Modelling multi-hazard risk assessment: A case study in the Yangtze River Delta, China

Baoyin Liu

Submitted in accordance with the requirements for the degree of
Doctor of Philosophy

The University of Leeds
School of Earth and Environment

August, 2015

The candidate confirms that the work submitted is his own, except where work which has formed part of jointly-authored publications has been included. The contribution of the candidate and the other authors to this work has been explicitly indicated below. The candidate confirms that appropriate credit has been given within the thesis where reference has been made to the work of others.

Some of the work in Chapters 1 and 2 of the thesis has been published in the jointly authored publications as follows:

Liu, B., Siu, Y. L., Mitchell, G., & Xu, W. (2013). Exceedance probability of multiple natural hazards: risk assessment in China's Yangtze River Delta. *Natural hazards*, *69*(3), 2039-2055.

Liu, B., Siu, Y. L., Mitchell, G., & Xu, W. (2014). The danger of mapping risk from multiple natural hazards. *Sustainability Research Institute Working Paper Series Working Paper* No. 61. Sustainability Research Institute, School of Earth and Environment, Leeds University, England.

Some of the work in Chapters 3, 4 and 5 of the thesis has been submitted for publication as follows:

Liu, B., Siu, Y. L., & Mitchell, G. A quantitative model for estimating risk from multiple interacting natural hazards: an application in northeast Zhejiang, China. *Stochastic Environmental Research and Risk Assessment*. In review.

Liu, B., Siu, Y. L., & Mitchell, G. Hazard interaction analysis for multi-hazard risk assessment: a systematic classification based on hazard-forming environment. *Natural Hazards and Earth System Sciences*. In review.

In these four papers, the candidate, Baoyin Liu, was the lead author and responsible for analysing the data and writing the paper. The joint authors had supervisory and advisory roles.

Publications

Peer-Reviewed Journal Papers

- **Liu, B**., Siu, Y. L., Mitchell, G., & Xu, W. (2013). Exceedance probability of multiple natural hazards: risk assessment in China's Yangtze River Delta. *Natural hazards*, *69*(3), 2039-2055.
- **Liu, B**., Siu, Y. L., Mitchell, G., & Xu, W. (2014). The danger of mapping risk from multiple natural hazards. *Sustainability Research Institute Working Paper Series Working Paper* No. 61. Sustainability Research Institute, School of Earth and Environment, Leeds University, England.
- **Liu, B**., Siu, Y. L., & Mitchell, G. A quantitative model for estimating risk from multiple interacting natural hazards: an application in northeast Zhejiang, China. *Stochastic Environmental Research and Risk Assessment*. In review.
- **Liu, B**., Siu, Y. L., & Mitchell, G. Hazard interaction analysis for multi-hazard risk assessment: a systematic classification based on hazard-forming environment. *Natural Hazards and Earth System Sciences*. In review.
- Ming, X., Xu, W., **Liu, B**., Du, J., Gu, Z., & Ge, Y. (2013). An overview of the progress on multi-risk assessment. *Journal of Catastrophology*, 28(1), 126-132.
- Ming, X., Xu, W., Li, Y., Du, J., **Liu, B**., & Shi, P. (2015). Quantitative multi-hazard risk assessment with vulnerability surface and hazard joint return period. *Stochastic Environmental Research and Risk Assessment*, 29(1), 35-44.

Book Chapters

- Xu, W., **Liu, B**., Ming, X., Chen, W., Hu, F., Zhang, Y., Tian, Y., & Yang, X. (2014). Natural hazard risk diagnosis. In W. Xu., et al., (Eds.), *Integrated Risk Governance: natural hazards and risk assessment in the Yangtze River Delta region*. Beijing: Science Press.
- Xu, W., Shi, P., Ming, X., **Liu, B**., Yang, G., Wan, R., Guo, J., Zhao, Y., & Zhao, T. (2014). General introduction of the Yangtze River Delta region. In W. Xu., et al., (Eds.), *Integrated Risk Governance: natural hazards and risk assessment in the Yangtze River Delta region*. Beijing: Science Press.

- Shi, P., Xu, W., Ming, X., **Liu, B**., Fang, J., Chen, W., Zhou, Y., Hu, F., & Zheng, J. (2014). Integrated natural hazards risk assessment in the Yangtze River Delta region. In P. Shi., et al., (Eds.), *Integrated Risk Governance: integrated natural hazards risk assessment and mapping in the Yangtze River Delta region. Beijing: Science Press*.

Conference Proceeding

- **Liu, B**., Siu, Y. L., Mitchell, G., & Xu, W. (2012). Multi-hazard risk assessment: a comparative evaluation of alternative approaches. *Third Conference of the International Society for Integrated Disaster Risk Management (IDRiM)*. Beijing Normal University, Beijing, China, 7th-9th September.

Acknowledgements

This thesis concludes four years of research as a PhD student at the School of Earth and Environment at the University of Leeds. I want to express my deepest appreciation to all who supported me during this period. Without their kind help and support, the past four years would have been much harder.

First and foremost, I would like to express my great gratitude to my excellent supervisors, Dr Yim Ling Siu and Dr Gordon Mitchell, for their unconditional and constant trust, support and guidance throughout my time in Leeds. They have been extremely patient and kind to help, encourage and comfort me when I faced many difficulties in both academic and daily life. Their helpful suggestions inspired me, and gave me an excellent foundation from which to complete this thesis.

I would also like to express my gratitude to my colleagues, both staff and PhD students, within the School of Earth and Environment and the School of Geography for their help and friendship. I am very grateful for the enjoyable life in Leeds.

I would especially like to thank Dr Wei Xu in Beijing Normal University, for his endless support and inspiration during my studies. I am also very grateful for his wonderful assistance during data collection.

I am most grateful to my family for their endless support while I am abroad. Without their help, I would not have been able to undertake this degree.

Special thanks also go to Professor Alan Pearman and Dr Guoyi Han for acting as examiners.

Abstract

Multi-hazard risk assessment (MHRA) has become a major concern in the risk study area, but existing approaches do not adequately meet the needs of risk mitigation planning. The main research gap in the existing approaches was identified that they cannot consider all hazard interactions when calculating possible losses.

Hence, an improved MHRA model, MmhRisk-HI (Model for multi-hazard Risk assessment with a consideration of Hazard Interaction), was developed. This model calculates the possible loss caused by multiple hazards, with an explicit consideration of interaction between different hazards. A more complete perspective, the regional disaster system perspective, was selected as the basic theory, and two categories of multi-hazard risk expressions were combined in the model construction. Hazard identification, hazard analysis, hazard interaction analysis, exposure analysis and vulnerability analysis are the five basic modules of the developed model. The concept of hazard-forming environment was introduced into the MHRA research as the basis for hazard identification, hazard analysis, and hazard interaction analysis. The methods used for exposure analysis depend on the scale of the region to be addressed and the assessment units. A Bayesian Network was adopted to calculate the loss ratio in the vulnerability analysis.

This developed model was applied into the Yangtze River Delta (YRD) and validated by comparison with an observed multi-hazard sequence. The validation results (simulation results are consistent with observed results in 76.36% of the counties, and the deviation of an estimated aggregate loss value from its actual value is less than 2.79%) show that this model can more effectively represent the real world, and that the outputs, possible loss caused by multiple hazards, obtained with the model are reliable. The outputs can additionally help to identify which area is at greatest risk (of loss), and allow a determination of the reasons that contribute to the greatest losses. Hence, it is a useful tool which can provide further information for planners and decision-makers concerned with risk mitigation.

Table of Contents

List of Tables

List of Figures

Abbreviations

AGSO	Australian Geological Survey Organization
AHP	Analytic Hierarchy Method
Armonia	Applied Multi-Risk Mapping of Natural Hazards for Impact Assessment
BN	Bayesian Network
CEC	Commission of the European Communities
DDRM	Délégation aux Risques Majeurs
DEM	Digital Elevation Model
EM	Expectation–Maximization
EM-DAT	Emergency Events Database
ESPON	European Spatial Planning and Observation Network
FEMA	Federal Emergency Management Agency
GDP	Gross Domestic Product
GIS	Geographic information system
IFRC	International Federation of Red Cross and Red Crescent Societies
ISDR	International Strategy for Disaster Reduction
IUGS	International Union of Geological Sciences
JRC	Joint Research Centre
MATRIX	New Multi-HAzard and MulTi-RIsK Assessment MethodS for Europe
MHRA	Multi-Hazard Risk Assessment
MLE	Maximum-Likelihood Estimation
MmhRisk-HI	Model for multi-hazard Risk assessment with a consideration of Hazard Interaction
Munich Re	Munich Reinsurance Company

OEP-EOP	Office of Emergency Preparedness of the Executive Office of the President of the United States
PCA	Principal Component Analysis
SCEMDOAG	South Carolina Emergency Management Division Office of the Adjutant General
SPSS	Statistic Package for Social Science
UNDP	United Nations Development Programme
UNDRO	United Nations Office of the Disaster Relief Co-Ordinator
YRD	Yangtze River Delta

Chapter 1

Introduction

1.1 Research background and research rationale

During the twenty-first century, with rapid development of the global economy and urbanization, society has been greatly affected by natural disasters (e.g. floods, droughts, earthquakes) (Figure 1.1). According to the report about natural disasters in the United Nations EM-DAT (Emergency Events Database) (2015) (Figure 1.2), losses and effects caused by these disasters have been increasing. In the field of risk studies, several methods have been developed for evaluating a single type of hazard such as earthquake, flood or typhoon, and some of which have been widely used for disaster risk reduction (e.g. Hall et al., 2003; Bonachea et al., 2009; Okuyama, 2008; Hsu et al., 2013).

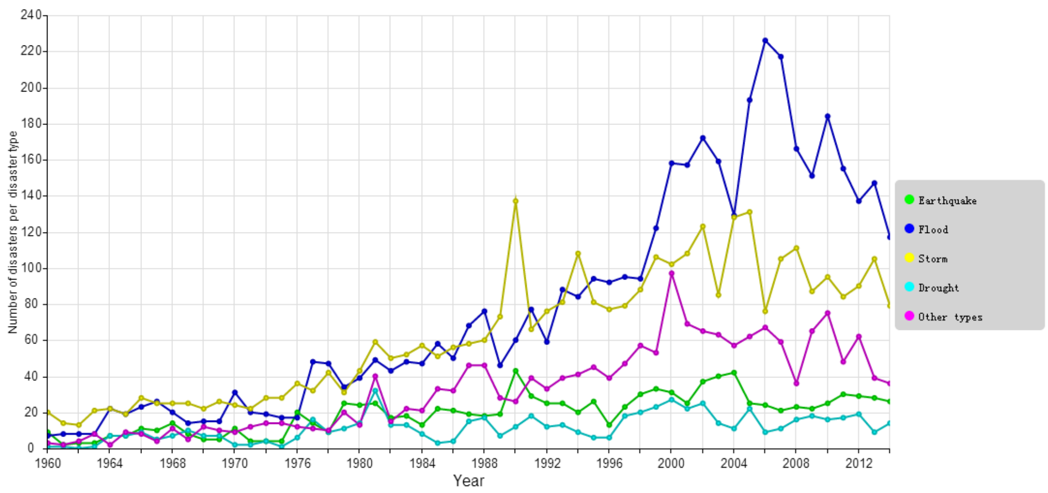

Figure 1.1 Total number of natural disasters from 1960 to 2014 (Source: The United Nations EM-DAT datasets)

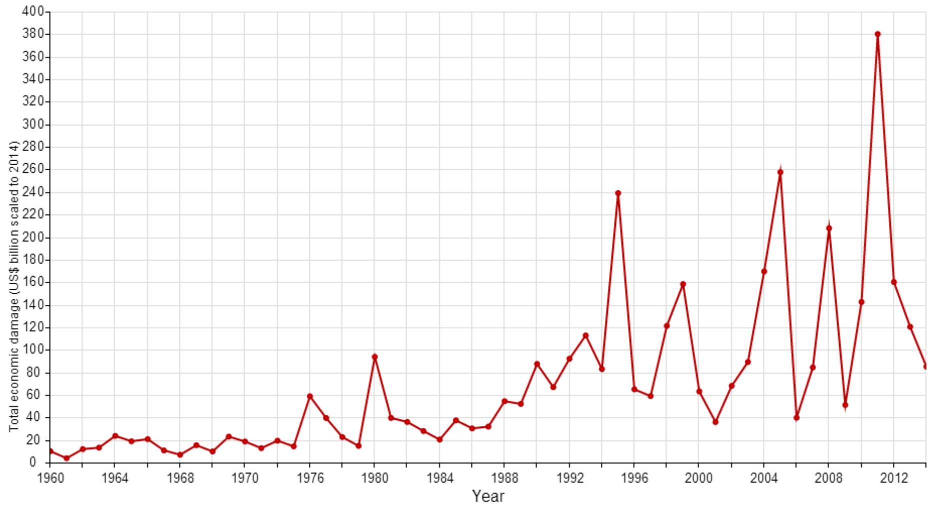

Figure 1.2 Total economic damage caused by natural disasters from 1960 to 2014 (Source: The United Nations EM-DAT datasets)

However, United Nations data (EM-DAT, 2015) reveal strong evidence that many world regions are subject to multiple hazards. In these areas, the impacts of one hazardous event are often exacerbated by interaction with other hazards; whilst some hazards occur one after another in a short period of time without an evident common cause. The short time period between events may reduce resilience and recovery, and hence is indicative of greater risk than when events are considered individually.

The 2011 Tohoku earthquake, which hit Japan on Friday, 11 March, 2011, is the costliest natural disaster in world history (economic cost was US$ 210 billion) (EM-DAT, 2011). The earthquake triggered a destructive tsunami. It reached the eastern coast of Honshu, Japan, with the wave up to 38m high (Norio et al., 2011). The tsunami also created a serious nuclear accident, the most critical of which was the level 7 meltdowns at three reactors in the Fukushima Daiichi Nuclear Power Plant complex (Tabuchi and Bradsher, 2011). The tsunami and subsequently the nuclear disaster are the main reasons to induce the huge loss (Norio et al., 2011).

Typhoon Haiyan, which was one of the strongest recorded storms ever to make landfall, swept through the Philippines on 11th November, 2013. The cyclone caused catastrophic destruction in the central Philippines. According to the United Nations EM-DAT (2013), the number of people killed was 7354. The huge casualties should also be attributed to the Bohol earthquake, a magnitude 7.2 earthquake which happened in the central Philippines one month before. During the earthquake, several government buildings, hospitals and numerous schools were partially or totally damaged; some bridges, including many along the National Road, were damaged in Bohol province. Bohol was a centre in which relief supplies (water, blankets etc.) were stored in the central Philippines. These stores have been emptied by the earthquake relief effort. Therefore, when Haiyan attacked, some provinces in the central Philippines were in the disaster reconstructions stage, which were more vulnerable than the pre-disaster stage. Most importantly the Philippines government did not get chance to replenish the relief supplies which were used in the earthquake in one month. The shortage of the relief supplies exacerbated the typhoon disaster and became the most important reason to induce huge casualties.

The 2011 Tohoku earthquake which led to a tsunami and subsequently the Fukushima Daiichi nuclear disaster is an example of one hazard exacerbated by interaction with other hazards. The Bohol earthquake-typhoon Haiyan case is an example of ‘crowding’, close proximity between events lower resilience to disaster and making recovery more difficult. Therefore, the problem is that by investigating single hazards in isolation to each other may lead to an underestimation of the compound (or ripple) effects of the events. To avoid this pitfall, more attention should be paid to multiple hazards risk.

Risk assessment is the core of risk management (Hester and Harrison, 1998; Schmidt et al., 2011; Komendantova et al., 2014). Multi-hazard risk assessment (MHRA) is the key step of integrated risk management (Carpignano et al., 2009; Frigerio et al., 2012; Marulanda et al., 2013). Thus, multiple hazards risk assessment has become a major concern in the risk study area. There are some studies and projects addressing this issue, e.g. the Australian Geological Survey Organisation (AGSO) Cities project for Australia (Granger and Trevor, 2000), Natural Hazard Index for Mega-cities (Munich Re, 2003), HAZUS-MH software for Risk Assessment in the USA (FEMA, 2004), World Bank’s Natural Disaster Hotspot analysis for whole global (Dilley et al., 2005), ESPON (European Spatial Planning and Observation Network) multi-hazard approach for the enlarged European Union (Schmidt-Thomé, 2006a), Calculation of the Total Place Vulnerability Index in the State of South Carolina, USA (SCEMDOAG, 2006), Regional RiskScape project for New Zealand (Schmidt et al., 2011), Central American Probabilistic Risk Assessment Program for Latin America and the Caribbean Region (Linares-Rivas, 2012), Integrated Risk Governance project for China (Shi et al., 2014).

However, these studies cannot provide enough information for risk mitigation planning (Komendantova et al., 2014, Scolobig et al., 2014), e.g. Natural

Hazard Index for Mega-cities (Munich Re, 2003) and ESPON multi-hazard approach (Schmidt-Thomé, 2006a) are best used to assess relative risk, but cannot calculate the possible loss and corresponding exceedance probability; Regional RiskScape project (Schmidt et al., 2011) and Integrated Risk Governance project for China (Shi et al., 2014) neglect the interaction between different hazards. Besides, some different approaches used in the same region may present totally different results (Liu et al., 2014), which may induce the planners and decision-makers to misunderstand the risk situation. Hence, developing an improved MHRA model, MmhRisk-HI (Model for multi-hazard Risk assessment with a consideration of Hazard Interaction), is the core of my research study.

1.2 Key terms and definitions

This section outlines several of the key terms used in the research aim and objectives (see section 1.3) to provide a consistent understanding. Further discussion surrounding the development of these terms is provided in Chapter 2.

- Natural hazard: extreme natural events arise from specific geophysical environments.
- Risk: expected loss and the probability of occurrence.
- Multi-hazard risk assessment: assess and map the expected loss due to the occurrence of various natural hazards on the social, environmental and economic settings in a given area.
- Hazard forming environment: the specific geophysical environment that natural hazards arise from.
- Exposure: the number, types and monetary value of elements that are under threat of hazard events.
- Vulnerability: the conditions determined by physical, social, economic, and environmental factors, which decide the potential extent of damage following exposure to hazard events.
- Exceedance probability: probability of an event being greater than or equal to a given value.
- Loss ratio: the ratio of total losses to the total value of the exposure.

1.3 Research aim and objectives

1.3.1 Research aim

The central aim of this research is to evaluate the existing MHRA approaches, and develop an improved quantitative technique that overcomes key limitations identified from the existing approaches, forming the basis of prudent planning and prioritized risk-mitigation measures.

1.3.2 Research objectives

There are six research objectives that contribute to the above research aim. These are:

1) To characterize the pattern of risk from multiple natural hazards
    a) Draw on data to show trends and outcomes in natural hazard events and multi-hazard events.
    b) Draw on case analysis to show the serious influence caused by multiple natural hazards.
2) To critically evaluate the theory and practice of MHRA
    a) Review the definition and basic components of natural disaster, summarise a relatively comprehensive definition for natural disaster and define terminology for each basic component.
    b) Review the definition of risk of natural hazard, and summarise a relative comprehensive definition.
    c) Review the definition of MHRA, and summarise a relative comprehensive definition.
    d) Review the basic theory of MHRA, summarise deficiencies in current theories, and identify the opportunities for enhancement.
    e) Review the conceptual model of MHRA, summarise deficiencies in current models, and identify the opportunities for enhancement.
    f) Evaluate the research scope of the existing MHRA approaches, summarise deficiencies in the current models, and identify the limitations for enhancement.
    g) Review the basic components for MHRA models (hazard identification and analysis, hazard interaction analysis, exposure analysis and vulnerability analysis) and corresponding methods,

summarise the deficiencies in current methods, and identify the limitations for enhancement.

3) To design a new methodology for MHRA, addressing key deficiencies identified in the existing approaches; to choose a case study area and collect relevant data

    a) Basic theory: describe the regional disaster system perspective for the improved MHRA model.

    b) Conceptual model: describe the conceptual basis of the improved MHRA model, and explain how it addresses the key deficiencies in existing models.

    c) Describe which methods are used in this research, and explain why choose these methods and how they address the key deficiencies in existing methods.

    d) From social, geographical and historical disasters to describe how the case study area is chosen.

    e) Describe which kinds of data are used and how these data are collected.

    f) Describe how to test the validity of the proposed model.

4) To construct an improved model (MmhRisk-HI) of MHRA

    a) Framework: describe the basic framework of MmhRisk-HI, which is a hybrid model, combining elements of risk index and mathematical statistics approaches. Hazard identification, hazard analysis, hazard interaction analysis, exposure analysis, and vulnerability analysis are the main components.

    b) Hazard identification: describe how to use stable factors in hazard-forming environment to identify the spatial distribution of hazards. This considers all possible hazard situations even if some hazards have long return periods.

    c) Hazard analysis: describe how to use multiple dimension information diffusion method to analyse the trigger factors for hazard magnitude-frequency analysis, and thus overcome the problem of limited historical observation (short observation period relative to return period).

    d) Hazard interaction analysis: describe how to analyse the hazard interaction and calculate the exceedance probability of multiple hazards occurrence based on the results of the hazard identification and hazard analysis modules. All possible relationships among different hazards are considered in this module.

e) Exposure analysis: describe how to analyse the distribution of exposure.

f) Vulnerability analysis: describe how to use Bayesian Network (BN) to calculate the loss ratio induced by multi-hazard of different degree, and reflect how vulnerability indicators from physical, social, economic and environmental domains influence overall vulnerability.

5) To apply MmhRisk-HI to test its utility

a) Model application: apply MmhRisk-HI in the Yangtze River Delta (YRD) to calculate the possible loss and corresponding exceedance probability caused by multiple hazards based on historical data from 1980-2012.

b) Model validation: the hazards that occurred in 2013 are simulated in this model. The simulated results are used to compare with the observed data.

c) Results analysis: analyse the results by risk maps.

6) To make recommendations for improving risk mitigation through the application of MHRA modelling

a) Discuss the strengths and limitations of MmhRisk-HI.

b) Discuss the effectiveness on risk mitigation of MmhRisk-HI.

c) Discuss the recommendations for policy and practice, and further research.

d) Depict the contributions of this research.

1.4 Framework of the research

Figure 1.3 depicts the research framework corresponding to the objectives set out above. Each objective is represented in the framework in the order depicted (reading top to bottom), with each of the six main boxes and their objectives reflecting the thesis structure (Chapter 1-6).

Chapter 1 is an introduction to the thesis, where the research background, rationale, aim and objectives are clarified. The frame of the research and structure of the thesis are delineated.

Chapter 2 is the literature review of MHRA. Firstly, this chapter introduces the definition of natural disaster and risk. Then, the definition, basic theory and conceptual model of MHRA are introduced. The research scope and basic components for the existing MHRA methods are presented at the end of this chapter.

Chapter 3 is the research design and methodology. This chapter interprets the basic theory and conceptual model used in this research. Then, the basic modules for MmhRisk-HI and the methods used for each module are introduced. After explaining the choice of study area and data needed, the methods used for model verification are introduced.

Chapter 4 is the MHRA model construction. The basic framework for the development of MmhRisk-HI is first introduced. Then, the construction of each module is presented, including hazard identification, hazard analysis, hazard interaction analysis, exposure analysis and vulnerability analysis.

Chapter 5 is the application of MmhRisk-HI in the YRD. The model is applied in the YRD to calculate the multi-hazard risk based on historical data from 1980-2012. The hazards that occurred in 2013 are simulated in this model. The simulated results are used to compare with the observed data.

Chapter 6 is the discussion and conclusion. Firstly, the strengths, limitations and effectiveness on risk mitigation of MmhRisk-HI are introduced, and then the recommendations for policy and practice and further research are discussed. Finally, contributions of this research are presented.

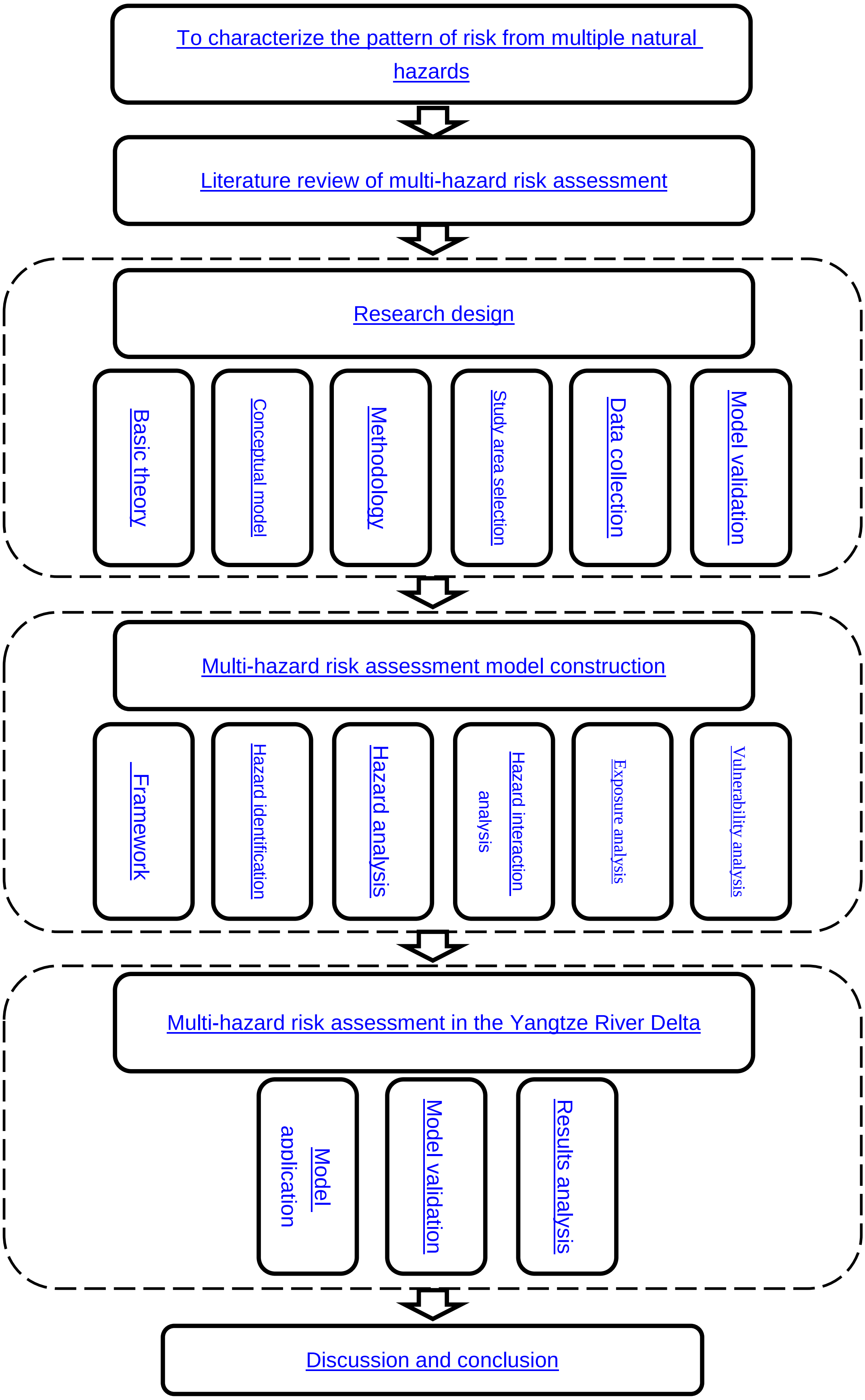

Figure 1.3 Framework of the research

Chapter 2

A review of multi-hazard risk assessment

This chapter firstly introduces the definition of natural disaster and its formation mechanism, and then presents the relevant definition of risk. It next discusses the basic theory and underlying conceptual model for assessing risk from multiple hazards (hereafter multi-hazard risk assessment, or MHRA), and reviews existing MHRA processes, before drawing a conclusion on the research gaps and opportunities in MHRA.

2.1 Definition of natural disaster

2.1.1 Natural disaster

Chapter 1 detailed how typhoons, floods, earthquakes and other natural disasters have greatly affected society recently. However, there is no widely accepted definition of disaster. The definition of disaster and its many components is contested and has been the subject of considerable debate in various disciplines. In contemporary academia, disasters are routinely divided into natural or human-made according to their cause (Rutherford and De Boer, 1983; Schmidt-Thomé, 2006a; Smith, 2013). Natural disasters including floods, volcanic eruptions, earthquakes, tsunamis, and other geologic processes are all adverse events resulting from natural processes of the Earth. Disasters caused by chemical or industrial accidents, environmental pollution, transport accidents, terrorist attack and political unrest are classified as human-made disaster since they are the direct result of human action. This research mainly focuses on natural disasters. Some definitions of disaster are listed in Table 2.1.

In adopting alternative perspectives, these scholars define natural disasters differently. Kates (1978), Alexander (1993) and Smith (2000) focus on the interaction among hazard and socio-economic environment/vulnerability. Cohen and Ahearn (1980), Keller et al. (1990) and Smith (2000) emphasize the consequence with loss of human life, material wealth, economic activity and ecological value. However, some common characteristics for natural disasters can be identified, namely that under a specific environment, natural hazard's interaction with vulnerability of exposures can result in serious damage to exposures in the affected area, with consequent loss of human life, material wealth, economic activity and ecological value. Thus, hazard-forming environment, natural hazard, exposure and vulnerability are the main components for natural disaster. These terms are further defined below to provide a consistent understanding.

Table 2.1 Definitions of disaster

Author	Year	Definition
Kates	1978	"Hazard potential occurring in nature, technology or society makes harmful interaction with human population, activities, and wealth and with the environments that humans value and need".
Whittow	1980	"A hazard is a perceived natural event which threatens both life and property-a disaster is the realization of this hazard".
Cohen and Ahearn	1980	"Extraordinary events that cause great destruction of property and may result in death, physical injury, and human suffering".
Keller et al.	1990	"An event which afflicts a community the consequences of which are beyond the immediate financial, material or emotional resources of the community".
Parker	1992	"An unusual natural or man-made event, including an event caused by failure of technological systems, which temporarily overwhelms the response capacity of human communities, groups of individuals or natural environments, and which causes massive damage, economic loss, disruption, injury and /or loss of life".
Alexander	1993	"Some rapid, instantaneous or profound impact of the natural environment upon the socio-economic system".
Smith	2000	"An event, concentrated in time and space, in which a community experiences severe danger and disruption of its essential functions, accompanied by widespread human, martial or environment losses, which often exceed the ability of the community to cope without external assistance".
Pelling	2003	"The outcome of hazard and vulnerability coinciding. Disaster is a state of disruption to systemic functions. Systems operate at a variety of scales, from individuals' biological and psychological constitutions or local socio-economic to urban infrastructure networks and the global political economy".
ISDR	2004	"A serious disruption of the functioning of a community or a society causing widespread human, material, economic or environmental losses which exceed the ability of the affected community or society to cope using its own resources".

2.1.2 Natural hazard

2.1.2.1 Definition of natural hazard

A natural hazard is a prerequisite of a natural disaster. As with natural disaster, there is no universally accepted definition of a natural hazard, and its definition has been the subject of considerable debate in various disciplines.

Table 2.2 Definitions of natural hazard

Author	Year	Definition
Burton and Kates	1963	"Those elements of the physical environment harmful to man and caused by forces extraneous to him."
Hewitt	1983	"The potential for damage that exists only in the presence of a vulnerable human community."
Royal Society	1986	A situation that in particular circumstances could lead to harm.
Blaikie et al.	1994	"The natural events that may affect different places singly or in combination at different times."
Alexander	2000	"An extreme geophysical event that is capable of causing a disaster."
McGuire et al.	2002	"An extreme natural event that poses a threat to people, their property and their possessions."
Pelling	2003	"The potential to harm individuals or human systems."
ISDR	2004	"A potentially damaging physical event, phenomenon and/or human activity, which if realized may cause the loss of life or injury, property damage, social and economic disruption or environmental degradation."
Smith and Petley	2009	"Extreme geophysical events, biological processes that release concentrations of energy or materials into the environment on a sufficiently large scale to pose major threats to human life and economic assets."

From Table 2.2, it is noticed that certain common features exist and they are:

1. Extreme natural events arise from specific geophysical environments.
2. Concentrations of energy are released into the environment.
3. The released energy produces major threats to human life and/or economic assets.

Given these features, it is proposed that a relatively comprehensive definition of natural hazard is: a natural event that arises from a specific geophysical environment, accompanied by concentrations of energy released to produce major threats to human life or economic assets.

2.1.2.2 Basic characteristics of natural hazard

As a “natural event”, the basic characteristics of natural hazards comprise space, time, magnitude and frequency (Kates, 1978; Alexander, 1993; Smith, 2000).

The space attribute firstly addresses geological location. This refers to the place of hazard occurrence. Avalanches, landslides, and earthquakes can ordinarily be mapped precisely. Droughts and cold waves are widespread in occurrence and are usually associated with a relatively large area. The second space attribute is the areal extent of the damage zone. In contrast to geological location, this represents the space influenced by a hazard event. Thus, for example, an earthquake’s geological location, is its hypocentre or epicentre (the position where the strain energy stored in the rock is first released), while its damage zone may cover thousands of square kilometres.

Time scale also comprises two attributes: time of occurrence and duration. Time of occurrence refers to the onset time of hazard occurrence. Some hazards tend to be seasonal phenomena, e.g. most typhoons which influence China develop in late summer and autumn. Duration refers to the time span or persistence of a hazardous event. Most hazards are easy to describe in this way, e.g. an avalanche may last for hours, a flood may persist for weeks, but some hazards are harder to estimate. For example, a drought which may last for years, or land degradation that could last years or centuries.

Magnitude refers to the strength or force of the hazard event. It is used to quantify the energy released by a natural hazard. Different types of hazards use different units to measure these factors, e.g. stream discharge for flood, wind speed for tornado. Therefore, it is hard to directly compare the magnitude of different hazards.

Frequency can be defined as how often a given magnitude of natural hazard occurs in the long-run. It also can be expressed as a recurrence interval or return period - the average length of time between hazards of a given magnitude. These factors vary considerably between different types of natural hazards, but they usually have a strong nonlinear relationship to magnitude. According to the magnitude-frequency rule, there will be many small events and few large ones over a sufficient interval of time (Wolman and Miller, 1960). Hence, the average return period of small-magnitude hazards is short and that of big-magnitude hazards is long (Alexander, 1993).

Generally speaking, time and space scales describe the timing of hazardous events, particularly any seasonality, and the area is covered by these hazards, whilst magnitude and frequency express the strength of hazards and how often they occur.

2.1.3 Hazard-forming environment

Given the definition of natural hazard as a “natural event”, natural hazard is a geophysical process which must therefore arise from a specific geophysical environment. The geophysical environment includes environmental factors in the atmosphere, hydrosphere, biosphere and lithosphere. These factors are the basic conditions for the occurrence of hazards (Park, 1994; Shi, 1996; McGuire et al., 2002). Natural hazards are also extreme natural events. Here, “extreme” means natural hazards are extraordinary compared to the normal natural event. The “extreme” is always caused by one or more environmental factors substantial departure in either the positive or the negative direction from their mean value, e.g. flood can be induced when the precipitation is above the normal level, while drought is easy to occur when it is below the normal level.

According to their contribution to natural hazard, the geophysical environmental factors can be categorized into two types. Factors in the first type form the background for the occurrence of natural hazards. Here, these factors are named as stable factors. They are the preconditions to hazards. These factors never change or change very little over a long time (hundreds or thousands of years), e.g. tectonic plates, landform, or the value of these factors stays within a relative stable range, e.g. annual average temperature, annual average precipitation. Compared to the stable factors, factors in the second type are constantly changing, e.g. daily precipitation, daily temperature. Substantial changes in these factors give rise to hazard. Therefore, they can be taken as trigger factors for natural hazards and they are the determinant factors for the frequency and magnitude of hazards. The fundamental characteristics of natural hazards are decided by these geophysical environmental factors (further analysis is presented in section 3.2.1). Hence, geophysical environmental factors are the determining factors for natural hazards, and the geophysical environment which consists of these factors can be defined as the “hazard-forming environment”.

2.1.4 Exposure

The term “exposure” also can be expressed as the “element at risk” (Alexander, 2000). It can be defined as the number, types and monetary value of property, infrastructure, natural environment, economic activities and population that are under threat of a hazard event in a given area (Alexander, 2000; Blanchard, 2005). A big magnitude earthquake in a sparsely populated area may result in few losses, but in a big city, the consequence may be terrible. Therefore, exposure analysis has an important role in understanding the extent of the damage and loss caused by natural disaster in a risk area (Daniel and Cothern, 2001).

2.1.5 Vulnerability

Vulnerability in the context of natural disasters was introduced from the social sciences in the 1970s (Schneiderbauer and Ehrlich, 2004; Birkmann, 2006). In 1972, the Office of Emergency Preparedness of the Executive Office of the President of the United States (OEP-EOP) (1972) presented a report in which vulnerability is recognized as the predisposition of communities or larger jurisdictions to be affected by a natural disaster. Since then, various definitions of vulnerability have emerged. Chambers (1989) introduced vulnerability as the “exposure to contingencies and stresses and the difficulty which some communities experience while coping with such contingencies and stresses”; Blaikie et al. (1994) defined vulnerability as “the characteristics of a person or group and their situation that influence their capacity to anticipate, cope with, resist and recover from the impact of a natural hazard”; Alexander (2000) proposed the notion of vulnerability as “the potential for casualty, destruction, damage, disruption or other forms of loss with respect to a particular element”; whilst the International Strategy for Disaster Reduction (ISDR) (2004) defined vulnerability as “the conditions determined by physical, social, economic, and environmental factors or processes, which increase the susceptibility of a community to the impact of hazards”.

These definitions reveal two basic types of vulnerability: biophysical and social (Pelling, 2003; Brooks, 2003). Biophysical vulnerability focuses on the potential extent of damage following exposure to hazardous events (Burton et al., 1993; Hilhorst and Bankoff, 2004; WBGU, 2005; Macchi et al., 2008). Social vulnerability refers to a pre-existing condition (including physical, social, economic and environmental factors) of an exposure that affects its ability to cope with the impact of hazard events (Downing et al., 2001; Allen, 2003; Cannon et al., 2003; Cutter et al., 2003). The aim of this thesis is to assess the risk caused by multiple hazards, with vulnerability assessment which is used to measure the possible loss for a given exposure, under conditions caused by hazard of varying degree, and to reflect how these conditions (including physical, social, economic and environmental factors) influence the possible loss. Hence, in this study, vulnerability is given a relatively broad definition as the conditions determined by physical, social, economic, and environmental factors, which decide the potential extent of damage following exposure to hazard events.

2.2 Definition of risk

As with the terms ‘natural disaster’, and ‘hazard’, there is no universally accepted definition of risk, and a range of definitions of risk from natural disaster exist (Table 2.3). These expressions reflect risk of natural disaster more comprehensively and most risk assessment approaches use these definitions or variants of them. However, the differences that occur mean that risk associated with natural hazards is commonly characterized in one of two distinct categories of risk assessment.

The first type defines risk as the probability of loss caused by the interactions between the vulnerability of exposure and the hazard. Risk is most commonly expressed as in equation (2-1) (ISDR, 2004):

$$\text{Risk} = \text{Hazard} \times \text{Vulnerability} \times \text{Exposure} \tag{2-1}$$

The second type describes risk as a product of the probability of occurrence of a hazardous event and the consequences of such an event for exposures (the magnitude of impact resulting from realization of the hazard). Risk is expressed as (IUGS, 1997):

$$\text{Risk} = \text{Probability} \times \text{Consequence} \tag{2-2}$$

The first expression biases the risk assessment process towards a greater consideration of the disaster formation mechanism (interaction of hazard and exposure). The second type emphasizes the possible consequences by assessing risk from the perspective of possibility of loss. The substantively different expressions to risk assessment are also evident in the field of MHRA.

Table 2.3 Risk definitions with reference to natural hazards

Author	Year	Definition	Expression
Fournier	1979	the possibility of a loss	$\text{Risk} = \text{Value} \times \text{Vulnerability} \times \text{Hazard}$
Blaikie et al.	1994	a compound function of hazard and vulnerability of exposure to that specific hazard	$\text{Risk} = \text{Hazard} \times \text{Vulnerability}$
Smith	1996	the possibility of a loss caused by disaster	$\text{Risk} = \dfrac{\text{Probability} \times \text{Loss}}{\text{Loss mitigation}}$
IUGS	1997	the probability of occurrence and the severity may cause toward human life, property and the environment	$\text{Risk} = \text{Probability} \times \text{Consequence}$
Tobin and Montz	1997	expected loss caused by disaster and the probability of the loss happened	$\text{Risk} = \text{Probability} \times \text{Consequence}$
Hurst	1998	the probability of occurrence and excepted loss	$\text{Risk} = \text{Probability} \times \text{Consequence}$
Alexander	2000	"the likelihood, or more formally the probability, that a particular level of loss will be sustained by a given series of elements as a result of a given level of hazard"	$\text{Total Risk} = \left(\Sigma \text{elements at risk}\right) \times \text{Hazard} \times \text{Vulnerability}$
Hahn et al.	2003	represented by hazard, vulnerability, exposure and coping capacities	$\text{Risk} = \text{Hazard} + \text{Exposure} + \text{Vulnerability-Coping Capacities}$
ISDR	2004	"The probability of harmful consequences, or expected losses (deaths, injuries, property, livelihoods, economic activity disrupted or environment damaged) resulting from interactions between natural hazards and vulnerable conditions"	$\text{Risk} = \text{Hazard} \times \text{Exposure} \times \text{Vulnerability}$
Dilley et al.	2005	the combination of three components: hazard, exposure, and vulnerability.	$\text{Risk} = \text{Hazard} \times \text{Exposure} \times \text{Vulnerability}$

2.3 Definition of multi-hazard risk assessment

Generally, MHRA is based on single-hazard risk assessment. The main advance of MHRA is that it puts different types of hazards into a single system for joint evaluation (Armonia, 2006; Di Mauro et al., 2006; Marzocchi et al., 2009; Carpignano et al., 2009). MHRA is a relatively new field, and there is currently no clear definition (Kappes et al., 2012; Komendantova et al., 2014). In principle, it takes into account the characteristics of each hazardous event (e.g. probability, frequency, magnitude), and their mutual interactions and interrelations (e.g. one hazard may occur repeatedly in time; different hazards may independently occur in the same place; different hazards may occur dependently in the same place) (Kappes et al., 2012; Marzocchi et al., 2012). The aim of MHRA is to have a holistic view of the total effects or impacts by assessing and mapping the expected loss due to the occurrence of various natural hazards on the social, environmental and economic settings in a given area (Dilley et al., 2005; Armonia, 2006; Gao et al., 2007; Kappes et al., 2012; Komendantova et al., 2014).

2.4 Basic theory of multi-hazard risk assessment

The understanding of disaster formation mechanism determines the strategy of risk assessment. Hence, perspective on the disaster formation mechanism forms the basic theory for risk assessment. The existing perspectives on the disaster formation mechanism basically can be divided into four types: natural hazard perspective, hazard-forming environment perspective, exposure perspective and regional disaster system perspective.

The natural hazard perspective holds that the occurrence of hazard is the main reason to induce disaster (Varnes, 1984; EL-Sabh and Murty, 1988; Mccall et al., 1992; Tucker, et al., 1994; Rossi et al., 1994; Busoni et al., 1995). Risk assessment based on this perspective mainly focuses on how to calculate the return periods of hazards. The assessment results help to improve the prediction accuracy of natural hazard, and provide technical parameters for the engineering construction, e.g. seismic intensity zoning, or flood risk division.

The hazard-forming environment perspective assumes that the change of environment is the main reason to induce the occurrence of disaster (McGuire et al., 2002), e.g. a rise in sea level makes flooding happen frequently in coastal lowlands, a decrease of relative humidity in dry areas expands the scope and increases relative strength of the drought (Parker, 1992). How to reconstruct the time and space distribution of natural disasters under regional environment evolution (climate change, landscape change and land cover change process) is the main problem under this perspective (Eddy et al., 1986; Philander, 1990; Parsons, 1995; Park, 1994; McGuire et al., 2002).

The exposure perspective states that the formation of the disaster is the result of exposure affected by natural hazard (Turner II and Meyer, 1991; Chung, 1994). Risk assessment based on this perspective focuses on how to monitor the change of exposures and evaluate the vulnerability for different exposures (Gong and Howarth, 1992).

In the process of disaster formation, hazard, hazard-forming environment and exposure, all are necessary. The natural hazard, hazard-forming environment and exposure perspectives all emphasize the dominant factors and ignore the other factors. Therefore, the regional disaster system perspective was produced to seek to integrate these alternative perspectives. The regional disaster system perspective contends that disaster is produced by social and natural factors together (Burton et al., 1993; Shi, 1996; Wisner et al., 2004). Disaster is a system composed by a variety of factors: hazard, exposure, hazard-forming environment. Risk assessment based on this perspective should calculate the possible loss and corresponding probability with considering the stability of the hazard-forming environment, probability of the hazard occurrence and the vulnerability of exposure together.

Natural disasters result from natural hazards interaction with vulnerability of exposure under a specific environment. The natural hazard, hazard-forming environment and exposure perspectives each only emphasize a single attribute for natural disaster. Therefore, the regional disaster system perspective which postulates disaster is produced by hazard, exposure, and hazard-forming environment together is more suitable for MHRA as an important theory basis. Some conceptual models of MHRA have been developed based on this perspective, which are discussed next.

2.5 Conceptual model of multi-hazard risk assessment

A conceptual model is a model made up of a composition of concepts, which are used to help understand relationships among factors in the model. A conceptual model of risk shows the relationship among factors that give rise to that risk. Some conceptual models of risk were expressed in section 2.2, and two distinct categories of conceptual model were summarised (equations 2-1 and 2-2 in section 2.2).

MHRA assesses the risk from multiple hazards, and building on the models of risk from a single hazard presented above, can be expressed in two fundamental conceptual models (Armonia, 2006; Di Mauro et al., 2006; Marzocchi et al., 2012):

$$\text{Risk} = \sum_{i=1}^{n} (\text{Hazard} \times \text{Vulnerability} \times \text{Exposure}) \tag{2-3}$$

$$\text{Risk} = \prod_{i=1}^{n} \text{Probability} \times \text{Consequence} \tag{2-4}$$

Where, *i = (1,2…n)* represents *i* types of hazards.

These two expressions cannot express the whole regional disaster system perspective. The first expression is biased towards interaction of hazard and exposure, whilst the second emphasizes the possible consequences by assessing risk from the perspective of possibility of loss. The substantively different conceptual approaches to MHRA have both been developed in practice.

2.6 Research scope of multi-hazard risk assessment

MHRA is a relatively new field, with little MHRA research conducted before 2000. There are three recognizable phases in the development of MHRA to date. At the beginning, research mainly focused on multiple hazards which affect a given area through the development of a synthetic indicator, which is effective in comparing the relative danger experienced by different areas (Granger and Trevor, 2000). From 2004, research moved from synthetic indicator evaluation to assessing integrated losses caused by multiple nature hazards in a given region and time period (FEMA, 2004). However, this research neglected the interaction between different hazards. Hence, in recent years, comprehensive MHRA research is proposed to assess the possible loss caused by multiple hazards with a consideration of domino effects (Marzocchi et al., 2009). These phases are further detailed below.

2.6.1 Synthetic indicator

Synthetic indicators of multiple hazards mainly use a risk index approach. The risk index approach addresses the factors that lead to a disaster. Risk is most commonly expressed as in equation 2-1 (Section 2.2) and calculated based on the conceptual model in equation 2-3 (Section 2.5). Selection of component indicators for hazard, vulnerability and exposure, and calculation of associated weights are key steps. The process is an extension of that used for an individual hazard, with risks from individual hazards aggregated in a unified multi-hazard risk index. Aggregation may proceed in two ways (Tables 2.4 and 2.5).

Category 1: This approach analyses the hazard, vulnerability and exposure to obtain the respective multi-hazard, vulnerability and exposure indices. The multi-hazard risk index is then calculated by summation (Munich Re, 2003; Schmidt-Thomé et al., 2003; Fleischhauer et al., 2005; Schmidt-Thomé, 2006a; Schmidt-Thomé, 2006b; SCEMDOAG, 2006). It can be expressed as:

$$R = f\left(\sum_{i=1}^{n} H_i, \sum_{i=1}^{n} V_i, \sum_{i=1}^{n} E_i\right) \qquad (2\text{-}5)$$

Where, R is Multi-hazard risk,
H_i is Hazard,
V_i is Vulnerability, and
E_i is Exposure.

Table 2.4 Multi-hazard risk assessment for synthetic indicator Category 1

Country (or Institution)	Study area	Hazards	Remarks
Australia (Australian Geological Survey Organisation) (Granger and Trevor, 2000)	Mackay (Australia)	Cyclone (flood, strong wind, storm tide).	Multi-hazard risk was calculated by combining the highest rank of the individual hazards and overall community vulnerability.
Munich Reinsurance Company (Munich Re, 2003)	Global	Earthquake, windstorm, flood, volcanic hazard, bush fire, frost.	Historical loss data was used to calculate the weight for each single hazard.
India (Khatsu and van Westen, 2005)	Kohima Town (India)	Earthquake, landslide, fire.	Multi-hazard map was created by overlaying single hazard map.
Europe (European Spatial Planning and Observation Network) (Schmidt-Thomé, 2006a)	The enlarged European Union (EU-29)	Avalanche, drought, earthquake, extreme temperature, flood, forest fire, landslide, storm surge, tsunami, volcanic hazard, winter and tropical storm, technological hazards.	The Delphi method was used to assign weight to each single hazard.
Cameroon (Thierry et al., 2008)	Mount Cameroon	Volcanic hazards, landslide, earthquake.	Geographic Information System (GIS) was used to combine each single hazard and element-at-risk.
Switzerland (Kunz and Hurni, 2008)	Switzerland	Flood, mass movements, snow avalanche.	Multi-hazard map was created by overlaying single hazard map.
The United States (SCEMDOAG, 2009)	The United States	Coastal events, dam failure, drought, flood, fog, geophysical events, human-induced hazard events, severe thunderstorm events, temperature extreme, wildfire, winter weather.	The multi-hazard index was constructed by aggregating the frequency of occurrence for each hazard with equal weight.

The Calculation of the Total Place Vulnerability Index in the State of South Carolina, USA (SCEMDOAG, 2006; SCEMDOAG, 2009) used this method to calculate a multi-hazard index, aggregating all hazards with equal weight. An urban multi-hazard risk analysis using GIS and remote sensing for Kohima Town, India (Khatsu and Van Westen, 2005) used ArcGIS software to overlay equal weighted, single hazard maps to generate a multi-hazard map. These methods do not fully reflect the spatial variability in various impacts of different hazards in an area. The Natural Hazard Index for Mega-cities (Munich Re, 2003) used average annual losses and probable maximum loss as indicators to decide weights for each hazard (in a ratio of 80:20 for each relevant hazard), but the key problem here is that the probable maximum loss for very infrequent large-scale disasters is unknown. The ESPON multi-hazard approach (Schmidt-Thomé et al., 2003; Fleischhauer et al., 2005; Schmidt-Thomé, 2006a; Schmidt-Thomé, 2006b) used the Delphi method to decide weights for each hazard. Delphi analysis draws on collective wisdom and absorbs useful ideas, which is assumed to make the result more accurate, but the process is relatively complicated and protracted, which makes it difficult to apply widely. Furthermore, results obtained by Delphi analysis may vary according to experience of participants involved (i.e. familiarity bias), and are sensitive to any events that occur during the deliberative process (availability bias).

Category 2: In this approach, each hazard risk index is first assessed individually for a given area. Weights are then assigned to each individual hazard risk and summation is used to derive the multi-hazard risk index (Wood et al., 2003; JRC, 2004; Bell and Glade, 2004; Dilley et al., 2005; Arnold et al., 2006; Sales et al., 2007; Wang et al., 2008; Wipulanusat et al., 2009; Mosquera-Machado and Dilley, 2009; Lung et al., 2013; Gruber and Mergili, 2013). This approach is expressed as:

$$R = \sum_{i=1}^{n} f\,(H_i, V_i, E_i) \qquad (2\text{-}6)$$

Where, R is Multi-hazard risk,
H_i is Hazard,
V_i is Vulnerability, and
E_i is Exposure.

Table 2.5 Multi-hazard risk assessment for synthetic indicator Category 2

Country (or Institution)	Study area	Hazards	Remarks
German (Bell and Glade, 2004)	Bíldudalur (NW-Iceland)	Snow avalanche, debris flow, rock fall.	Multi-hazard risk map was created by overlaying single hazard risk maps with equal weight.
United Nations Development Programme (UNDP, 2004)	Global	Earthquake, tropical cyclone, flood, drought.	Multi-hazard risk index was calculated by aggregating single-hazard risk index.
Europe (Joint Research Centre) (Lavalle et al., 2005)	Europe	Flood, forest fire, drought, heat wave.	Multi-hazard risk index was calculated by aggregating single-hazard risk index.
World Bank (Dilley et al., 2005)	Global	Earthquake, cyclone, flood, landslide, drought, volcanic hazards.	Multi-hazard risk index was calculated as the sum of single-hazard risk index.
Thailand (Wipulanusat et al., 2009)	Pak Phanang basin (Thailand)	Drought, flood.	Multi-hazard risk map was created by overlaying single hazard risk map.
China (Shi, 2011)	China	Earthquake, typhoon, flood, drought, landslide and debris flow, sandstorm, snow, hail, storm surge, frost, forest fire, grassland fire.	The frequency of occurrence for each hazard was used to decide the weight.

Applications in this category calculate multi-hazard risk by aggregating single hazard risk using ArcGIS or other GIS software. Examples include the Joint Research Centre (JRC)-Multi-risk Approach (Wood et al., 2003; JRC, 2004; Sales et al., 2007), a Multi-Hazard Analysis in the village of Bíldudalur, Iceland (Bell and Glade, 2004), the World Bank's methodology for Natural Disaster Hotspot analysis (Dilley et al., 2005; Arnold et al., 2006), the Délégation aux Risques Majeurs (DDRM) multi-risk approach (Fleischhauer, 2005), and a MHRA using GIS and remote sensing in the Pak Phanang Basin, Thailand (Wipulanusat et al., 2009). These methods suffer the same drawback of the Category 1 methods, in that the multi-hazard risk index is calculated by aggregating all single hazard risks with equal weight, which does not adequately reflect the various impacts of different hazards present in the same area.

Most methods in both aggregation approaches (equations 2-5 and 2-6) suffer the drawback that the multi-hazard risk index is calculated by aggregating all single hazard risks with equal weight, which does not adequately reflect the varied impacts of different hazards present in the same area. Whilst both aggregation methods have advanced MHRA and can be used to better compare the relative degree of danger between different areas, these applications utilise hazard, vulnerability and exposure to assess the final multi-hazard risk without a consideration of probabilities and exceedance probabilities, and thus these approaches cannot reflect the real risk in the study areas. Thus the risk index is useful in a relative sense, but is less helpful in an absolute sense for determining total losses.

2.6.2 Integrated losses

To overcome the problem with the synthetic indicator approach, where losses were estimated in a relative but not absolute sense, an alternative approach was developed. The integrated losses from the multiple hazards approach mainly uses mathematical statistics to estimate absolute losses from multiple natural hazards. The mathematical statistics approach is based upon the analysis of observed natural disasters with risk a product of the probability of occurrence of a hazardous event and the consequences of such an event for exposures (the intensity of impact resulting from realization of the hazard). Risk is most commonly expressed as in equation 2-2 (Section 2.2) and calculated based on the conceptual model in equation 2-4 (Section 2.5). The equation is the basic model for the mathematical statistics method and its associated loss curve is shown in Figure 2.1. X-axis is the loss (damage) associated with the disaster, and y-axis is the exceedance probability for the corresponding loss (probability of loss being greater than or equal to a given value). Through application of this approach, an exceedance probability-loss curve can be built, which shows the likelihood of losses of different magnitudes, and which is used to estimate and evaluate risk of future disasters. Both parametric and nonparametric methods are used to estimate the required probabilities. Some applications have been listed in Table 2.6.

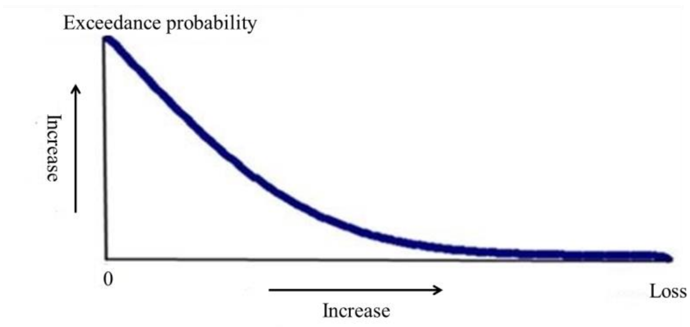

Figure 2.1 Exceedance probability-loss curve

Table 2.6 Multi-hazard risk assessment for integrated losses

Country (or Institution)	Study area	Hazards	Remarks
The United States (FEMA, 2004)	The United States	Flood, hurricane, earthquake.	Parametric method and historical information were used to produce loss estimates.
German (Grünthal et al., 2006)	Cologne (Germany)	Storm, flood, earthquake.	Parametric method.
The Netherlands (Van Westen, 2008)	Tegucigalpa (Honduras)	Landslide, flood, earthquake, technological hazards.	Historical information and parametric method were used to estimate annual loss.
New Zealand (Schmidt et al., 2011)	Hawke's Bay (New Zealand)	Earthquake, storm, flood.	Synthetic loss curves were developed by a combination of nonparametric and parametric methods.
Central American Probabilistic Risk Assessment Program (Linares-Rivas, 2012)	Latin America and the Caribbean Region	Earthquake, hurricane, volcanic hazards, flood, tsunami, landslide.	Historical information and parametric method were used to estimate annual loss for several return periods.
China (Liu et al., 2013)	Yangtze River Delta (China)	Flood, typhoon.	Nonparametric method was used to calculate possible loss in different multi-hazard return periods.

The mathematical theory in the parametric method assumes that disaster losses follow a known distribution function (curve). Historical loss data sets are often used to estimate the distribution function parameters that are then used to calculate the probability distribution. This methodology has been widely used in risk assessment. For instance, Grünthal et al. (2006) calculated exceedance probability-mean wind speed curves for windstorm risk assessment using Schmidt and Gumbel distributions (Gumbel, 1958). Stedinger et al. (1992) estimated parameters by the method of moments for Gumbel type, Pearson type III, Weibull and lognormal curves, and Grünthal et al. (2006) used these distributions to build exceedance probability-discharge curves for flood risk assessment.

There is sometimes a lack of historical observations needed to properly estimate the losses, so it can be difficult to develop a probability distribution function that reflects the real situation for parameter estimation. In these circumstances, a nonparametric method is used, which may employ histogram density estimation, kernel density estimation or information diffusion to derive probability estimates. Histogram density estimation first draws a histogram and curve according to varying degree of disaster, then based on the curve type, adopts a moving average (using exponential smoothing or other methods) to analyse historical loss data. A mathematical statistics model can then be built to reflect the functional relationship between disaster degree and frequency. However, the results obtained with this method are crude and are greatly influenced by the interval choice. In order to overcome the disadvantages of histogram density estimation, Rosenblatt (1956) and Parzen (1962) proposed the use of kernel density estimation. Kernel density estimates are closely related to histograms, but can be endowed with properties such as smoothness or continuity by using a suitable kernel. However, the key problem of how to choose an appropriate smoothing parameter still remains. The information diffusion method was introduced by Huang (1997) to overcome this problem, and improve the accuracy of natural disaster risk assessment. The information diffusion method can use sample data to assess natural disaster risk, and Huang (2000) showed it to be about 28% more efficient than histogram density estimation.

The mathematical statistics method expresses risk as probabilistic loss, and is useful in estimating and evaluating losses from potential future disaster. It gives more consideration to the probability of occurrence but relative to the risk index approach, exposure and vulnerability are neglected. Besides, it also neglects the interaction between different hazards.

2.6.3 Comprehensive multi-hazard risk assessment

Evidently, the integrated losses approach, itself developed to address deficiencies in the synthetic indicators approach, is not without its drawbacks, and this resulted in further development work to produce a more comprehensive MHRA process. Compared to the first two phases, there is however relatively little research that attempts this more comprehensive approach. Comprehensive multi-hazard risk assessment tries to assess the possible loss with a consideration being the interaction between different hazards in MHRA process (Marzocchi et al., 2012; Selva, 2013; Mignan et al., 2014). However, the research that does exist mainly focuses on the domino (cascade, triggering) effect in practical application, whereby one hazardous event triggers another (e.g. landslide induced by earthquake, flood induced by storm) (Marzocchi et al., 2012; Frolova et al., 2012).

There is no universally accepted method in this scope, but hazard matrix and event tree are the commonly used methods. Kappes et al. (2010) proposed a matrix to identify the possible triggering effect within seven hazards in an alpine region. Gill and Malamud (2014) analysed 21 hazards and built a hazard matrix which focuses on hazard interactions where one hazard triggers another or increases the probability of others occurring. Marzocchi et al. (2009, 2012) employed event tree to analyse multi-hazard risk due to triggering effects in Italy. For each hazard, the triggering events were identified by qualitative analysis according to a database of hazards. Then, a set of scenarios were defined by identifying the possible chain of triggering events. The event tree was used in this step to simulate the possible chain of events. The related triggering events were arranged in the tree structure as branches, and probabilities of single branches were quantified. Frolova et al. (2012) identified technological accidents (fires, explosions, release of chemical materials) triggered by earthquakes according to the distribution of shaking intensity in Russia. The MATRIX (New Multi-HAzard and MulTi-RIsK Assessment MethodS for Europe) project (Garcia-Aristizabal and Marzocchi, 2013) adopted event-tree and fault-tree strategies to identify the domino effects scenarios in Naples (volcanic earthquakes and seismic swarms triggered by volcanic activity), Guadeloupe (rainfall-and earthquake-triggered landslides), and Cologne (earthquake-triggered embankment/flood defence dyke failures). Eshrati et al. (2015) also proposed elaboration of event tree is the useful method to analyse the potential consequences of domino effects in more detail by simulating the possible chain of triggering events.

Research on synthetic indicator is effective in comparing the relative danger experienced by different areas, but it has no representation of the real risk situation in those areas (i.e. in terms of assessing losses it is useful in a relative but not absolute sense). In order to solve this problem, research moved from synthetic indicator evaluation to assessing integrated losses caused by multiple nature hazards in a given region and time period. However, this research neglected the interaction between different hazards. Hence, in the most recent phase, more comprehensive MHRA research is proposed to assess the possible loss caused by multiple hazards in a given time with a consideration of the domino effect. These studies typify a rather small body of work on comprehensive MHRA. In practice, the interaction between different natural hazards is complex and ever-changing, and simply addressing the domino effect is not enough to cover all situations, as two hazards can occur independently without evident common cause, yet in close proximity, spatially, temporally, or both (the specific time frame should be defined in each specific case). Thus, a significant intellectual gap in the current MHRA research needs to be filled.

2.7 Basic components for multi-hazard risk assessment

MHRA aims for a more comprehensive view of the total effects or impacts by assessing and mapping expected loss due to the occurrence of various natural hazards on the social, environmental and economic settings in a given area. The basic components of MHRA include hazard identification, hazard analysis, hazard interaction analysis, exposure analysis and vulnerability analysis (Marzocchi et al., 2009; Komendantova et al., 2014). These elements are discussed further below, after which conclusions are drawn on the research gaps in MHRA.

2.7.1 Hazard identification

Hazard identification is used to identify which kinds of natural hazards influence a given area and summarise the spatial distribution of these hazards (Bell and Glade, 2004; Schmidt et al., 2011). Spatial distribution decides which pattern of hazard-response is needed in a given area. Below, some commonly used methods for hazard identification are discussed. These methods are used in assessment of risk from both single- and multiple-hazards.

2.7.1.1 Historical data analysis

Historical data is past-periods data, collected from historical texts, newspaper reports, diaries, and maps. Historical data describes the past, but planning involves the future. Therefore, historical data analysis is an approach of analysing what happened in the past to discover patterns or relations which are useful in projecting the future value of significant variables.

Many studies make use of this approach to analyse the spatial distribution of hazards (Munich Re, 2003; UNDP, 2004). Spatial distribution of natural hazards can be summarised by analysing the influence situation of each hazard in the past. However, this approach relies on extensive historical data (at least 20 years), which is hard to obtain for some areas. Additionally, because the occurrence of hazard is a random event, historical data may not contain all the possible hazard situations, especially as some hazards have a long return period (e.g. volcanic eruption).

2.7.1.2 Social survey

In the absence of historical data, social survey can be used to collect the relevant data. Systematic social survey is used to collect data from people living in a specific geographic, cultural, or administrative area. The social survey is one of the best known and most widely used investigative approaches in the social sciences, most commonly manifest as a questionnaire or interview. Researchers use this approach to collect information on the hazard situation during past years from local residents, then summarise the spatial distribution of these hazards. Survey generally only applies on a local scale because the social survey is resource intensive in terms of time and human resources. Furthermore, it generally relies upon respondents living in the surveyed area for 20 years or more, with an even spatial distribution in the study area (Ge et al., 2008). In addition, the data collected by social survey also face the same problem as historical data. The data may not contain all the possible hazard situations, especially as some hazards have a long return period.

Therefore, the significant gap in hazard identification is that the data collected may not reflect all the possible hazard situations due to some hazards having long return periods. This problem is exacerbated in the case of MHRA which must address multiple and interacting hazards (see below) where return periods of hazard interactions may be longer than single hazards.

2.7.2 Hazard analysis

Hazard analysis, that is magnitude-frequency analysis, analyses the probability of hazard occurrence of different magnitudes in a given area (Petak and Atkisson, 1982; UNDRO, 1991). As mentioned in section 2.1.2.2, there is a strong nonlinear relationship between magnitude and frequency. According to the magnitude-frequency rule, there will be many small events and few large ones over a sufficient interval of time (Wolman and Miller, 1960). Hence, the average return period of small-magnitude hazards is short and that of big-magnitude hazards is long (Alexander, 1993). The mathematical statistics method is the commonly used method (Section 2.6.2) with both parametric and nonparametric methods used to estimate the required hazard occurrence probabilities. The existing research on hazard analysis mainly relies on the historical disaster data (FEMA, 2004; Grünthal et al., 2006). However, many disaster databases tend to record loss data rather than the magnitude data, e.g. EM-DAT (2015). Hence, the lacking of hazard magnitude data is the main gap in hazard analysis.

2.7.3 Hazard interaction analysis

The existing research on hazard interaction in MHRA mainly focuses on the domino effect, introduced in Section 2.6.3, with hazard matrix and event tree the commonly used methods (Marzocchi et al., 2012; Gill and Malamud, 2014; Eshrati et al., 2015). They analyse hazard interaction beginning with given information about the primary hazard, which triggers another or increases the probability of others occurring. However, the interaction between different natural hazards is complex and dynamic, and the domino effect is not enough to cover all situations. For example, two hazards may occur independently without evident common cause, but in close proximity, spatially, temporally, or both. Hence the relationships between different natural hazards need a systematic classification to facilitate improved MHRA.

2.7.4 Exposure analysis

Exposure analysis is used to analyse the spatial distribution of people, infrastructure or other valued assets at risk. There are three methods to exposure analysis in a risk area: official statistics analysis (Dilley et al., 2005; Schmidt-Thomé, 2006a), on-site survey (Khatsu and Van Westen, 2005) and remote sensing image analysis (Wang et al., 2008). Any combinations of these methods can be applied in exposure analysis to meet the data requirements. Official statistical data can be obtained easily, but data collection units are mainly based on government administrative division which may not map well to hazard zones. On-site survey can produce more detailed and targeted data, but it generally applies only on a local scale as it is time and resource intensive to collect. Remote sensing image provides wide area coverage, but that raster format (i.e. an image) means that the information conveyed is more limited in scope.

2.7.5 Vulnerability analysis

Vulnerability assessment is used to measure the possible loss for a given exposure, under conditions caused by hazard of varying degree, and to reflect how these conditions (including physical, social, economic and environmental indicators) influence the possible loss (Cutter, 1996; Villagran, 2006). The assessment methods fall into two types based on the development of either a vulnerability index or vulnerability curve (fragility curve).

2.7.5.1 Vulnerability index

The vulnerability index method is mainly used in synthetic indicators analysis. Various factors from physical, social, economic and environmental are selected as indicators to assess vulnerability index. Munich Re (2003) calculated a vulnerability index from: standard of preparedness/safeguards, building class vulnerability (including residential construction vulnerability and commercial construction vulnerability) and general vulnerability (building density and quality of construction). Schmidt-Thomé (2006a) built a vulnerability index from three aspects: economic, societal and ecological, using indicators of national and regional Gross Domestic Product (GDP), population density, and fragmented natural areas respectively.

A vulnerability index can be obtained by aggregating these indicators using an appropriate weight, which recognizes that indictors may each make a different contribution to vulnerability. Deriving an appropriate weight for each indicator is the key problem in this method. Weight derivation methods used include the weighted summation method (Moss et al., 2001), Principal Component Analysis (PCA) (Cutter et al., 2000), the Analytic Hierarchy Method (AHP) (Thirumalaivasan et al., 2003) and the fuzzy comprehensive evaluation method (Dixon, 2005).

This method can reflect how physical, social, economic and environmental factors influence vulnerability, but cannot measure the relationship between loss and hazard with different degree.

2.7.5.2 Vulnerability curve

The vulnerability curve is mainly used in integrated loss assessment. It is always expressed by a curve or table, used to measure the relationship between loss ratio and hazard of different degree. The core content of this method is to build a damage model (Penning-Rowsell and Chatterton, 1977; Suleman et al., 1988):

$$D = f(h) \tag{2-7}$$

Where, *D* means damage rate,

h represents hazard in different degree, and

f is the function to calculate the damage degree to hazard with different degree.

The function is mainly deduced from historic disaster data or valuation surveys. With historic disaster data, the one-to-one relationship between hazard magnitude and loss ratio is built according to the historical disaster situation, then curve fitting, neural network or other mathematical methods are used to build the vulnerability curve (Hohl et al., 2002; Dutta et al., 2003). With valuation surveys, the value of different exposures are estimated based on land cover, land use, exposure type, and other information, and then surveys or questionnaire are used to find the one-to-one relationship between hazard magnitude and loss ratio. A vulnerability curve can then be built (Penning-Rowsell and Chatterton, 1977; Smith, 1994).

In contrast to the vulnerability index, the curve method can measure the relationship between loss and hazard in different degree, but cannot reflect how physical, social, economic and environmental factors influence vulnerability.

2.8 Summary and conclusion on research gaps

This chapter has provided a review of literature addressing the key concepts, theories and practice relevant to advancing research in MHRA.

Section 2.1 discussed the definition of natural disaster and its formation mechanism. Natural disaster was defined as: under a specific environment, natural hazard's interaction with vulnerability of exposures can result in serious damage to exposures of the affected area, with consequent loss of human life, material wealth, economic activity and ecological value. The hazard-forming environment, hazard, exposure and vulnerability are the main components of a natural disaster.

Section 2.2 discussed the definition of risk from natural disasters. Risk is commonly characterized in one of two distinct categories. The first type defines risk as the probability of loss caused by the interactions between the vulnerability of exposure and the hazard. The second type describes risk as a product of the probability of occurrence of a hazardous event and the consequences of such an event for exposures.

Section 2.3 introduced MHRA. The aim of MHRA is to have a holistic or comprehensive view of the total effects or impacts by assessing and mapping the expected loss due to the occurrence of various multiple natural hazards on the social, environmental and economic settings in a given area.

Section 2.4 then reviewed the basic theory of MHRA. The natural hazard perspective, the hazard-forming environment perspective and the exposure perspective emphasize the dominant factors but ignore other relevant factors. The regional disaster system perspective, postulates that disaster is produced by hazard, exposure, and hazard-forming environment together, is thus seen as a more suitable theory for MHRA.

Section 2.5 provided two conceptual model of MHRA. One addresses the interaction of hazard and exposure, the other emphasizes the possible consequences.

Section 2.6 then reviewed and discussed the research scope of MHRA. The synthetic indicator of multiple hazards affecting a given area mainly uses the risk index method, with results obtained used to compare the relative danger between different areas, but with no reflection of the real risk situation in these areas. Integrated losses mainly rely on the mathematical statistic method to calculate possible losses caused by multiple nature hazards in a given region and time period. However, these MHRA research studies ignore the interaction between different hazards. The existing comprehensive MHRA research considers domino effects in loss assessment, but the domino effect is not enough to cover all hazard interaction situations.

Section 2.7 discussed the basic components of MHRA which comprise hazard identification, hazard analysis, hazard interaction analysis, exposure analysis and vulnerability analysis. For hazard identification, historical data analysis and social survey are commonly used methods. Parametric and nonparametric methods are frequently used to estimate the required probabilities in hazard analysis. Hazard interaction analysis mainly relies on hazard matrix or event tree methods. There are three methods to evaluate exposure in risk area: official statistics analysis, on-site survey and remote sensing image analysis. The methods for vulnerability assessment can be summarised into two types: vulnerability index and vulnerability curve.

On the basis of the literature review, the main research gap identified with respect to MHRA is that the existing MHRA methods cannot consider all hazard interactions when calculating possible losses. MHRA needs to assess the possible loss due to the occurrence of various natural hazards on the social, environmental and economic settings in a given area. Furthermore it should take into account the characteristics of each hazardous event, and their mutual interactions and interrelations, but existing research focuses only on domino effects. However, the interaction between different natural hazards is complex and dynamic, and simply addressing the domino effect is not enough to cover all situations. Besides, there are also some gaps in the conceptual model and basic components for MHRA.

The regional disaster system perspective is more suitable for MHRA, and two conceptual models of MHRA have been developed based on this perspective. However, these two conceptual models cannot express the whole regional disaster system perspective. Hazard identification and hazard analysis both face the data problem. The data collected for hazard identification may not reflect all the possible hazard situations, particularly for some hazards that have a long return period. Additionally, many disaster databases do not provide the magnitude data which is necessary for hazard analysis. In the hazard interaction analysis, the relationships between different natural hazards are complex, and a systematic classification is needed to ensure that sufficient possible hazard interactions are addressed. In vulnerability analysis, a method is also needed to calculate the loss ratio induced by multi-hazard with different degree, and to reflect how physical, social, economic and environmental factors influence vulnerability. The research that follows aims to address these gaps and develop a more complete MHRA model. The research design and approaches used are discussed in the next chapter.

Chapter 3

Research design and methodology

The research gaps of the MHRA were introduced in Chapter 2. The focus of Chapter 3 is to explain how these identified gaps are filled in this study. The basic theory and conceptual model used in this research are first presented. Then, the basic modules for the proposed MHRA model (MmhRisk-HI) and the methods used for each module are introduced. After explaining the choice of study area and data needed, the methods used for model validation are introduced.

3.1 Basic theory and conceptual model

As discussed in Chapter 2, the natural hazard perspective, the hazard-forming environment perspective and the exposure perspective emphasize a single attribute of natural disaster. The regional disaster system perspective, postulates that disaster is produced by hazard, exposure, and hazard-forming environment acting together (Shi, 1996; Wisner et al., 2004), and so is a more complete perspective and more suitable as basic theory for MHRA.

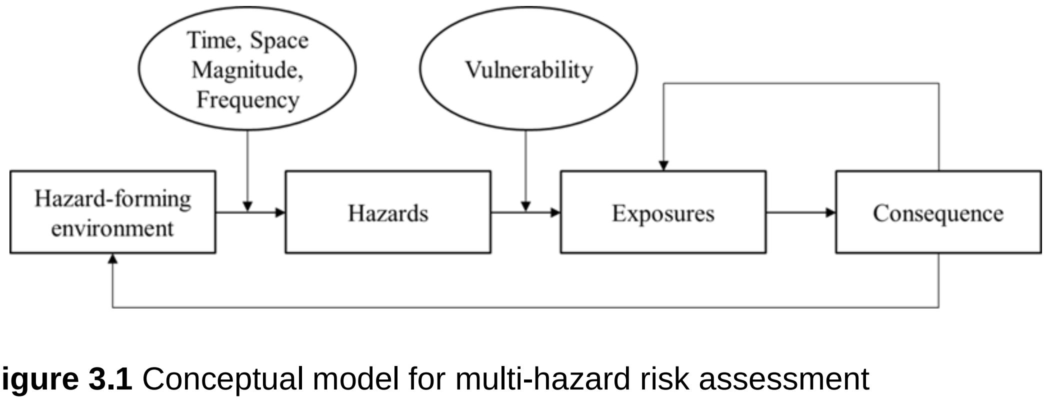

Figure 3.1 Conceptual model for multi-hazard risk assessment

Based on the regional disaster system perspective, the conceptual model for MHRA can be developed as shown in Figure 3.1. Some hazards can occur in close proximity, spatially, temporally, or both in a specific hazard-forming environment. The time, space, magnitude and frequency of these hazards are determined by the hazard-forming environment. The hazards' interaction with vulnerability of exposures results in serious consequence. The induced consequence influences the hazard-forming environment. The influenced hazard-forming environment has a chance to produce new hazards. In addition, the induced consequence also influences the distribution of exposures. The consequence includes widespread losses of human life, material wealth, economic activity and ecological value. These losses mean some exposures are partially or totally destroyed, thus the quantity of these exposures could be changed. Besides, in the recovery stage, local residents tend to redistribute the exposures according to the loss situation in consequence, thus the location of some exposures also could be changed.

Two basic multi-hazard risk expressions were introduced in Chapter 2.

$$\text{Risk} = \sum_{i=1}^{n} (\text{Hazard} \times \text{Vulnerability} \times \text{Exposure}) \tag{3-1}$$

$$\text{Risk} = \prod_{i=1}^{n} \text{Probability} \times \text{Consequence} \tag{3-2}$$

Where, $i = (1,2\ldots n)$ represents i types of hazards.

These two expressions cannot express the whole regional disaster system perspective. According to the regional disaster system perspective, MHRA should calculate the possible loss considering the stability of the hazard-forming environment, and the probability of the hazard occurrence and the vulnerability of exposure. Therefore, this research considers these two categories of expressions together.

3.2 Multi-hazard risk assessment model

MHRA seeks a holistic view of the total effects or impacts by assessing and mapping the expected loss due to the occurrence of various natural hazards on the social, environmental and economic settings in a given area. This research explores and constructs a new MHRA model (MmhRisk-HI) to calculate the possible loss caused by multiple hazards, with an explicit consideration of interaction between different hazards. This model takes advantage of the merits of both the risk index method and the mathematical statistics method. This can be achieved by analysing risk considering the disaster formation mechanism, and calculating possible loss and corresponding probability of loss under different natural hazard scenarios. Hazard identification, hazard analysis, hazard interaction analysis, exposure analysis and vulnerability analysis are the component modules. The approaches used for each module are introduced in detail below.

3.2.1 Hazard-forming environment analysis

Chapter 2 described how each natural hazard arises from a specific hazard-forming environment. The geophysical environmental factors in the hazard-forming environment were categorized into two types. The first are relative stable factors which construct the precondition for the occurrence of natural hazards, whilst the second are trigger factors, which determine the frequency and magnitude of hazards. Different combinations of geophysical environmental factors can induce different hazards. Hence, hazard-forming environment analysis is useful in hazard identification, hazard analysis and hazard interaction analysis. The hazard-forming environments for some major hazards are next discussed.

3.2.1.1 Hazard-forming environment and natural hazards

For illustrative purpose, this section discusses the relationship between some specific major hazards and their hazard-forming environments.

Earthquake

An earthquake is one of the most destructive of natural hazards. An earthquake is a sudden and violent shaking of the ground caused by the sudden breaking and movement of tectonic plates of the earth's crust (Alexander, 1993). Earthquakes are caused mostly by tectonic movement in the earth’s crust, thus the distribution of earthquake tends to follow crustal plate boundaries (Nishenko and Buland, 1987; Pacheco et al., 1993). Hence, the plate boundary can be used as the precondition (stable factor) to earthquake, and the movement of the earth’s crust is treated as the trigger factor. The movement of the earth’s crust is hard to observe, thus seismic moment is generally used in practical application (Aki and Richards, 2002).

Tropical Cyclone

Tropical cyclone is the generic name for storms with swirling atmospheric disturbance occurring in tropical or subtropical maritime regions (McGuire et al., 2002). Cyclones are called by other names in different parts of the world, with common terms including "Hurricane" in the Caribbean and the Atlantic Ocean, "Tropical storm" in the Indo-Pacific region, and "Typhoon" in the north-west Pacific (IFRC, 2013). The formation of tropical cyclones is a topic of extensive ongoing research and is not fully understood, but a series of factors are necessary including: 1) Five degrees of latitude away from the Equator; 2) Vast and warm ocean; 3) Water temperature at least 26.5 °C down to a depth of at least 50 m; 4) Low amounts of weak vertical wind shear; 5) A pre-existing system of disturbed weather; 6) High humidity (Gray, 1979; Henderson-Sellers et al., 1998; McGuire et al., 2002). Of these factors, the first two are stable factors as the preconditions and the last four belong to the trigger factors in hazard-forming environment.

In contrast to other hazards, tropical cyclones can move thousands of kilometres (Smith, 2013), hence, in an inland area, the distance to the origins of tropical cyclone can be used as the precondition (stable factor) for tropical cyclone identification. The movement of tropical cyclones is accompanied by strong winds and heavy rain, and a series of hazards (e.g. strong winds, floods) induced by the changes of winds and rainfall are the reasons to cause loss in the track (Smith, 2013). Thus, tropical cyclone is viewed as the changes of wind speed and rainfall, and these changes can be used as trigger factors to measure the magnitude of the series of hazards in the track (the types of hazards in the series are decided by the hazard-forming environment in the track).

Flood

As the most common of all natural hazards, flood can be defined as a temporary inundation of land area by water from any source (Alexander, 1993; Kron, 2005; CEC, 2006). There are several classification schemes for floods in the relevant literature (French and Holt, 1989; Perry, 2000; Berz et al., 2001; Bronstert, 2003; Kron, 2005; Jonkman, 2005), e.g. Berz et al. (2001) and Kron (2005) classified floods in three main types: river flood, flash flood and storm surge; Jonkman (2005) divided floods into six types: coastal floods, flash floods, river floods, drainage problems, tsunamis and tidal waves. Nevertheless these classification schemes cannot better reflect the difference in hazard-forming environment for different floods. Hence, four types of floods are distinguished in this study: slow kinds riverine flood, fast kinds riverine flood, coastal flood and pluvial flood. The definitions of these four types of floods are introduced below.

Riverine (fluvial) flooding[1] is where water overtops the banks of a river to take it outside its regular boundaries (Jonkman, 2005). The dynamics of riverine flooding vary with terrain. Slow kinds riverine flood occurs in relatively

[1] In this thesis, floods which originate from lakes and reservoirs are grouped into riverine flooding.

flat areas, land may stay covered with shallow, slow-moving floodwater for days or even weeks (Kron, 2005). Fast kinds riverine flood occurs in hilly and mountainous areas, it is characterized by a rapid rise in water, high velocities that occur in an existing river channel over a short period (Alexander, 1993). Besides, an important feature of riverine flood is that the ground becomes fully saturated, thus the soil's capacity to store water is exceeded, and consequently increase overland flow and runoff to rivers (Kron, 2005). Hence, the preconditions (stable factors) to slow kinds riverine flood can be summarised as: 1) flat and low-lying terrain; 2) river basins; 3) land surface with poor water infiltration capacity, and the preconditions to fast kinds riverine flood are: 1) hilly or mountainous terrain; 2) river basins; 3) land surface with poor water infiltration capacity. Surplus water beyond the capacity of a river is the only reason for riverine flood. Hence, the trigger factors to these two kinds of river flood are basically same. Several trigger factors can cause a river flood, of which the most common is heavy rainfall, other factors include melting of snow and ice and high tides (Barredo, 2007).

Coastal flood occurs when a normally dry coastal area is inundated by sea water (McGuire et al., 2002). Hence, coastal floods occur mainly in low-lying coasts. The preconditions (stable factors) to coastal flood include: 1) flat and low-lying terrain; 2) coastal area; 3) land surface with poor water infiltration capacity. Coastal flood can be induced by several trigger factors including storm surges induced by tropical cyclones, tidal waves and tsunamis (McGuire et al., 2002; Barredo, 2007).

Pluvial flood (ponding) is the phenomenon where surface water accumulates as input exceeds runoff rate, and is common in low-lying areas with poor water absorption ability (Falconer et al., 2009; Zhou et al., 2012). The preconditions (stable factors) to pluvial flood are mainly: 1) flat and low-lying terrain; 2) land surface with poor water infiltration capacity. The most common trigger factor for pluvial flood is heavy rainfall (Maksimović et al., 2009).

Landslide

Landslide is the most common hazard in many mountainous and hilly areas. It can be defined as a geological phenomenon which includes a wide range of ground movements with rock and soil over a sloping surface (Varnes, 1958). Landslides mainly happen in hilly areas with land surface with poor water absorption ability (Varnes, 1984; Guzzetti et al., 1999). The preconditions (stable factors) to landslide are: 1) hilly or mountainous terrain; 2) slope material with poor water absorption capacity. Landslides occur when the stability of the slope changes from a stable to an unstable condition. Trigger factors which can change the stability of the slope mainly include: 1) heavy rainfall which increases the pressure of material on the slope; and 2) earthquake which reduces the resisting (shear) forces of the slope (Varnes, 1984; Kuriakose et al., 2009).

Drought

Drought is markedly different to tropical cyclone, flood and the other natural hazards described above as it develops slowly and has a prolonged existence, and may persist for several years (Alexander, 1993; Smith, 2000). Drought can be simply defined as a condition of abnormal weather resulting in a shortage of water (Dracup et al., 1980; Wilhite and Glantz, 1985; McKee et al., 1993). It is common to divide drought in three main types: meteorological drought (a prolonged period with less than average precipitation), agricultural drought (droughts that affect crop production) and hydrological drought (water reserves such as aquifers, lakes and reservoirs fall below the statistical average) (Hisdal and Tallaksen, 2000; Smith and Petley, 2009). Drought results in a shortage of water, and meteorological drought usually precedes the other kinds of drought (Hisdal and Tallaksen, 2000).

Lack of rainfall within a given period is taken as the direct physical processes leading to drought (Smith and Petley, 2009), hence, lack of rainfall can be treated as the main trigger factor. Drought can easily occur in areas with low annual average precipitation and high annual average temperature (Alexander, 1993). Water reserves such as aquifers, lakes and reservoirs, can help to reduce the susceptibility to drought. Therefore, the preconditions (stable factors) to drought are: 1) low annual average precipitation; 2) high annual average temperature; 3) low drainage density; 4) land surface with poor water absorption capacity.

3.2.1.2 Stable factors for hazard identification

Hazard identification is used to identify which kinds of natural hazards influence a given area, and address the spatial distribution of these hazards (Bell and Glade, 2004; Schmidt et al., 2011). The stable factors as precondition for major natural hazards were summarised in the previous section. According to the characteristic of these environmental factors, the spatial distribution of natural hazards in a region can be deduced (The Yangtze River Delta as an example is shown in Sections 3.3.2 and 5.1.1).

The relationship between stable factors and major natural hazards can be expressed as:

$$S(H_k)=f(SF_1,SF_2,\dots SF_j)\quad (j=1,2\dots n) \tag{3-3}$$

Where, for any given area, $S(H_k)$ is susceptibility to Hazard k, given stable factors SF_j.

Stable factors analysis identifies hazard from environmental factors rather than historical data, thus can consider all possible hazard situations even if some hazards have long return periods, e.g. a city located on a crustal plate boundary means an earthquake could influence this city, even if there was no earthquake over an observed period of decades or more.

3.2.1.3 Trigger factors for hazard analysis

Hazard analysis is used to analyse the probability of hazard occurrence of different magnitudes in a given area (Petak and Atkisson, 1982; UNDRO, 1991). The trigger factors for major natural hazards are summarised in section 3.2.1.1. Substantial changes in trigger factors are the main reason that hazards are induced, thus trigger factors can be used to estimate both the frequency and magnitude of hazards. The change degree in trigger factors represents the magnitude of hazards, and the probability of change in trigger factors represents the probability of hazards. The relationship between trigger factors and natural hazards can be expressed as:

$$f(p_{ti})=p(h_j) \tag{3-4}$$

One trigger factor induces one hazard.

$$f(p_{ti})=p(h_1,h_2\dots h_j) \tag{3-5}$$

One trigger factor induces multiple hazards.

$$f(p_{t1},p_{t2}\dots\ p_{ti})=p(h_j) \tag{3-6}$$

Multiple trigger factors induce one hazard.

$$f(p_{t1},p_{t2}\ldots\ p_{ti}) = p(h_{1,}h_2\ldots h_j) \tag{3-7}$$

Multiple trigger factors induce multiple hazards.

Where, p_{ti} is the probability of the change in trigger factor *i*, and $p(h_j)$ *is* the probability of hazard *j*.

Compared to the hazard magnitude data, most of the data for trigger factors are easy to collect, e.g. daily precipitation, daily wind speed. Hence, trigger factors for hazard analysis can effectively be used to solve the data problem in the existing methods.

3.2.2 Multi-dimension information diffusion method

Changes in trigger factors can be used to measure the probability of the occurrence of hazards. This can be achieved using a mathematical statistics approach to define a function to determine event magnitude and frequency. The information diffusion method was developed by Huang (1997) based on the molecular diffusion theory. This method addresses the difficulty of establishing event probabilities from short historical records (or for records of long return period events) and helps improve natural disaster risk assessment, making it more accurate than that achieved with histogram density estimation and kernel density estimation (Huang, 2000). It can be used to assess the probability of occurrence of hazards of different magnitudes.

Taking pluvial flood as an example, and as mentioned in section 3.2.1, daily rainfall can be used as a trigger factor to express the pluvial flood hazard magnitude. T_i $(i=1,2,\cdots m)$ expresses daily rainfall in each historical pluvial flood disaster.

The rainfall universe is selected as:

$$U_t = \{u_{1,} u_2 \cdots u_n\} = \{1, 2 \cdots \mathrm{n\ mm}\} \tag{3-8}$$

Equation (3-9) is then used to diffuse the information carried by each sample point T_i to all the points in the rainfall universe:

$$f_i(u_j) = \frac{1}{h\sqrt{2\pi}} \exp[-\frac{(T_i - u_j)^2}{2h^2}] \quad (i = 1, 2 \cdots m;\ j = 1, 2 \cdots n) \tag{3-9}$$

Huang (1997) deduced equation (3-10) for the calculation of the diffusion coefficient *h.* It is determined by the minimum and maximum values of the samples (*a* and *b*, respectively), and the sample size *m*.

$$h = \begin{cases} 0.8146(b-a), 1 < m \leq 5, \\ 0.5690(b-a), m = 6, \\ 0.4560(b-a), m = 7, \\ 0.3860(b-a), m = 8, \\ 0.3362(b-a), m = 9, \\ 0.2986(b-a), m = 10, \\ 2.6851(b-a)/(m-1), 11 \leq m. \end{cases} \tag{3-10}$$

The information distribution $\mu_i(u_j)$ is derived from normalising equations (3-11) and (3-12), and the result is a continuous probability density function:

$$C_i = \sum_{j=1}^{n} f_i(u_j) \tag{3-11}$$

$$\mu_i(u_j) = \frac{f_i(u_j)}{C_i} \tag{3-12}$$

The probability distribution $p(u_j)$ at u_j can be calculated using equations (3-13) and (3-14). $p(u_j)$ is the probability distribution of 1 to n mm daily rainfall.

$$q(u_j) = \sum_{i=1}^{m} \mu_i(u_j) \tag{3-13}$$

$$p(u_j) = \frac{q(u_j)}{\sum_{j=1}^{n} q(u_j)} \tag{3-14}$$

Finally, exceedance probability on magnitude of pluvial flood hazard $P(u_j)$ is derived as shown in equation (3-15).

$$P(u_j) = \sum_{k=j}^{n} p\left(u_k\right) \tag{3-15}$$

However, this method only can assess one factor, while some hazards are induced by multiple trigger factors. The normal diffusion function (equation 3-9) is same as the normal distribution. Hence, multiple dimension information diffusion can be deduced based on the multivariate normal distribution (equation 3-16).

$$f_X(x_1, x_2, \cdots x_N) = \frac{1}{(2\pi)^{N/2} \left|\boldsymbol{\Sigma}\right|^{1/2}} \exp\{-\frac{1}{2}(x - \mu)^T \Sigma^{-1}(x - \mu)\} \tag{3-16}$$

Where, μ is mean value, and
Σ is symmetric covariance matrix.

Taking two dimensions as example, the basic diffusion function can be expressed as equation[2] (3-17):

$$f_i(u_j, v_k) = \frac{1}{2\pi h_x h_y \sqrt{1-r^2}} \exp\{-\frac{1}{2(1-r^2)}[\frac{(x_i-u_j)^2}{h_x{}^2} - 2r\frac{(x_i-u_j)(y_i-v_k)}{h_x h_y} + \frac{(y_i-v_k)^2}{h_y{}^2}]\} \tag{3-17}$$

Where, $XY=\{(x_1,y_1), (x_2,y_2) \ldots (x_m, y_m)\}$ expresses sample data,
$U=\{u_1,u_2,\ldots u_j,\ldots u_s\}$ is universe for X ,
$V=\{v_1,v_2,\ldots v_k,\ldots v_t\}$ is universe for Y ,
h_x is diffusion coefficient for X,
h_y is diffusion coefficient for Y, and
r is the correlation coefficient between X and Y.

3.2.3 The basic relationships among hazards

The relationships between different natural hazards are complex. However, as mentioned in 2.7.3, the existing research on hazard interaction in MHRA

[2] Huang et al. (2013) also proposed an equation for two dimension information diffusion, but in their equation, the correlation coefficient between two factors is neglected.

mainly focuses on the domino effect in practical application (Marzocchi et al., 2012; Frolova et al., 2012; Eshrati et al., 2015). Therefore, a systematic classification of these relationships is presented below, to facilitate their inclusion in the MHRA model. It is proposed to classify these relationships into four types according to the trigger factors of each hazard.

Independent relationship

Here, the changes in trigger factors which induce hazard A are independent of that which induce hazard B. Hence, the occurrences of these two hazards are independent, e.g. typhoon and earthquake have no relationship with each other.

Mutex relationship

The changes in trigger factors which induce hazard A and which induce hazard B are mutually exclusive. It means hazard A and hazard B cannot occur together, e.g. drought and pluvial flood cannot happen at the same time.

Parallel relationship

The changes in one or some trigger factors have the chance to induce more than one hazard A_1, A_2…A_n at the same time. The relationship of hazards A_1, A_2…A_n is parallel. For example, fast kinds riverine flood and landside induced by heavy rainfall can be taken as a parallel relationship.

Series relationship

Hazard A induces changes in some trigger factors, and then the changes in these trigger factors induce hazard B. Hazard A and hazard B are the series relationship.

Using this classification based on a trigger factors analysis is useful as it helps to ensure all possible relationships among different hazards are considered. It can effectively fill the gap in existing methods which to date only consider domino effects.

3.2.4 Exposure analysis methods selection

As mentioned in section 2.7.4, official statistics analysis, on-site survey and remote sensing image analysis are three commonly used approaches to evaluate the number or value of exposure in a risk area (i.e. the people or valued assets at risk). On-site survey generally applies on a very local scale as it is time and resource intensive to collect, remote sensing image provides data in raster format, whilst official statistical data are based on government administrative division. Hence, the method selected for exposure analysis mainly depends on the scale of the area to be assessed, and the data available for that area. That is, exposure analysis method selection is application specific.

3.2.5 Bayesian network for vulnerability analysis

As mentioned in section 2.7.5, vulnerability index and vulnerability curve are two commonly used methods for vulnerability assessment. A vulnerability curve can reflect the relationship between loss ratio and hazard, but cannot reflect how physical, social, economic and environmental factors influence vulnerability. Conversely, a vulnerability index can reflect how physical, social, economic and environmental factors influence vulnerability, but cannot measure the relationship between loss and hazard by degree. This research therefore uses a Bayesian network (BN) to consider both of these together.

A BN is a probabilistic graphical model that encodes probabilistic interdependencies among a set of random variables (Jensen and Nielsen, 2007). It is a good method for modelling uncertainties and interactions between related factors, and has been applied in risk areas, e.g. earthquake risk management (Bayraktarli et al., 2006); landslide risk assessment (Straub, 2005) and flood risk assessment (Li et al., 2010).

A BN is based on Bayes' theorem, which is a method of inference used to update the probability estimate for a hypothesis according to some evidence. The common form of Bayesian theorem is:

$$P(A|B) = \frac{P(B|A)P(A)}{P(B)} \tag{3-18}$$

Where, $P(A)$ and $P(B)$ are probabilities of A and B, $P(A|B)$ and $P(B|A)$ are the conditional probabilities of A given B and B given A.

Let $X = \{X_1, X_2, \cdots X_n\}$ be random variables, a BN is a directed acyclic graph consisting of these variables as nodes, and the joint probability function of X is given as (Pourret et al., 2008):

$$P(X_1, X_2, \cdots X_n) = \prod_{i=1}^{n} P(X_i | pa(X_i)) \tag{3-19}$$

Where, $pa\ (X_i)$ is the parent set of variables X_i, such that there is an edge from each $pa\ (X_i)$ node to node X_i in the graph.

A simple BN for vulnerability analysis in this thesis is illustrated in Figure 3.2. Trigger factors in the hazard-forming environment are selected as hazard-related indicators to measure the probability of the occurrence of multiple hazards with different magnitudes. Vulnerability-related indicators for exposure are constructed from physical, social, economic and environmental factors (e.g. Cutter, et al., 2003; Villagran, 2006; Schmidt-Thomé, 2006a; SCEMDOAG, 2009). Loss ratio (*L*) is the root node, V_i *is* the ith node of the vulnerability-related indicators and V_{tj} *is* the jth node of the hazard-related indicators. Loss ratio is a parent of vulnerability-related indicators V_i and hazard-related indicators V_{tj}. Then historic loss data for trigger factors with different magnitudes and the corresponding vulnerability-related indicators data can be input into this model to calculate the conditional probabilities of indicators given loss ratio, $P(V_i|L)$ and $P(V_{tj}|L)$. These conditional probabilities are used to calculate the joint probability $P(L, V_i, V_{tj})$, which can be used to assess the future loss ratio with different value of vulnerability-related indicators and trigger factors (more details are introduced in section 4.6).

Thus, a BN is an optimal model to calculate the loss ratio induced by multi-hazards of different degree, whilst also addressing vulnerability using vulnerability indicators from physical, social, economic and environmental domains.

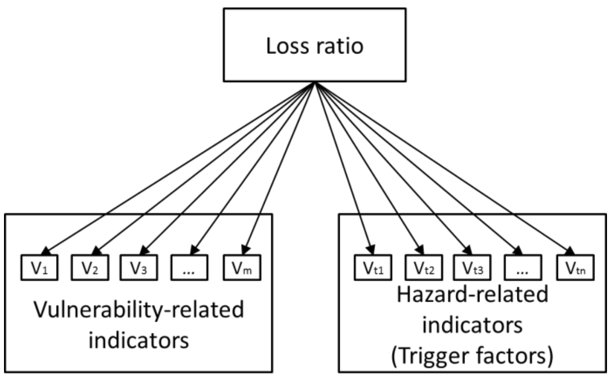

Figure 3.2 A simple Bayesian network framework for vulnerability analysis

Chapter 2 concluded with a discussion of the principal research gaps in MHRA. So far in Chapter 3, I have set out the conceptual structure of an improved MHRA model, and the methods proposed for specific components within the model, which seek to address the identified deficiencies in existing MHRA models. Chapter 4 and Chapter 5 will further demonstrate the model through real world application; however, in advance of that application, the case study area and supporting data are described next.

3.3 Case study area

The Yangtze River Delta (YRD) (Figure 3.3) in China’s central eastern coastal area was selected as the region to trial the improved MHRA model. The YRD covers an area of 110,000 km^2, about 1.1% of China's total land area. This region was chosen for several reasons.

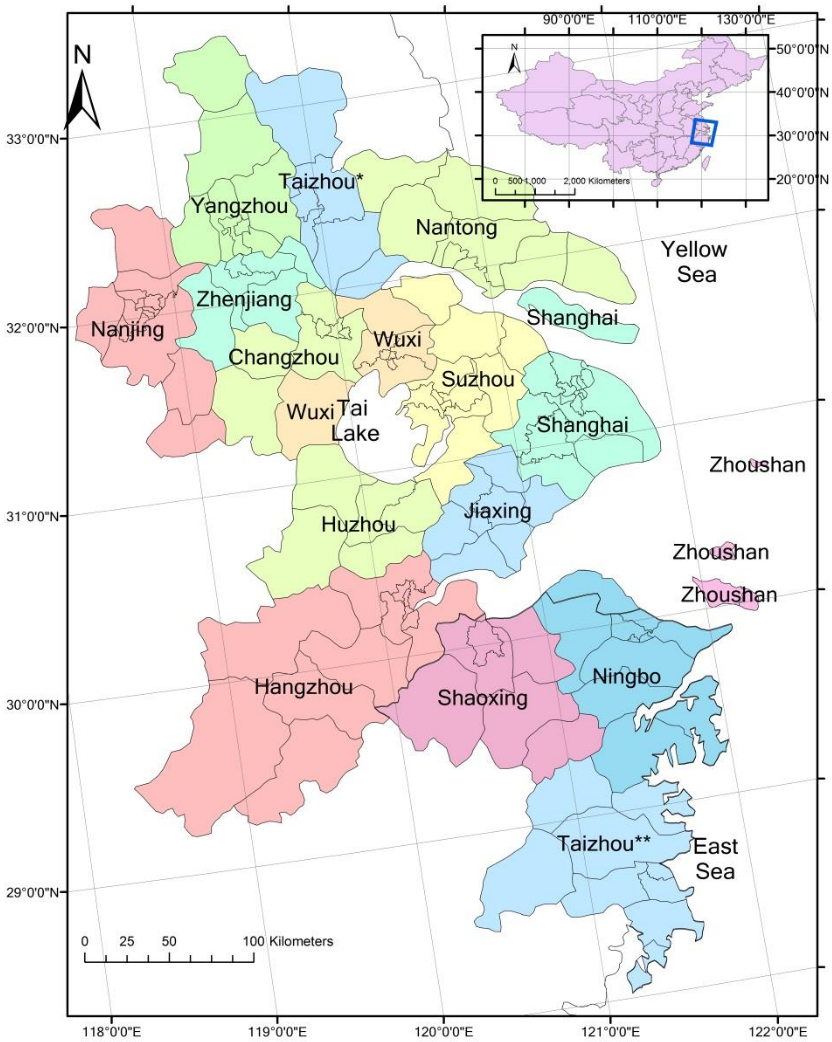

(Note that Taizhou is in Jiangsu Province and Taizhou** is in Zhejiang province.)*

Figure 3.3 The Yangtze River Delta region in China

First, the YRD is highly prone to and is increasingly vulnerable to damage from multiple hazards. According to historical data, in China, 16% of all typhoons that occurred between 1950 and 2012 made landfall in this region, and nearly 30% influenced the region. The region was hit by catastrophic floods in 1991 and 1999, which cause direct economic losses of 11 and 14.1 billion Yuan respectively (Wu and Guan, 1999; Ou and Wu, 2001). Besides, the region is also influenced by drought, earthquake, landslide and other disasters. Secondly, the YRD is one of the country's main economic regions. With both population density and economic activity growing, this already vulnerable region is becoming increasingly dangerous to natural disasters. This growing vulnerability, combined with occurrence of several different natural hazards, makes the area a suitable region in which to research multi-hazard risk appraisal.

3.3.1 Administrative division

As shown in Table 3.1, the YRD comprises the Shanghai municipality and 15 prefecture-level cities in Jiangsu and Zhejiang provinces (hereafter "city"), and comprises 139 county level cities and counties (hereafter "county").

Table 3.1 Administrative division of the Yangtze River Delta Region

Provincial level	Prefectural level	Area (km^2)	County level
Shanghai		6,340	Huangpu, Luwan, Xuhui, Changning, jing'an, Putuo*, Zhabei, Hongkou, Yangpu, Minghang, Baoshan, Jiading, Pudong New, Jinshan, Songjiang, Qingpu, Fengxian, Chongming
Jiangsu	Nanjing	6,596	Xuanwu, Baixia, Qinhuai, Jianye, Gulou, Xiaguan, Pukou, Qixia, Yuhuatai, Jiangning, Liuhe, Lishui, Gaochun
	Suzhou	8,488	Canglang, Pingjiang, Jinchang, Huqiu, Wuzhong, Xiangcheng, Changshu, Zhangjiagang, Kunshan, Wujiang, Taicang
	Wuxi	4,788	Chong'an, Nanchang, Beitang, Xishan, Huishan, Binhu, Jiangyin, Yixing
	Changzhou	4,385	Tianning, Zhonglou, Qishuyan, Xinbei, Wujin, Liyang, Jintan
	Zhenjiang	3,799	Jingkou, Runzhou, Dantu, Danyang, Yangzhong, Jurong
	Nantong	8,544	Chongchuan, Gangzha, Hai'an, Rudong, Qidong, Rugao, Tongzhou, Haimen
	Yangzhou	6,678	Guangling, Hanjiang, Weiyang, Baoying, Yizheng, Gaoyou, Jiangdu
	Taizhou*	5,794	Hailing, Gaogang, Xinghua, Jingjiang, Taixing, Jiangyan
Zhejiang	Hangzhou	16,847	Shangcheng, Xiacheng, Jianggan, Gongshu, Xihu, Binjiang, Xiaoshan, Yuhang, Tonglu, Chun'an, Jiande, Fuyang, Lin'an
	Ningbo	9,816	Haishu, Jiangdong, Jiangbei, Beicang, Zhenhai, Jinzhou, Xiangshan, Ninghai, Yuyao, Cixi, Fenghua
	Jiaxing	3,915	Nanhu, Xiuzhou, Jiashan, Haiyan, Haining, Pinghu, Tongxiang
	Huzhou	5,794	Wuxing, Nanxun, Deqing, Changxing, Anji
	Shaoxing	8,256	Yuecheng, Shaoxing, Xinchang, Zhuji, Shangyu, Shengzhou
	Zhoushan	1,440	Dinghai, Putuo**, Daishan, Shengsi
	Taizhou**	9,413	Jiaojiang, Huangyan, Luqiao, Yuhuan, Sanmen, Tiantai, Xianju, Wenling, Linhai

(*Note that Putuo* is in Shanghai city and Putuo** is in Zhoushan city*.)

3.3.2 Geophysical environment

The YRD, facing the Pacific to the east, is a typical floodplain with low, flat terrain and numerous rivers, lakes and canals. It is highly prone to various natural hazards.

Lithosphere

The YRD is located in the Yangtze platform, which is a relatively stable platform without distribution of volcanic belts (Zhang et al., 2009). Hence, there is no volcano eruption in this region. Strong destroying earthquakes (over 7 magnitude) are unlikely to happen, but earthquakes between 3 to 6 magnitudes influence this area frequently (Xu et al., 2014).

Atmosphere

Being situated in a subtropical high-pressure belt, the YRD has a moist monsoon climate with annual rainfall above 1,000 mm (Figure 3.4). A long wet Plum rain season (a wet season caused by precipitation along a persistent stationary front for nearly two months during the late spring and early summer between eastern China, South Korea, and Japan) is the main reason to induce slow kinds riverine floods and pluvial floods. Rainfall caused by typhoon mainly occurs in August and September, which easily induces various serious floods due to high intensities and short durations. In addition, storms which occur in hilly areas also can induce landslides.

Hydrosphere

As shown in Figure 3.5, this region is downstream of the Yangtze and Qiantang Rivers and their many tributaries, and channel density is more than 0.5 km of river per km^2 (National Atlas Compilation Committee, 1999). The Tai Lake Basin Area, with some 36,000 km^2 of water, is also within the region (Ou and Wu, 2001). These factors make the YRD liable to frequent riverine floods.

Landform

The YRD is coastal and an oceanic landform between Eurasia and the Pacific, so the coastal areas are susceptible to typhoons and coastal floods. As shown in Figures 3.6 and 3.7, in the YRD, the northern areas are plains below an average altitude of 200 metres, whilst the southern areas are hilly and below an average altitude of 1,000 metres. Hence, the northern plain areas are vulnerable to pluvial floods, and southern hilly areas are likely to be influenced by some fast kinds riverine floods and landslides.

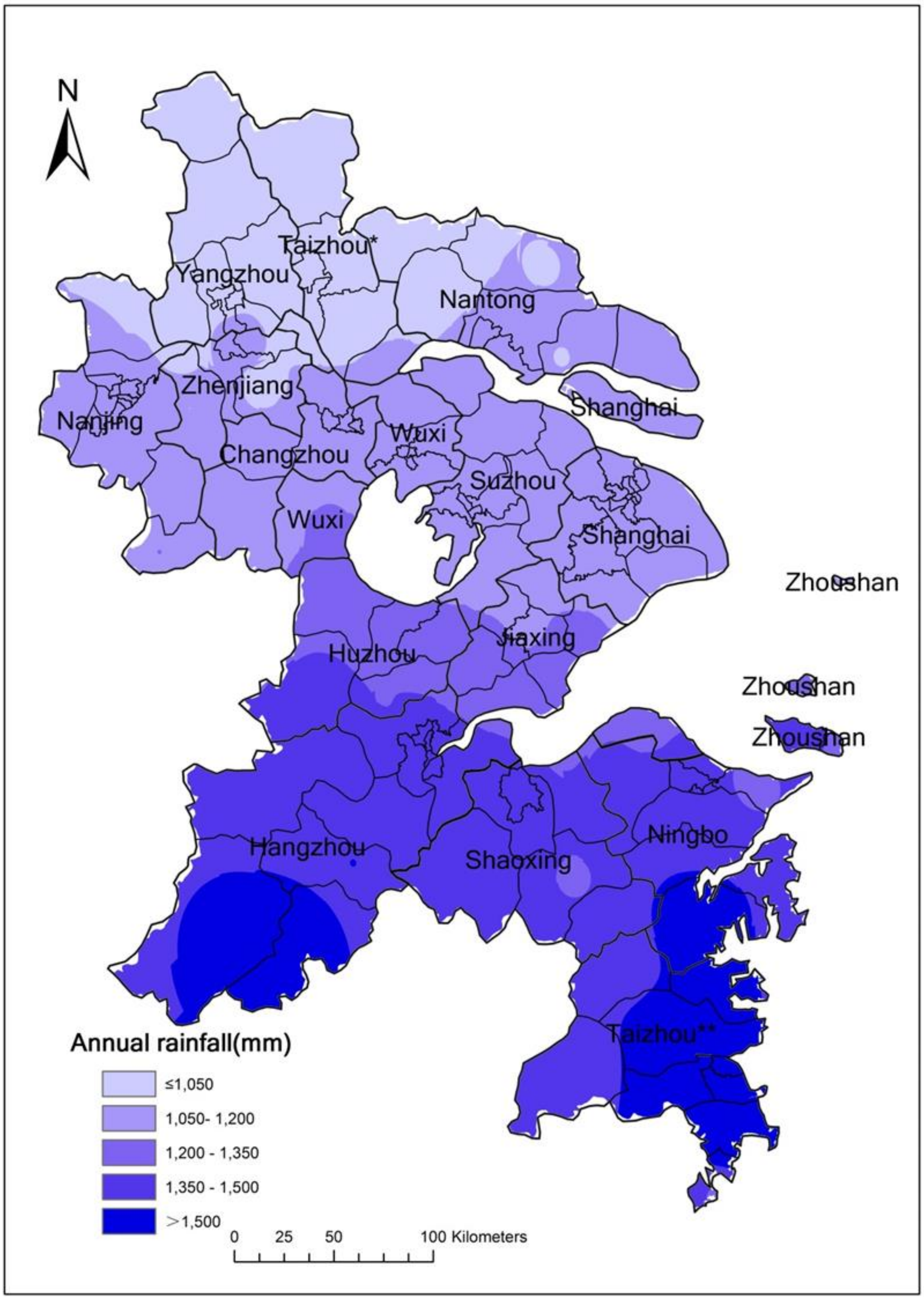

Figure 3.4 Average annual rainfall of the Yangtze River Delta

Figure 3.5 River system and drainage of the Yangtze River Delta

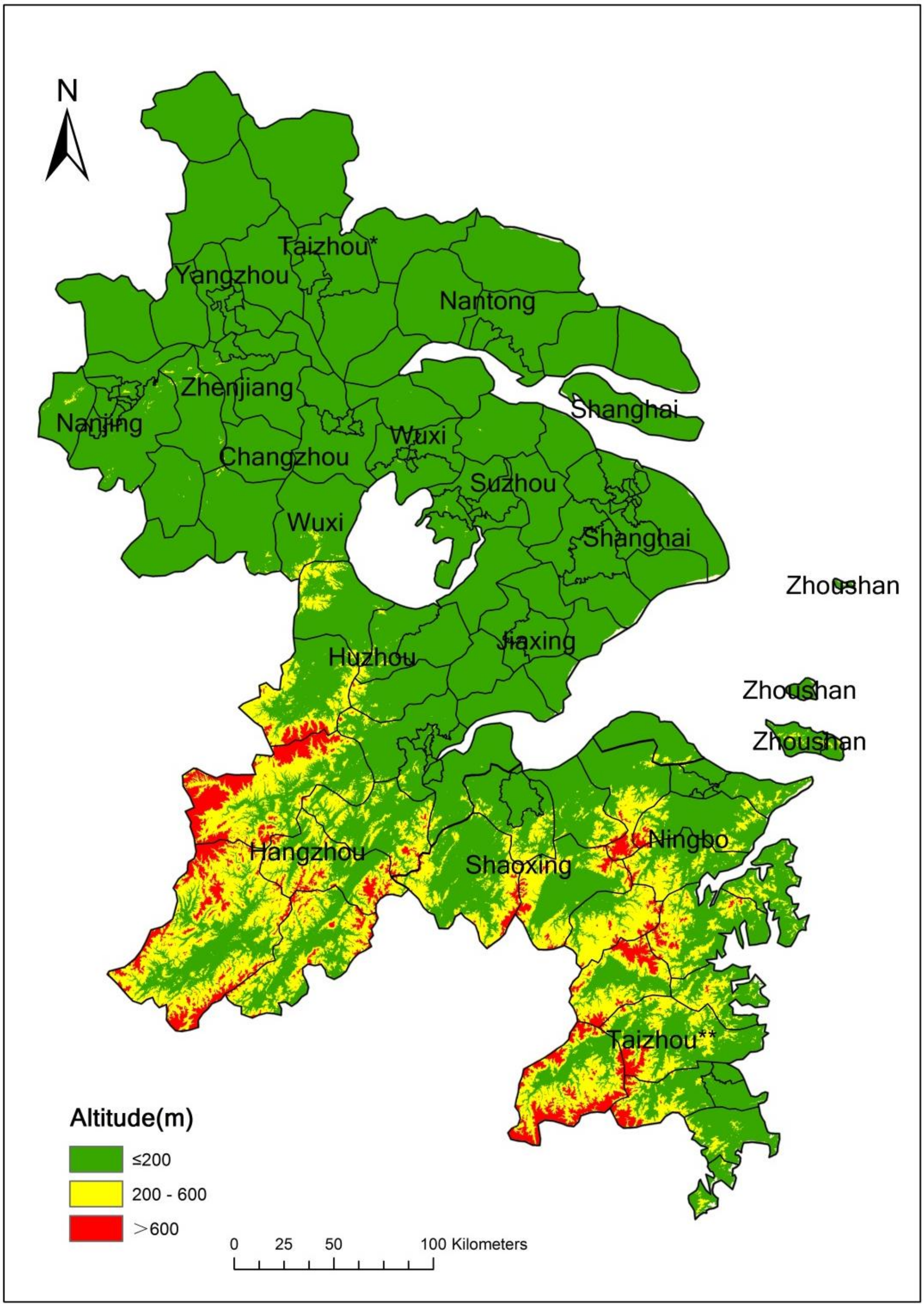

Figure 3.6 Landform of the Yangtze River Delta

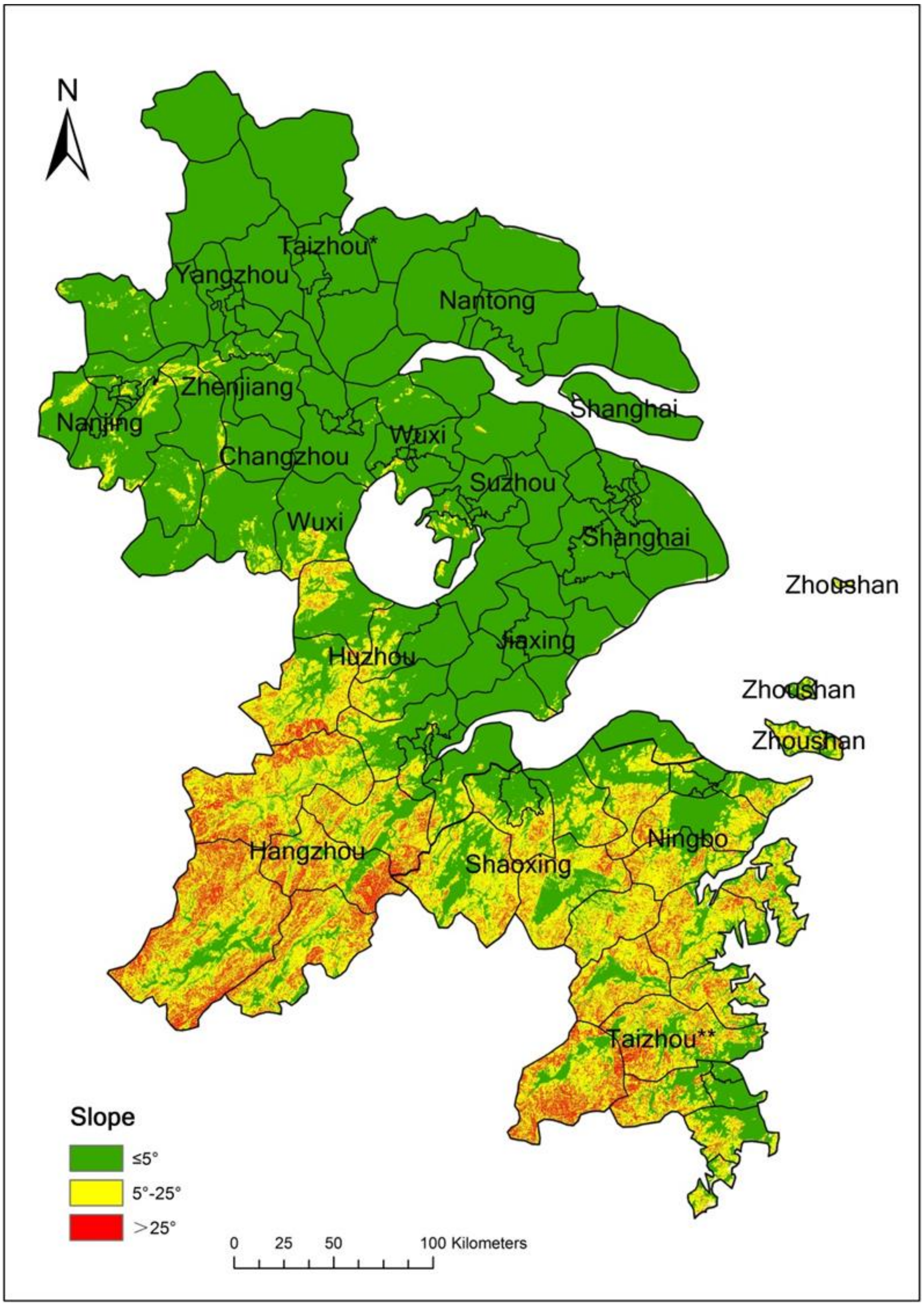

Figure 3.7 Ground slope of the Yangtze River Delta

3.3.3 Socioeconomic environment

The YRD covers an area of 110,000 km^2, only about 1.1% of China's total land area. However, its population at the end of 2012 stood at 108.4 million, accounting for about 8.01% of China's total population. Indeed, the delta is one of the most densely populated regions on earth (World Bank, 2014). Shanghai has the highest population density, more than 3600 per km^2 in 2012. As shown in Figure 3.8, counties with higher population density are mainly located in the north-eastern part of the region.

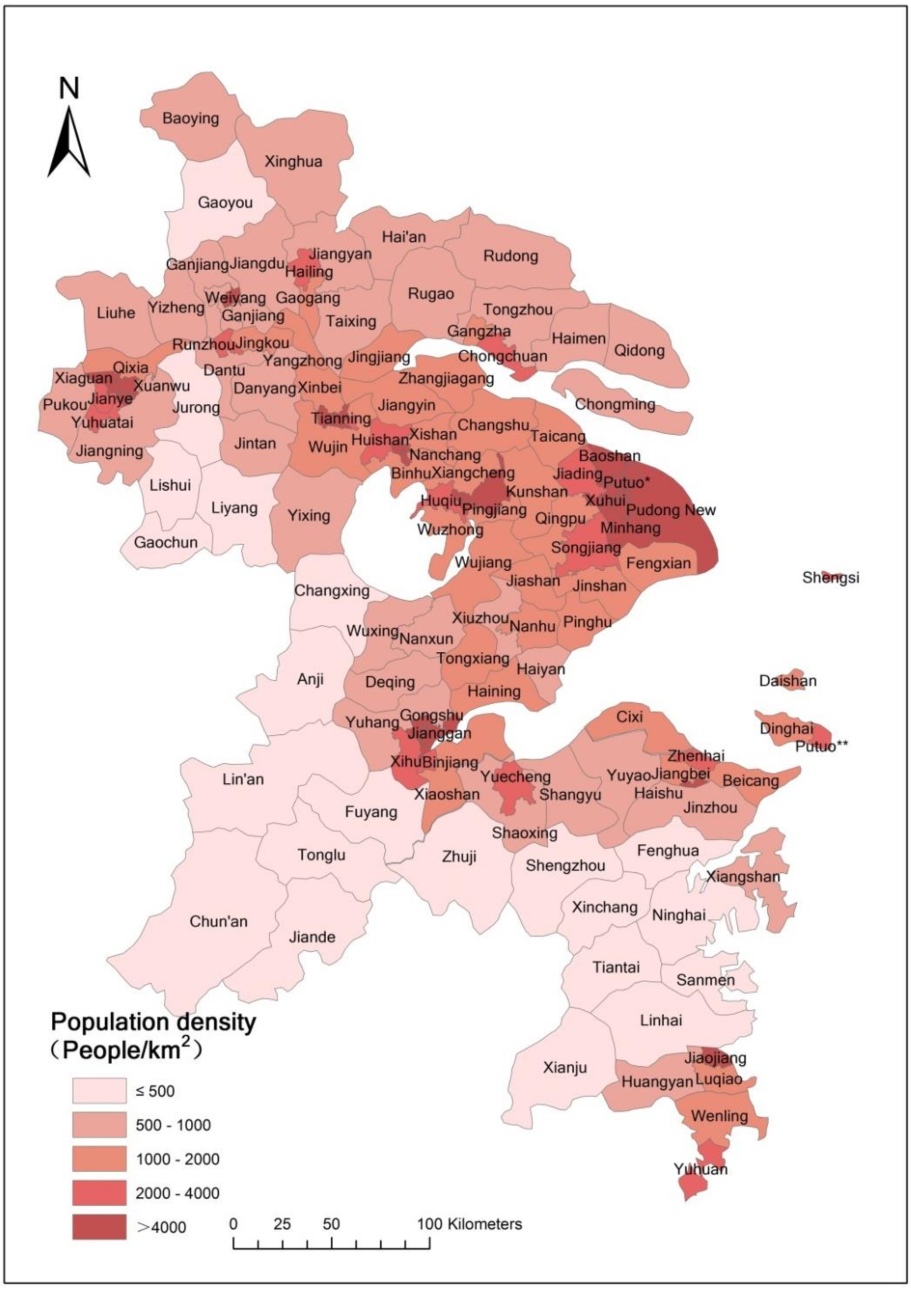

Figure 3.8 Population density in the Yangtze River Delta in 2012

GDP reached 8,700 billion in 2012, representing 17.3% of the national economy. The distribution of GDP is similar to that of population: Shanghai has the largest GDP per km^2 in the region and countries with higher GDP per unit area are also mainly located in the north-eastern part of the region (Figure 3.9).

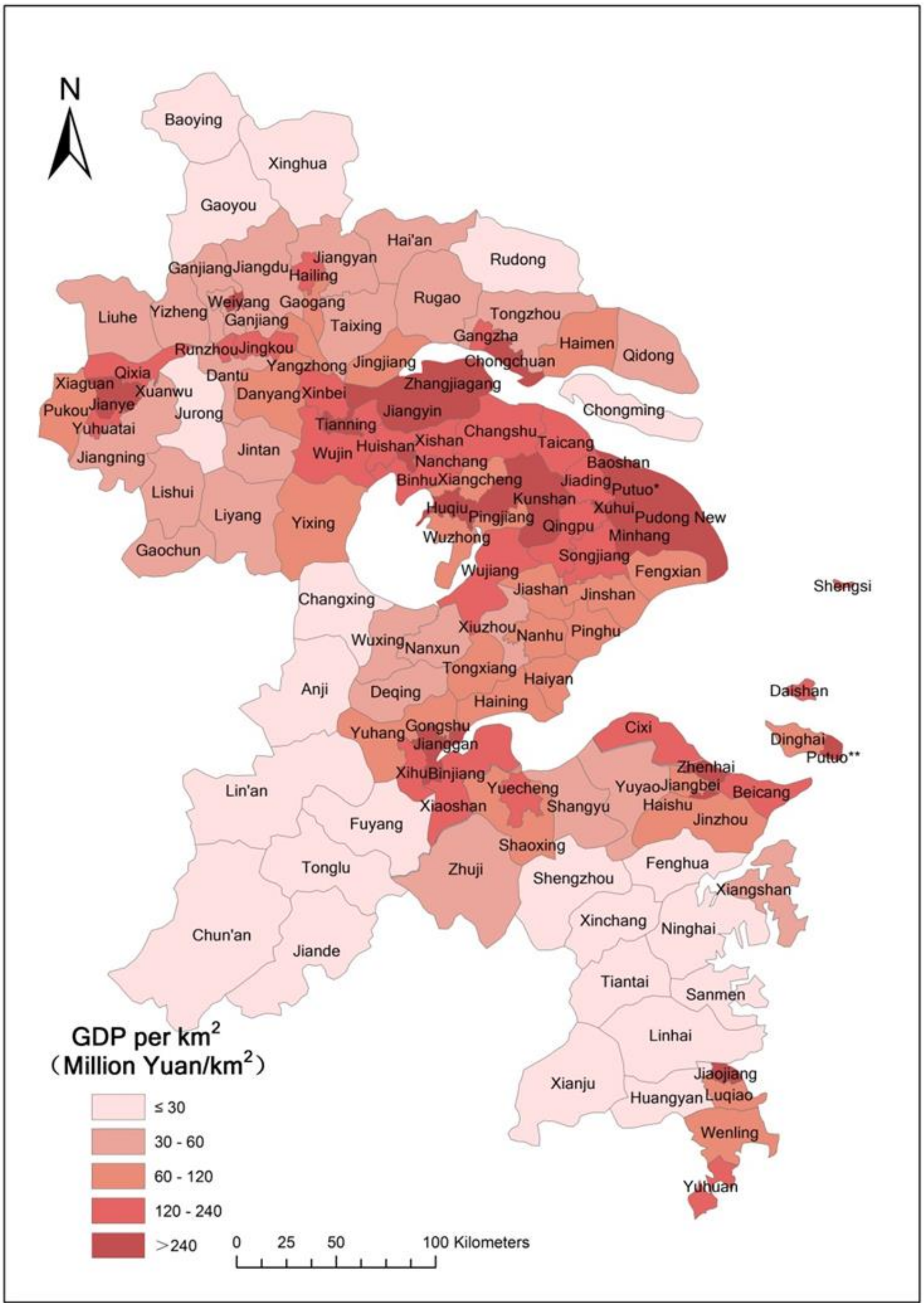

Figure 3.9 GDP per km^2 in the Yangtze River Delta in 2012

As shown in Figures 3.10 and 3.11, population density and GDP per unit area both show rapid growth over the past 20 years. This rising population density and GDP per unit area mean rising exposure and vulnerability to natural hazards.

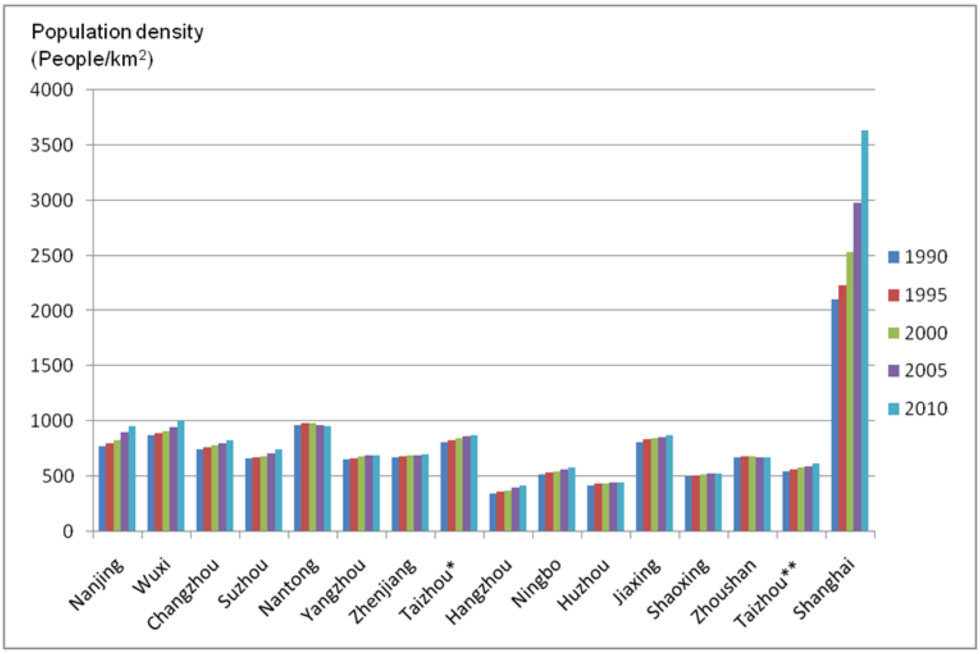

Figure 3.10 Population density for each city in the Yangtze River Delta

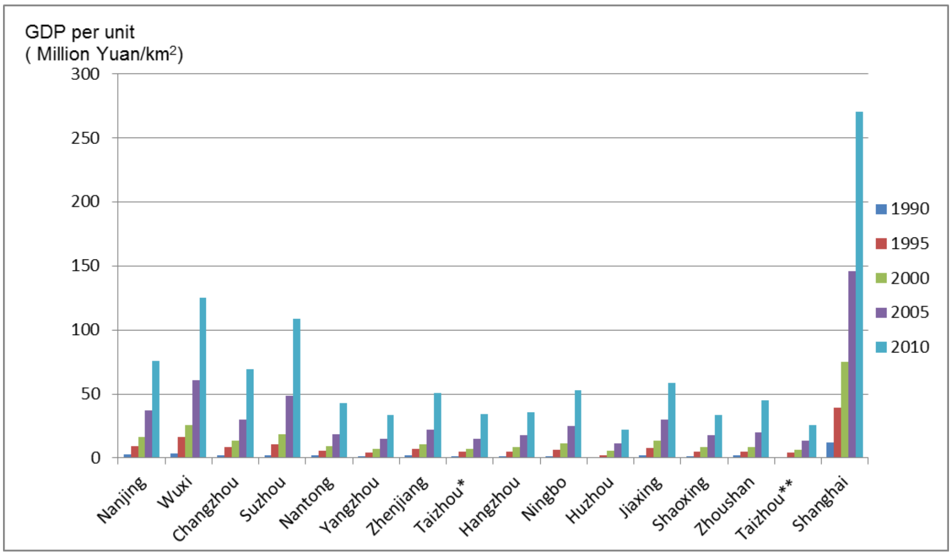

Figure 3.11 GDP per km^2 for each city in the Yangtze River Delta

Due to its geophysical environment, the YRD is evidently highly prone and increasingly vulnerable to damage from multiple hazards, and as one of the country's main economic regions, due to the recent and rapid growth in population and GDP, this already vulnerable region is becoming increasingly dangerous to natural disasters. This growing vulnerability, combined with occurrence of several different natural hazards, makes the area a suitable region in which to research multi-hazard risk appraisal.

3.4 Data collection

In this thesis, the YRD is selected as a case study area with county level as appraisal unit. There are three types of data needed to implement the proposed MHRA model: environmental data, disaster data and socioeconomic data.

Environmental data includes: meteorological data, river system and drainage, digital elevation model (DEM) and plate structure. The meteorological data were downloaded from 24 meteorological stations (Figure 3.12) in the YRD. These 24 meteorological stations recorded daily meteorological data from 1980 to 2013, which is a more suitable basis for hazard-forming environment analysis. The river system and drainage and tectonic plate structure were extracted from the Atlas of Natural Disaster Risk of China (Shi, 2011), and DEM was download from National Aeronautics and Space Administration (2011).

Disaster data includes the disaster type, time, place, and direct economic loss for each disaster in the YRD from 1980 to 2013. The Meteorological Department and the Civil Administration Department record data based on the county level in China, and the assessment unit for this research is also the county level. Hence, data collected from the Meteorological Department and the Civil Administration Department is more suitable for this research.

Socioeconomic data includes GDP, income of residents (income of rural residents, income of urban residents), population (population density), gender (gender ratio), age (age structure), telecommunication (number of mobile phone users, number of fixed line phone users, number of internet users), transport route (road length), medical condition (number of medical institutions and beds, medical technical personnel), and social dependency (number of residents covered by subsistence allowances, number of employed) in each county from 1980 to 2013. Hence, statistics yearbooks in each city in the YRD based on government administrative division are the best data sources.

Figure 3.12 Meteorological sites in the Yangtze River Delta

3.5 Model validation

Model validation is the process of determining the degree to which a model is an accurate representation of the real world from the perspective of the intended uses of the model (Thacker et al., 2004). Validation checks the accuracy of the model's representation of the real system. A model should be built for a specific purpose or set of objectives and its validity determined for that purpose.

There are several approaches that can be used to validate a model, ranging from subjective reviews to objective statistical tests. Broadly speaking, there are three approaches to model validation and any, or a combination of them, could be applied as appropriate to the different aspects of a particular model (Oreskes et al., 1994; Thacker et al., 2004; Sargent, 2004). These approaches include those based on expert intuition, theoretical results, and real system measurements. There is much subjectivity in expert intuition, and the choice of experts substantively influences results. A theoretical results approach is limited as it can only provide a crude validation of the model due to the fact that practice is not always consistent with theory. Comparison of observed and modelled data is the most reliable and preferred way to validate a model, but in practice, this is often not feasible because of various difficulties (cost, measurement, timing etc.) of obtaining observed data for validation purposes.

Model validation is a difficult problem in MHRA and tends to be impracticable due to the structure of the models used. Results obtained by the risk index approach are relative danger degree not the real loss. They cannot compare the observed loss data directly. The mathematical statistics approach is to estimate absolute loss from multiple natural hazards with different exceedance probabilities, but exceedance probabilities mean uncertainty in the results, so it is hard to validate by the observed data.

In this research, a MHRA model (MmhRisk-HI) is developed and used to estimate potential loss caused by multiple hazards in the YRD. Besides estimating loss from multiple natural hazards with different exceedance probabilities, this model also can simulate different multiple natural hazards scenarios to estimate the corresponding loss. Thus, the model draws on historical data from 1980-2012 in the YRD. In order to test the effectiveness of the developed MHRA model, the hazards that happened in 2013 in the YRD will be simulated in this model. The simulated results will be used to compare with the observed data.

3.6 Summary and conclusion

This chapter discussed the research design and approaches used to explore and address current limitations in MHRA. The choice of study area, data required, and methods used for model validation were also introduced.

Section 3.1 developed the conceptual model for MHRA based on the regional disaster system perspective. MHRA should calculate the possible loss considering the stability of the hazard-forming environment, probability of the hazard occurrence, interaction among hazards and the vulnerability of exposure. Hence, two categories of multi-hazard risk expressions will be considered together in the proposed model (MmhRisk-HI) construction.

Section 3.2 introduced five basic modules of MmhRisk-HI and the methods used in each module. The first module is hazard identification which includes a stable factors analysis to identify hazard from environmental factors rather than historical data. In doing so, it can take all possible hazard situations into consideration even if some hazards have long return periods. The hazard analysis module adopts changes in trigger factors to predict the frequency and magnitude of hazards, after which a multiple dimension information diffusion method is proposed to develop more complete magnitude and frequency function to overcome the problem of limited historical observation (short observation period relative to return period). The third module addresses hazard interaction analysis based on the trigger factors. The relationships among hazards were systematized for the first time in the MHRA field to provide a more complete view of hazard interaction than simply the domino effect. A four-class categorization scheme of hazard interactions was developed: independent, mutex, parallel and series relationships. The trigger factors analysis helps to ensure all possible relationships among different hazards are considered. The exposure analysis module can draw on official statistics, on-site survey and remote sensing image to provide data in different scales and units to characterize population and assets at risk. The methods used for exposure analysis are not pre-determined and depend on the scale of the region to be addressed and the assessment units. The final module addresses vulnerability analysis. Here a BN is considered a good method to calculate the loss ratio induced by multi-hazard with different degree, and reflect how physical, social, economic and environmental factors influence vulnerability. Trigger factors in the hazard-forming environment are selected as hazard-related indicators to measure the probability of the occurrence of multiple hazards of different magnitudes. Vulnerability-related indicators for exposure are constructed from physical, social, economic and environmental factors. Historic loss data for trigger factors with different magnitudes and the corresponding vulnerability-related indicators data can then be input into this model to calculate the conditional probabilities of indicators given loss. These conditional probabilities can be used to assess the future loss.

In section 3.3, the YRD case study area was introduced, and reasons for its selection as a case study area for multi-hazard risk appraisal were given. Due to its geophysical environment, the YRD is highly prone, and is increasingly vulnerable to, damage from multiple hazards. More importantly, as one of the country's main economic regions, due to the recent and rapid growth in population and GDP, this already vulnerable region is becoming increasingly dangerous to natural disasters.

Section 3.4 introduced the data needed in this research. Detailed environmental data was obtained from 24 meteorological stations in the YRD and the Atlas of Natural Disaster Risk of China. According to the assessment units, disaster data was collected from the Meteorological Department and the Civil Administration Department of China, and socioeconomic data was downloaded from statistics yearbooks.

Section 3.5 introduced the approach for model validation. Comparison with a real system is the most reliable and preferred way to validate a model. Hence, in order to test the effectiveness of the developed MHRA model (MmhRisk-HI), the hazards that occurred in 2013 will be simulated in this model. The simulated results will be used to compare with the observed data.

In the next chapter, a detailed account is given on the construction of MmhRisk-HI for the YRD based on the approach and methods discussed in this chapter.

Chapter 4

Multi-hazard risk assessment model construction

The research design and study area, the Yangtze River Delta (YRD) were introduced in Chapter 3. Chapter 4 discusses the construction of a multi-hazard risk assessment (MHRA) model (MmhRisk-HI) based on the approach and methods discussed in Chapter 3. The basic framework for MmhRisk-HI is introduced in section 4.1, after which the construction of the five component modules is discussed in turn, before finally drawing some conclusion on the MmhRisk-HI development in section 4.7.

4.1 Framework

The aim of MHRA is to gain a holistic view, through assessing and mapping, of the total expected loss due to the occurrence of various natural hazards on the social, environmental and economic settings in a given area. This research explores and constructs a model (MmhRisk-HI) to calculate the possible loss caused by multiple hazards, with an explicit consideration of interaction between different hazards. This model takes advantage of the merits of both risk index and mathematical statistics methods. This is achieved by analysing risk considering the disaster formation mechanism (considering hazard, vulnerability and exposure), and calculating possible loss and corresponding probability of loss under different natural hazard scenarios.

The basic research framework of MmhRisk-HI is shown in Figure 4.1. There are two main components (shown by the dotted lines) containing five modules in total (solid line boxes within dotted line boxes): hazard identification, hazard analysis, hazard interaction analysis, exposure analysis, and vulnerability analysis.

The first main component, including hazard identification, hazard analysis, and hazard interaction analysis modules, is used to calculate the exceedance probability of multiple hazards occurrence. The hazard-forming environment is divided into two factor types, stable factors and trigger factors. Stable factors are analysed to identify the spatial distribution of hazards with the Entropy-weight method in the hazard identification module; the hazard analysis module is built based on a multiple dimension information diffusion method to analyse the trigger factors for hazard magnitude-frequency analysis. The hazard interaction analysis module then analyses the hazard interaction and calculates the exceedance probability of multiple hazards occurrence based on the results of the hazard identification and analysis modules.

The second component focuses on the calculation of the possible loss caused by multiple hazards with different exceedance probabilities. The methods used for exposure analysis depend on the scale of the region to be addressed and the assessment units. A Bayesian network (BN) is used to measure the relationship between loss and multiple hazards with exceedance probability considering the relevant vulnerability indicators in the vulnerability analysis module.

Finally, a multi-hazard risk map can be drawn addressing the probability of multi-hazard occurrence and corresponding loss.

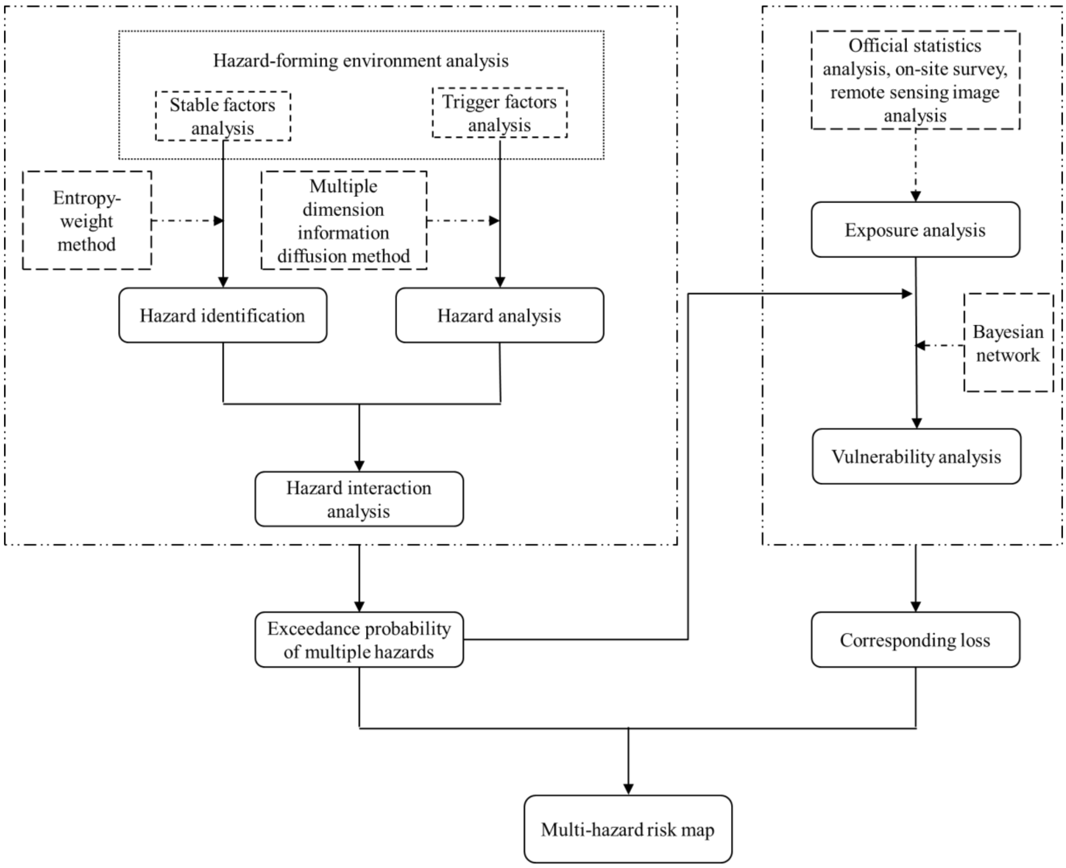

Figure 4.1 Framework of MmhRisk-HI

4.2 Hazard identification

Hazard identification is the process used to identify which kinds of natural hazards influence a given area. It also addresses the spatial distribution of these hazards in the study area. As described in Chapter 3, stable factors in the specific geophysical environment determine the preconditions for the occurrence of a specific natural hazard. According to the characteristics of these environmental factors, the spatial distribution of natural hazards in a region can be deduced. The relationship between stable factors and major natural hazards can be expressed as:

$$S(H_k)=f(SF_1,SF_2,\ldots SF_j) \quad (j=1,2\ldots n) \tag{4-1}$$

Where, S is susceptibility,
H is hazard,
SF is stable factors, and
for any given area, $S(H_k)$ is susceptibility to hazard k, given stable factors SF_j.

Taking the YRD as an example, in the module, the susceptibility of each assessment unit (county) to each hazard can be calculated as:

$$S_i(H_k)=\sum_{j=1}^{n} w_j \; Nor\left(SF_j\right)_i \tag{4-2}$$

Where, for any given county i,
S is susceptibility,
H is hazard,
SF is stable factors,
$S_i(H_k)$ is susceptibility to hazard k, given stable factors SF_j,
$Nor(SF_j)_i$ is the normalization of stable factor j in county i, and
w_j is the weight for stable factor j.

The weight w_j is calculated using the entropy-weight method (Qiu, 2002). Information entropy is a general measure of uncertainty (Shannon, 1948). Here, it measures the amount of useful information in the indicator provided. The greater the entropy, the greater the uncertainty, the amount of useful information that the indicator provides is small. That is, when the difference in one indicator between different assessment units is small, the entropy is great, it illustrates that this indicator provides less useful information, and the weight of this indicator should be set correspondingly small. On the other hand, if the difference is large and the entropy is small, the weight would be big (Zou et al., 2006; Qi et al., 2010).

First, assume X denotes the initial data matrix, $X=\{x_{ij}\}_{m\times n}$ $(i=1,2\ldots m;\ j=1,2\ldots n)$ whereas m represents the number of assessment units and n represents the number of stable factors. As the dimension of each indicator is different, equation (4-3) is used to standardise the initial data matrix to the standardised matrix $Y=\{y_{ij}\}_{m\times n}$ $(i=1,2\ldots m;\ j=1,2\ldots n)$.

$$y_{ij} = \frac{x_{ij}}{\sum_{i=1}^{m} x_{ij}},\ 0 \le y_{ij} \le 1 \tag{4-3}$$

Information entropy for each indicator e_j is derived from equation (4-4):

$$e_j = -k\sum_{i=1}^{m} y_{ij} \ln y_{ij} \tag{4-4}$$

The coefficient k is determined by the sample size m. ln represents the natural logarithm in equations (4-4) and (4-5).

$$k = \frac{1}{\ln m} \tag{4-5}$$

The information utility value for each indicator h_j is derived from equation (4-6), and the weight for each indicator w_i is calculated using equation (4-7).

$$h_j = 1 - e_j \tag{4-6}$$

$$w_j = \frac{h_j}{\sum_{j=1}^{n} h_j} \tag{4-7}$$

The susceptibility of assessment units (counties in our case) to each hazard is then mapped to show the spatial distribution of single hazards in the whole study area. ArcGIS software is used to aggregate the spatial distribution of single hazards to show the spatial distribution of multi-hazard.

4.3 Hazard analysis

There is a strong nonlinear relationship between natural hazard event magnitude and frequency. Hazard analysis is the process used to analyse this relationship, to give the probability of hazard occurrence of different magnitudes in a given area. The relationships between trigger factors and major natural hazards were discussed in Chapter 3. Substantial changes in some trigger factors are the main reason that some hazards are induced, hence, trigger factors can be used to estimate both the frequency and magnitude of hazards, with the change of degree in them representing the magnitude of hazards, and the probability of changes in them representing the probability of hazards. This can be achieved using a mathematical statistics approach to define a function to determine event magnitude and frequency. The information diffusion method has been introduced as an efficient method to assess the probability of occurrence of hazards of different magnitudes. However, this method can only assess one factor, while some hazards are induced by multiple trigger factors. Hence, the multiple dimension information diffusion method is adopted to measure the exceedance probability of the changes of trigger factors in this module.

Taking typhoons in the YRD as an example, typhoons do not originate in the YRD region, yet the whole region is still influenced by typhoons (which develop in the north western part of the Pacific Ocean between 180° and 100°E). In contrast to other hazards, typhoons move thousands of kilometres. The movement of typhoon is accompanied by strong winds and heavy rain, and a series of hazards induced by the changes of winds and rainfall are the reasons to cause loss in the track. Thus, typhoon can be viewed as the changes of wind speed and rainfall, and these changes can be used as the trigger factors to measure the magnitude of the series of hazards in the track. Hence, maximum daily rainfall and maximum wind speed during each historical typhoon record are selected to measure the frequency and magnitude of these hazards in the typhoon track.

$XY=\{(x_1,y_1),\ (x_2,y_2)\ \dots(x_m,\ y_m)\}$ expresses maximum wind speed x_i and maximum daily rainfall y_i in m group historical typhoon disaster record.

The wind speed universe is defined as:

$$U=\{u_1, u_2 \cdots u_s\}(j=1,2\cdots s) \tag{4-8}$$

The daily rainfall universe is defined as:

$$V=\{v_1, v_2 \cdots v_t\}(k=1,2\cdots t) \tag{4-9}$$

Multiple dimension information diffusion method has been introduced in section 3.2.2. Here, two dimension information diffusion (equation 4-10) is used to diffuse the information carried by each sample set *{XY}$_i$* to all the sampling points.

$$f_i(u_j, v_k)=\frac{1}{2\pi h_x h_y \sqrt{1-r^2}}\exp\{-\frac{1}{2(1-r^2)}[\frac{(x_i-u_j)^2}{h_x{}^2}-2r\frac{(x_i-u_j)(y_i-v_k)}{h_x h_y}+\frac{(y_i-v_k)^2}{h_y{}^2}]\} \tag{4-10}$$

The marginal distribution of a two dimension normal distribution is normal distribution. Hence, it can be deduced that if given a fixed value u_j in the wind speed universe, the information carried by maximum daily rainfall y_i will diffuse to the rainfall universe V following normal distribution (equation 4-11); the same thing to wind speed x_i when given a fixed value v_k in the rainfall universe (equation 4-12).

$$f_i(v_k)=\frac{1}{h_y\sqrt{2\pi}}\exp[-\frac{(y_i-v_k)^2}{2h_y{}^2}] \tag{4-11}$$

$$f_i(u_j)=\frac{1}{h_x\sqrt{2\pi}}\exp[-\frac{(x_i-u_j)^2}{2h_x{}^2}] \tag{4-12}$$

Therefore, the method used to decide the diffusion coefficient in one dimension information diffusion also can be used here. It is determined by the minimum and maximum values of the samples (a and b respectively), and the sample size m.

The value of h_x and h_y are then determined, for a given value of m, as:

$$h_x = \begin{cases} 0.8146(b_x - a_x), 1 < m \le 5, \\ 0.5690(b_x - a_x), m = 6, \\ 0.4560(b_x - a_x), m = 7, \\ 0.3860(b_x - a_x), m = 8, \\ 0.3362(b_x - a_x), m = 9, \\ 0.2986(b_x - a_x), m = 10, \\ 2.6851(b_x - a_x) / (m-1), 11 \le m. \end{cases} \tag{4-13}$$

$$h_y = \begin{cases} 0.8146(b_y - a_y), 1 < m \le 5, \\ 0.5690(b_y - a_y), m = 6, \\ 0.4560(b_y - a_y), m = 7, \\ 0.3860(b_y - a_y), m = 8, \\ 0.3362(b_y - a_y), m = 9, \\ 0.2986(b_y - a_y), m = 10, \\ 2.6851(b_y - a_y) / (m-1), 11 \le m. \end{cases} \tag{4-14}$$

r is the correlation coefficient between *X* and *Y*.

$$r = \frac{E[(X - E(X))(Y - E(Y))]}{\sqrt{D(X)}\sqrt{D(Y)}} = \frac{E[(X - E(X))(Y - E(Y))]}{\sqrt{E(X^2) - (E(X))^2}\sqrt{E(Y^2) - (E(Y))^2}} \tag{4-15}$$

The information distribution $\mu_i(u_j, v_k)$ is derived from normalising equations (4-16) and (4-17), and the result can be expressed as a continuous probability density function.

$$C_i = \sum_{j=1}^{s} \sum_{k=1}^{t} f_i(u_j, v_k) \tag{4-16}$$

$$\mu_i(u_j, v_k) = \frac{f_i(u_j, v_k)}{C_i} \tag{4-17}$$

The probability distribution $p(u_j, v_k)$ at (u_j, v_k) can be calculated using equations (4-18) and (4-19), where $p(u_j, v_k)$ denotes the probability distribution of wind speed and daily rainfall sets.

$$q(u_j, v_k) = \sum_{i=1}^{\mathrm{m}} \mu_i(u_j, v_k) \tag{4-18}$$

$$p(u_j, v_k) = \frac{q(u_j, v_k)}{\sum_{j=1}^{s}\sum_{k=1}^{t} q(u_j, v_k)} \quad (4\text{-}19)$$

Finally, exceedance probability on each set is derived as shown in equation (4-20):

$$P(u_j, v_k) = \sum_{g=j}^{s}\sum_{h=k}^{t} p(u_g, v_h) \quad (4\text{-}20)$$

The exceedance probability distribution $P(u_j, v_k)$ and the corresponding maximum wind speed and maximum daily rainfall can then be used to measure the magnitude-frequency of the series of hazards in the typhoon track.

Hence, based on the trigger factors and multiple dimension information diffusion method, the probability of hazard occurrence of different magnitudes in a given area can be calculated.

4.4 Hazard interaction analysis

Hazard interaction analysis is used to calculate the probability of multiple hazards occurring together, given different types of possible relationships. The relationships between different natural hazards were categorized into four types (section 3.2.3) and in this hazard interaction module, the probability of multiple hazards occurring together is calculated based on the trigger factors in the hazard-forming environment.

4.4.1 Independent relationship analysis

The Independent relationship is where there is no evident common cause between two different hazards. This means that the changes in trigger factors which induce hazard A are independent of those which induce hazard B. The relationship between these trigger factors and hazards can be expressed as:

$$f(p_{t1}, p_{t2} \ldots p_{ti}) = p(h_A) \quad (4\text{-}21)$$

$$f(p_{ti+1}, p_{ti+2} \ldots p_{tn}) = p(h_B) \quad (4\text{-}22)$$

Where, p_{ti} is the probability of the change in trigger factor i, and
$p(h_j)$ *is* the probability of hazard j occurrence.

The changes in trigger factors $t_1,t_2\dots t_i$ are independent of changes in trigger factors $t_{i+1},t_{i+2}\dots t_n$. If the changes in these trigger factors occur together, then hazard A and hazard B happen together. Hence, the probability of these two hazards occurring together can be calculated as:

$$P(A\cap B)= p(h_A)\times p(h_B)= f(p_{t1},p_{t2}\dots p_{ti})\times f(p_{ti+1},p_{ti+2}\dots p_{tn}) \tag{4-23}$$

Where, p_{ti} is the probability of the change in trigger factor i, and
$p(h_j)$ *is* the probability of hazard j occurrence.

4.4.2 Mutex relationship analysis

A Mutex relationship is where hazard A and hazard B are mutually exclusive, and so cannot occur together. The changes in trigger factors for these hazards can be expressed as:

$$f(p_{ti+})=p(h_A) \tag{4-24}$$

$$f(p_{ti-})=p(h_B) \tag{4-25}$$

Where, $_{ti+}$ represents the trigger factor i departure in positive direction from its mean value,

$_{ti-}$ represents the trigger factor i departure in the negative direction from its mean value,

p_{ti} is the probability of the change in trigger factor i, and

$p(h_j)$ *is* the probability of hazard j occurrence.

One trigger factor cannot move in two directions simultaneously, hence, the probability of these two hazards occurring together can be expressed as:

$$P(A\cap B)= 0 \tag{4-26}$$

4.4.3 Parallel relationship analysis

A change in one (or several) trigger factors may induce more than one hazard A_1, A_2……A_n at the same time. Thus hazards A_1, A_2……A_n are in a parallel relationship. This relationship between trigger factors and these hazards can be expressed as:

$$\begin{gathered} f(p_{t1},p_{t2}\ldots\ p_{ti})=\ p(h_{A1}) \\ f(p_{t1},p_{t2}\ldots\ p_{ti})=\ p(h_{A2}) \\ \ldots \\ f(p_{t1},p_{t2}\ldots\ p_{ti})=\ p(h_{An}) \end{gathered} \tag{4-27}$$

Where, p_{ti} is the probability of the change in trigger factor *i*, and $p(h_j)$ *is* the probability of hazard *j* occurrence.

Hazards A_1, A_2……A_n constitute a hazard group, with all hazards in the group induced by the same trigger factor(s). Hence, the frequency and magnitude of this hazard group are determined by the changes in these trigger factors. The probability of this hazard group (Hazards A_1, A_2……A_n) occurring can be expressed as:

$$P(A_1 \cap A_2 \cap \ldots \cap A_n) = f(p_{t1},p_{t2}\ldots\ p_{ti}) \tag{4-28}$$

Where, p_{ti} is the probability of the change in trigger factor *i*, and $p(h_j)$ *is* the probability of hazard *j* occurrence.

4.4.4 Series relationship analysis

If Hazard A induces changes in some trigger factors, and the changes in these trigger factors then induce hazard B, hazards A and B are in a series relationship. This can be expressed as:

$$f(p_{t1},p_{t2}\ldots\ p_{ti})=p(h_A)\rightarrow f(p_{ti+1},p_{ti+2}\ldots\ p_{tn})\ =\ p(h_B) \tag{4-29}$$

Where, p_{ti} is the probability of the change of trigger factor *i*, and $p(h_j)$ *is* the probability of hazard *j* occurrence.

The changes of trigger factors $t_1, t_2 \ldots t_i$ induce the hazard A, then hazard A cause the changes of trigger factors $t_{i+1}, t_{i+2} \ldots t_n$. The changes of trigger factors $t_{i+1}, t_{i+2} \ldots t_n$ induce hazard B. Hence, the probability of Hazard A and B occurring together can thus be expressed as:

$$P(A \cap B) = p(h_A) \times p(h_B) = f(p_{t1}, p_{t2} \ldots p_{ti}) \times f(p_{ti+1}, p_{ti+2} \ldots p_{tn} \mid h_A) \quad (4\text{-}30)$$

Where, p_{ti} is the probability of the change of trigger factor i,

$p(h_j)$ *is* the probability of hazard j, and

$p_{tn} \mid h_A$ is the probability of the change of trigger factor n given the magnitude of hazard A occurrence.

Hence, based on the four basic hazard interaction relationships described above, the probability of multiple hazards occurring together can be calculated in this module.

Let us now to turn to the second main component of the MHRA model, which focuses on the calculation of the possible loss caused by multiple hazards with different exceedance probabilities. This comprises exposure and vulnerability analysis modules.

4.5 Exposure analysis

Exposure analysis is used to determine the spatial distribution of the elements at risk (e.g. people, infrastructure). This is usually achieved using analysis of data contained in official statistical reports, or that obtained via on-site survey or remote sensing image. These data sources vary considerably in their characteristics: on-site survey data may be very detailed, but generally only exists on a very local scale as it is time and resource intensive to collect. Conversely remote sensing image provides wide area coverage, but that raster format means that the information conveyed is more limited in scope. Official statistical data, are based on government administrative division and commonly represent an intermediate point, in terms of functional resolution.

This module thus selects the exposure analysis method mainly based on the scale of the area to be assessed, and the data available for that area. Taking the YRD case study area as an example, the assessment unit is the county level (government administrative division), so official statistics analysis is the method to be used. From these official statistical data, the number and monetary value of exposure in each county can be obtained. ArcGIS software is then used to map the number or value of the exposure in each spatial assessment unit.

4.6 Vulnerability analysis

In the vulnerability analysis module, vulnerability assessment is used to measure the possible loss for a given exposure, under conditions caused by multiple hazards of varying degree, and to determine how these conditions (including physical, social, economic and environmental factors) influence the possible loss. A vulnerability curve can reflect the relationship between loss ratio and hazard, but cannot reflect how physical, social, economic and environmental factors influence vulnerability. Conversely, a vulnerability index can reflect how physical, social, economic and environmental factors influence vulnerability, but cannot measure the relationship between loss and hazard by degree. Thus, a Bayesian network (BN), which is an optimal model to calculate the loss ratio induced by multi-hazard of different degree, and which can reflect how physical, social, economic and environmental factors influence vulnerability, is used in this module. Determining the BN structure and estimating conditional probabilities are the two key parts in the BN, discussed further below.

4.6.1 Structure of Bayesian network

A BN is a complete model of the system of interest, including its component variables and the probabilistic relationships between them. To construct a BN, the variables of indicators should first be identified. In this module, a BN modelling framework is constructed according to domain knowledge (e.g. Cutter et al., 2003; Villagran, 2006; Alexander, 2000). As shown in Figure 4.2, the loss ratio, which is assumed to be a parent of vulnerability- and hazard-related indicators, is the root node. Trigger factors are chosen to construct the set of hazard-related indicators which represent the magnitude of multiple hazards. Indicators in the economic, social, physical and environmental domains are chosen to construct the sets of vulnerability-related indicators (e.g. Cutter et al., 2003; Villagran, 2006; Schmidt-Thomé, 2006a; SCEMDOAG, 2009).

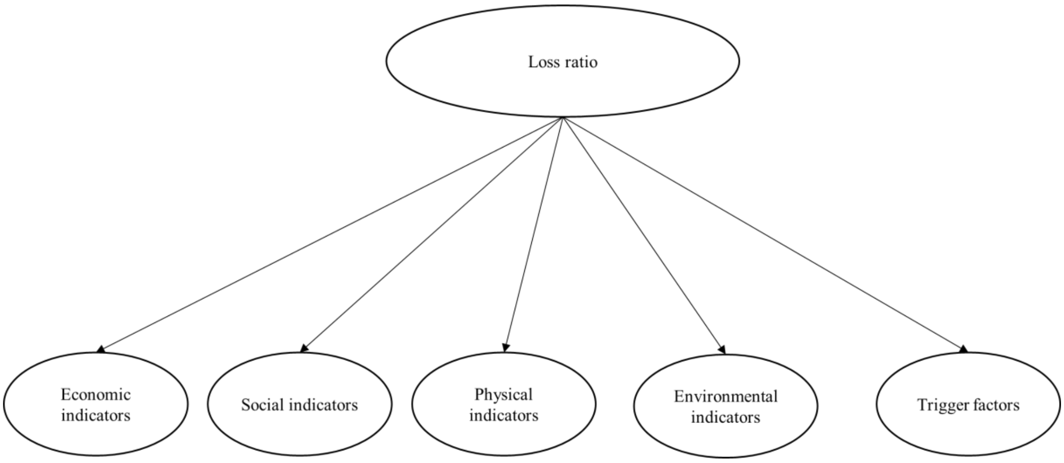

Figure 4.2 Generic Bayesian network framework for vulnerability analysis

Table 4.1 Some possible vulnerability-related indicators

Domain	**Indicator**
Economic	• GDP/capita
	• Income of residents
Social	• Population density
	• Gender ratio
	• Age structure
	• Telecommunication
	• Transport route
	• Medical condition
	• Social dependency
	• Risk perception
	• Warning system
	• Institutional preparedness
	• Educational achievement
Physical	• Technical infrastructure
Environmental	• Significant natural areas
	• Fragmented natural areas

Table 4.1 lists some possible vulnerability-related indicators, the details of these indicators are described below.

- GDP/capita: high GDP/capita means more economic activities under threat of hazard events (Blaikie et al., 1994; Schmidt-Thomé, 2006a).
- Income of residents: high income means residents have more personal resources to absorb losses and speed up the recovery after a disaster (Hewitt, 1997; Cutter et al., 2003; SCEMDOAG, 2009).
- Population density: high population density means more population under threat of hazard events (Puente, 1999; Pelling, 2003).
- Gender ratio: females are often more vulnerable than males, because females tend to have limited education, lower incomes and family care responsibilities (Cutter et al., 2003; SCEMDOAG, 2009; Yavinsky, 2012).
- Age structure: children and old people are more vulnerable to hazard than young adults due to the limited physical strength (Cutter et al., 2000; Ngo, 2001).
- Telecommunication: high telecommunication capacity supports fast and precise hazard information transmission, thus targeted measures can be adopted quickly (Blaikie et al., 1994; Puente, 1999).
- Transport route: good traffic condition makes it easy to evacuate people and to distribute emergency rescue and relief materials (Platt, 1991; Villagran, 2006).
- Medical condition: good medical services ensure wounded people get fast and effective treatment after a disaster, thus the recovery period after a disaster can be shortened (Morrow, 1999; Cutter et al., 2003).
- Social dependency: people who are totally dependent on social services almost have no personal resources to absorb losses, and require more support in the post-disaster period, thus they are more vulnerable than the employed (Cutter et al., 2003; SCEMDOAG, 2009).
- Risk perception: it measures the ability of an individual to discern and understand the characteristics and severity of risk from hazard events (Slovic, 2000). Understanding of the risk is helpful in taking effective measures to cope with disasters, thus people with low risk perception are more vulnerable than those with high risk perception (Armas, 2006; Smith, 2013).
- Warning system: disaster warning system is used to send early warning to those who might be affected by a coming disaster, thus a good warning system is useful for people to prepare for the disaster

and act effectively to mitigate its influence (McGraw et al., 1997; Zschau and Küppers, 2003).

- Institutional preparedness: it indicates regulations or procedures which have been developed to deal with some possible disaster situations (e.g. emergency response plan). Good institutional preparedness helps to cope with disasters quickly and effectively (Haque, 2000; Schmidt-Thomé, 2006a).
- Educational achievement: higher education means people can understand information about hazard events better and take more effective measures to cope with disasters (Cutter et al., 2003; SCEMDOAG, 2009).
- Technical infrastructure: it indicates some facilities which are used to respond to hazard events (e.g. fire trucks, steamboats, helicopters etc.). Good technical infrastructure makes it easy to evacuate people and control disaster situation (Schmidt-Thomé, 2006a).
- Significant natural areas: areas with special natural values (e.g. national parks) are considered more vulnerable, because they are unique and hard to recover (Schmidt-Thomé, 2006a).
- Fragmented natural areas: fragmented natural areas are vulnerable because the nature in larger undisturbed areas recovers faster than that in smaller areas (Schmidt-Thomé, 2006a).

In this framework, the indicators used to construct vulnerability-related indicators should be independent. Factor analysis is a classical statistical method to detect structure in the relationships between variables or indicators (Russell, 2002). In this module, based on the SPSS (Statistic Package for Social Science) statistics software, Principal Component Analysis (PCA) (Jolliffe, 2002) is adopted to make distinct the principal component, and then the commonly used varimax rotation strategy (Osborne, 2008) is used to calculate the factor loading in each principal component (Polit and Beck, 2008). The factors (vulnerability-related indicators) with highest loading in each principal component are then selected to construct the BN.

Based on the hazard analysis and hazard interaction analysis, trigger factors can be used to measure the probability of the occurrence of multiple hazards with different magnitudes. Trigger factors are thus chosen to construct the set of hazard-related indicators which represent the magnitude of multiple hazards. Hazard-related indicators for multiple hazards with different relationships are shown in Figure 4.3.

In Figure 4.3a, hazard A and hazard B are an independent relationship. The changes in trigger factors $t_1, t_2 \ldots t_i$ which induce hazard A are independent of the changes in trigger factors $t_{i+1}, t_{i+2} \ldots t_n$ which induce hazard B. The two trigger factor groups ($t_1, t_2 \ldots t_i$) and ($t_{i+1}, t_{i+2} \ldots t_n$) can be used to measure the frequency and magnitude of hazard A and B respectively. Hence, the trigger factor group ($t_1, t_2 \ldots t_i$) is chosen as hazard-related indicator to represent the magnitude of hazard A, and the trigger factor group ($t_{i+1}, t_{i+2} \ldots t_n$) is chosen as hazard-related indicator to represent the magnitude of hazard B.

In Figure 4.3b, hazards $A_1, A_2 \ldots A_n$ represent a parallel relationship. Hazards $A_1, A_2 \ldots A_n$ are all induced by the changes in the same trigger factors $t_1, t_2 \ldots t_i$. The frequency and magnitude of this hazard group ($A_1, A_2 \ldots A_n$) are determined by the changes in these trigger factors. Hence, the trigger factor group ($t_1, t_2 \ldots t_i$) is chosen as the hazard-related indicator to represent the magnitude of group ($A_1, A_2 \ldots A_n$).

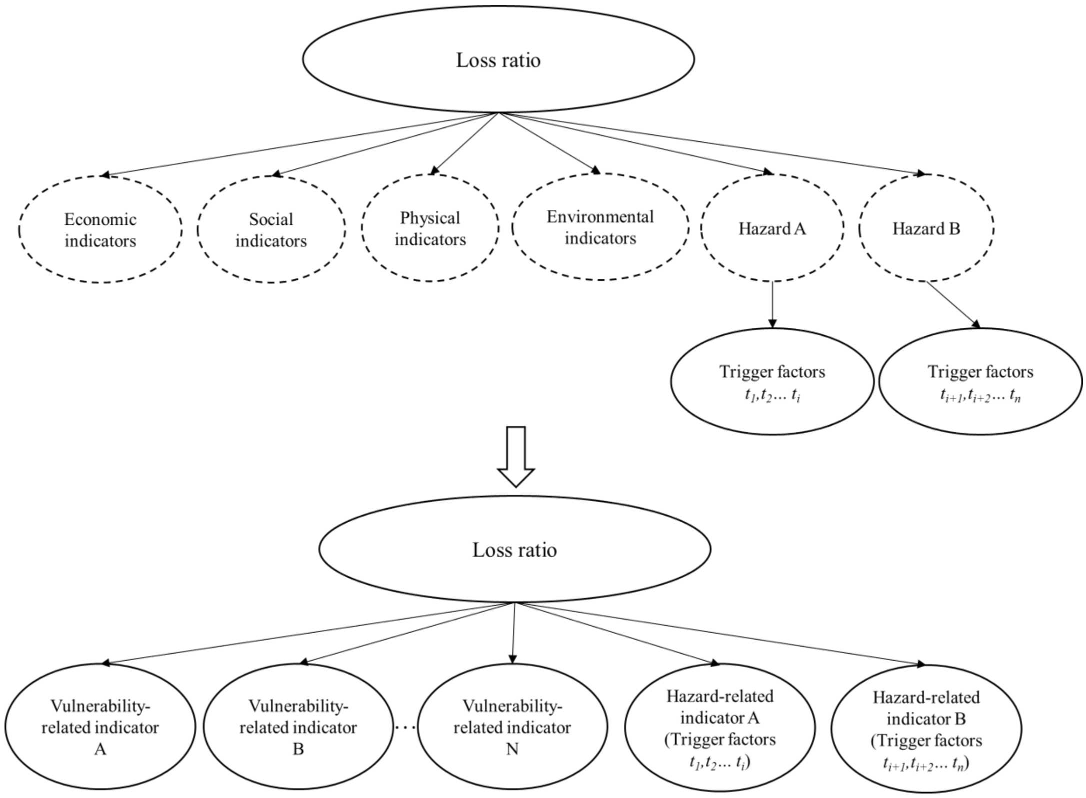

(a) Independent relationship

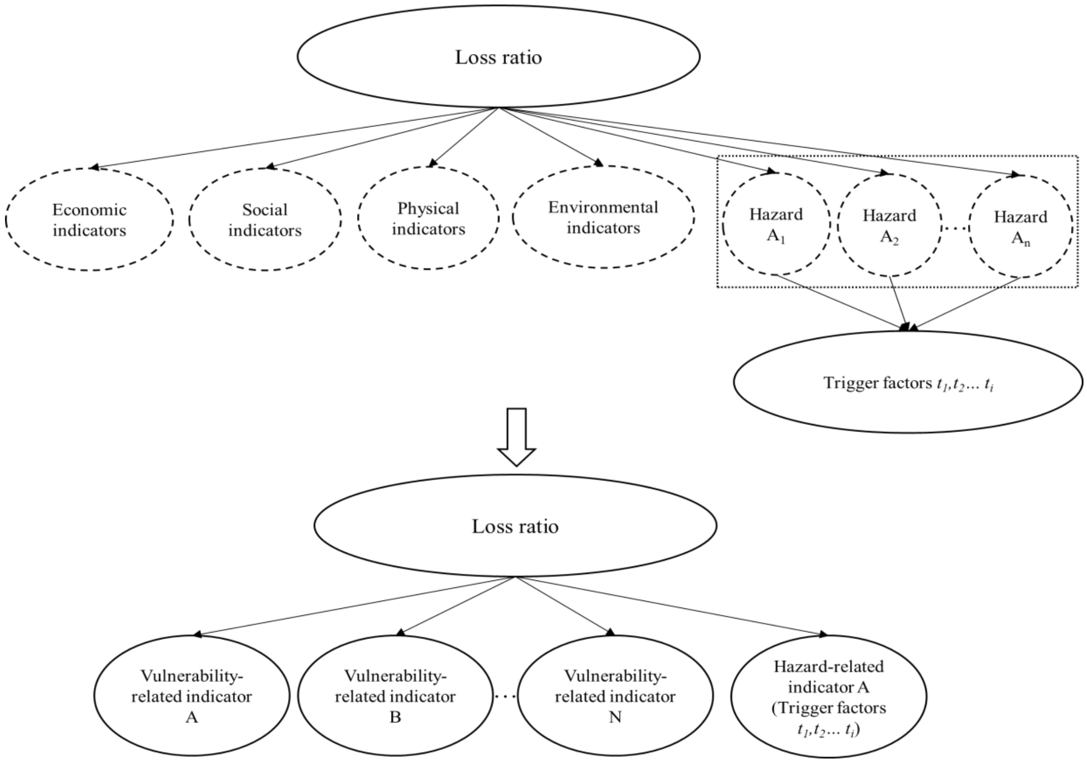

(b) Parallel relationship

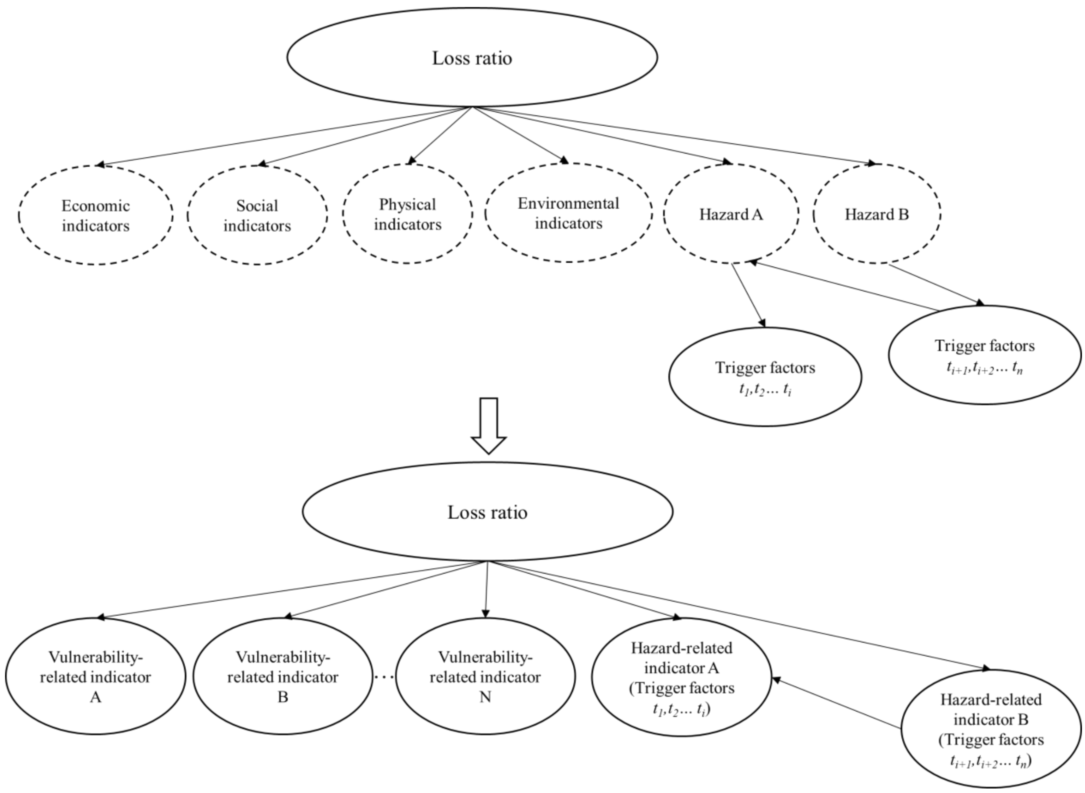

(c) Series relationship

Figure 4.3 Bayesian network frameworks for vulnerability analysis of multiple hazards with different relationships

In Figure 4.3c, hazard A and hazard B represent the series relationship. The changes in trigger factors t_1, $t_2 \ldots t_i$ induce hazard A, then the hazard A induces the changes in trigger factors $t_{i+1}, t_{i+2} \ldots t_n$. The changes in trigger factors t_{i+1}, $t_{i+2} \ldots t_n$ induce hazard B. Hence, the trigger factor group (t_1, $t_2 \ldots t_i$) is chosen as the hazard-related indicator to represent the magnitude of hazard A, and the trigger factor group (t_{i+1}, $t_{i+2} \ldots t_n$) is chosen as the hazard-related indicator to represent the magnitude of hazard B. The probability and degree of the changes in the trigger factor group (t_{i+1}, $t_{i+2} \ldots t_n$) are determined by the magnitude of hazard A, that is, the changes in the trigger factor group (t_1, $t_2 \ldots t_i$).

Hazards in mutex relationship cannot occur together, so the mutex relationship is not mentioned here.

4.6.2 Determining the conditional probability

A conditional probability measures the probability of an event given that another event has occurred. Once a BN framework is constructed, the conditional probability of each node given their parent nodes should be determined, that is, the conditional probability of a vulnerability-related indicator or hazard-related indicator given a loss ratio should be determined in this module (equation 4-31).

$$p(v_{kj} \mid L_i) \tag{4-31}$$

Where, L_i represent the i state of loss ratio L, $i=1,2,\ldots m$, and

v_{kj} represents the j state of vulnerability-related indicator or hazard-related indicator k, k=1,2, …s, $j=1, 2,\ldots n$.

Table 4.2 lists three commonly used methods for estimation of the conditional probability. When applied to a complete observed data set, maximum-likelihood estimation (MLE), a well-known statistical method is used to provide estimates for the model's parameters (the conditional probabilities) (Redner and Walker, 1984; Grossman and Domingos, 2004). If the model relies on incomplete observed data, an expectation–maximization (EM) algorithm, an iterative method for finding maximum likelihood estimates of parameters (conditional probabilities) in statistical models, can be used (Lauritzen, 1995; Friedman, 1998). When there is no observed data for the model, the model's parameters (conditional probabilities) can be estimated according to the domain knowledge (Heckerman et al., 1995; Liao and Ji, 2009). Hence, in this module, the methods used for estimation of conditional probabilities are determined according to the observed data situation.

Table 4.2 Methods for estimation of the conditional probability

Data situation	Methods
Complete observed data	Maximum-likelihood estimation
Incomplete observed data	Expectation-Maximization algorithm
Without observed data	Based on the Domain knowledge

4.6.3 Vulnerability assessment

In this step, given the above conditional probability, the joint probability (equation 4-32) is used to estimate the posteriori probability of the target loss ratio.

$$\begin{aligned} p(L, v_1, v_2, \cdots v_k \cdots v_s) &= p(L)\, p(v_1, v_2, \cdots v_k \cdots v_s \mid L) \\ &= p(L) \prod_{k=1}^{s} p(v_k \mid L) \end{aligned} \tag{4-32}$$

Where, L is the target variable loss ratio, and

v_k is the vulnerability-related indicator or hazard-related indicator k.

When the states of all vulnerability-related indicators and hazard-related indicators are given as j, the probability of loss ratio L_i occurring can be calculated based on the posteriori probability of the target loss ratio.

$$P(L_i) = \frac{p(L_i, v_{1j}, v_{2j}, \cdots v_{kj} \cdots v_{sj})}{\sum_{i=1}^{m} p(L_i, v_{1j}, v_{2j}, \cdots v_{kj} \cdots v_{sj})} \tag{4-33}$$

Where, L_i represent the i state of loss ratio L, $i=1,2,\ldots m$, and

v_{kj} represents the j state of vulnerability-related indicator or hazard-related indicator k, $k=1,2, \ldots s$.

Then the vulnerability, with given all vulnerability-related indicators and hazard-related indicators states j, can be calculated as equation (4-34).

$$Vul = \sum_{i=1}^{m} L_i \times P(L_i) \quad (4\text{-}34)$$

Where, L_i is the i state loss ratio with given all vulnerability-related indicators and hazard-related indicators states j, and

$P(L_i)$ is the corresponding probability of the target loss ratio L_i occurred.

The vulnerability with other states of vulnerability-related and hazard-related indicators can be calculated in the same way. This module can thus calculate the loss ratio induced by multi-hazards of different degree (different states in hazard-related indicators), whilst also addressing vulnerability using vulnerability-related indicators from physical, social, economic and environmental domains.

At this point, and based on the hazard identification, analysis, and interaction analysis, the exceedance probability of multiple hazards can be determined, and the corresponding loss calculated as the result of the exposure and vulnerability analyses (equation 4-35).

$$\textit{Loss} = \textit{Exposure} \times \textit{Vulnerability} = \textit{Value of the exposure} \times \textit{Loss ratio} \quad (4\text{-}35)$$

With the help of ArcGIS software, the possible loss caused by multi-hazard with different exceedance probabilities in each spatial assessment unit can be mapped. These maps can be used to identify which area is a high risk (large loss) area. Furthermore, through the hazard identification and vulnerability assessment, the kinds of hazards and types of vulnerability-related indicators that underpin large potential losses in a given area can be identified. This is significant, as such information supports, guides and targets the development of appropriate prevention and mitigation measures.

4.7 Summary and conclusion

This chapter has discussed the construction of a MHRA model (MmhRisk-HI) based on the approach and methods discussed in Chapter 3. The model calculates the possible loss caused by multiple hazards, with an explicit consideration of interaction between different hazards. It takes advantage of the merits of both risk index method and mathematical statistics method.

There are two main components in the MmhRisk-HI. The first component, including hazard identification, hazard analysis, hazard interaction analysis, is used to calculate the exceedance probability of multiple hazards occurrence. Stable factors are analysed to identify the spatial distribution of hazards with the Entropy-weight method in the hazard identification module. This considers all possible hazard situations even if some hazards have long return periods. The hazard analysis module is based on the multiple dimension information diffusion method to analyse the trigger factors for hazard magnitude-frequency analysis, and thus overcomes the problem of limited historical observation (short observation period relative to return period). The hazard interaction analysis module analyses the hazard interaction and calculates the exceedance probability of multiple hazards occurrence based on the results of the hazard identification and hazard analysis modules. All possible relationships among different hazards are considered in this module.

The second main component of the MmhRisk-HI focuses on the calculation of the possible loss caused by multiple hazards with different exceedance probabilities. In the exposure analysis module, the methods used for exposure analysis depend on the scale of the region to be addressed and the assessment units. The BN, used for vulnerability assessment, calculates the loss ratio induced by multi-hazard of different degree (different states in hazard-related indicators), and reflects how vulnerability-related indicators from physical, social, economic and environmental domains influence overall vulnerability.

Based on the hazard identification, analysis, and interaction analysis, the exceedance probability of multiple hazards can be calculated. The corresponding potential loss can then be calculated as the result of exposure analysis and vulnerability analysis. Finally, risk maps can be drawn with the exceedance probability of multi-hazard occurrence and corresponding loss. These maps can help to identify areas at high risk within the study region. With the results of the hazard identification and vulnerability assessment, the hazards and vulnerability-related indicators that underpin a high risk in a given area also can be identified.

The MmhRisk-HI fills a key research gap in the existing MHRA methods. This model calculates the possible loss caused by multiple hazards, with an explicit consideration of interaction between different hazards. The final results obtained in this model can help to identify which area is the high risk (large loss) area, and allow a determination of the reasons that contribute to large potential losses (high risk). In the next chapter, the YRD is used as a case study area to show the application of this model.

Chapter 5

Multi-hazard risk assessment in the Yangtze River Delta

The Yangtze River Delta (YRD) was introduced as a suitable region for multi-hazard risk appraisal in Chapter 3, and the construction of an improved multi-hazard risk assessment (MHRA) model, MmhRisk-HI, was introduced in Chapter 4. In this chapter, Chapter 5, the data from 1980-2012 are input to MmhRisk-HI to calculate the possible loss caused by multiple hazards and corresponding exceedance probability in the YRD. After model validation in section 5.2, the model results are analysed in section 5.3.

5.1 Model application

The YRD in China's central eastern coastal area was selected as the region to trial the improved MHRA model, MmhRisk-HI. The framework for MmhRisk-HI was introduced in Chapter 4, and the theoretical basis of the component modules (hazard identification, hazard analysis, hazard interaction analysis, exposure analysis, and vulnerability analysis) was discussed. The application of these modules in the overall MHRA model is discussed below.

5.1.1 Hazard identification in the Yangtze River Delta

The hazard identification module is used to identify which kinds of natural hazards occur in a given area and summarise the spatial distribution of these hazards. As mentioned in Chapter 3, the YRD, facing the Pacific to the east, is a typical floodplain with low, flat terrain and numerous rivers, lakes and canals. It is highly prone to various natural hazards. Due to the abundant rainfall and high channel density, the whole YRD is liable to frequent riverine floods. The YRD is coastal and an oceanic landform between Eurasia and the Pacific, so the coastal areas are susceptible to typhoons and coastal floods. The northern plain areas which are below an average altitude of 200 metres are vulnerable to pluvial floods, and southern hilly areas are likely to be influenced by some landslides and fast kinds riverine floods. The YRD is located in a relatively stable geological platform. Strong destroying earthquakes (over 7 magnitude) are unlikely to happen. Hence, this case study mainly focuses on typhoon, flood (slow kinds riverine flood, fast kinds riverine flood, coastal flood and pluvial flood) and landslide.

5.1.1.1 Stable factors selection in the Yangtze River Delta

Chapter 3 discussed how stable factors in the specific geophysical environment determine the preconditions for the occurrence of a specific natural hazard. According to the characteristic of these stable factors, the spatial distribution of natural hazards in a region can be deduced. Hence, stable factors for various hazards should first be identified for each county (139 in total) in the YRD.

Table 5.1 lists the stable factors selected as the preconditions to various hazards in the YRD. Typhoons cannot originate in the YRD region. However, typhoons which develop in the north western part of the Pacific Ocean can move thousands of kilometres, accompanied by strong winds and heavy rain to influence the whole YRD region. Hence, the distance to the origins of typhoon can be used as the stable factor for typhoon identification. Here, the north western part of the Pacific Ocean is at the south east of the YRD, so susceptibility to typhoon in the south eastern part of the YRD is higher than in the north western part. Therefore, the distance from each county to the south eastern most point of the YRD is selected as the stable factor to measure susceptibility to typhoon (Ho et al., 2004; Yuan et al., 2006).

Elevation and slope obtained from a Digital elevation model (DEM) can be used to express terrain (Bolstad and Stowe, 1994; Moore et al., 1999; Wilson and Gallant, 2000). Hence, the elevation and slope are calculated based on a DEM in each county. Lower average elevation area with slope ≤ 5 degree is used to represent flat and low-lying terrain. Higher average elevation area with slope>25 degree is used to represent hilly or mountainous terrain in this research (Yesilnacar and Topal, 2005; Fernández and Lutz, 2010).

Coastal belt buffer area is selected to represent the area exposed to coastal flood, and stream (lake, reservoir) buffer area is selected to represent the area exposed to riverine flood (Lane et al., 2003; Merz et al., 2007). Based on the historical disaster data, Fang et al. (2011) proved that the best coastal belt buffer distance for coastal flood risk assessment in the YRD is 20km, and the best stream (lake, reservoir) buffer distance for riverine flood risk assessment in the YRD is listed in Table 5.2. These buffer distances are thus adopted in this research.

Table 5.1 Stable factors as hazard preconditions in each county of the Yangtze River Delta

Hazards	Preconditions	Stable factors selection
Typhoon	Distance to origin	The distance to the south eastern most point of the YRD
Slow kinds riverine flood	Flat and low-lying terrain	Average elevation
		Percentage of slope ≤ 5 degree area
	River basins	Percentage of stream (lake, reservoir) buffer area
	Land surface with poor water infiltration capacity	Percentage of land cover with poor water infiltration capacity area
		Percentage of soil with poor water infiltration capacity
Fast kinds riverine flood	Hilly or mountainous terrain	Average elevation
		Percentage of slope >25 degree area
	River basins	Percentage of stream (lake, reservoir) buffer area
	Land surface with poor water infiltration capacity	Percentage of land cover with poor water infiltration capacity area
		Percentage of soil with poor water infiltration capacity
Coastal flood	Flat and low-lying terrain	Average elevation
		Percentage of slope ≤ 5 degree area
	Coastal region	Percentage of coastal belt buffer area
	Land surface with poor water infiltration capacity	Percentage of land cover with poor water infiltration capacity area
		Percentage of soil with poor water infiltration capacity
Pluvial flood	Flat and low-lying terrain	Average elevation
		Percentage of slope ≤ 5 degree area
	Land surface with poor water infiltration capacity	Percentage of land cover with poor water infiltration capacity area
		Percentage of soil with poor water infiltration capacity
Landslide	Hilly or mountainous terrain	Average elevation
		Percentage of slope >25 degree area
	Slope material with poor water absorption capacity	Percentage of land cover with poor water infiltration capacity area
		Percentage of soil with poor water infiltration capacity

Due to lack of some soil data and land cover data, land surface with poor water infiltration capacity is not considered in this study. These factors should be considered if such data are available.

Table 5.2 Buffer distance for different waterbodies in the Yangtze River Delta

Waterbody	Buffer distance (km)
Main rivers and first level branches in the basins (e.g. Yangtze river, Qiantang river)	8
Second level and below second level branches	6
Lakes, reservoirs (area>100km^2)	8
Lakes, reservoirs (area between 10-100km^2)	6
Lakes, reservoirs (area<10km^2)	4

(Note that the river classification follows the China's rivers name code (The Office of State Flood Control and Drought Relief Headquarters, 2000).)

(Sources: Fang et al., 2011; Xu et al., 2014)

5.1.1.2 Spatial distribution of single hazard in the Yangtze River Delta

With the given stable factors indicators, the susceptibility of each county to each hazard can be calculated based on the entropy-weight method.

$$S_i(H_k) = \sum_{j=1}^{n} w_j \; Nor\left(SF_j\right)_i \tag{5-1}$$

Where, for any given county *i*,
S is susceptibility,
H is hazard,
SF is stable factors,
$S_i(H_k)$ is susceptibility to hazard *k*, given stable factors SF_j,
$Nor(SF_j)_i$ is the normalization of stable factor *j* in county *i*, and
w_j is the weight for stable factor *j*.

The weights for stable factors to various hazards calculated by the entropy-weight method (equations 4-3 to 4-7) are shown in Table 5.3. Based on these weights, the susceptibility of each county to each individual hazard can be obtained. The results are shown in Figures 5.1 to 5.6.

Table 5.3 Weight for each stable factor in the Yangtze River Delta

Hazards	Stable factors	Entropy	Weight
Typhoon	The distance to the south eastern most point of the YRD	-	1
Slow kinds riverine flood	Average elevation	0.9923	0.1475
	Percentage of slope ≤ 5 degree area	0.9787	0.4073
	Percentage of stream (lake, reservoir) buffer area	0.9768	0.4452
Fast kinds riverine flood	Average elevation	0.8318	0.4001
	Percentage of slope >25 degree area	0.7868	0.5073
	Percentage of stream (lake, reservoir) buffer area	0.9611	0.0926
Coastal flood	Average elevation	0.9833	0.1399
	Percentage of slope ≤ 5 degree area	0.9616	0.3222
	Percentage of coastal belt buffer area	0.9360	0.5380
Pluvial flood	Average elevation	0.9923	0.2658
	Percentage of slope ≤ 5 degree area	0.9788	0.7342
Landslide	Average elevation	0.8318	0.4409
	Percentage of slope >25 degree area	0.7868	0.5591

Figure 5.1 shows that counties in the south eastern YRD are more susceptible to typhoon than those in the north western part. Figures 5.2 and 5.5 show that the distribution of slow kinds riverine flood and that of pluvial flood are similar, with counties in the north more susceptible than those in the south due to the terrain difference. Figures 5.3 and 5.6 show that the distribution of fast kinds riverine flood and that of landslide are basically the

same, with counties which are most susceptible to these two kinds of hazards mainly located in the south western part of the YRD. Figure 5.4 shows that counties in the northern coastal region are more susceptible to coastal flood than those in the southern coastal region.

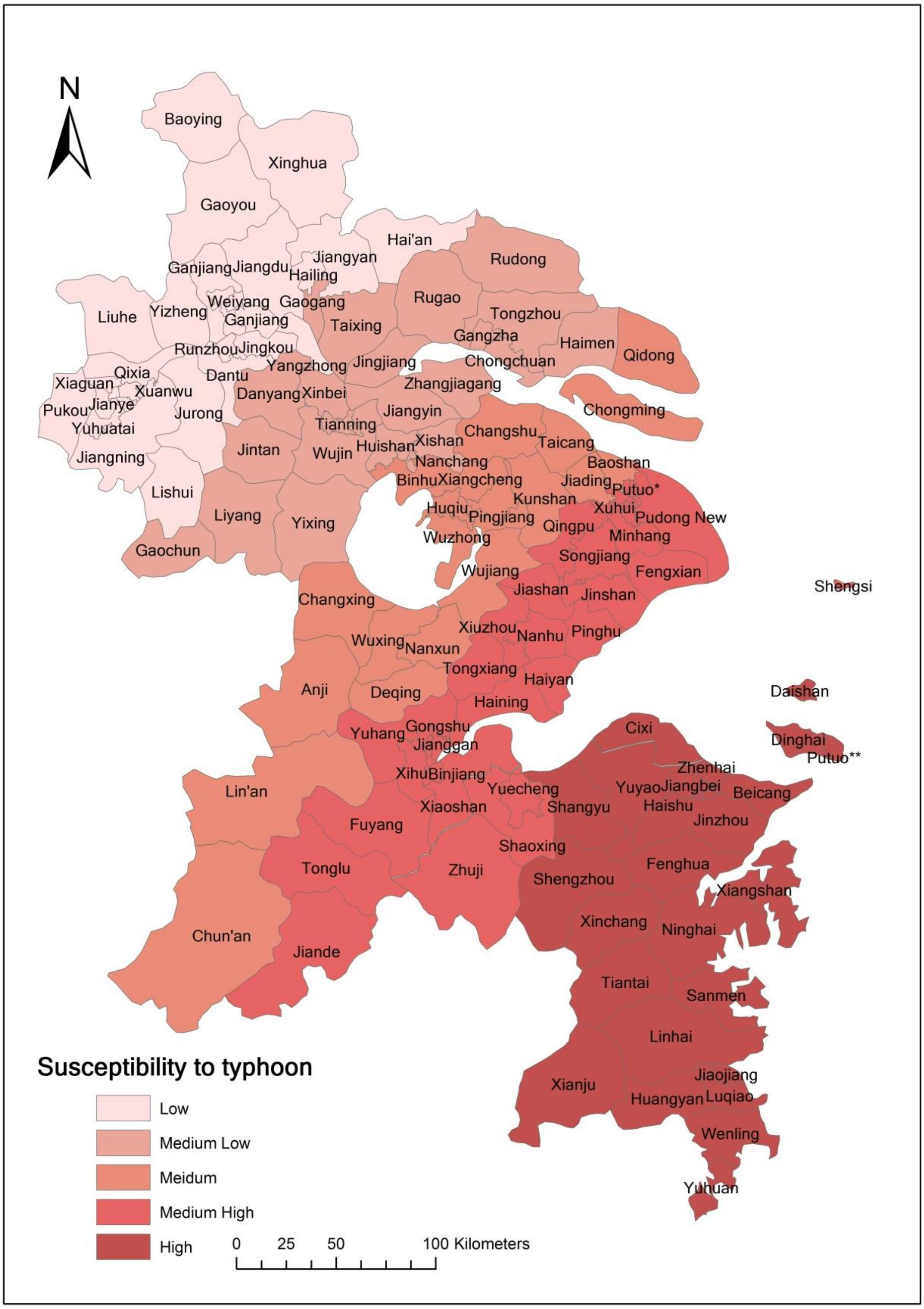

Figure 5.1 Spatial distribution of typhoon in the Yangtze River Delta

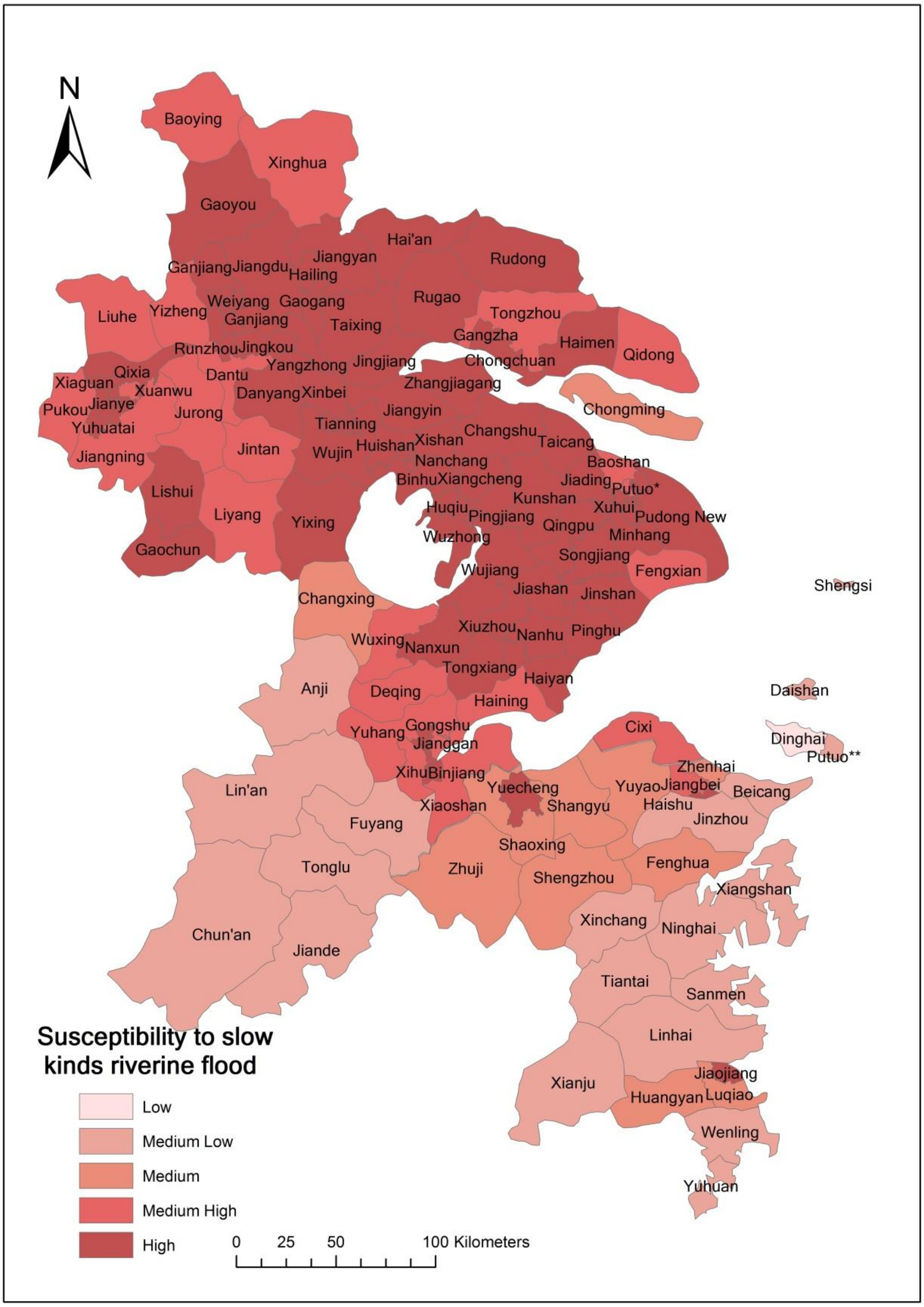

Figure 5.2 Spatial distribution of slow kinds riverine flood in the Yangtze River Delta

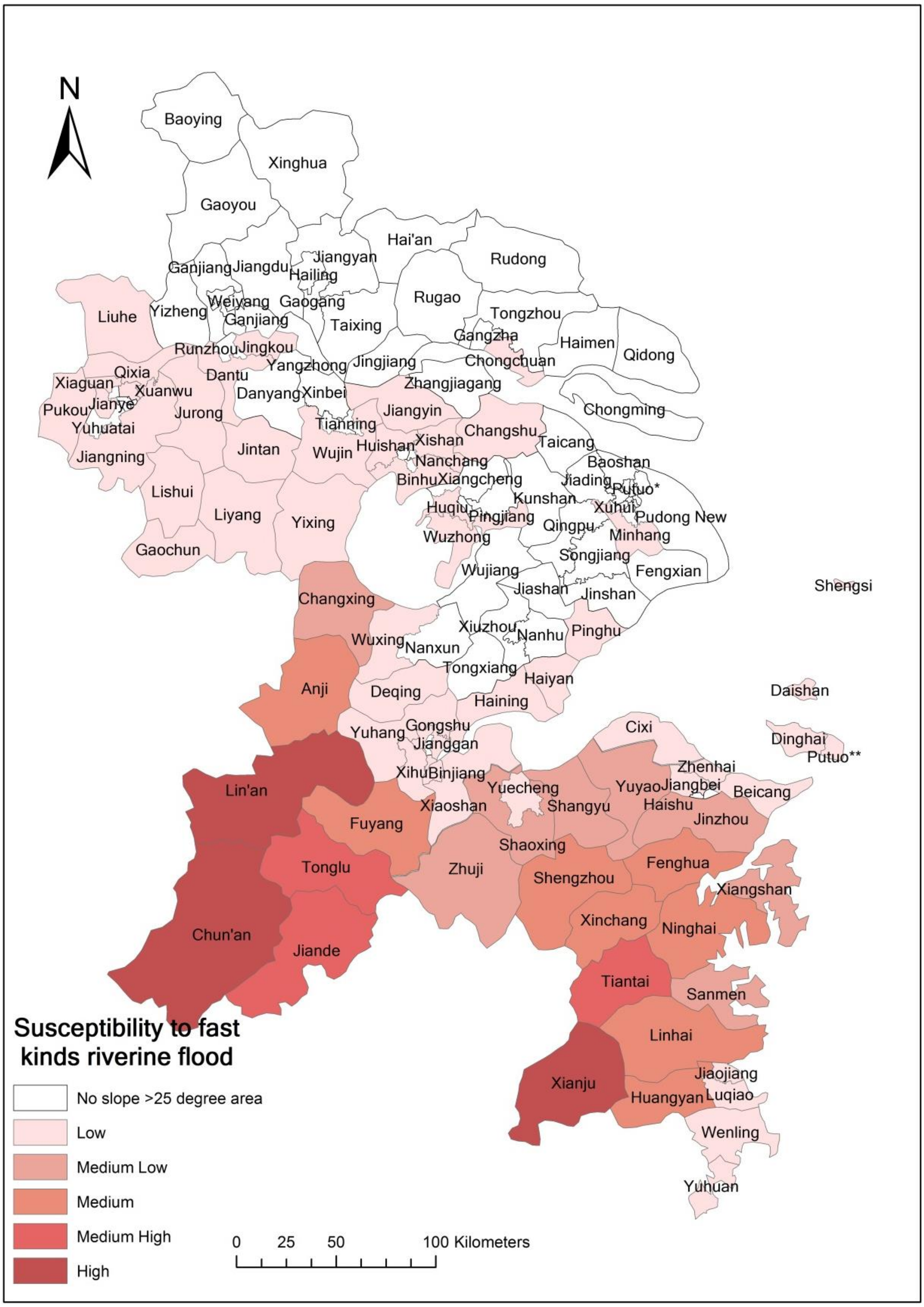

Figure 5.3 Spatial distribution of fast kinds riverine flood in the Yangtze River Delta

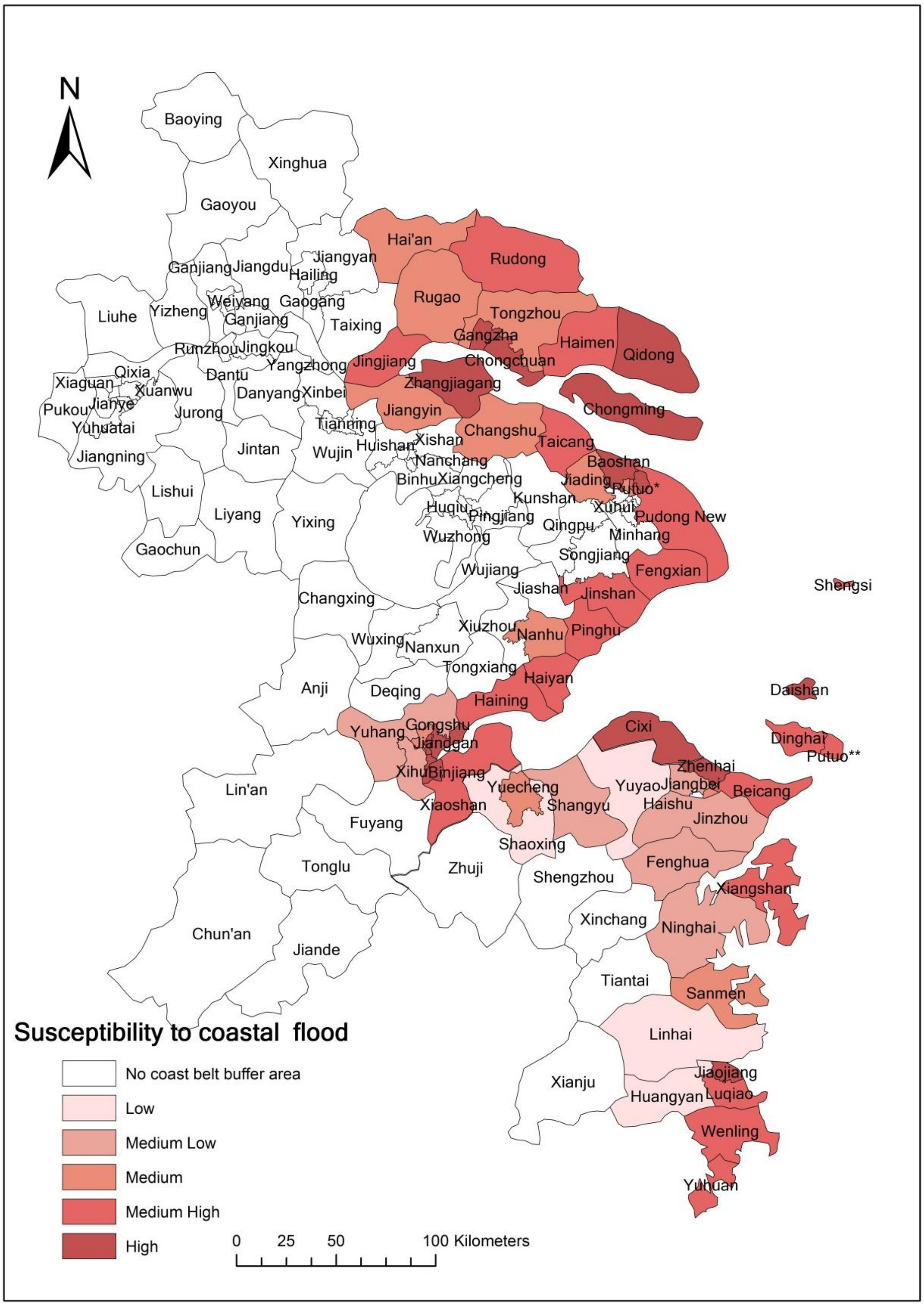

Figure 5.4 Spatial distribution of coastal flood in the Yangtze River Delta

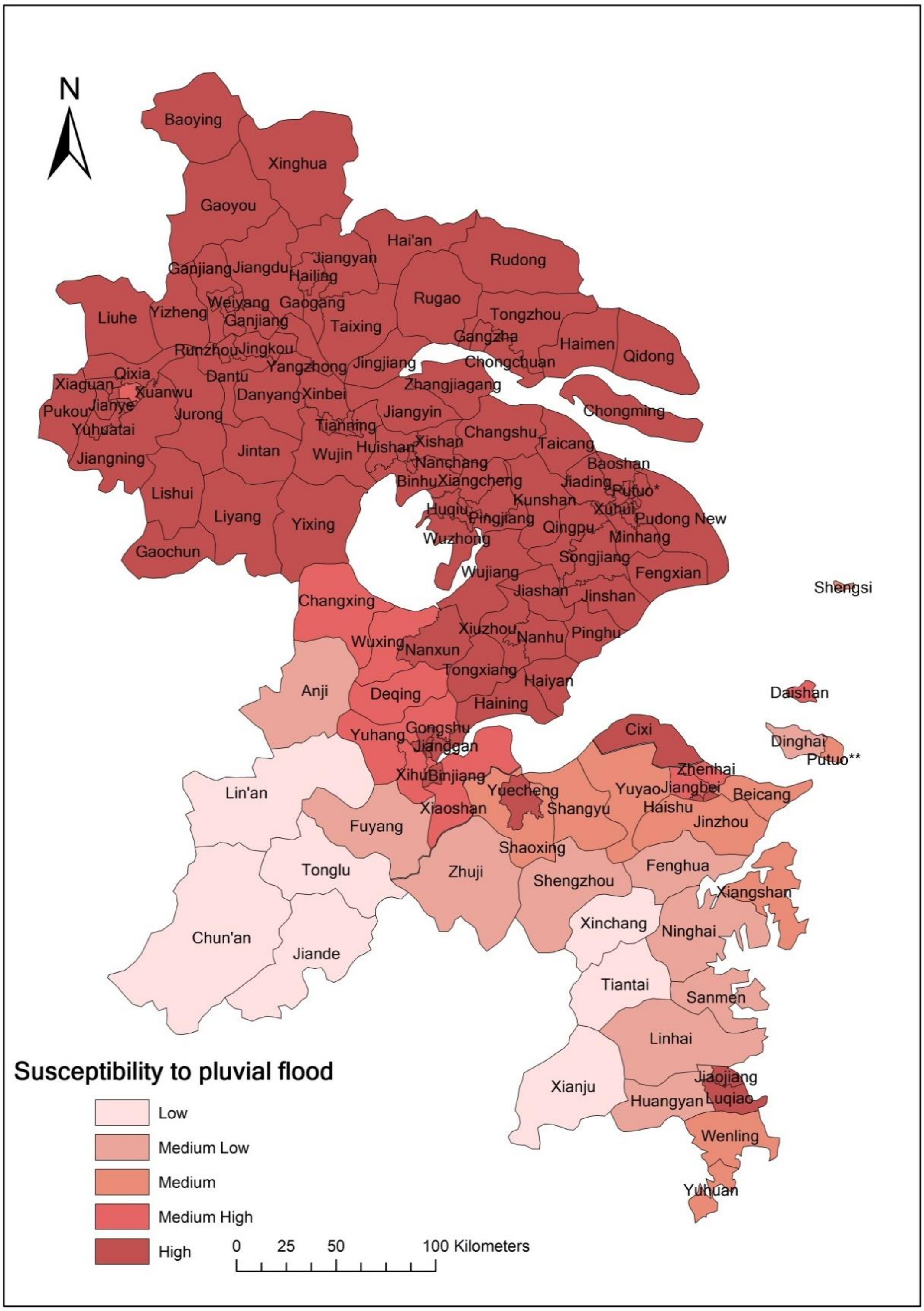

Figure 5.5 Spatial distribution of pluvial flood in the Yangtze River Delta

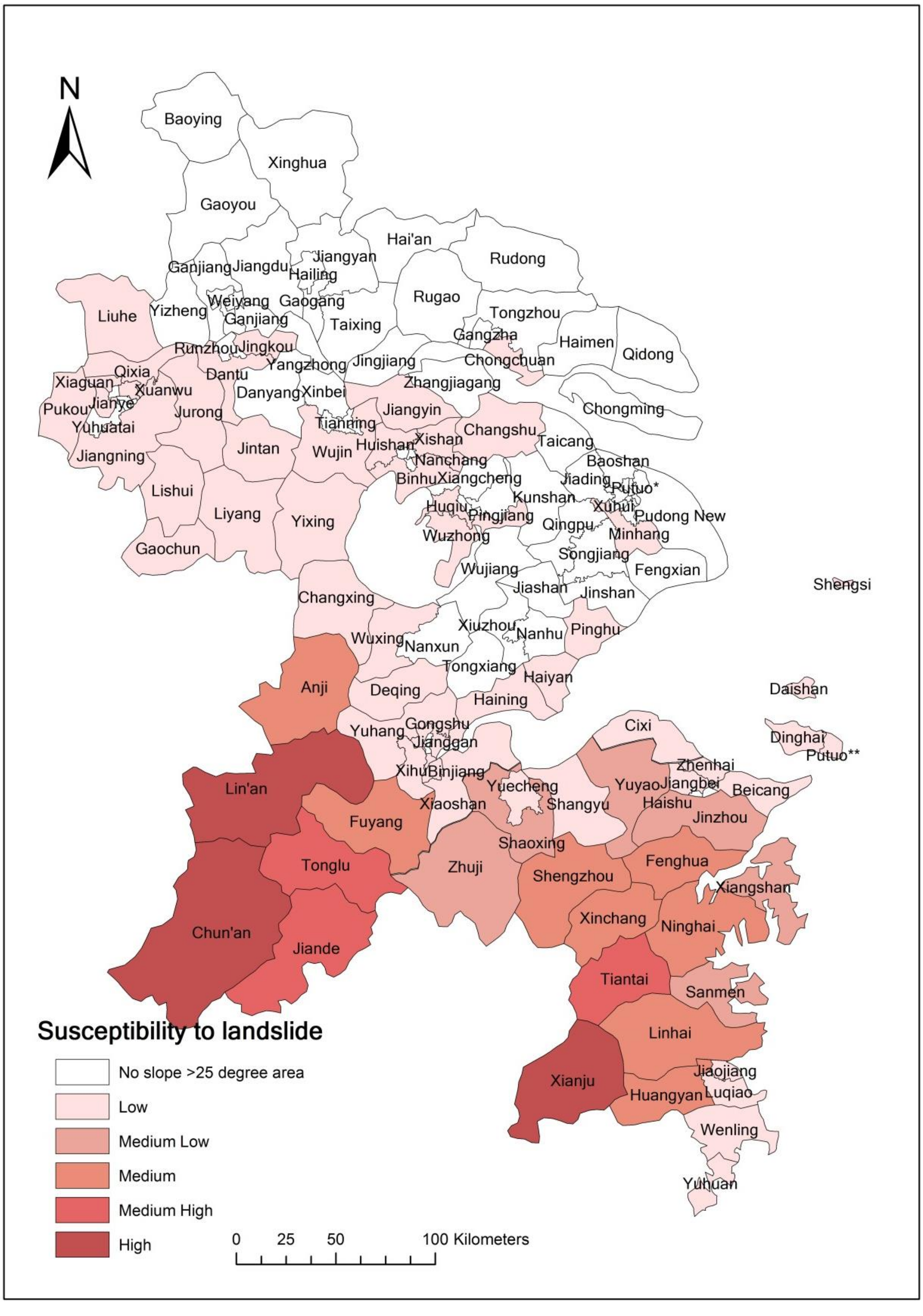

Figure 5.6 Spatial distribution of landslide in the Yangtze River Delta

5.1.1.3 Spatial distribution of multi-hazard in the Yangtze River Delta

Based on the single hazard maps (Figures 5.1 to 5.6), the whole YRD area is divided into four zones according to the types of hazards in each county (Figure 5.7). Counties in zone I are susceptible to three kinds of hazards, typhoon, slow kinds riverine flood and pluvial flood. Counties in zone II are susceptible to four kinds of hazards, typhoon, slow kinds riverine flood, pluvial flood and coastal flood. Counties in zone III are susceptible to five kinds of hazards, typhoon, slow kinds riverine flood, fast kinds riverine flood, pluvial flood and landslide. Counties in zone IV are susceptible to all six natural hazards (as zone III plus coastal flood), typhoon, slow kinds riverine flood, fast kinds riverine flood, pluvial flood, coastal flood and landslide. The susceptibility of each county to each hazard in the four zones is shown in Appendix A. This regionalization is helpful in identifying the multi-hazard situation in each county, and thus is the basis for hazard interaction analysis.

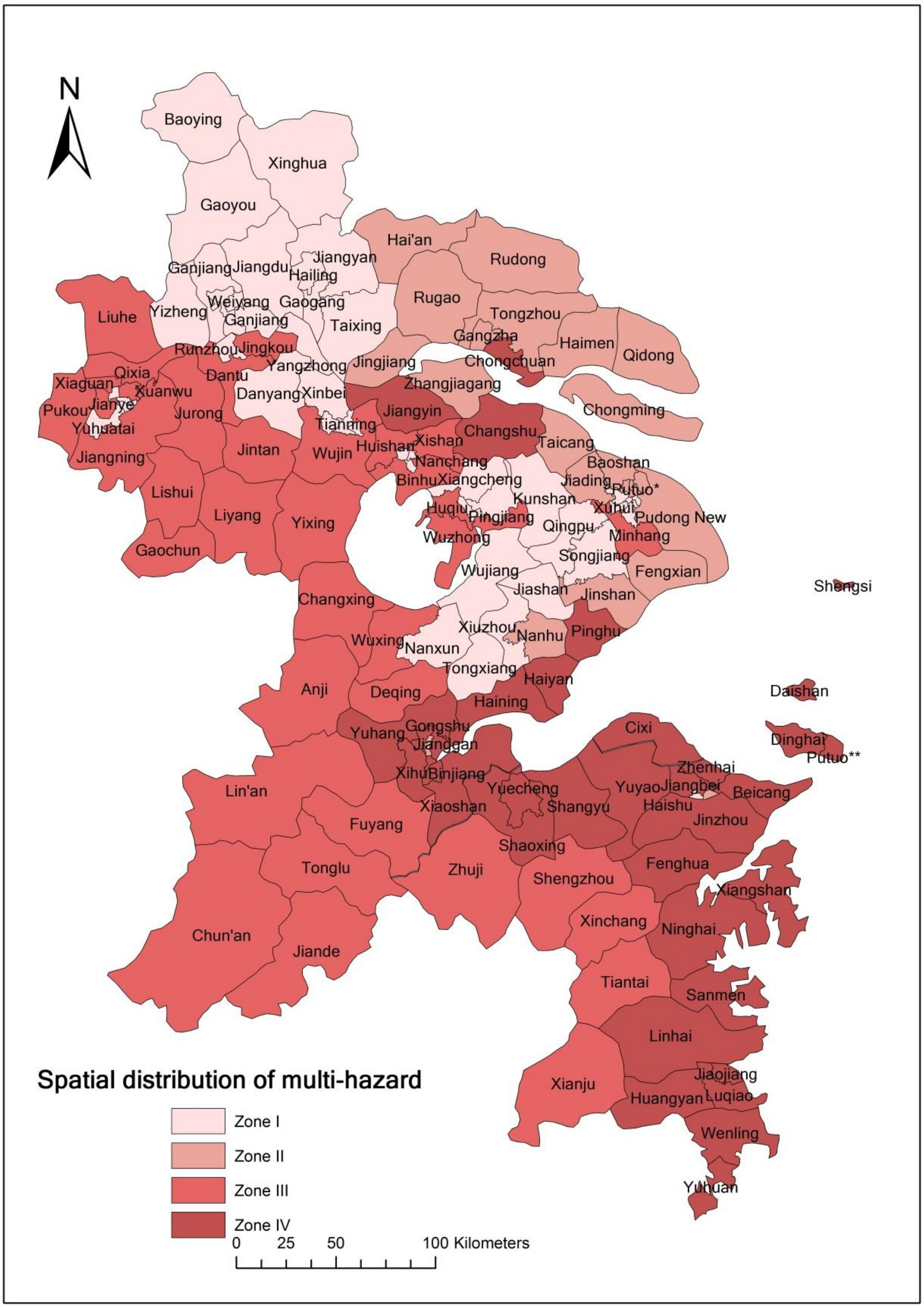

Figure 5.7 Spatial distribution of multi-hazard in the Yangtze River Delta

Zone I: typhoon, slow kinds riverine flood, pluvial flood. Zone II: typhoon, slow kinds riverine flood, pluvial flood and coastal flood. Zone III: typhoon, slow kinds riverine flood, fast kinds riverine flood, pluvial flood and landslide Zone IV: typhoon, slow kinds riverine flood, fast kinds riverine flood, pluvial flood, coastal flood and landslide.

5.1.2 Hazard analysis in the Yangtze River Delta

Various natural hazards have been identified for the YRD. As mentioned in section 2.1.2.2, for these natural hazard events, a strong nonlinear relationship between event magnitude and frequency exists. Hazard analysis is the process used to analyse this relationship, to give the probability of occurrence of hazards of different magnitudes.

5.1.2.1 Trigger factors selection in the Yangtze River Delta

The relationships between trigger factors and major natural hazards were discussed in Chapter 3. Substantial changes in trigger factors are the main reason that some hazards are induced, thus trigger factors can be used to estimate both the frequency and magnitude of hazards, with the change of degree in trigger factors representing the magnitude of hazards, and the probability of the change in trigger factors representing the probability of the hazard. Hence, trigger factors for various hazards should first be identified for hazard analysis in the YRD.

Table 5.4 lists the possible trigger factors for hazards in the YRD according to the hazard-forming environment. As stated in section 3.2.1.1, the movement of typhoon is accompanied by strong winds and heavy rain, and a series of hazards induced by the changes of winds and rainfall are the reasons to cause loss in the track. Thus, typhoon can be viewed as changes of wind speed and rainfall, with these changes used as the trigger factors to measure the magnitude of the series of hazards in the track.

In the YRD, all flood types and landslide might be induced in the typhoon track, hence maximum daily rainfall and maximum wind speed during the typhoon period are selected to measure the frequency and magnitude of these hazards. Besides, non-typhoon rainfall is also the main reason to induce all flood types and landslide in the YRD; thus, the maximum daily rainfall during the non-typhoon rainfall days is also selected as the trigger factor for these hazards. Slow kinds riverine flood and coastal floods can also be induced by high tides, but due to a lack of tide level data, high tides are not included in the MHRA YRD model. Maximum daily rainfall and maximum wind speed data from 1980 to 2012, collected from 24 meteorological stations in the YRD are used in the analysis (Figure 3.12).

Table 5.4 Trigger factors for hazards in the Yangtze River Delta

Hazards	Trigger factors	Factors selection
Typhoon	Typhoon is viewed as the changes of wind speed and rainfall	Maximum daily rainfall
		Maximum wind speed
Slow kinds riverine flood	Typhoon	Maximum daily rainfall
		Maximum wind speed
	Non-typhoon rainfall	Maximum daily rainfall
	High tides	Maximum tide level
Fast kinds riverine flood	Typhoon	Maximum daily rainfall
		Maximum wind speed
	Non-typhoon rainfall	Maximum daily rainfall
Coastal flood	Typhoon	Maximum daily rainfall
		Maximum wind speed
	Non-typhoon rainfall	Maximum daily rainfall
	High tides	Maximum tide level
Pluvial flood	Typhoon	Maximum daily rainfall
		Maximum wind speed
	Non-typhoon rainfall	Maximum daily rainfall
Landslide	Typhoon	Maximum daily rainfall
		Maximum wind speed
	Non-typhoon rainfall	Maximum daily rainfall

5.1.2.2 Exceedance probability calculation in the Yangtze River Delta

With the given trigger factor indicators, the frequency and magnitude of various hazards in each county can be calculated based on the multiple dimension information diffusion method.

Maximum daily rainfall and maximum wind speed during each historical typhoon are selected to measure the frequency and magnitude of the four flood types, and landslide induced by the typhoon. The probability distribution of the rainfall and wind speed sets is calculated by the two dimension information diffusion method (equations 4-10 to 4-20). The wind speed universe is defined as {0, 1, 2,…50}m/s, and the daily rainfall universe is defined as {0, 10, 20,…500}mm. The information carried by each sample set (maximum daily rainfall and maximum wind speed in the historical typhoon record) is diffused to these two universes according to the diffusion function. The results in 24 meteorological sites are shown in Appendix B, and 3 sites are used as cases to be shown in Figure 5.8.

In Figure 5.8, x-axis is the maximum daily rainfall, z-axis is the maximum wind speed, and y-axis is the exceedance probability of the corresponding rainfall and wind speed sets. From Figure 5.8, the maximum daily rainfall and maximum wind speed with different exceedance probabilities in these 24 meteorological sites can be obtained. Then, a spatial interpolation technique is used to estimate the rainfall and wind distribution in the whole YRD. According to the literature, Kriging performs best amongst spatial interpolation techniques for meteorological data (Tabios and Salas, 1985; Li et al., 2006; Di Piazza et al., 2011), and thus Kriging is adopted in this research. Exceedance probabilities of 5% and 10% are shown in Figures 5.9 and 5.10 for maximum daily rainfall and wind speed respectively, with further results shown in Appendix C. For example, Figure 5.9a shows that the probability of maximum daily rainfall being equal to or greater than the value shown in this Figure is 5%. The maximum daily rainfall distribution and maximum wind speed distribution with exceedance probabilities of 5% and 10% are basically similar. The value in the south eastern part is higher than the north western part.

Using the same method, the maximum daily rainfall distribution with different exceedance probabilities in non-typhoon rainfall also can be calculated. This can be used to measure the frequency and magnitude of flood and landslide induced by the non-typhoon rainfall.

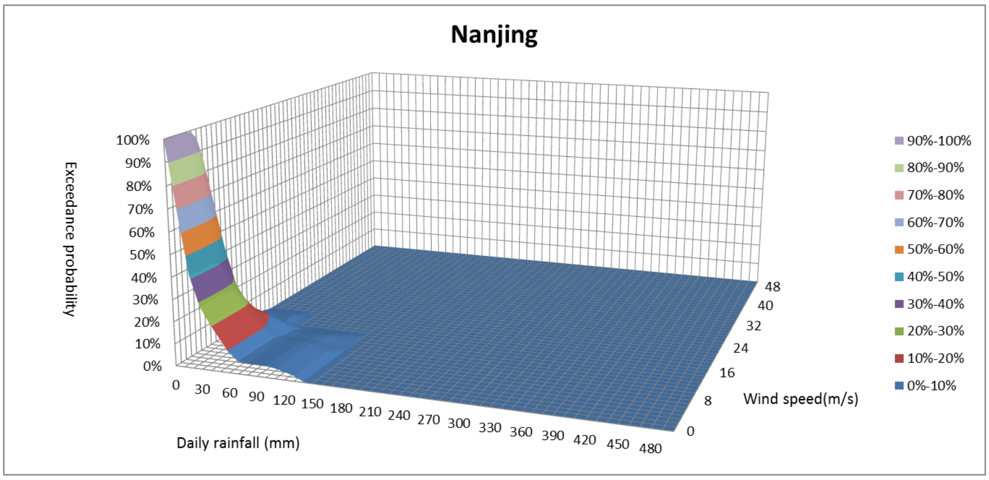

(a) Nanjing

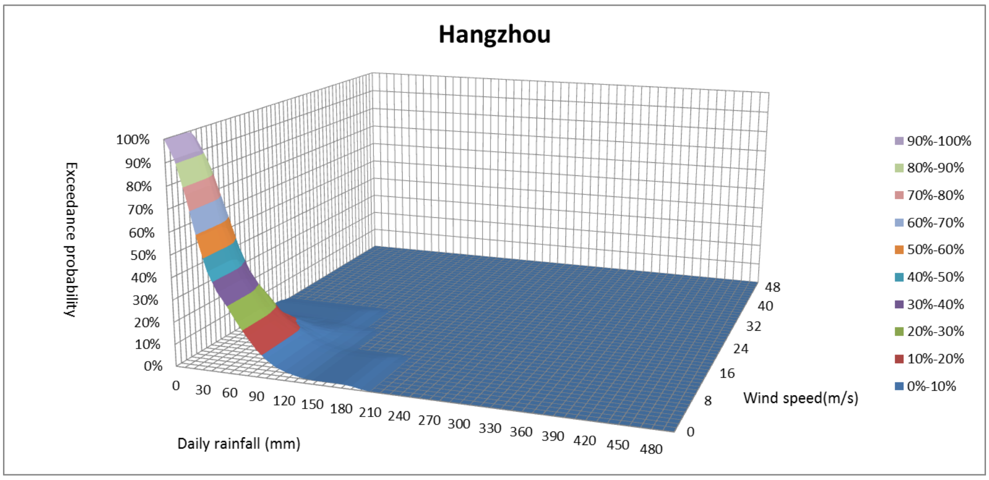

(b) Hangzhou

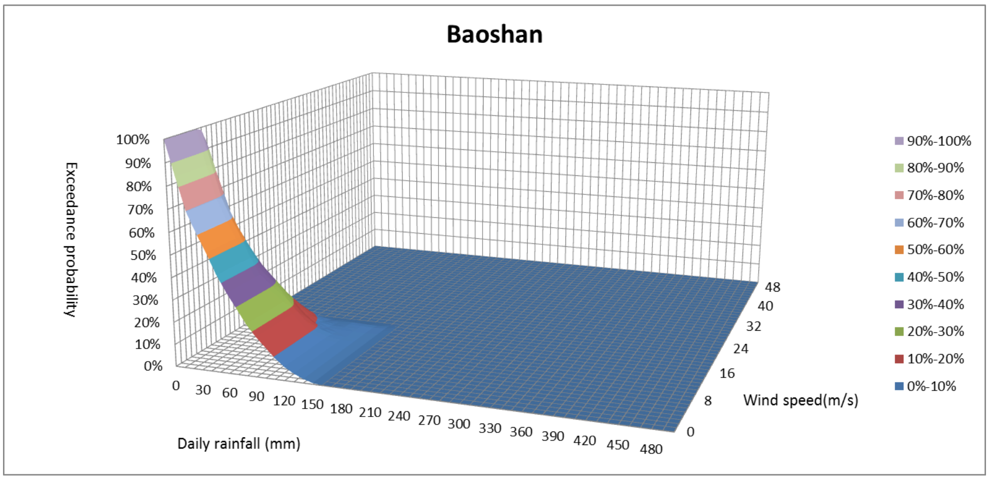

(c) Baoshan

Figure 5.8 Exceedance probability distribution of rainfall and wind speed sets

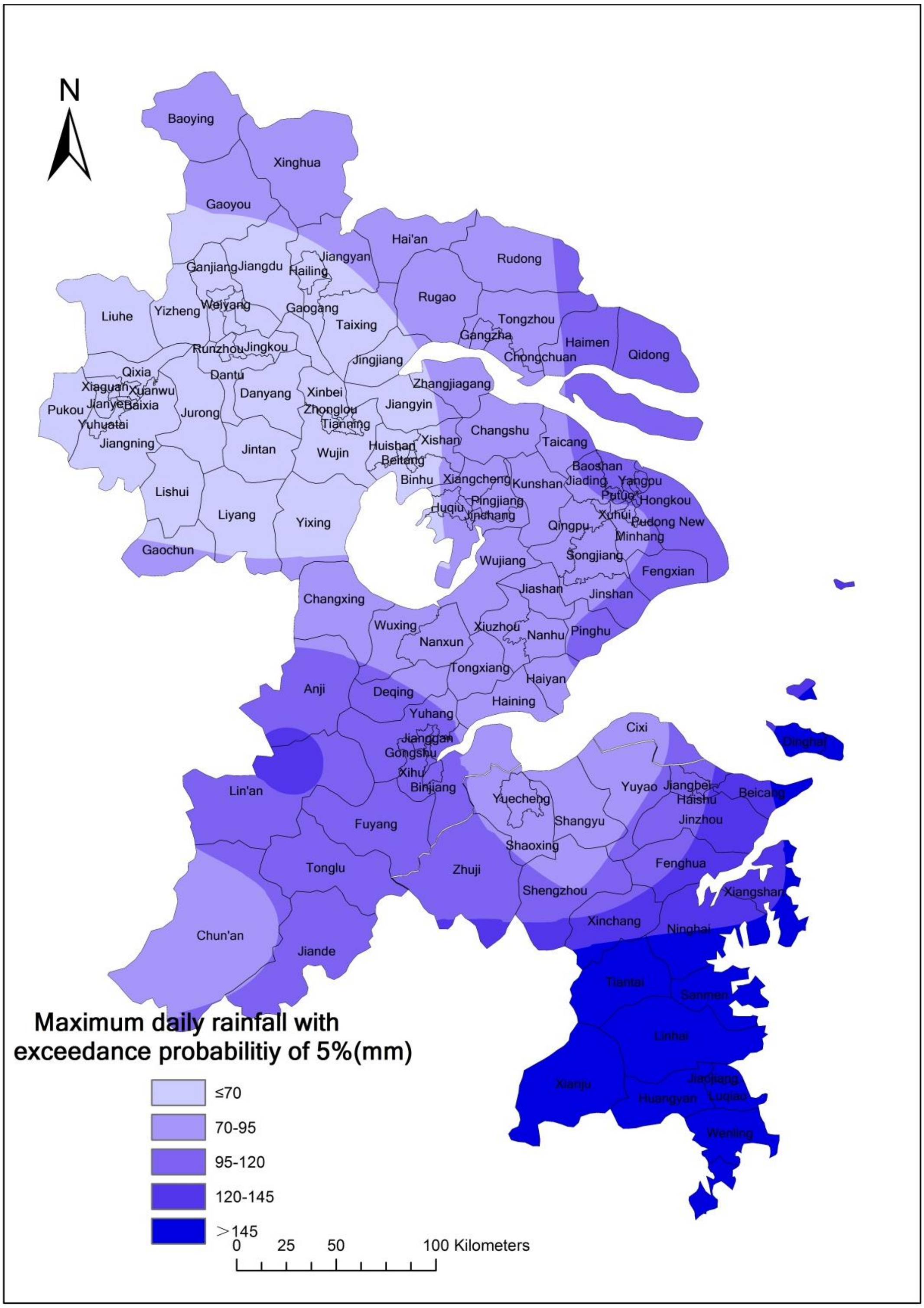

(a) Maximum daily rainfall distribution with exceedance probability of 5%

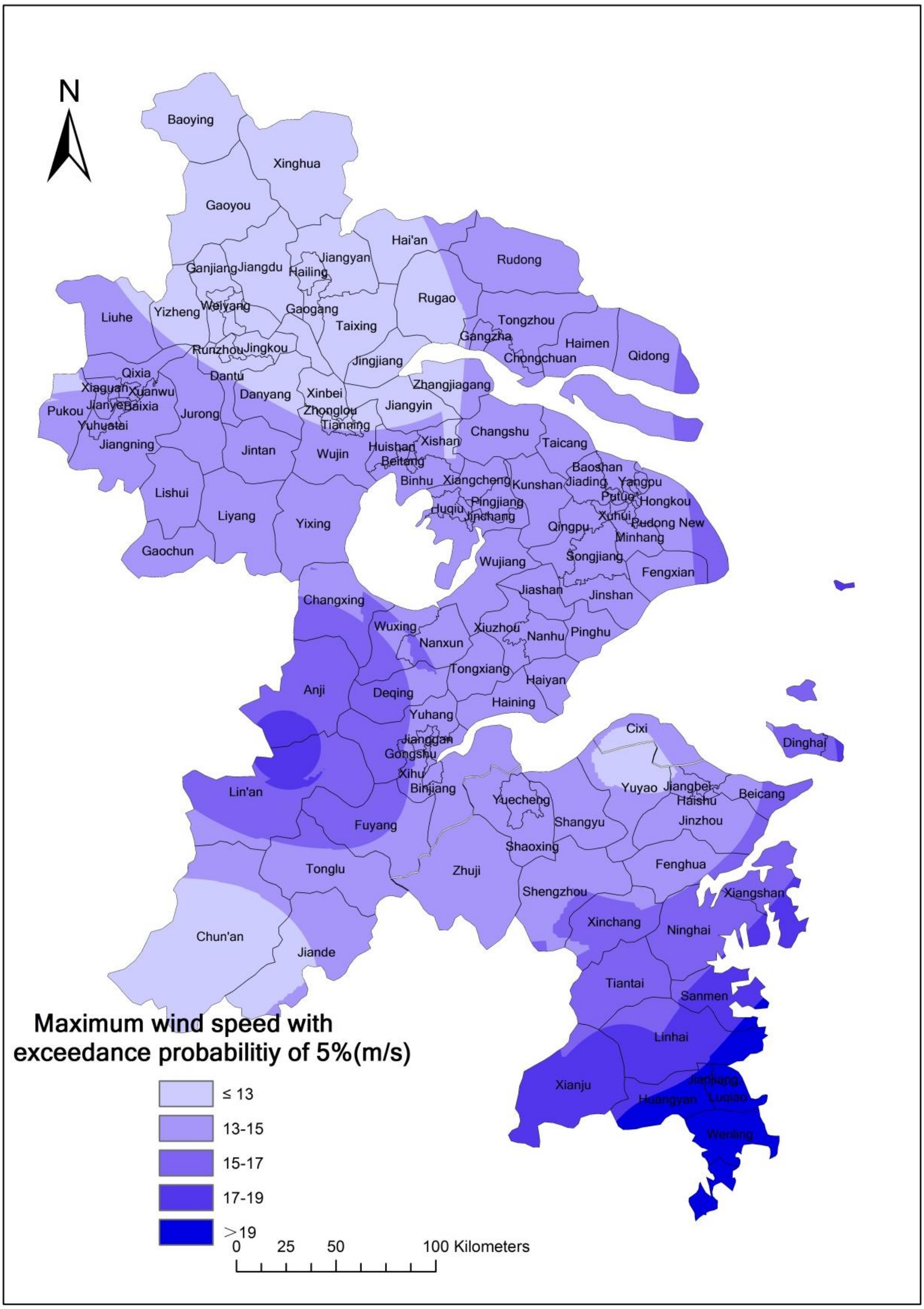

(b) Maximum wind speed distribution with exceedance probability of 5%

Figure 5.9 Distribution of maximum daily rainfall and maximum wind speed with exceedance probability of 5%

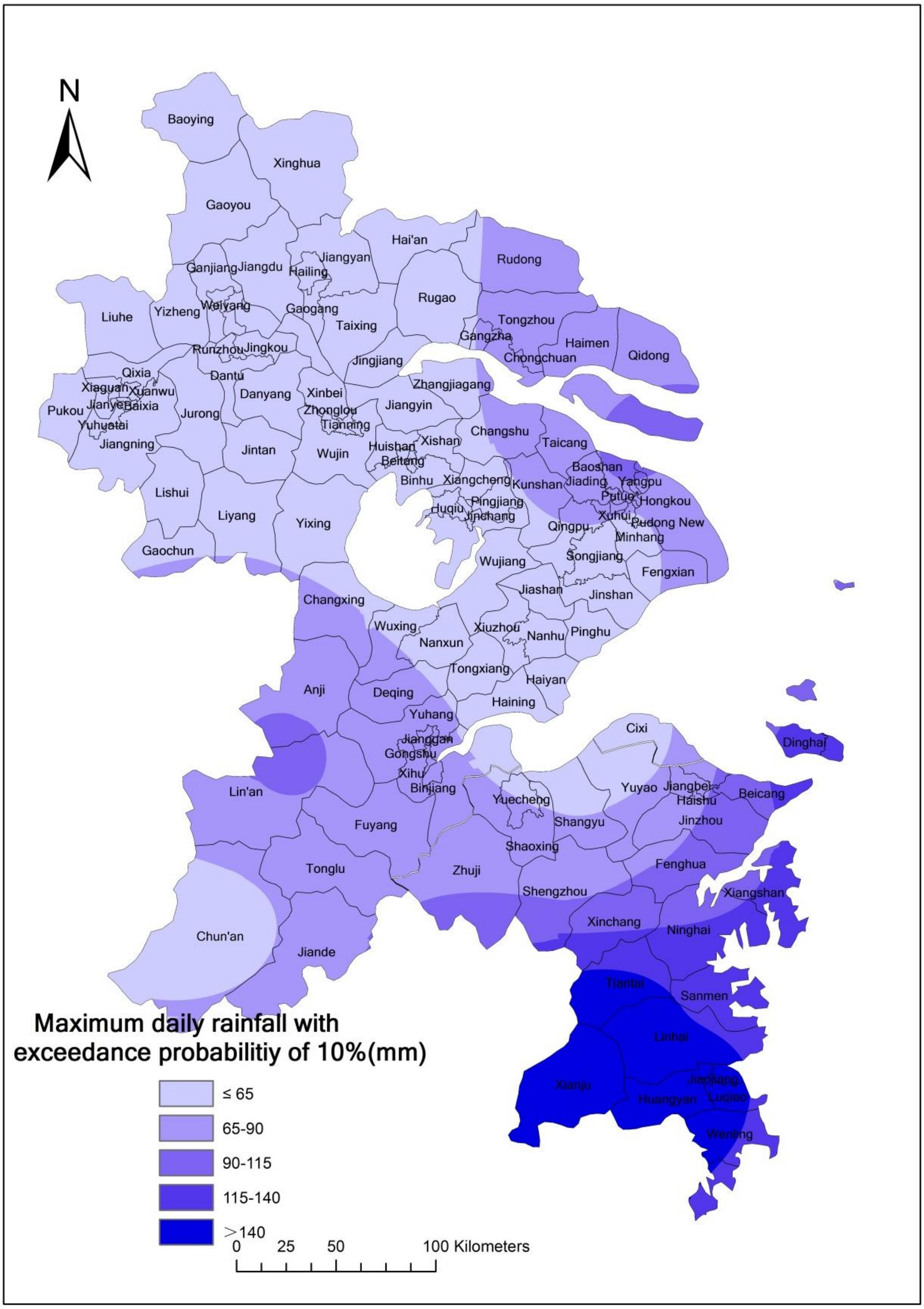

(a) Maximum daily rainfall distribution with exceedance probability of 10%

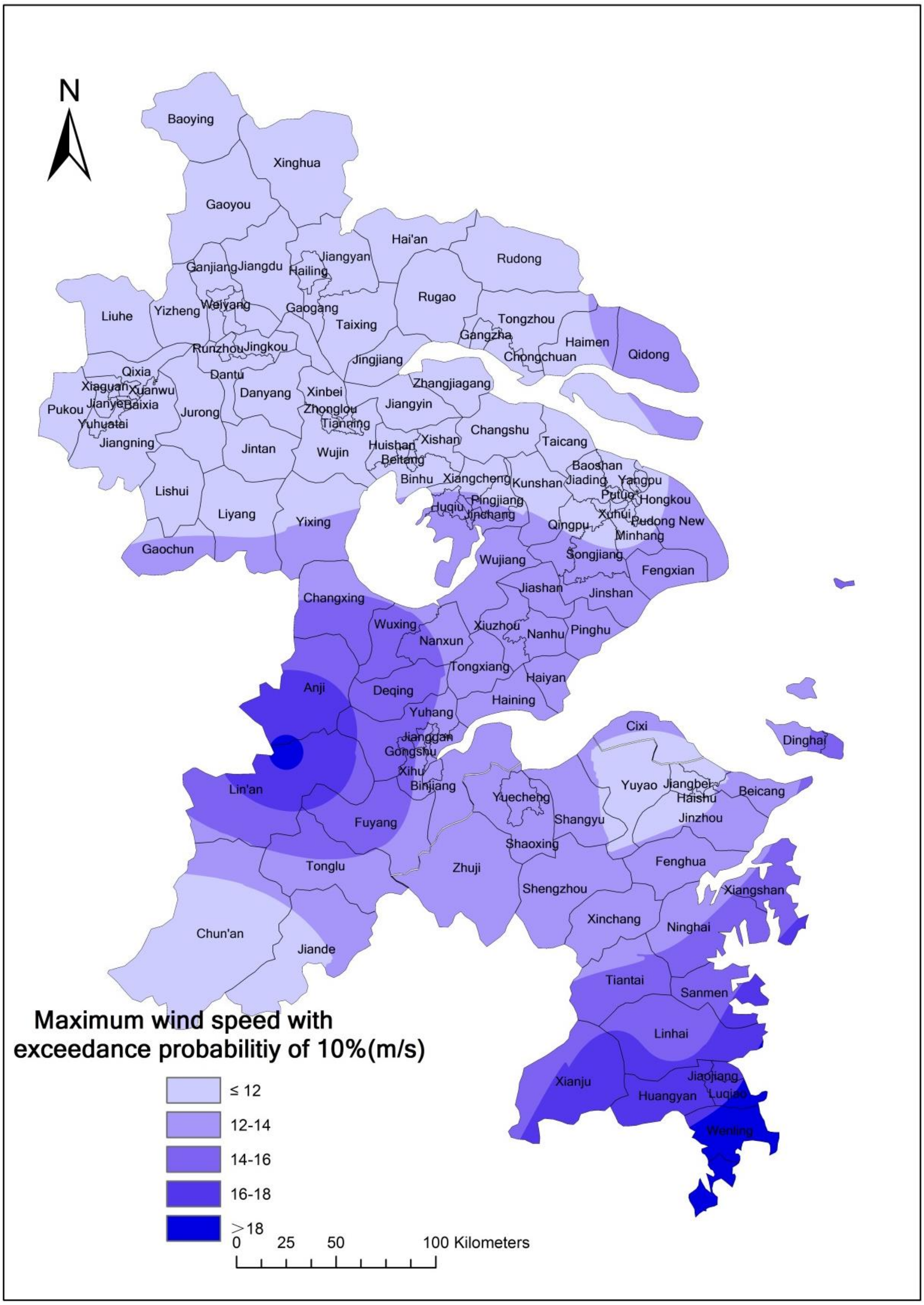

(b) Maximum wind speed distribution with exceedance probability of 10%

Figure 5.10 Distribution of maximum daily rainfall and maximum wind speed with exceedance probability of 10%

5.1.3 Hazard interaction analysis in the Yangtze River Delta

Hazard interaction analysis is used to calculate the probability of multiple hazards occurring together, given different types of possible relationships. In Figure 5.7 (section 5.1.1), the YRD was divided into four zones according to the types of hazards. Hazard interaction is analysed respectively in these four zones. According to the trigger factors for various hazards in the YRD, the relationships among multiple hazards in the YRD can then be shown (Figures 5.11 to 5.14).

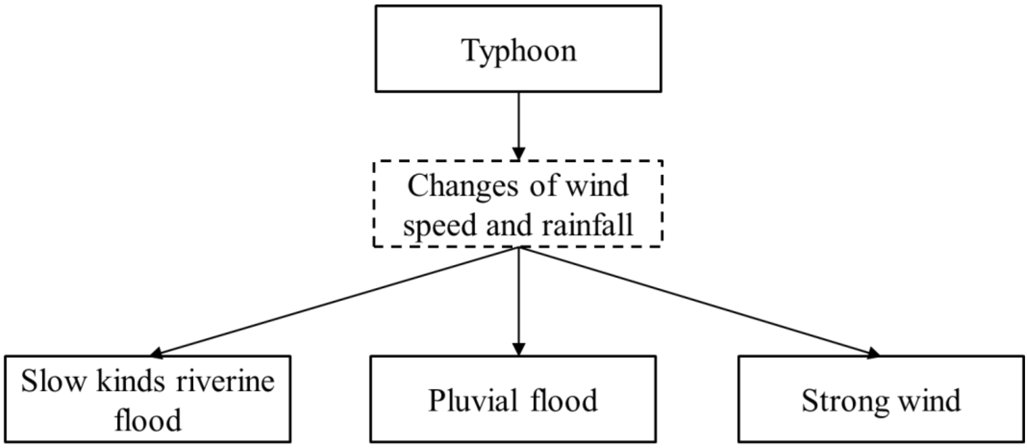

(a) Typhoon as trigger factor

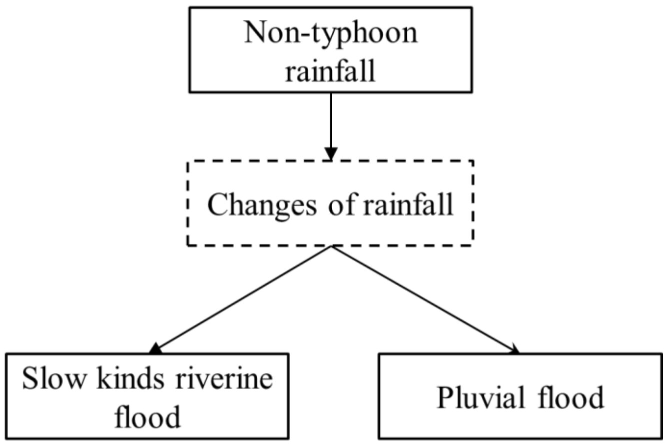

(b) Non-typhoon rainfall as trigger factor

Figure 5.11 The relationships among multiple hazards in zone I in the Yangtze River Delta

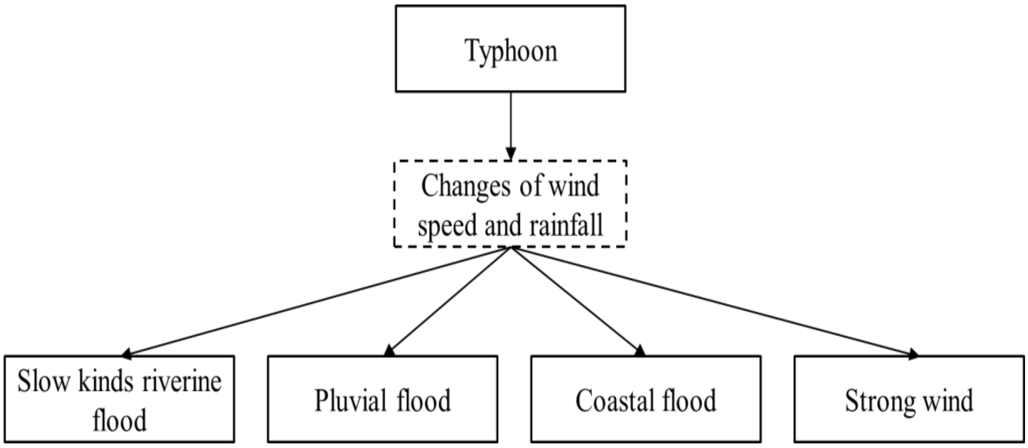

(a) Typhoon as trigger factor

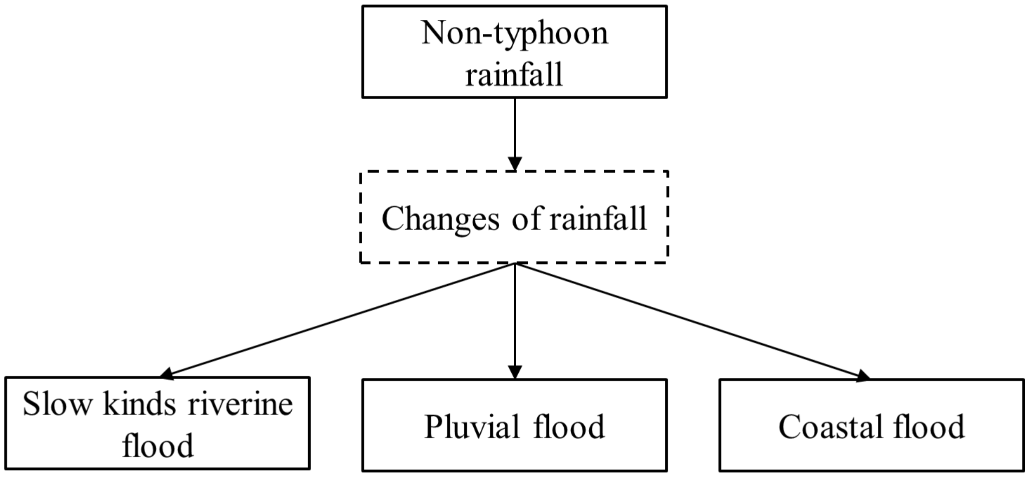

(b) Non-typhoon rainfall as trigger factor

Figure 5.12 The relationships among multiple hazards in zone II in the Yangtze River Delta

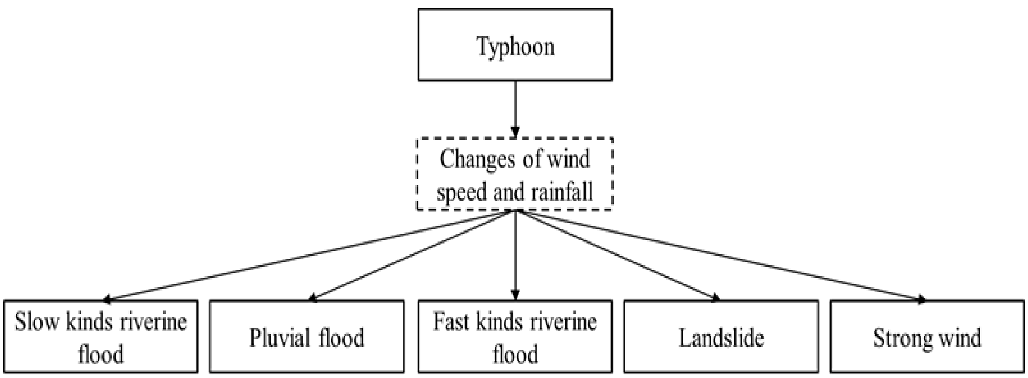

(a) Typhoon as trigger factor

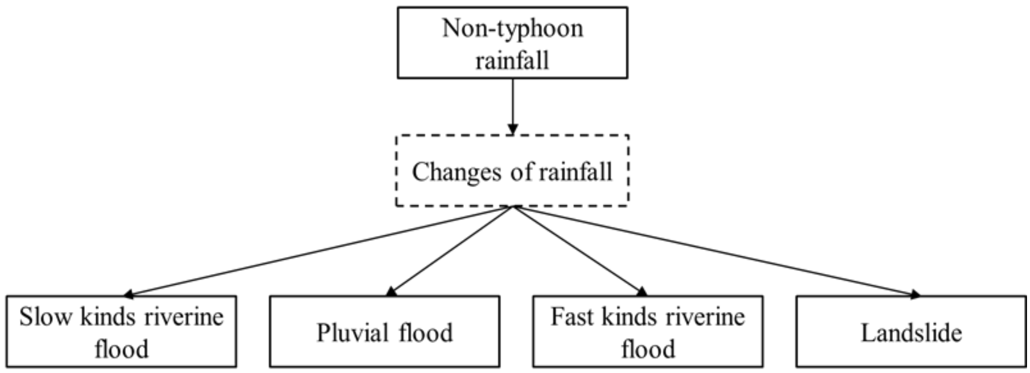

(b) Non-typhoon rainfall as trigger factor

Figure 5.13 The relationships among multiple hazards in zone III in the Yangtze River Delta

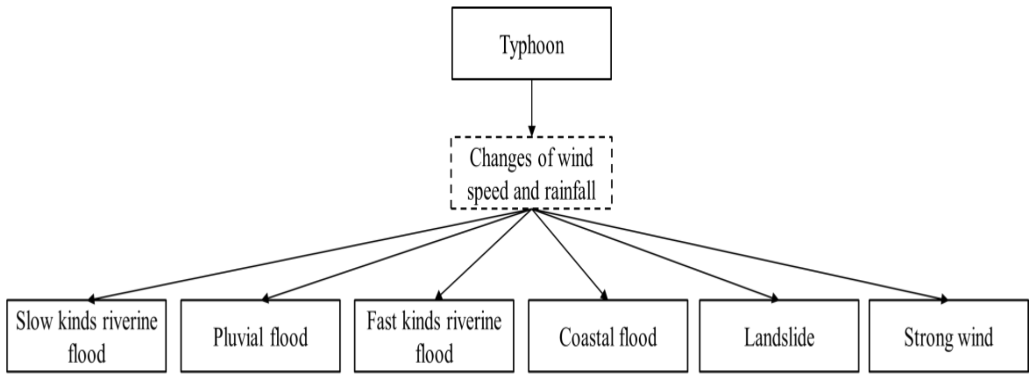

(a) Typhoon as trigger factor

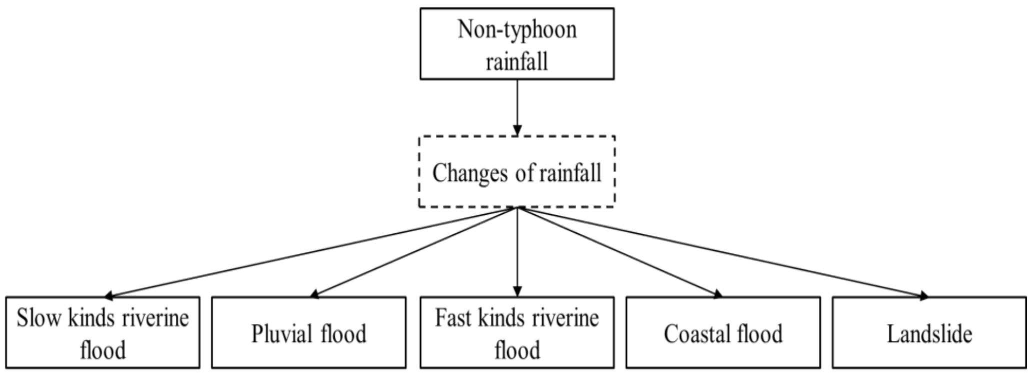

(b) Non-typhoon rainfall as trigger factor

Figure 5.14 The relationships among multiple hazards in zone IV in the Yangtze River Delta

Take Figure 5.11a as an example: typhoon is viewed as the trigger factor, with changes of wind speed and rainfall, which induce slow kinds riverine flood, pluvial flood and strong wind. These three kinds of hazards are in a parallel relationship and constitute a hazard group with each hazard induced by common trigger factors (wind speed and rainfall). Hence, the frequency and magnitude of this hazard group are determined by the changes in wind speed and rainfall. The exceedance probability of this hazard group (slow kinds riverine flood, pluvial flood and strong wind) occurring with different magnitudes can be expressed (equation 5-2) as:

$$EP(H_s \cap H_p \cap H_w) = EP(wind\ speed,\ rainfall) \tag{5-2}$$

Where, H_s is slow kinds riverine flood,

H_p is pluvial flood,

H_w is strong wind, and

EP(wind speed, rainfall) is the exceedance probability of the corresponding maximum daily rainfall and maximum daily wind speed sets, calculated in the hazard analysis.

In the same way, the exceedance probabilities of multiple hazards in other zones also can be calculated.

Zone I: Non-typhoon rainfall as trigger factor.

$$EP(H_s \cap H_p) = EP(non\text{-}typhoon\ rainfall) \tag{5-3}$$

Zone II: Typhoon as trigger factor.

$$EP(H_s \cap H_p \cap H_c \cap H_w) = EP(wind\ speed,\ rainfall) \tag{5-4}$$

Zone II: Non-typhoon rainfall as trigger factor.

$$EP(H_s \cap H_p \cap H_c) = EP(non\text{-}typhoon\ rainfall) \tag{5-5}$$

Zone III: Typhoon as trigger factor.

$$EP(H_s \cap H_p \cap H_f \cap H_l \cap H_w) = EP(wind\ speed,\ rainfall) \tag{5-6}$$

Zone III: Non-typhoon rainfall as trigger factor.

$$EP(H_s \cap H_p \cap H_f \cap H_l) = EP(non\text{-}typhoon\ \ rainfall) \qquad (5\text{-}7)$$

Zone IV: Typhoon as trigger factor.

$$EP(H_s \cap H_p \cap H_c \cap H_f \cap H_l \cap H_w) = EP(wind\ \ speed,\ \ rainfall) \qquad (5\text{-}8)$$

Zone IV: Non-typhoon rainfall as trigger factor.

$$EP(H_s \cap H_p \cap H_c \cap H_f \cap H_l) = EP(non\text{-}typhoon\ \ rainfall) \qquad (5\text{-}9)$$

Where, H_s is slow kinds riverine flood,
H_p is pluvial flood,
H_w is strong wind,
H_f is fast kinds riverine flood,
H_c is coastal flood,
H_l is landslide,

EP(non-typhoon rainfall) is the exceedance probability of the corresponding maximum non-typhoon daily rainfall, calculated in the hazard analysis, and

EP(wind speed, rainfall) is the exceedance probability of the corresponding maximum daily rainfall and maximum daily wind speed sets, calculated in the hazard analysis.

5.1.4 Exposure analysis in the Yangtze River Delta

Exposure analysis is used to analyse the spatial distribution of the elements at risk. This research takes the economic loss as an example, with GDP selected as the exposure indicator (Section 3.3.3 shows the rapid growth in the YRD GDP over the past 20 years). The assessment unit in the YRD is the county level (government administrative division), so the official statistics analysis method is used. From these official statistics, GDP in each county can be obtained, and mapped using ArcGIS. Figure 5.15 shows that countries with higher GDP in 2013 are mainly located in the north eastern part of the region.

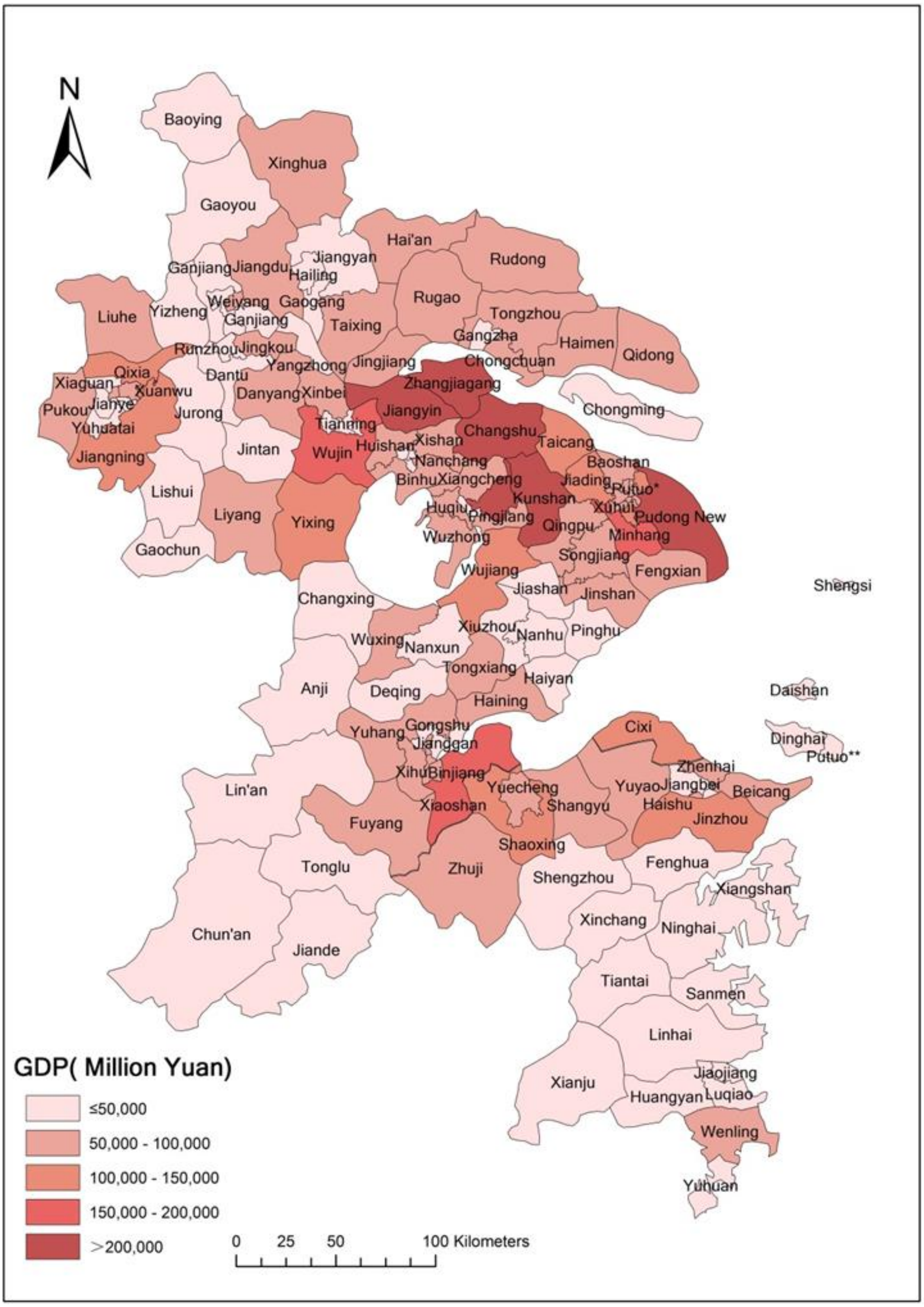

Figure 5.15 GDP distribution in the Yangtze River Delta in 2013

5.1.5 Vulnerability analysis in the Yangtze River Delta

Vulnerability assessment is used to measure the possible loss for a given exposure, under conditions caused by multiple hazards of varying degree, and to determine how these conditions (including physical, social, economic and environmental factors) influence the possible loss. A Bayesian network (BN), an optimal model to calculate the loss ratio induced by multi-hazard of different degree, and which can reflect how physical, social, economic and environmental factors influence vulnerability, is used in this module. Determining the BN structure and estimating conditional probabilities are the two key parts in the BN.

5.1.5.1 Structure of Bayesian network for vulnerability analysis in the Yangtze River Delta

A BN is a complete model of the system of interest, including its component variables and the probabilistic relationships between them. To construct a BN, the indicators should first be identified. As shown in section 4.6.1, indicators in the economic, social, physical and environmental domains are chosen to construct sets of vulnerability-related indicators. In the YRD, the relevant indicators are selected as shown in Table 5.5. Among these indicators, GDP per km^2, population density and percentage of residents covered by subsistence allowances show the same directional trend with vulnerability, that is, as the value of these indicators increases, the value of vulnerability increases; the other indicators show the opposite directional trend with the vulnerability. In order to unify the directional trend of these indicators with vulnerability, the reciprocal of the GDP per km^2, population density, and 1-percentage of residents covered by subsistence allowances are used in Factor analysis. Principal Component Analysis (PCA) is adopted to make distinct the principal component. Table 5.6 shows eight principal components selected based on the cumulative of variance, then a varimax rotation strategy is used to calculate the factor loading in each principal component. The number of mobile phone users per 10,000 persons (a proxy for income of residents, and telecommunication condition), doctors per 10,000 persons (a proxy for hospital beds and doctor situation), reciprocal of the population density (a proxy for population density and road length per 10,000 persons), reciprocal of the GDP per km^2, number of medical institutions per km^2, percentage of population age >15 and < 65, percentage of male residents and percentage of employed, which are with highest loading in each principal component (bold figures in Table 5.6), are selected as vulnerability-related indicators to construct the BN.

Table 5.5 Vulnerability indicators in the Yangtze River Delta

Domain	Indicator	Indicator in the YRD
Economic	GDP/capita	GDP per km^2
	Income of residents	Income of urban residents
		Income of rural residents
Social	Population density	Population density
	Gender ratio	Percentage of male residents
	Age structure	Percentage of population with age above 15 and under 65
	Telecommunication	Number of mobile phone users per 10,000 persons
		Number of fixed line phone users per 10,000 persons
		Number of internet users per 10,000 persons
	Transport route	Road length (km) per km^2
		Road length (km) per 10,000 persons
	Medical condition	Number of medical institutions per km^2
		Number of hospital beds per 10,000 persons
		Number of doctors per 10,000 persons
	Social dependency	Percentage of employed
		Percentage of residents covered by subsistence allowances
	Risk perception	-----
	Warning system	-----
	Institutional preparedness	-----
	Educational achievement	-----
Physical	Technical infrastructure	-----
Environmental	Significant natural areas	-----
	Fragmented natural areas	-----

(*Note: ----- represents the data is not available in these indicators. These indicators should be considered if such data are available.*)

Table 5.6 Factor loadings in each principal component in the Yangtze River Delta

Vulnerability indicators	Component							
	1	2	3	4	5	6	7	8
Reciprocal of the GDP per km^2	-.294	-.151	.137	**-.865**	-.072	.121	.158	-.068
Income of urban residents	.849	.125	.128	.325	.035	-.243	-.070	.166
Income of rural residents	.829	.190	.105	.328	.079	-.213	-.174	.161
Reciprocal of the population density	-.146	-.021	**.884**	-.303	-.209	-.036	.110	-.011
Percentage of male residents	-.270	-.237	.226	-.212	-.220	-.018	**.815**	-.083
Percentage of population with age above 15 and under 65	-.226	.046	-.002	-.103	.063	**.954**	-.001	-.061
Number of mobile phone users per 10,000 persons	**.916**	.254	.005	.066	.058	-.081	-.069	.190
Number of fixed line phone users per 10,000 persons	.851	.263	.099	.177	.056	-.162	-.191	.182
Number of internet users per 10,000 persons	.850	.355	-.086	-.059	.042	.054	-.113	.150
Road length (km) per km^2	.793	-.001	.094	.274	.384	-.002	.023	.079
Road length (km) per 10,000 persons	.428	-.010	.859	.164	.036	.029	.079	.011
Number of medical institutions per km^2	.128	.211	-.147	.056	**.916**	.066	-.155	.005
Number of hospital beds per 10,000 persons	.347	.807	-.066	.057	.220	-.023	-.189	.015
Number of doctors per 10,000 persons	.248	**.889**	.020	.133	.073	.068	-.066	.082
Percentage of employed	.485	.093	-.006	.085	.011	-.085	-.075	**.853**
1-Percentage of residents not covered by subsistence allowances	-.692	-.412	-.051	.048	.018	.145	.391	-.005
Cumulative % of Variance	49.4%	63.1%	72.0%	77.8%	82.8%	86.6%	89.7%	92.8%

Here, the YRD being struck by two consecutive typhoons is taken as an example of the vulnerability analysis. For data reasons, it is assumed that when two consecutive typhoons occur in the model, they do so within 60 days of each other. However, in reality, consecutive typhoons that occur 10 days apart may imply different risk to those 60 days apart. If sufficient data were available, the 60 day time frame could be divided into intervals (e.g. the second typhoon forms within 30 days of the first, versus 31-60 days after the first), and vulnerability could be analysed in each interval to make the assessment more accurate.

Maximum daily rainfall and maximum daily wind speed in each typhoon are selected as trigger factors to construct the set of hazard-related indicators which represent the magnitudes of multiple hazards. The first and second typhoons have an independent relationship. Based on the hazard interaction analysis in section 5.1.3, the BN framework in the four zones of the YRD can be constructed as shown in Figure 5.16. The BN framework in all four zones can be simplified into the same structure, as shown in Figure 5.17. Hence, the framework in Figure 5.17 is used as the basic structure of BN for vulnerability analysis in the YRD.

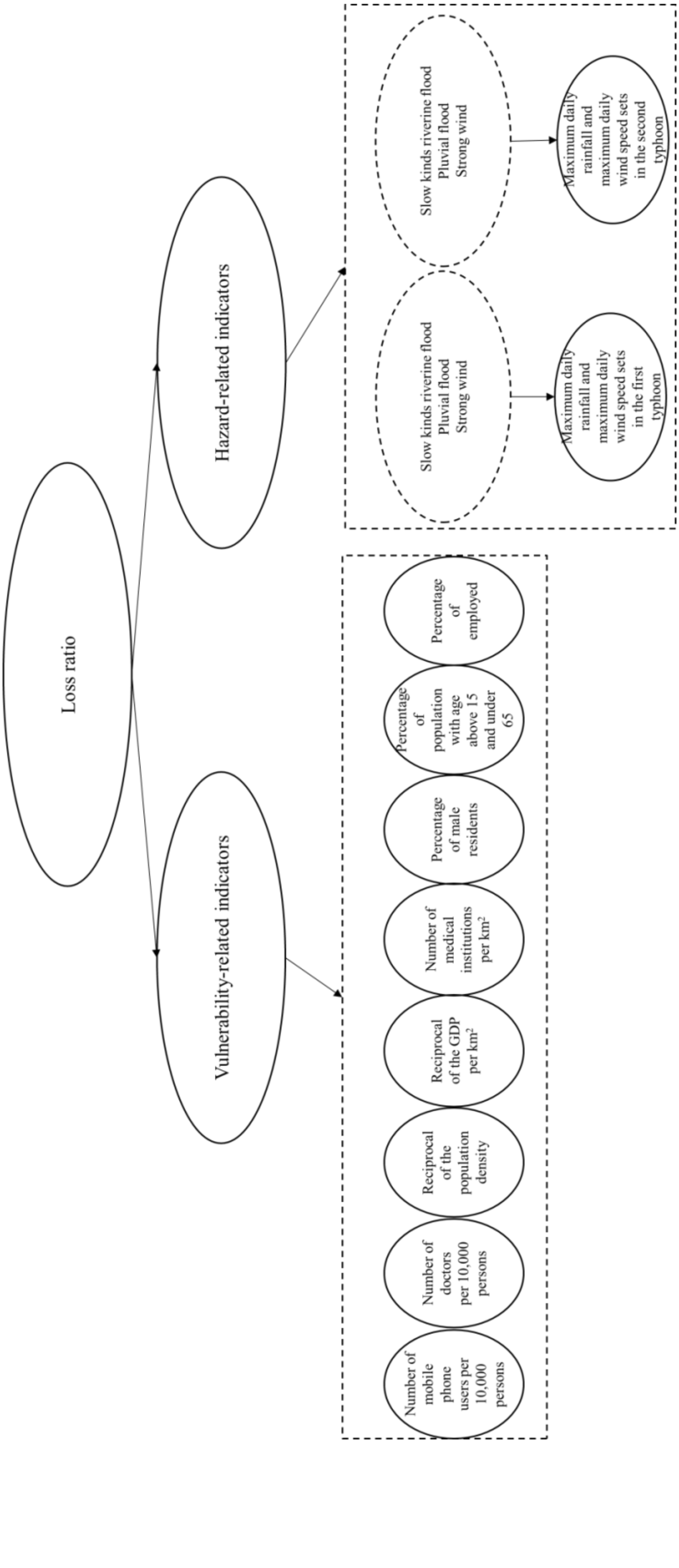

Loss ratio
Vulnerability-related indicators
Hazard-related indicators
Number of mobile phone users per 10,000 persons
Number of doctors per 10,000 persons
Reciprocal of the population density
Reciprocal of the GDP per km²
Number of medical institutions per km²
Percentage of male residents
Percentage of population with age above 15 and under 65
Percentage of employed
Slow kinds riverine flood Pluvial flood Strong wind
Maximum daily rainfall and maximum daily wind speed sets in the first typhoon
Slow kinds riverine flood Pluvial flood Strong wind
Maximum daily rainfall and maximum daily wind speed sets in the second typhoon

(a) Zone I

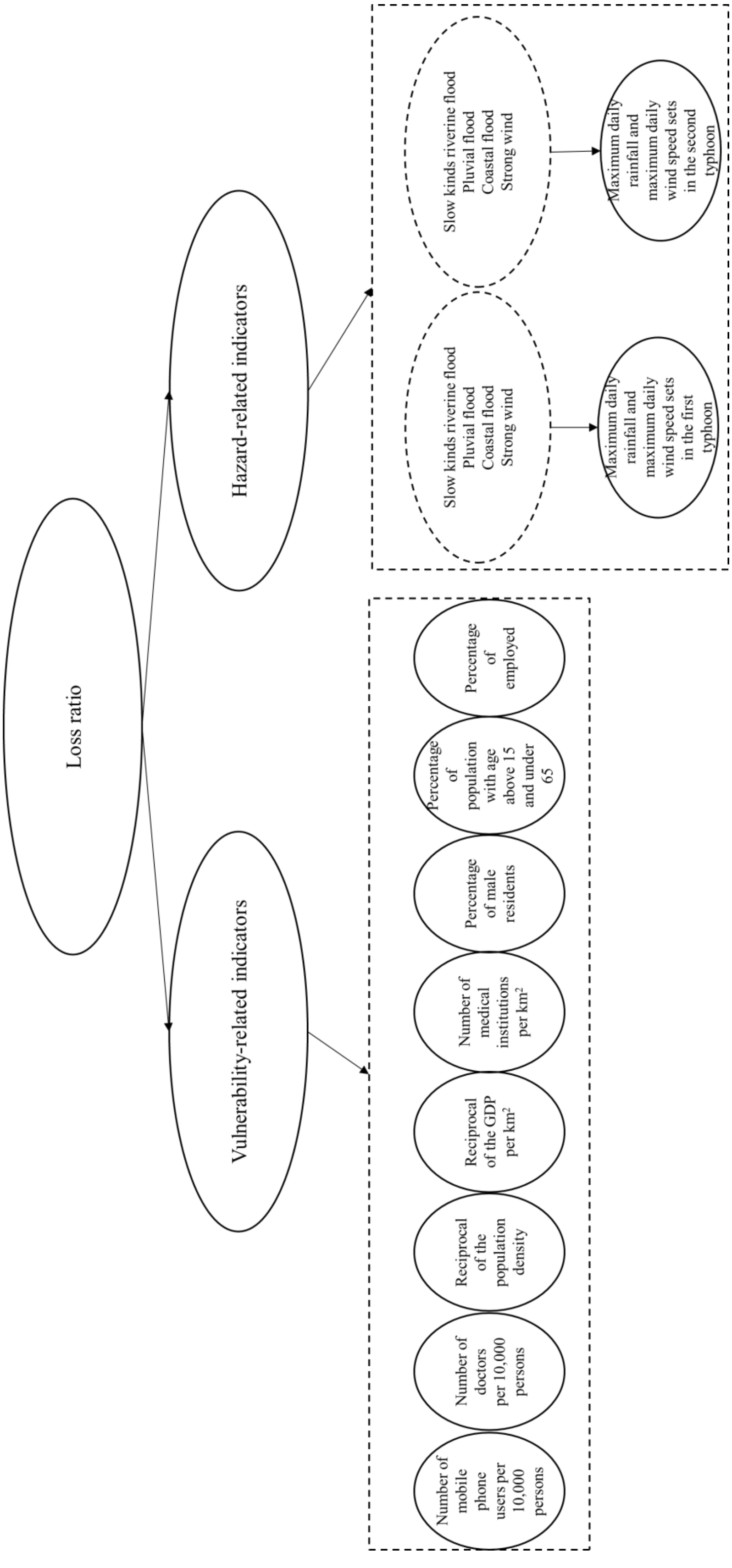
Loss ratio
Vulnerability-related indicators
Hazard-related indicators
Number of mobile phone users per 10,000 persons
Number of doctors per 10,000 persons
Reciprocal of the population density
Reciprocal of the GDP per km^2
Number of medical institutions per km^2
Percentage of male residents
Percentage of population with age above 15 and under 65
Percentage of employed
Slow kinds riverine flood Pluvial flood Coastal flood Strong wind
Maximum daily rainfall and maximum daily wind speed sets in the first typhoon
Slow kinds riverine flood Pluvial flood Coastal flood Strong wind
Maximum daily rainfall and maximum daily wind speed sets in the second typhoon

(b) Zone II

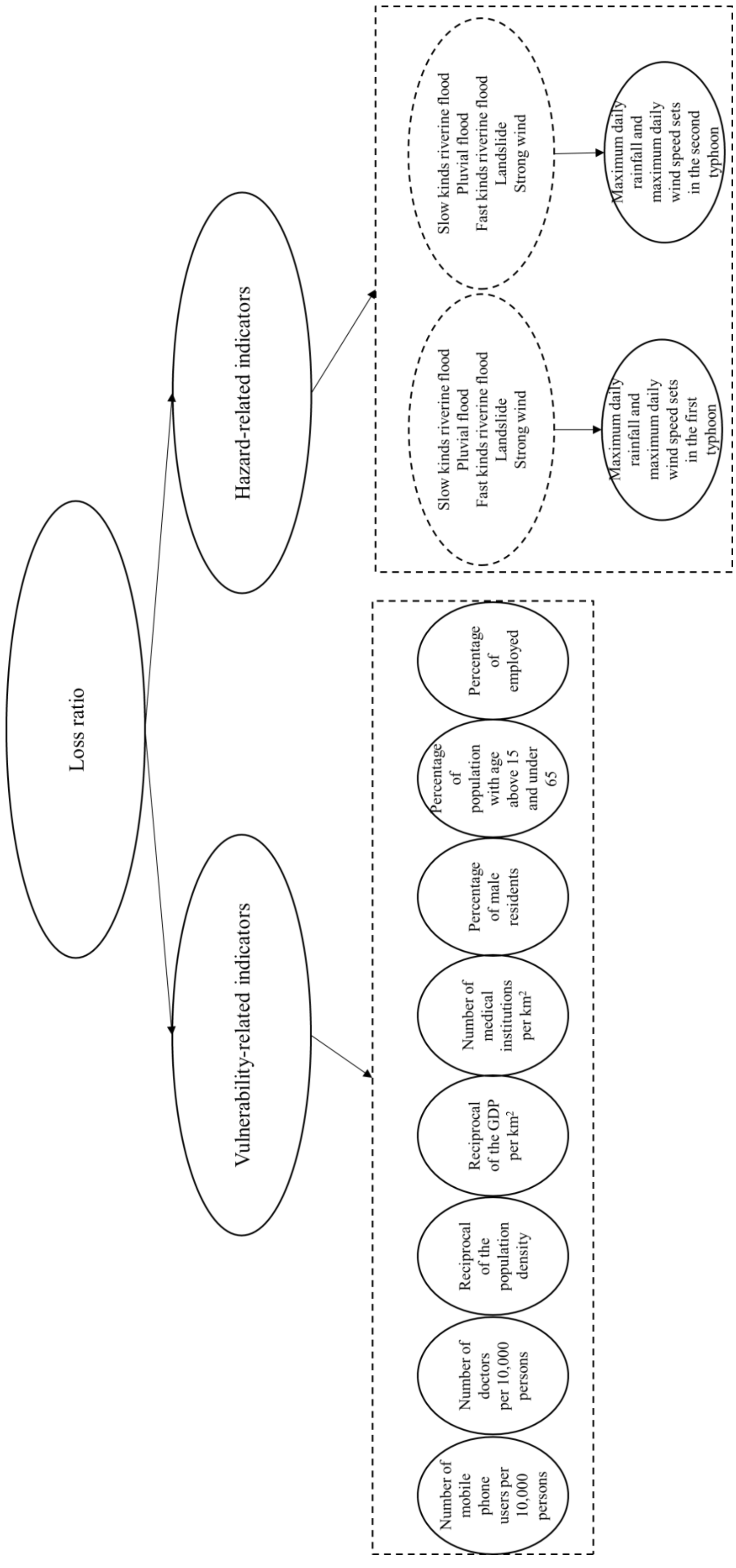

Loss ratio
Hazard-related indicators
Vulnerability-related indicators
Slow kinds riverine flood
Pluvial flood
Fast kinds riverine flood
Landslide
Strong wind
Maximum daily rainfall and maximum daily wind speed sets in the first typhoon
Slow kinds riverine flood
Pluvial flood
Fast kinds riverine flood
Landslide
Strong wind
Maximum daily rainfall and maximum daily wind speed sets in the second typhoon
Number of mobile phone users per 10,000 persons
Number of doctors per 10,000 persons
Reciprocal of the population density
Reciprocal of the GDP per km²
Number of medical institutions per km²
Percentage of male residents
Percentage of population with age above 15 and under 65
Percentage of employed

(c) Zone III

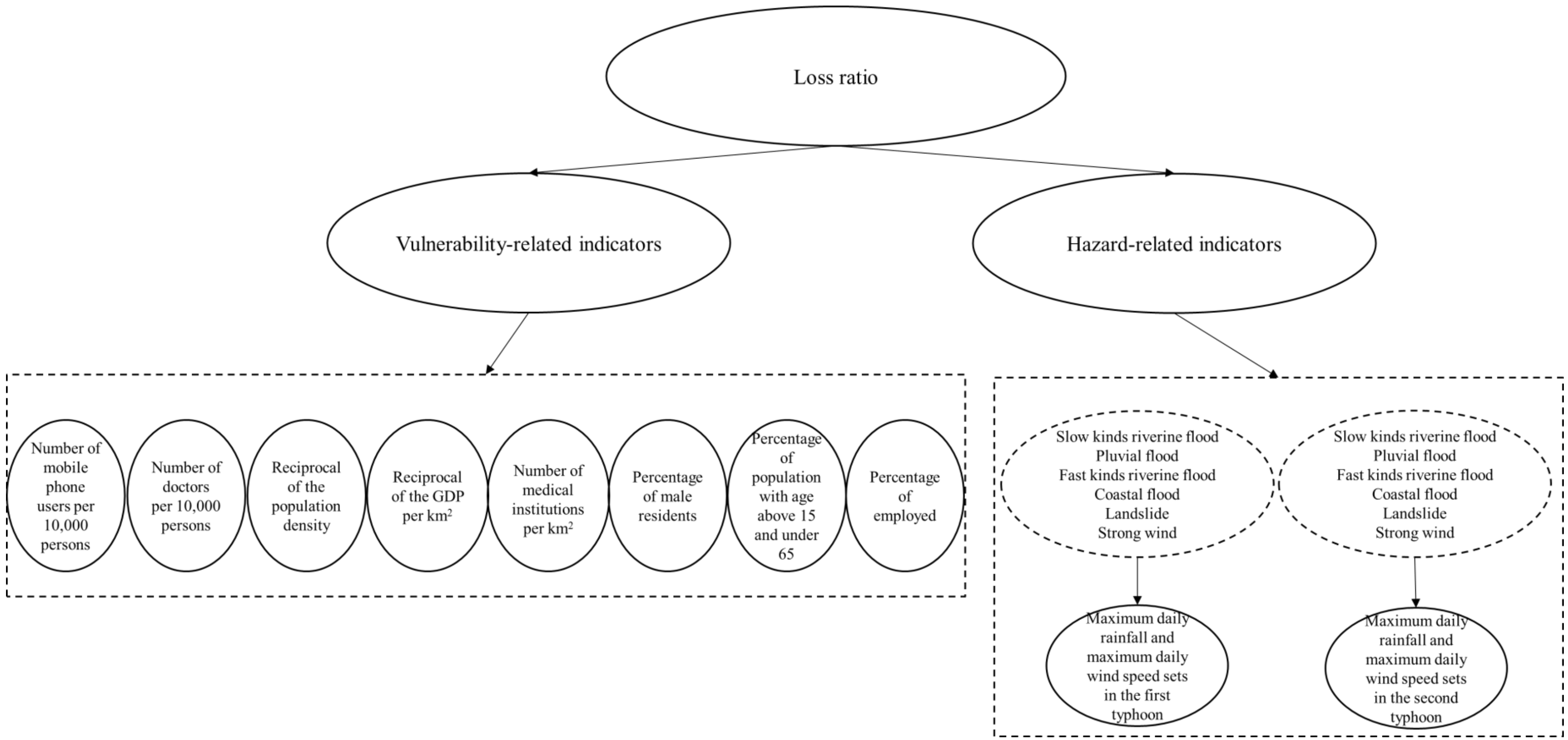

(d) Zone IV

Figure 5.16 BN framework for vulnerability analysis in four zones in the Yangtze River Delta

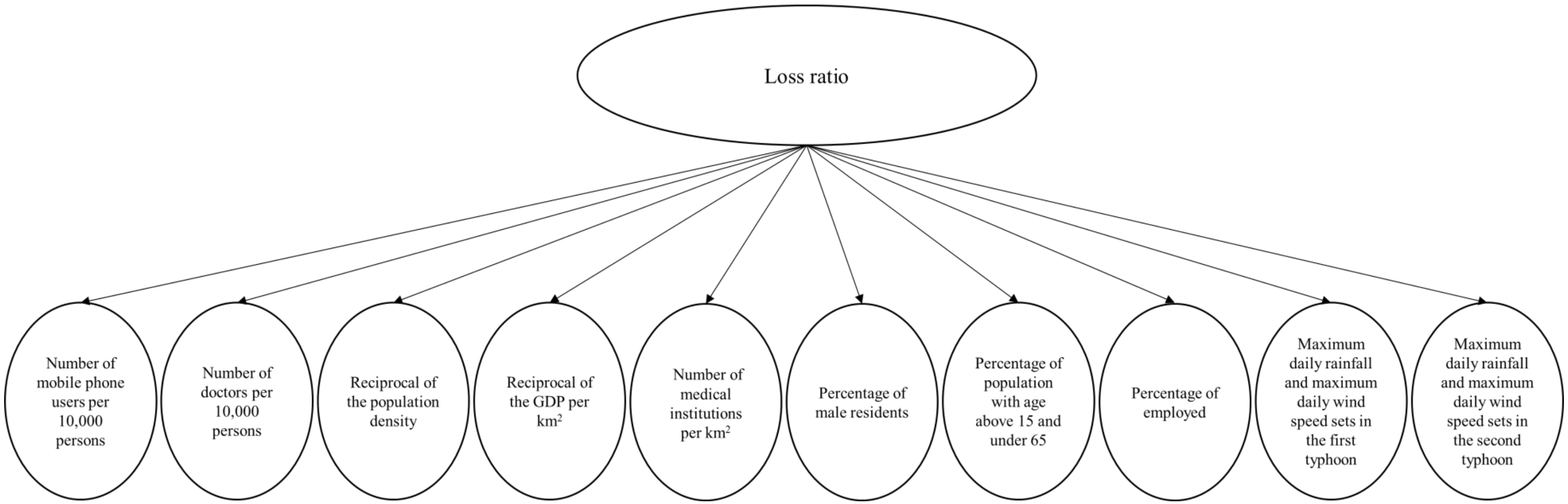

Figure 5.17 Basic structure of BN for vulnerability analysis in the Yangtze River Delta

5.1.5.2 Determining the conditional probability in the Yangtze River Delta

A conditional probability measures the probability of an event given that another event has occurred. In this model, once a BN framework is constructed, the conditional probability of a vulnerability-related indicator or hazard-related indicator given a loss ratio should be determined (equation 5-10).

$$p(v_{kj} \mid L_i) \tag{5-10}$$

Where, L_i represents the i state of loss ratio L, $i=1,2,\ldots m$, and

v_{kj} represents the j state of vulnerability-related indicator or hazard-related indicator k, $k=1,2, \ldots s, j=1, 2,\ldots n$.

In this example, the loss ratio is divided into six states, eight vulnerability-related indicators are all divided into five states, and the hazard-related indicators (maximum daily rainfall and maximum daily wind speed sets) are divided into eight states (Table 5.7). Based on the historic disaster data from 1980 to 2012, the aggregate losses caused by two consecutive typhoons were collected, and the corresponding data for vulnerability-related indicators were collected (from the relevant statistics yearbook) to construct a complete observed data set. Then maximum-likelihood estimation (MLE) is used to provide estimates of the conditional probabilities. Taking the number of mobile phone users per 10,000 persons in state one (M_1) as an example, the probability of loss ratio in state one (L_1), and the conditional probability of M_1 given L_1 can be calculated using equations 5-11 and 5-12.

$$p(L_1)=\frac{Number(L=L_1)}{Total\ number\ of\ samples} \tag{5-11}$$

$$p(M_1 \mid L_1)=\frac{Number(M=M_1, L=L_1)}{Number(L=L_1)} \tag{5-12}$$

The calculated conditional probabilities are shown in Appendix D, with some exemplar data shown in Table 5.8. As shown in Table 5.8 (a), the value of

$p(M_1 \mid L_1)$ is 0.58, that means when loss ratio is in state one, the probability of mobile phone users per 10,000 persons in state one is 0.58. In addition, the conditional probability $p(M \mid L)$ decreases gradually from mobile phone users state one (M_1) to state five (M_5) in each loss ratio state. This means the loss mainly occurs in the areas with fewer mobile phone users.

With these conditional probabilities, the joint probability (equation 5-13) is used to estimate the posteriori probability of the target loss ratio, which is the basis for the vulnerability calculation.

$$\begin{aligned} p(L, v_1, v_2, \cdots v_k \cdots v_s) &= p(L)\, p(v_1, v_2, \cdots v_k \cdots v_s \mid L) \\ &= p(L) \prod_{k=1}^{s} p(v_k \mid L) \end{aligned} \tag{5-13}$$

Where, L is the target variable loss ratio, and

v_k is the vulnerability-related indicator or hazard-related indicator k.

Table 5.7 Different states of factors in Bayesian network

Factor	States
Number of mobile phone users per 10,000 persons (M)	M_1<2500 phone users/10,000 persons 2500 phone users/10,000 persons≤M_2<5000 phone users/10,000 persons 5000 phone users/10,000 persons≤M_3<7500 phone users/10,000 persons 7500 phone users/10,000 persons≤M_4<10000 phone users/10,000 persons M_5≥10,000 phone users/10,000 persons
Number of doctors per 10,000 persons (D)	D_1<10 doctors/10,000 persons 10 doctors/10,000 persons≤D_2<15 doctors/10,000 persons 15 doctors/10,000 persons≤D_3<20 doctors/10,000 persons 20 doctors/10,000 persons≤D_4<25 doctors/10,000 persons D_5≥25 doctors/10,000 persons
Reciprocal of the population density (Pd)	Pd_1<(1/1000) km^2/ persons (1/1000) km^2/ persons≤Pd_2<(1/750) km^2/ persons (1/750) km^2/ persons≤Pd_3< (1/500) km^2/ persons (1/500) km^2/ persons≤Pd_4<(1/250) km^2/ persons Pd_5≥(1/250) km^2/ persons
Reciprocal of the GDP per km^2 (G)	G_1<(1/30) km^2/ million yuan (1/30) km^2/ million yuan≤G_2<(1/20) km^2/ million yuan (1/20) km^2/ million yuan≤G_3<(1/10) km^2/ million yuan (1/10) km^2/ million yuan≤G_4<(1/5) km^2/ million yuan G_5≥(1/5) km^2/ million yuan
Number of medical institutions per km^2 (Mi)	Mi_1<0.02 medical institutions/km^2 0.02 medical institutions/km^2≤Mi_2<0.03 medical institutions/km^2 0.03 medical institutions/km^2≤Mi_3<0.04 medical institutions/km^2 0.04 medical institutions/km^2≤Mi_4<0.05 medical institutions/km^2 Mi_5≥0.05 medical institutions/km^2
Percentage of population with age above 15 and under 65 (Pa)	Pa_1<72% 72%≤Pa_2<73.5% 73.5%≤Pa_3<75% 75%≤Pa_4<76.5% Pa_5≥76.5%
Percentage of male residents (Ma)	Ma_1<50% 50%≤Ma_2<50.5% 50.5%≤Ma_3<51% 51%≤Ma_4<51.5% Ma_5≥51.5%
Percentage of employed (E)	E_1<50% 50%≤E_2<60% 60%≤E_3<70% 70%≤E_4<80% E_5≥80%
Maximum daily rainfall and maximum daily wind speed sets in the first typhoon (WRf)	WRf_1(W<10m/s, R<50mm) WRf_2(W<10m/s, 50mm≤R) WRf_3(10m/s≤W<20m/s, R<50mm) WRf_4(10m/s≤W<20m/s, 50mm≤R<150mm) WRf_5(10m/s≤W<20m/s, R≥150mm) WRf_6(W≥20m/s, R<50mm) WRf_7(W≥20m/s, 50mm≤R<150mm) WRf_8(W≥20m/s, R≥150mm)
Maximum daily rainfall and maximum daily wind speed sets in the second typhoon (WRs)	WRs_1(W<10m/s, R<50mm) WRs_2(W<10m/s, 50mm≤R) WRs_3(10m/s≤W<20m/s, R<50mm) WRs_4(10m/s≤W<20m/s, 50mm≤R<150mm) WRs_5(10m/s≤W<20m/s, R≥150mm) WRs_6(W≥20m/s, R<50mm) WRs_7(W≥20m/s, 50mm≤R<150mm) WRs_8(W≥20m/s, R≥150mm)
Loss ratio (L)	L_1=0% 0%<L_2<0.5% 0.5%≤L_3<1% 1%≤L_4<5% 5%≤L_5<10% L_6≥10%

Table 5.8 Example conditional probability tables of vulnerability-related and hazard-related indicators given loss ratio

(a) Conditional probability table of number of mobile phone users per 10,000 persons (M) given loss ratio (L)

p(M/L)	M_1	M_2	M_3	M_4	M_5
L_1	0.58	0.16	0.1	0.1	0.05
L_2	0.44	0.16	0.19	0.1	0.11
L_3	0.59	0.05	0.25	0.06	0.05
L_4	0.66	0.14	0.14	0.03	0.04
L_5	0.72	0.09	0.15	0.02	0.02
L_6	0.77	0.13	0.07	0.02	0

(b) Conditional probability table of number of doctors per 10,000 persons (D) given loss ratio (L)

p(D/L)	D_1	D_2	D_3	D_4	D_5
L_1	0.11	0.34	0.36	0.09	0.1
L_2	0.07	0.25	0.37	0.17	0.15
L_3	0.13	0.25	0.5	0.08	0.05
L_4	0.11	0.38	0.33	0.15	0.03
L_5	0.15	0.43	0.3	0.11	0.02
L_6	0.13	0.46	0.33	0.06	0.02

(*Note that M_1 to M_5, L_1 to L_6, and D_1 to D_5 are defined in Table 5.7)*

5.1.5.3 Vulnerability assessment in the Yangtze River Delta

Based on the posteriori probability of the target loss ratio obtained above, when the states of all vulnerability-related indicators and hazard-related indicators are given as *j*, the probability of loss ratio L_i occurring can be calculated (equation 5-14).

$$P(L_i)=\frac{p(L_i,v_{1j},v_{2j},\cdots v_{kj}\cdots v_{10j})}{\sum_{i=1}^{6}p(L_i,v_{1j},v_{2j},\cdots v_{kj}\cdots v_{10j})} \tag{5-14}$$

Where, L_i represents the *i* state of loss ratio *L*, *i=1,2,…6*, and v_{kj} represents the *j* state of vulnerability-related indicator or hazard-related indicator *k*, *k=1,2, …10*.

Then the vulnerability, with given all vulnerability-related indicators and hazard-related indicators states *j*, can be calculated as equation (5-15).

$$\begin{aligned} Vul = {} & P(L_1)\times L_{1mean}+P(L_2)\times L_{2mean}+P(L_3)\times L_{3mean} \\ & +P(L_4)\times L_{4mean}+P(L_5)\times L_{5mean}\times P(L_6)\times L_{6mean} \end{aligned} \tag{5-15}$$

Where, L_{imean} represents the mean value in each L state,
L_{1mean}=0%,
L_{2mean}=0.25%,
L_{3mean}=0.75%,
L_{4mean}=3%,
L_{5mean}=7.5%,
L_{6mean}=1/2(10%+Maximum loss ratio in historical data), and
$P(L_i)$ is the corresponding probability of the target loss ratio L_i occurring.

The vulnerability with other states of vulnerability-related and hazard-related indicators can be calculated in the same way.

Here, data for vulnerability-related indicators in 2013 are taken as example. Assume all counties in the YRD are influenced by typhoons at the same magnitude (that is maximum daily rainfall and maximum daily wind speed sets in the first typhoon are at the same state in all counties and those in the second are also the same), vulnerabilities are calculated to show the vulnerability distribution in the YRD. Three examples are shown in Figures 5.18 to 5.20. Figure 5.18 shows the vulnerability distribution when all counties are influenced by typhoon twice consecutively with the maximum daily rainfall and maximum daily wind speed sets both in state 2. Figure 5.19 shows the sets both in state 4 and Figure 5.20 shows those both in state 8.

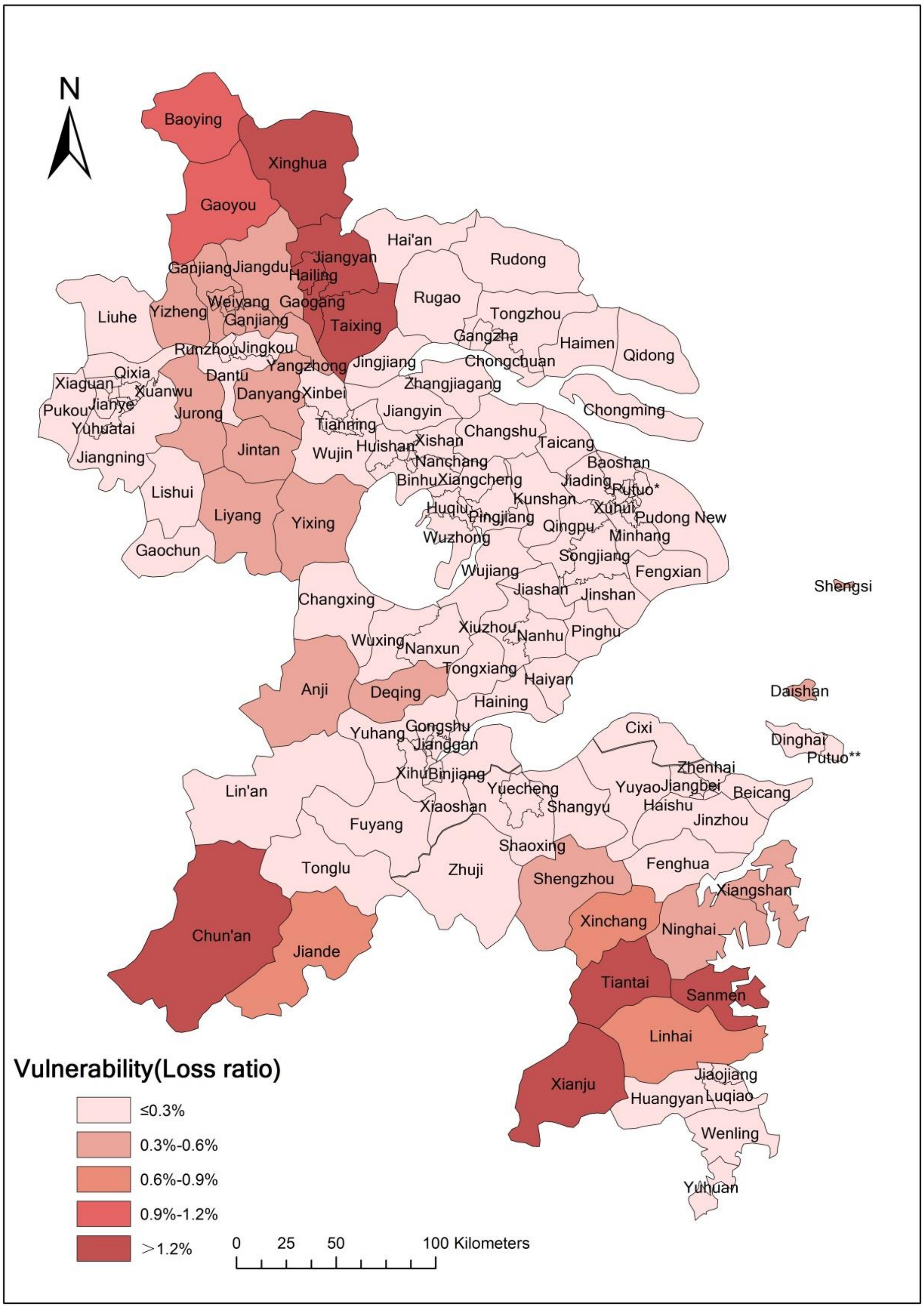

Figure 5.18 Vulnerability distribution influenced by two consecutive typhoons with (maximum daily) rainfall and wind speed sets both in state 2

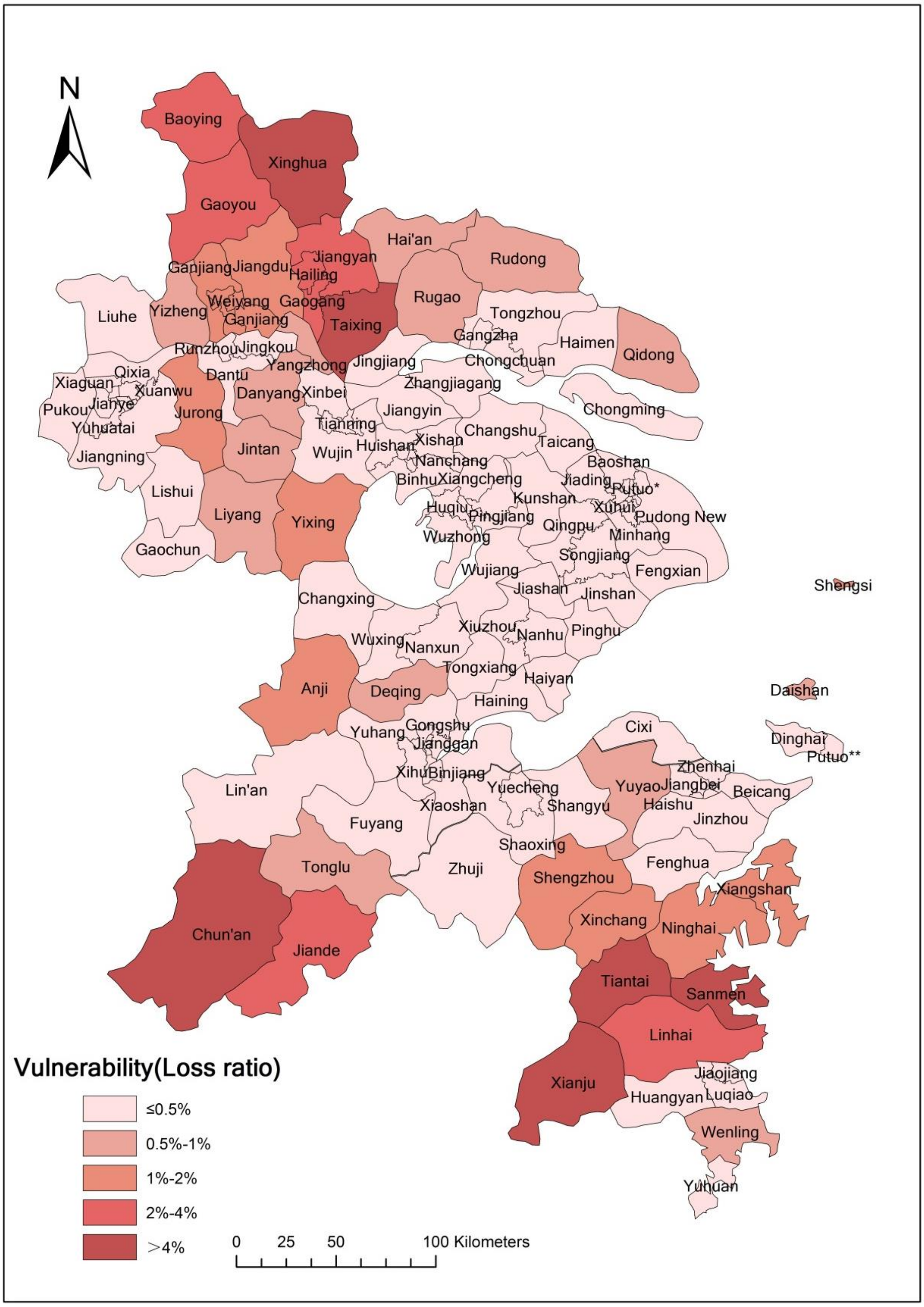

Figure 5.19 Vulnerability distribution influenced by two consecutive typhoons with (maximum daily) rainfall and wind speed sets both in state 4

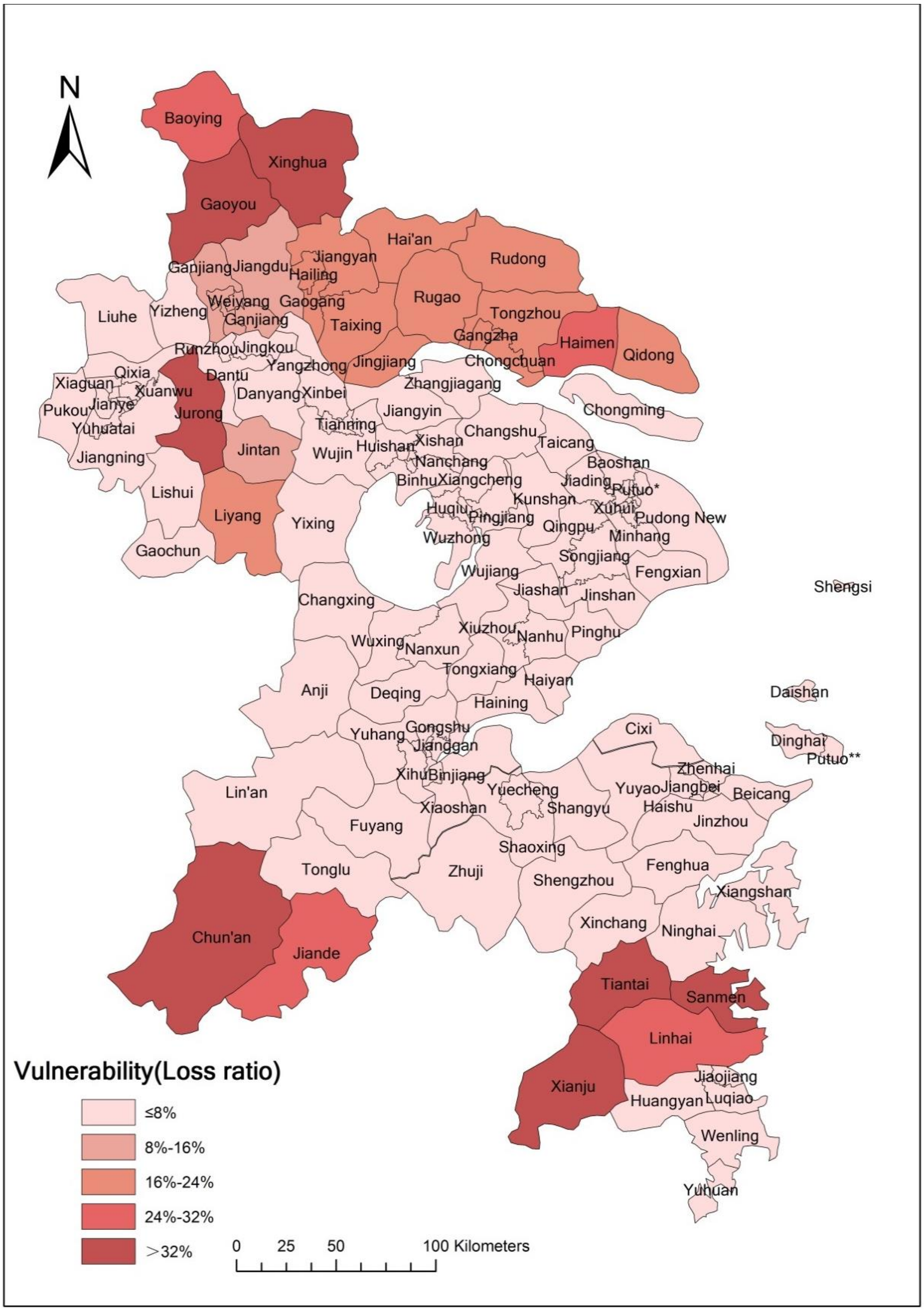

Figure 5.20 Vulnerability distribution influenced by two consecutive typhoons with (maximum daily) rainfall and wind speed sets both in state 8

The vulnerability distributions in Figures 5.18 to 5.20 are essentially the same. Counties with higher vulnerability are mainly located far from the metropolitan areas. Fewer mobile phone users, doctors and medical institutions are the main reasons to induce higher vulnerability in these counties. According to the Factor Analysis (section 5.1.5.1), the lower number of mobile phone users shows that the income of residents is lower and telecommunication condition is poorer. The lower number of doctors and medical institutions indicates that medical responses services are relatively undeveloped in these counties. Hence, the higher vulnerability in these counties is due to the relatively lower income of residents, poor telecommunication condition and less developed medical service.

Using this module, the vulnerability distribution influenced by other multiple hazards types also can be calculated.

5.1.6 Multi-hazard risk assessment

At this point, and based on the hazard identification, analysis, and interaction analysis, the exceedance probability of multiple hazards can be determined, and the corresponding loss calculated as the result of the exposure and vulnerability analyses (equation 5-16).

$$Loss = Exposure \times Vulnerability = Value\ of\ the\ exposure \times Loss\ ratio \quad (5\text{-}16)$$

Taking the YRD in 2013 influenced by consecutive typhoons as an example, assume the maximum daily rainfall distribution and maximum wind speed distribution of the first typhoon is with exceedance probability of 10%, and the second is with exceedance probability of 5%. According to the hazard identification, analysis, and interaction analysis, the magnitude of multiple hazards can be expressed by the maximum daily rainfall distribution and maximum wind speed distribution in Figures 5.9 and 5.10. With these rainfall and wind speed distributions, the vulnerability distribution can be calculated by the vulnerability assessment module. Finally, the corresponding loss is calculated as equation 5.16. The results are shown in Figure 5.21. Counties with higher loss are mainly located in the south eastern part of the region. The reasons for these higher losses are analysed further below (section 5.3).

The loss distribution influenced by typhoon with other exceedance probabilities can also be calculated by this model - see Appendix E for further results. Besides, using this module, the loss distribution that arises through other hazard combinations can also be calculated.

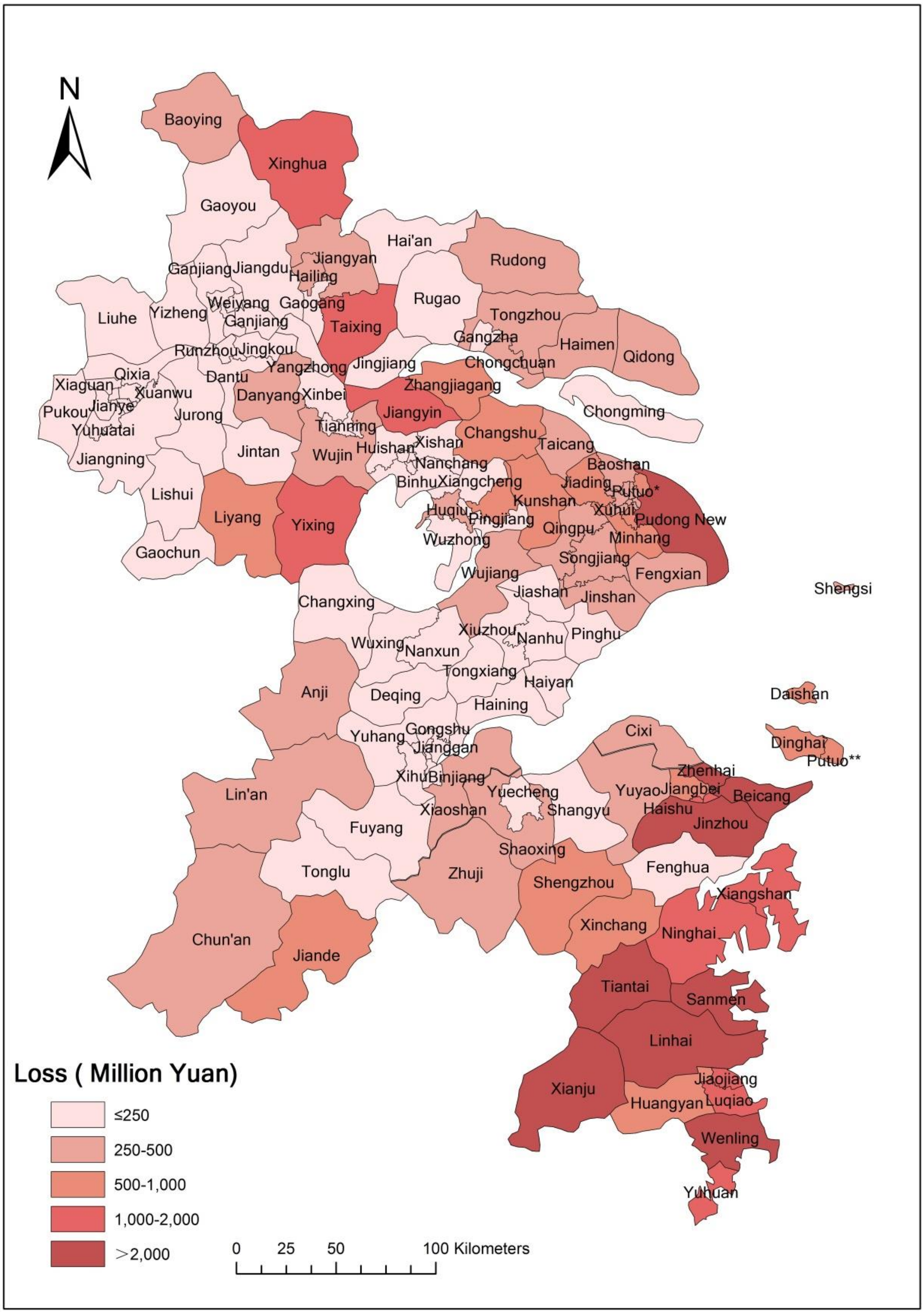

Figure 5.21 Loss distribution influenced by two typhoons with exceedance probability of 10% and exceedance probability of 5%

5.2 Model validation

Model validation is used to check the accuracy of the model's representation of the real system. In this research, MmhRisk-HI is developed and used to estimate potential loss caused by multiple hazards in the YRD. In order to test the effectiveness of this model, the hazards that occurred in 2013 are simulated in this model. The simulated results are compared to the observed data.

In 2013, the YRD was influenced by typhoon Trami (21st August) and typhoon Fitow (7th October) consecutively. According to the hazard identification, analysis, and interaction analysis, the magnitude of multiple hazards induced by typhoon in the YRD can be expressed by the maximum daily rainfall and maximum wind speed. The data about maximum daily rainfall and maximum wind speed in these typhoons were collected from 24 meteorological stations in the YRD, then spatial interpolation technique is used to estimate the rainfall and wind value in each county. With these hazard-related indicators (maximum daily rainfall and maximum wind speed) and vulnerability-related indicators described using data for 2013, the vulnerability module (based on historical data from 1980 to 2012) is used to estimate the probability of loss ratio in each county induced by these two typhoons. The estimated results and the observed real loss ratio in 55 counties in Zhejiang Province are shown in Table 5.9 (The real loss data in Jiangsu and Shanghai in 2013 is not available).

Table 5.9 The estimated results and observed real loss ratio in 55 counties in Zhejiang Province

	Estimated probability of loss ratio L_i occurring						Real loss ratio
	L_1=0%	**0%< L_2<0.5%**	**0.5%≤ L_3<1%**	**1%≤ L_4<5%**	**5%≤ L_5<10%**	**L_6≥10%**	
Shangcheng	1.62%	**98.00%**	0.31%	0.07%	0.00%	0.00%	0.01%
Xiacheng	1.62%	98.00%	0.31%	0.07%	0.00%	0.00%	0.00%
Jianggan	0.79%	**99.08%**	0.11%	0.02%	0.00%	0.00%	0.02%
Gongshu	1.62%	**98.00%**	0.31%	0.07%	0.00%	0.00%	0.03%
Xihu	1.62%	**98.00%**	0.31%	0.07%	0.00%	0.00%	0.28%
Binjiang	1.46%	97.80%	0.53%	0.21%	0.00%	0.00%	0.00%
Xiaoshan	0.61%	**99.27%**	0.10%	0.02%	0.00%	0.00%	0.49%
Yuhang	1.03%	**98.61%**	0.28%	0.08%	0.00%	0.00%	0.49%
Tonglu	10.07%	**86.07%**	1.56%	2.29%	0.00%	0.00%	0.16%
Chun'an	**93.64%**	4.78%	0.74%	0.41%	0.02%	0.41%	0.00%
Jiande	**55.55%**	38.22%	1.16%	4.57%	0.13%	0.36%	0.00%
Fuyang	3.76%	**95.13%**	0.51%	0.59%	0.00%	0.00%	0.27%
Lin'an	33.57%	**64.42%**	1.27%	0.73%	0.00%	0.00%	0.41%
Haishu	0.75%	98.82%	0.36%	0.06%	0.00%	0.00%	1.06%
Jiangdong	0.75%	**98.82%**	0.36%	0.06%	0.00%	0.00%	0.44%
Jiangbei	0.00%	0.00%	0.00%	**99.57%**	0.43%	0.00%	4.04%
Beicang	0.50%	**97.90%**	0.88%	0.72%	0.00%	0.00%	0.10%
Zhenhai	1.10%	**98.49%**	0.29%	0.11%	0.00%	0.00%	0.33%
Jinzhou	0.00%	0.00%	0.00%	**98.01%**	1.99%	0.00%	4.91%
Yuyao	0.00%	0.00%	0.00%	97.63%	2.37%	0.00%	26.62%
Cixi	0.00%	0.00%	0.00%	**98.56%**	1.44%	0.00%	1.96%
Fenghua	0.00%	0.00%	0.00%	99.77%	0.23%	0.00%	6.76%
Xiangshan	0.00%	0.00%	0.00%	**97.99%**	2.01%	0.00%	1.58%
Ninghai	0.00%	0.00%	0.00%	**98.87%**	1.13%	0.00%	1.08%
Nanhu	0.00%	0.00%	0.00%	89.84%	10.16%	0.00%	0.83%
Xiuzhou	0.00%	0.00%	0.00%	**89.87%**	10.13%	0.00%	4.73%
Pinghu	0.00%	0.00%	0.00%	**91.64%**	8.36%	0.00%	1.16%
Haining	0.00%	0.00%	0.00%	**73.04%**	26.96%	0.00%	1.92%
Tongxiang	0.00%	0.00%	0.00%	**90.58%**	9.42%	0.00%	1.37%
Jiashan	0.00%	0.00%	0.00%	**90.58%**	9.42%	0.00%	2.28%
Haiyan	0.00%	0.00%	0.00%	97.56%	2.44%	0.00%	5.63%
Wuxing	4.66%	94.92%	0.37%	0.04%	0.00%	0.00%	0.66%
Nanxun	0.00%	0.00%	0.00%	**98.75%**	1.25%	0.00%	1.50%
Deqing	0.00%	0.00%	0.00%	**98.28%**	1.72%	0.00%	1.42%
Changxing	0.00%	0.00%	0.00%	**99.07%**	0.93%	0.00%	1.07%
Anji	0.00%	0.00%	0.00%	93.37%	6.63%	0.00%	7.54%
Yuecheng	1.45%	**98.18%**	0.33%	0.05%	0.00%	0.00%	0.08%
Shaoxing	0.00%	0.00%	0.00%	96.16%	3.84%	0.00%	0.55%
Shangyu	0.00%	0.00%	0.00%	**92.00%**	8.00%	0.00%	2.75%
Zhuji	7.03%	**89.86%**	1.44%	1.67%	0.00%	0.00%	0.02%
Shengzhou	8.77%	**63.45%**	6.65%	20.78%	0.35%	0.00%	0.09%
Xinchang	5.95%	**52.34%**	3.17%	37.97%	0.57%	0.00%	0.27%
Dinghai	3.01%	**93.09%**	2.07%	1.79%	0.03%	0.00%	0.10%
Putuo**	4.08%	**94.02%**	1.43%	0.46%	0.01%	0.00%	0.18%
Daishan	7.29%	**77.66%**	5.81%	8.96%	0.29%	0.00%	0.12%
Shengsi	6.72%	**71.91%**	4.05%	16.44%	0.88%	0.00%	0.02%
Jiaojiang	3.58%	**92.16%**	3.41%	0.83%	0.01%	0.00%	0.19%
Huangyan	5.20%	4.99%	7.74%	**58.89%**	5.30%	17.89%	1.19%
Luqiao	3.58%	**92.16%**	3.41%	0.83%	0.01%	0.00%	0.17%
Wenling	8.42%	**60.32%**	5.23%	25.13%	0.90%	0.00%	0.21%
Linhai	9.61%	31.25%	16.01%	35.75%	5.17%	2.21%	0.66%
Yuhuan	3.74%	69.94%	1.98%	13.96%	10.38%	0.00%	0.95%
Sanmen	0.00%	0.00%	0.00%	**54.90%**	4.99%	40.11%	1.89%
Tiantai	3.81%	3.97%	13.91%	65.10%	3.52%	9.70%	0.90%
Xianju	3.16%	2.53%	6.62%	**67.25%**	5.92%	14.51%	1.16%

As shown in Table 5.9, among these 55 counties, the real loss ratio in 42 counties (76.36%) falls into the loss ratio state (L_i) which has the highest estimated probability (bold figures in Table 5.9). Taking Shangcheng as an example, the real loss ratio in this county is 0.01%, which falls into the loss ratio state 2 ($0\%<L_2<0.5\%$). In the corresponding estimated results, the estimated probability of L_2 occurring in Shangcheng is 98%, which is the highest among all six loss ratio states. In addition, the total estimated loss in these 55 counties is 51,893.39 million yuan compared to the actual loss of 50,485.43 million yuan, the deviation of an estimated aggregate loss value from its actual value is less than 2.79%. Hence, this developed MHRA model, MmhRisk-HI, can represent the real system, and the estimated results of this model can reflect the real loss situation.

5.3 Results analysis

The model developed in this research fills a key research gap in the existing MHRA methods. It calculates the possible loss caused by multiple hazards, with an explicit consideration of interaction between different hazards. The final results obtained in this model can help to identify which area is a high risk (large potential loss) area, and allow a determination of the reasons that contribute to those large potential losses (high risk).

Compared to the recent comprehensive MHRA research which only considers domino effect, MmhRisk-HI calculates the possible loss with an explicit consideration of all possible relationships between different hazards, e.g. the first typhoon and the second one are independent relationship in this case study. The short time period between two typhoons means the area is more vulnerable as it has not recovered immediately from the first typhoon. Previous MHRA methods assume there is no change in vulnerability, and calculate the loss in each typhoon individually with the same vulnerability, then aggregate the losses. Thus the results cannot reflect the real loss situation. In MmhRisk-HI, the vulnerability analysis module (section 5.1.5) addresses this issue by considering the magnitudes of these two typhoons together in hazard-related indicators. These two typhoons are treated as a multiple hazards group, and the relevant vulnerability-related indicators correspond to this group rather than a single typhoon. Hence, the results obtained in the model are more reliable.

Besides, this model can help to identify the reasons that contribute to large potential losses. Take the loss distribution in Figure 5.21 as an example.

Linhai, Tiantai, Xianju, Sanmen, Jinzhou, Pudong New, Beicang, Zhenhai and Wenling are in the highest risk area. Risk is determined by the magnitude of multiple hazards, vulnerability and value of exposure. According to the hazard, hazard interaction, exposure and vulnerability analysis before, Pudong New is in the highest risk area due to its highest exposure value; Linhai, Jinzhou, Beicang, Zhenhai and Wenling are at highest risk due to the highest magnitude of multiple hazards; the reason for highest risk at Tiantai, Xianju and Sanmen is the interaction with the highest magnitude of multiple hazards and the highest vulnerability. Thus different factors contribute to high risk.

Furthermore, through the hazard identification and vulnerability assessment, the kinds of hazards and types of vulnerability-related indicators that underpin large potential losses in a given area also can be identified. Based on the spatial distribution of multi-hazard (Figure 5.7 and Appendix A) which are obtained in hazard identification, the kinds of hazards that underpin the highest risk in the highest risk counties in Figure 5.21 can be summarised. Wenling, Sanmen, Linhai, Beicang, Zhenhai and Jinzhou are influenced by both slow and fast kinds riverine flood, pluvial flood, coastal flood and landslide; Tiantai and Xianju are at more danger from slow and fast kinds riverine floods, pluvial flood and landslide; Pudong New is influenced by slow kinds riverine flood, pluvial flood and coastal flood. Among them, fast kinds riverine flood and landslide in Xianju and pluvial flood in Pudong New are the most dangerous. Tiantai, Xianju and Sanmen have the highest vulnerability among the nine highest risk counties. According to the vulnerability-related indicator data, the smaller value of mobile phone users, doctors and medical institutions are the main reasons to induce higher vulnerability in these counties. The relatively small number of mobile phone users indicates that income of residents is relatively low and telecommunication condition is poor. The smaller value of doctors per head and medical institutions per km^2 represent that medical services are less developed.

In conclusion, MmhRisk-HI provides more reliable results (possible loss caused by multiple hazards) with an explicit consideration of interaction between different hazards, and can also be used to explore the reasons that contribute to large potential losses (high risk). Hence, this model is a useful tool which can provide better information to planners and decision-makers to make decisions on risk mitigation planning.

5.4 Summary and conclusion

This chapter applied the developed MHRA model, MmhRisk-HI, to the YRD and validated this model by comparison with a real system. The final results (possible loss caused by multiple hazards) obtained in this model are more reliable, due to an explicit consideration of interaction between different hazards. The results help to identify which areas are high potential loss areas, and allow a determination of the reasons that contribute to those large potential losses.

Section 5.1 applied the MmhRisk-HI in the YRD. In the hazard identification, the whole YRD area was divided into four zones according to the multiple hazards in each county. In the hazard analysis, typhoon was viewed as changes of wind speed and rainfall, and these changes can be used as the trigger factors to measure the magnitude of the series of hazards in the typhoon track. In the YRD, slow kinds riverine flood, fast kinds riverine flood, pluvial flood, coastal flood and landslide can all be induced in the typhoon track. Hence, maximum daily rainfall and maximum wind speed during the typhoon days were selected to measure the frequency and magnitude of these hazards, with the probability distribution of the rainfall and wind speed sets calculated by the two dimension information diffusion method. The relationships among multiple hazards in the YRD were analysed respectively in four zones which were divided by hazard identification. In the exposure analysis, GDP in 2013 in the YRD was used as an example. A BN was used to assess vulnerability. Indicators in the economic, social, physical and environmental domains were chosen to construct the sets of vulnerability-related indicators. The YRD struck by typhoon consecutively (twice within 60 days) was taken as example, and the vulnerability distribution with different exceedance probabilities of maximum daily rainfall and maximum wind speed sets in 2013 were calculated. Finally, the YRD influenced by two typhoons with exceedance probability of 10% and exceedance probability of 5% were investigated as an example application, and the corresponding loss distribution was calculated.

Section 5.2 used the model to simulate typhoon Trami (21st August) and typhoon Fitow (7th October) which struck the YRD in 2013. The simulated results were used to compare with the observed data in a model validation exercise. The validation results demonstrate that MmhRisk-HI can effectively represent the real world, both in terms of the geographical distribution of risk from multiple natural hazard, and aggregate loss value.

Results were further discussed in Section 5.3, with particular reference to the identification of different factors contributing to similar high risk. Compared to the recent comprehensive MHRA research which only considers the domino effect, MmhRisk-HI calculates the possible loss with an explicit consideration of all possible relationships between different hazards. Thus the final results obtained in this model are more reliable. Besides, based on the loss distribution in the YRD (influenced by two typhoons with exceedance probabilities of 10% and 5% respectively), the reasons that contribute to large potential losses were analysed.

It is concluded that MmhRisk-HI is a useful and improved MHRA tool which can provide further information for planners and decision-makers to make decisions on risk mitigation planning. In the final chapter, strengths and limitations of the model, and its role in effective risk mitigation are discussed, followed by a consideration of the overall contribution of the work and further research needs.

Chapter 6

Discussion and conclusion

This thesis began by setting out the rationale for the research and its aim and objectives (Chapter 1) which were to address capability gaps in existing multi-hazard risk assessment (MHRA) identified in Chapter 2. Chapter 3 discussed how to fill these gaps and introduced the case study area, the Yangtze River Delta (YRD). Chapter 4 discussed the construction of a new multi-hazard risk assessment (MHRA) model, MmhRisk-HI, based on the approach and methods discussed in Chapter 3, and this model was then applied and validated in the YRD to test its utility (Chapter 5). This final chapter includes a critical reflection on the MmhRisk-HI, including a discussion of its strengths and limitations, possible role and effectiveness in risk mitigation and associated planning. The recommendations for policy and practice, and further research are also identified. The chapter concludes by depicting the crux of each chapter and summarising the specific contributions this research has made to the field of natural hazard risk assessment.

6.1 Critical evaluation

Every model has strengths as well as limitations, and MmhRisk-HI is no exception. The specific strengths and limitations are discussed in detail below.

6.1.1 Strengths of MmhRisk-HI

The central aim of this research is to develop an improved MHRA model (MmhRisk-HI) that overcomes key limitations identified from the existing approaches. Thus, there are some strengths of this model compared with the existing MHRA approaches.

1) The biggest strength of this model is that it calculates the possible loss caused by multiple hazards, with an explicit consideration of all possible relationships among those hazards. The synthetic indicator of multiple hazards mainly uses the risk index method, with results used to compare the relative danger between different areas, but with no reflection of the real loss situation in these areas. Estimating integrated losses mainly relies on the mathematical statistics method to calculate possible losses caused by

multiple nature hazards in a given region and time period. However, this approach neglects the interaction between different hazards. To date, MHRA research reported in the literature proposes to assess possible losses caused by multiple hazards in a given time only through consideration of the domino effect. This approach to MHRA represents a rather small set of possible multi-hazard risks, as in practice, the interaction between different natural hazards is more complex. Therefore, simply addressing the domino effect is not enough to cover all situations as two hazards can occur independently without evident common cause, yet in close proximity, spatially, temporally, or both (as exemplified by the case study presented in Chapter 5 where the YRD is struck consecutively by typhoon).

In MmhRisk-HI, the hazard interaction analysis module analyses the hazard interaction and calculates the exceedance probability of multiple hazards occurrence based on the results of the hazard identification and hazard analysis modules. All possible relationships among different hazards can, in theory, be considered. Then the Bayesian network (BN), used in the vulnerability assessment module, calculates the possible loss ratio induced by multiple hazards with different exceedance probabilities. Hence, this new MHRA model is a more advanced model which considers all possible relationships among different hazards in risk assessment, and the results obtained in this model are possible losses which better reflect the real loss situation in a given area.

2) In terms of model design, this model is built upon a more comprehensive perspective of natural disaster than previous models. Risk of disaster from natural hazard must consider the process of disaster formation, including hazard, hazard-forming environment and exposure. However, prior approaches are variously based on the natural hazard perspective, the hazard-forming environment perspective or the exposure perspective which emphasize the dominant factors relevant to that perspective and ignore the other factors (Gong and Howarth, 1992; Busoni et al., 1995; McGuire et al., 2002). In MmhRisk-HI, the regional disaster system perspective is used, and put into practice. The regional disaster system perspective postulates that disaster is produced by the integration of hazard, exposure and hazard-forming environment (Shi, 1996; Wisner et al., 2004), and is a more complete perspective than those applied in prior models, and more suitable for MHRA.

MmhRisk-HI based on the regional disaster system perspective calculates the possible loss and corresponding probability of loss considering the stability of the hazard-forming environment, probability of the hazard occurrence and the vulnerability of exposure in an integrated model. During the modelling, the process of multi-hazard risk formation can be clearly expressed; for instance, hazards arise from specific hazard-forming environment; loss induced by the interaction of hazards and vulnerability of exposure. Although the risk index method emphasizes that risk is produced by hazard, vulnerability and exposure together, this risk index method estimates risk only by adding multi-hazard, vulnerability and exposure indices together. As a result, this calculation process is too simplistic and cannot reflect how risk is actually produced and propagated. Mathematical statistic method and the existing comprehensive MHRA research cannot show how hazards arise from a specific hazard-forming environment. Hence, compared to the existing MHRA approaches, MmhRisk-HI based on the regional disaster system perspective is more complete, clearly shows the multiple hazards risk formation process, and can better represent the real system.

3) Another strength of MmhRisk-HI is that it calculates multi-hazard risk by integrating two fundamental conceptual models together. These two conceptual models have particular advantages that have led to their widespread use and yet, they have disadvantages that can be addressed through their integration. The risk index approach calculates risk based on the first conceptual model, which addresses the interaction of hazard and exposure, but neglects the probability of risk. The mathematical statistics approach relies on the second conceptual model, which emphasizes the possible consequences by assessing risk from the perspective of possibility of loss, but cannot identify the reasons that contribute to high risk. In this thesis, a new MHRA model was developed by considering these two fundamental conceptual models together. MmhRisk-HI is thus produced which can estimate the possible losses induced by multi-hazards with different exceedance probabilities, and which also allows for a determination of the reasons that contribute to large potential losses (as it is important with respect to developing risk mitigation strategies and plans).

4) MmhRisk-HI is the first of its kind to introduce the concept of hazard-forming environment into the MHRA research. The hazard-forming environment includes environmental factors in the atmosphere, hydrosphere, biosphere and lithosphere. These environmental factors are the basic conditions for the occurrence of hazards. According to their contribution to natural hazard, these environmental factors were categorized into two types. Factors in the first type form the background to the occurrence of natural

hazards, and are stable factors acting as preconditions to hazards. These stable factors never change or change very little over a long time (hundreds or thousands of years), e.g. tectonic plates, landform, or the value of these factors stays within a relative stable range, e.g. annual average temperature, annual average precipitation. In contrast, factors in the second type (trigger factors) are constantly changing, e.g. daily precipitation, daily temperature. Substantial changes in trigger factors give rise to hazards.

Stable factors in the specific geophysical environment determine the preconditions for the occurrence of a specific natural hazard. According to the characteristic of these environmental factors, the spatial distribution of natural hazards in a region can be deduced. Stable factors analysis identifies hazard from environmental factors and it can consider all possible hazard situations even if some hazards have long return periods. Thus, stable factor analysis in this new MHRA model helps to fill a significant gap in existing hazard identification as observed hazard events may not reflect all possible hazard situations due to the long return period of some hazards.

Substantial changes in trigger factors is the main reason that some hazards are induced; hence, trigger factors can be used to estimate both the frequency and magnitude of hazards in the model, with the change of degree in trigger factors representing the magnitude of hazards, and the probability of change in them representing the probability of hazards. Compared to hazard magnitude data, most data for trigger factors are easy to collect such as daily precipitation, daily wind speed. Hence, trigger factors for hazard analysis can effectively be used to solve the data problem in existing methods.

In addition, in the hazard interaction module, the relationships among hazards were systematized for the first time in the MHRA research field, based on trigger factors analysis. A four class hazard interaction categorization was developed: independent, mutex, parallel and series relationships. The development of this categorization basically ensures that all possible relationships among different hazards are considered in the new MHRA model. Thus, trigger factors analysis can effectively fill the gap in existing methods which to date only consider domino effects.

Therefore, hazard-forming environment analysis (stable factors and trigger factors analysis) in MmhRisk-HI helps fill the gaps in existing hazard identification, hazard analysis and hazard interaction analysis.

5) A further strength of MmhRisk-HI is the use of a BN for vulnerability assessment. A vulnerability curve can reflect the relationship between loss ratio and hazard, but cannot reflect how physical, social, economic and environmental factors influence vulnerability. Conversely, a vulnerability index can reflect how physical, social, economic and environmental factors influence vulnerability, but cannot measure the relationship between loss and hazard by degree.

In MmhRisk-HI, a BN modelling framework was constructed according to domain knowledge (section 4.6.1). The loss ratio, which is assumed to be a parent of vulnerability- and hazard- related indicators, was the root node. Based on the hazard analysis and hazard interaction analysis, the corresponding trigger factors were chosen to construct the set of hazard-related indicators which represent the magnitude of multiple hazards. Indicators in the economic, social, physical and environmental domains were chosen to construct the sets of vulnerability-related indicators. Then, historic loss data was input into the model to calculate the conditional probability of a vulnerability-related indicator or hazard-related indicator given a loss ratio. These conditional probabilities can be used to assess the future loss. Thus, BN can calculate the loss ratio induced by multi-hazard of different degree (different states in hazard-related indicators), and can reflect how vulnerability-related indicators from physical, social, economic and environmental domains influence overall vulnerability.

MHRA is used to calculate the loss induced by multiple hazards. Some hazards may hit a given area consecutively in a short time. The short interval between these hazards means vulnerability cannot recover immediately. Existing MHRA research usually assumes there is no change in vulnerability, and calculates the loss in each hazard individually, with the same vulnerability, then sums to obtain the final loss. Thus, the final results cannot reflect the real loss situation, where vulnerability may vary according to prior events. In MmhRisk-HI, BN in a vulnerability analysis module is used to address this issue by considering the magnitude of hazards together in hazard-related indicators. These hazards are treated as a multiple hazards group, and the relevant vulnerability-related indicators correspond to this group rather than the component single hazards. Hence, the results obtained in MmhRisk-HI are more reliable.

6) Model validation is a difficult problem in MHRA and tends to be impracticable due to the structure of the models used. Results obtained by the risk index approach are the relative danger degree not the real loss (so

cannot be compared to observed losses directly), whilst the mathematical statistics approach estimates absolute loss from multiple natural hazards with different exceedance probabilities, but these exceedance probabilities imply uncertainty in the results and therefore, it is hard to validate against observed data.

Through its more comprehensive model design, MmhRisk-HI can be validated through comparison of modelled and observed data, with the model used to simulate different multiple natural hazards scenarios and estimate the corresponding loss. In the YRD case study, MmhRisk-HI was used to simulate consecutive events, typhoon Trami (21st August) and typhoon Fitow (7th October) which struck the YRD in 2013. The simulated results were then compared to the observed data, with good agreement. The validation results thus demonstrate that MmhRisk-HI can represent the real world risk situation with greater confidence.

Collectively, these strengths ensure MmhRisk-HI developed in this research is an advanced and powerful model for MHRA, and is a useful tool for risk mitigation.

6.1.2 Limitations of MmhRisk-HI

All models are abstractions of the real world, and imperfect. Some recognised limitations of the model are discussed below.

1) A change in one (or several) trigger factors may induce more than one hazard at the same time. In MmhRisk-HI, these hazards are treated as a multiple hazards group, with all hazards in the group induced by the same trigger factor(s). The frequency and magnitude of this hazard group are determined by the changes in these trigger factors. Thus, these trigger factors can be used as hazard-related indicators to represent the magnitude of this hazard group in vulnerability assessment. In this way, the results obtained in this model are more reliable (point 5 in section 6.1.1). However, these results cannot show how much loss is induced by each single hazard in the hazard group.

In reality, it is also hard to distinguish how much loss is induced by each single hazard. For example, during a typhoon, it is hard to distinguish how much loss can be attributed to strong winds and how much loss is induced by different types of floods. Indeed, in the historical disaster record, only records of loss induced by the whole typhoon are made, rather than for the constituent hazards. Nevertheless, in theory, if historical loss data in each single hazard were available, MmhRisk-HI could be used to calculate the loss situation in each single hazard with different exceedance probabilities.

2) In the vulnerably assessment module, vulnerability-related indicators, hazard-related indicators and the loss ratio which are used in the BN are all divided into different states: in the YRD case, the loss ratio was divided into six states, the eight vulnerability-related indicators were divided into five states, and the hazard-related indicators were divided into eight states. This introduces some data smoothing, but samples in the same state do have some differences, for example, in the YRD case, the loss ratio state 2 is $0\%<L2<0.5\%$; thus, a sample with value 0.01% and that with 0.49% are in the same state and yet, these two samples are treated as if they were the same in this model; in reality, the difference between loss ratio 0.01% and 0.49% is still substantial.

The state classification is determined by the number of samples. If the number of samples is big enough, the interval in each state can become small, and can even transfer the discrete interval into continuous value in each state.

3) In this thesis, this model took the YRD as a case study, and assessed the multi-hazard risk at regional scale. The results can show the risk difference in different counties (assessment unit) but cannot show the difference at local scale. For example, it does not differentiate risk between urban and rural areas. The new model, as currently applied, only assesses the multi-hazard risk at the regional scale. However, the theoretical framework is more broadly applicable, and with adequate data, the model could be developed for other scales (global, national, and local). Hence, with sufficient environmental data, disaster data and socioeconomic data at local scale, the multi-hazard risk difference between urban and rural area could be identified by this model.

6.2 Role in risk mitigation

MHRA is performed primarily for the purpose of providing information and insight to those who make decisions about how that risk should be managed. The synthetic indicator based risk index method is effective in comparing the relative danger experienced by different areas and analysing the reasons that contribute to any identified high risk areas, but it cannot calculate the absolute loss value. Integrated losses using the mathematical statistics method can calculate the absolute loss value caused by multiple nature hazards in a given region and time period, but it cannot analyse the reasons that contribute to high risk. In principle, these two approaches could be applied in parallel to provide more complete information on which to base risk management decisions. However, this is not in practice, and indeed, a comparative analysis has shown that when applied to a common region, these two methods give very different and often contradictory results (Liu et al., 2014). Hence, these two methods are hard to consider together in risk mitigation, and a more comprehensive model is required.

MmhRisk-HI developed in this research calculates the possible loss caused by multiple hazards, with an explicit consideration of interaction between different hazards. The final results obtained in this model can help to identify which areas are at high risk (of large loss), and allow a determination of the reasons that contribute to those large potential losses (high risk). Hence, it is a useful tool which can provide further information for planners and decision-makers concerned with risk mitigation. More specifically the model could be used to provide the following types of risk mitigation decision support.

1) Support optimal investment in disaster mitigation

The final results obtained in MmhRisk-HI are potential absolute loss induced by multiple hazards with different exceedance probabilities. Compared to the existing MHRA research, the results derived from MmhRisk-HI are more reliable with an explicit consideration of interaction between different hazards. These loss values can help planners and decision-makers to understand the possible future losses in a given area. Based on this possible loss situation, decisions on an appropriate level of disaster investment can be made.

2) Support targeting of disaster mitigation measures

MmhRisk-HI can help to identify the reasons that contribute to large potential losses (high multiple hazards magnitude, high vulnerability and high exposure value). Furthermore, the kinds of hazards and types of vulnerability-related indicator that underpin large potential losses also can be identified. Thus, this MHRA model can help planners and decision-makers deeper understand the factors that underpin high risk, and they can then take appropriate mitigation measures (informed by the investment analysis identified above), which could be strategic (e.g. land use plans), or tactical (e.g. building codes, warning and emergency response systems). For example, high risk in one county may be due to undeveloped medical services, which if developed could reduce potential losses. Thus, support for risk mitigation may be targeted both functionally and geographically.

3) Provide a reference for economic development planning

MmhRisk-HI identifies multi-hazard risk geographically, with an understanding of the hazard and vulnerability factors that contribute to that risk. Thus, the model can usefully inform economic development plans and strategic land use plans, by directing development to locations where risk level is more appropriate to the development of interest (for example, high vulnerability critical infrastructure, should be located in a low multi-hazard risk area). Better knowledge of the natural hazard risk could also lead to mitigation measures that are not just spatial (build elsewhere), but which are design oriented (e.g. appropriate flood protection measures, or building codes that require adequate provision of shelters in areas at high typhoon risk).

In addition to public planners and decision-makers, MmhRisk-HI could also be useful to the insurance industry in terms of setting insurance premiums that better reflect multi-hazard risk, and in establishing a multi-hazard risk insurance system. The spatial distribution of multi-hazard can also help local residents understand which kinds of natural hazards influence their living areas and the susceptibility to these hazards, thus enhancing public risk awareness and informing local risk management.

6.3 Recommendations

6.3.1 Recommendations for policy and practice

As mentioned above, the model developed in this thesis is a useful tool to form the basis of prudent planning and prioritized risk-mitigation measures. In this section, some recommendations for policy and practice are discussed.

1) MHRA should be embedded in economic development planning and land use planning. If public planners and decision-makers made planning without considering the MHRA, some high vulnerability critical infrastructure could be located in a high multi-hazard risk area. This situation may easily lead to huge loss when some hazards occur. Embedding the MHRA in planning can effectively avoid this situation. As mentioned in section 6.2, MHRA identifies multi-hazard risk geographically and helps adjust land use and development strategies accordingly. Furthermore, based on the MHRA, public planners

and decision-makers can forecast future disaster situations, and thus bundle some proper protective measures into planning to avoid the risk of disaster.

2) Disaster emergency management should transfer from single hazard to multiple hazards. The traditional disaster emergency management, which mainly focuses on single hazard, is relatively useless in some multiple hazards scenarios (Scolobig et al., 2014). Taking the Philippines case in Chapter 1 as an example (the central Philippines was struck consecutively by the Bohol earthquake and typhoon Haiyan), we note that the Philippines government found it difficult to cope with the second disaster, typhoon Haiyan, due to a shortage of relief supplies. In this thesis, the developed model, MmhRisk-HI, identifies which kinds of hazards occur in a given area and calculates the probability of these hazards occurring together. It effectively helps disaster managers to understand the possible multiple hazards situations in the future, thus they can design emergency response plans and mechanisms to cope with these multiple hazards scenarios rather than single hazard. In addition, MmhRisk-HI also assesses the possible loss caused by multiple hazards in each assessment unit. These loss assessments support disaster managers who can, for example, prepare sufficient emergency supplies for multiple hazards scenarios, and allocate them effectively to each unit.

3) There is a need to enhance public awareness of multi-hazard risk. Generally, public awareness of primary hazard risks has been well established, while that of the subsequent hazards risks (e.g. hazards triggered by the primary hazard) is less established (Scolobig et al., 2014; Komendantova et al., 2014). This means most local residents do not realize the subsequent hazards risks after the first disaster. Thus, when these subsequent hazards occur, residents are ill prepared and slow to take effective measures. As mentioned in section 6.2, the spatial distribution of multi-hazard identified in MmhRisk-HI helps local residents to discern and understand the characteristics and severity of risk from multiple hazards scenarios, thus this model is useful for enhancing public awareness of multi-hazard risk.

4) Risk communication between researchers and decision-makers should be strengthened. Due to differences in knowledge, it is not always easy for researchers to communicate the MHRA results or risk information to decision-makers (Komendantova et al., 2014). In this research, MmhRisk-HI can simulate different multiple natural hazards scenarios to estimate the corresponding loss. Take the figures in Appendix E as an example, where

hundreds of scenarios with different vulnerability-related indicators and multiple natural hazards intensity were simulated by the model. Hence, when decision-makers want to know the risk situation in a given area, the model can be applied to simulate all possible scenarios for the area, and provide a loss distribution with upper (worst case scenarios) and lower bounds (best case scenarios). These bounds can help decision-makers understand the extent of uncertainty of the risk, thus increasing confidence in the risk assessment results.

6.3.2 Recommendations for further research

Some limitations of MmhRisk-HI have been discussed above, and these form an appropriate basis for recommendations for further research to test and refine the model. These research needs are discussed further below.

1) In this thesis, MmhRisk-HI was applied in the YRD to assess the loss distribution influenced by consecutive typhoons with different exceedance probabilities. The validation results proved that MmhRisk-HI can more effectively represent the real world, and that the results obtained with the model are reliable. In theory, using this model, the loss distribution that arises through other hazard combinations in other areas can also be calculated. Hence, MmhRisk-HI will be used in more cases (different areas, different multi-hazard groups) in the future to prove that it is superior in its performance to previous approaches.

2) Section 6.1.2 notes that MmhRisk-HI developed in this research cannot distinguish how much loss is induced by each single hazard in multiple hazards situation. In this model, the susceptibility degree to each hazard can be summarised based on the spatial distribution of multi-hazard, but the susceptibility degree is the relative danger degree rather than the real loss situation. Understanding the loss induced by each single hazard could help decision-makers take more targeted mitigation measures, so if for example, strong winds contribute to 90% of loss during a typhoon, more measures should be taken for resisting strong winds rather than pluvial flood and other floods hazards. In theory, if historical loss data in each single hazard were available, MmhRisk-HI could be used to calculate the loss situation in each single hazard. However, in reality, it is also hard to distinguish how much loss is induced by each single hazard. Thus, there is no historical loss data about each single hazard in multiple hazards situations. Hence, how to address this issue without historical loss data will become a difficult problem in the future.

3) The second limitation (section 6.1.2) relates to the vulnerably assessment module, where the vulnerability-related indicators, hazard-related indicators and loss ratio are, in the BN, grouped into common states, despite differences across samples in each state. As the range in each state reduces, variability across component samples falls. The range is determined by the number of samples. However, in reality, there is not enough sample data in most areas. Hence, how to reduce the sample difference in the same state with the limited sample data will become a tough issue in the future.

4) MHRA research at the regional scale, as demonstrated here for the YRD, provides useful information for disaster mitigation and economic development planning. However, a great need is also to better understand the multi-hazard risk that exists at a more local scale, particularly the city-region scale. The world is increasingly urban, and rapid urbanization is underway in parts of the world, with more people, critical infrastructure, and wealth crowded into urban areas, which are thus at particular risk from multiple hazards. Urban risk assessment, and particularly MHRA at small-scale (city region, local and community scale) is needed to inform improved disaster mitigation. The model developed in this thesis is well placed to tackle this challenge.

5) Uncertainty is inherent in natural disaster risk. It is widely acknowledged that uncertainty analysis in risk assessment is important for decision-making and risk management (e.g. Bell and Glade, 2004; Schmidt et al., 2011), but approaches for uncertainty analysis are still rare in the MHRA area (Vangwlsten, 2013). Uncertainty is commonly classified into two kinds: aleatory uncertainty (it is due to the natural randomness of a system) and epistemic uncertainty (it is due to limited knowledge about the system and lack of data) (Matthies, 2007; Der Kiureghian and Ditlevsen, 2009). Rohmer (2012) divided the epistemic uncertainty into four additional types: epistemic - data, epistemic - models, epistemic - parameters and epistemic - science. Some sources of uncertainty in MmhRisk-HI are listed in Table 6.1. These uncertainties are spread throughout the whole MHRA process. Hence, how to reduce these uncertainties will become a difficult problem in the future.

Table 6.1 Some sources of uncertainty in MmhRisk-HI

Source of uncertainty	Type	Reason
Hazard identification	Aleatory	The intrinsically random variability of some environmental factors.
	Epistemic: data	Inexact measurement techniques of some environmental factors.
	Epistemic: models parameters	The selection of classification standard for susceptibility to each hazard.
	Epistemic: science	Some unknown environmental factors which could influence the distribution of natural hazards.
Hazard analysis	Aleatory	The intrinsically random variability of hazard occurrence.
	Epistemic: data	Inexact measurement techniques and the limited historical data.
	Epistemic: models parameters	The selection of spatial interpolation technique.
	Epistemic: science	Some unknown trigger factors which could induce natural hazards.
Hazard interaction analysis	Aleatory	The intrinsically random variability of hazard occurrence.
	Epistemic: science	Some unknown relationships between different natural hazards.
Exposure analysis	Aleatory	The number of exposure at a given time in a given area is random variability.
	Epistemic: data	Inexact measurement techniques.
Vulnerability analysis	Aleatory	The value of some vulnerability-related indicators is random variability.
	Epistemic: data	Inexact measurement techniques and the limited historical data.
	Epistemic: models parameters	The state classification for vulnerability-related indicators, hazard-related indicators and the loss ratio is determined by the number of samples.
	Epistemic: science	Some unknown vulnerability-related indicators which could influence the loss ratio.

6.4 Conclusion

In concluding this study, a brief overview of the research and key advances made are presented.

6.4.1 Research overview

Multiple hazards risk assessment has become a major concern in the risk study area, but existing approaches do not adequately meet the needs of risk mitigation planning, hence an improved MHRA approach, and associated tool, was developed. The central aim of this research is to evaluate the existing MHRA approaches, and develop an improved quantitative technique that overcomes key limitations identified from the existing approaches, forming the basis of more prudent planning and prioritized risk-mitigation measures.

Chapter 2 provided a review of literature addressing the key concepts, theories and practice relevant to advancing research in MHRA. On the basis of the literature review, the main research gap in the existing MHRA was identified that existing MHRA methods cannot consider all hazard interactions when calculating possible losses. Some gaps in the conceptual model and basic components for MHRA were also identified.

Chapter 3 discussed the research design and approaches used to explore and address current limitations in MHRA. A more complete perspective, the regional disaster system perspective, was selected as the basic theory for model construction, and two categories of multi-hazard risk expressions were combined in the model construction. Hazard identification, hazard analysis, hazard interaction analysis, exposure analysis and vulnerability analysis are the basic modules of the new MHRA model, MmhRisk-HI. Hazard-forming environment analysis is the basis for hazard identification, hazard analysis, and hazard interaction analysis. The methods used for exposure analysis depend on the scale of the region to be addressed and the assessment units. A BN was adopted to calculate the loss ratio in the vulnerability analysis.

Chapter 4 discussed the construction of MmhRisk-HI based on the approach and methods discussed in chapter 3. The model calculates the possible loss caused by multiple hazards, with an explicit consideration of interaction between different hazards.

Chapter 5 applied MmhRisk-HI to the YRD and validated the model by comparison with an observed multi-hazard sequence. The validation results proved that MmhRisk-HI can more effectively represent the real world, and that the outputs (possible loss caused by multiple hazards) obtained with the model are reliable. The outputs can additionally help to identify which area is at greatest risk (of loss), and allow a determination of the reasons that contribute to the greatest losses.

Chapter 6 discussed the strengths, limitations and effectiveness on risk mitigation of MmhRisk-HI. Six strengths of this model were discussed. The greatest strength is that the model calculates the possible loss caused by multiple hazards, with an explicit consideration of all possible relationships among different hazards. The effectiveness on risk mitigation of this model shows it is a useful tool to form the basis of prudent planning and prioritized risk-mitigation measures.

6.4.2 Contributions

There are several innovations in this research that represent significant contributions to the science of risk assessment, and practical use in risk mitigation. These are:

1) The main contribution of this research is that it constructs a more sophisticated and improved MHRA model (MmhRisk-HI), which calculates the possible loss caused by multiple hazards, with an explicit consideration of all possible interaction between different hazards. It takes advantage of the merits of both risk index method and mathematical statistics methods. This new model has been validated through comparison with a real world multi-hazard event sequence. Model validation is a highly desirable step in model development, but a process that has previously proved intractable in MHRA due to the nature of the existing models. The validation results proved that MmhRisk-HI can effectively represent the real system, with outputs (possible loss caused by multiple hazards) more reliable than those from existing MHRA approaches.

2) This research applied the regional disaster system perspective in the model construction. The regional disaster system perspective postulates that disaster is a product of hazard, exposure, and hazard-forming environment together. Unlike other disaster perspectives that emphasise one or other of these elements, the regional disaster system perspective is a more complete and balanced perspective of multi-hazard risk formation. Thus, the model built on the regional disaster system perspective can better represent real world risk.

3) This research also introduced the concept of the hazard-forming environment into MHRA research. Natural hazards must arise from a specific

hazard-forming environment. Geophysical environmental factors in the hazard-forming environment determine the fundamental characteristics of natural hazards (space, time, magnitude and frequency). Hazard-forming environment analysis (stable factors and trigger factors analysis) can therefore help to fill gaps in existing hazard identification, hazard analysis and hazard interaction analysis. In the hazard interaction module, the relationships among hazards were also systematized for the first time in the MHRA field, using trigger factor analysis. A four class categorization was developed with hazard relationships defined as either: independent, mutex (mutually exclusive), parallel or series. This categorization ensures that all possible relationships among different hazards are considered in the model.

4) Finally, it is concluded that MmhRisk-HI developed here is a useful tool to form the basis of prudent planning and prioritized risk-mitigation measures. The final results obtained from the model are potential absolute loss induced by multiple hazards with different exceedance probabilities. The absolute loss can support more optimal investment in disaster mitigation measures. This model can help to identify the reasons that contribute to large potential losses, and the kinds of hazards and types of vulnerability-related indicators that underpin large potential losses. This can help planners and decision-makers to better target multi-hazard risk mitigation measures (both functionally, and geographically). Furthermore, this model also can help planners and decision-makers to develop and adjust national and strategic land use and economic development plans that are more sensitive to risk from multiple natural hazards.

Bibliography

Aki, K., & Richards, P. G. (2002). *Quantitative seismology* (2nd ed.). California: University Science Books.

Alexander, D. (1993). *Natural disasters*. London: UCL Press.

Alexander, D. (2000). *Confronting catastrophe, new perspectives on natural disaster*. Harpenden: Terra.

Allen, K. (2003). Vulnerability reduction and the community-based approach. In M. Pelling (Ed.), *Natural Disasters and Development in a Globalising World* (pp170-184). New York: Routledge.

Armas, I. (2006). Earthquake risk perception in Bucharest, Romania. *Risk Analysis*, 26(5), 1223-1234.

Armonia (Applied Multi-Risk Mapping of Natural Hazards for Impact Assessment). (2006). *Applied multi-risk mapping of natural hazards for impact assessment. Report on new methodology for multi-risk assessment and the harmonisation of different natural risk maps*. Genova: Armonia, European Community.

Arnold, M., et al. (2006). *Natural disaster hotspots case studies*. Washington, D.C: World Bank.

Barredo, J. I. (2007). Major flood disasters in Europe: 1950–2005. *Natural Hazards*, 42(1), 125-148.

Bayraktarli, Y. Y., et al. (2006). Capabilities of the Bayesian probabilistic networks approach for earthquake risk management. *First European Conference on Earthquake Engineering and Seismology*. Geneva, Switzerland.

Bell, R., & Glade, T. (2004). Quantitative risk analysis for landslides? Examples from Bíldudalur, NW-Iceland. *Natural Hazards and Earth System Science*, *4*(1), 117-131.

Berz, G., et al. (2001). World map of natural hazards–a global view of the distribution and intensity of significant exposures. *Natural Hazards,* 23(2-3), 443–465.

Birkmann, J. (2006). Measuring vulnerability to promote disaster-resilient societies: conceptual frameworks and definitions. In J. Birkmann (Ed.), *Measuring vulnerability to natural hazards* (pp 9–54). UNU Press.

Blaikie, P., Cannon, T., Davis, I. & Wisner, B. (1994). *At risk: natural hazards, people's vulnerability, and disasters.* New York: Routledge.

Blanchard, W. (2005). *Select emergency management-related terms and definitions, vulnerability assessment techniques and applications (VATA)*. NOAA Coastal Services Center. Retrieved from http://www.csc.noaa.gov/vata/glossary.html.

Bolstad, P. V., & Stowe, T. (1994). An evaluation of DEM accuracy: elevation, slope, and aspect. *Photogrammetric Engineering and Remote Sensing*, *60*(11), 1327-1332.

Bonachea, J., Remondo, J., Terán, D., Díaz, J. R., González‐Díez, A., & Cendrero, A. (2009). Landslide risk models for decision making. *Risk Analysis*, 29(11), 1629-1643.

Bronstert, A. (2003). Floods and climate change: interactions and impacts. *Risk Analysis*, *23*(3), 545-557.

Brooks, N. (2003). Vulnerability, risk and adaptation: A conceptual framework. *Tyndall Centre for Climate Change Research Working Paper*, 38, 1-16.

Burton, I., & Kates, R. W. (1963). Perception of Natural Hazards in Resource Management, The. *Nat. Resources J.*, 3, 412.

Burton, I., Kates, R. W. & White, G. F. (1993) *The Environment as Hazard* (2nd ed). New York: The Guildford Press.

Busoni, E., Sanchis, P. S., Calzolari, C., & Romagnoli, A. (1995). Mass movement and erosion hazard patterns by multivariate analysis of landscape integrated data: the Upper Orcia River Valley (Siena, Italy) case. *Catena*, 25(1), 169-185.

Cannon, T., Twigg, J., & Rowell, J. (2003). *Social vulnerability, sustainable livelihoods and disasters.* London: DFID.

Carpignano, A., Golia, E., Di Mauro, C., Bouchon, S., & Nordvik, J. P. (2009). A methodological approach for the definition of multi-risk maps at regional level: first application. *Journal of Risk Research*, 12(3-4), 513–534.

CEC (Commission of the European Communities). (2006). *Proposal for a*

Directive on the assessment and management of floods (COM (2006)15 final). Brussels : Commission of the European Communities.

Chambers, R. (1989). Editorial introduction: vulnerability, coping and policy. *IDS bulletin*, 20(2), 1-7.

Chung, R. M. (Ed.). (1994). *Natural Disaster Studies. An Investigative Series of the Committee on natural Disasters.* Washington D.C: National Academy Press.

Cohen, R. E., & Ahearn, F. L. (1980). *Handbook for mental health care of disaster victims.* Baltimore: The Johns Hopkins University Press.

Cutter, S. L. (1996). Societal responses to environmental hazards. *International Social Science Journal*, 48(150), 525-536.

Cutter, S. L., Boruff, B. J., & Shirley, W. L. (2003). Social vulnerability to environmental hazards*. *Social science quarterly*, 84(2), 242-261.

Cutter, S. L., Mitchell, J. T., & Scott, M. S. (2000). Revealing vulnerability of people and place: A case study of Geogretown county, South Carolina. *Annals of the association of American Geographer*, 90(4), 713-737.

Daniel, M. B. III., & Cothern, R. C. (2001). *Introduction to risk analysis: a systematic approach to science-based decision making.* Rockville: Government Institutes.

Der Kiureghian, A., & Ditlevsen, O. (2009). Aleatory or epistemic? Does it matter? *Structural Safety*, *31*(2), 105-112.

Di Piazza, A., Conti, F. L., Noto, L. V., Viola, F., & La Loggia, G. (2011). Comparative analysis of different techniques for spatial interpolation of rainfall data to create a serially complete monthly time series of precipitation for Sicily, Italy. *International Journal of Applied Earth Observation and Geoinformation*, 13(3), 396-408.

Dilley, M., et al. (2005). *Natural disaster hotspots, a global risk analysis.* Washington, D.C: World Bank.

Di Mauro, C., Bouchon, S., Carpignana, A., Golia, E., & Peressin, S. (2006). Definition of multi-risk maps at regional level as management tool: experience gained by civil protection authorities of Piemonte region. *5th conference on risk assessment and management in the civil and industrial settlements*. University of Pisa, Italy.

Dixon, B. (2005). Groundwater vulnerability mapping: A GIS and fuzzy rule based Integrated Tool. *Applied Geography*, 25(4), 327-347.

Downing, T. E., Butterfield, R., Cohen, S., Huq, S., Moss, R., Rahman, A., Sokona, Y., & Stephen, L. (2001). *Vulnerability Indices: Climate Change Impacts and Adaptation* (UNEP Policy Series, No. 3, Nairobi 07/2001; 3). Nairobi: UNEP.

Dracup, J. A., Lee, K. S., & Paulson, E. G. (1980). On the definition of droughts. *Water Resources Research*, 16(2), 297-302.

Dutta, D., Herath, S., & Musiake, K. (2003). A mathematical model for flood loss estimation. *Journal of Hydrology*, 277(1-2), 24-49.

Eddy, J. A., et al. (1986). *Global Change in the Greosphere Biosphere.* Washington, D.C: National Academy Press.

EL-Sabh, M. I., & Murty, T. S. (1988). *Natural and Man-made Hazards, Holland.* Dordrecht: D. Reidel Publishing Company.

EM-DAT (Emergency events database) (2011) *The OFDA/CRED International Disaster Database.* Universite ́ Catholique de Louvain, Brussels. Retrieved from http://www.cred.be/emdat.

EM-DAT (Emergency events database) (2013) *The OFDA/CRED International Disaster Database.* Universite ́ Catholique de Louvain, Brussels. Retrieved from http://www.cred.be/emdat.

EM-DAT (Emergency events database) (2015) *The OFDA/CRED International Disaster Database.* Universite ́ Catholique de Louvain, Brussels. Retrieved from http://www.cred.be/emdat.

Eshrati, L., Mahmoudzadeh, A., & Taghvaei, M. (2015). Multi hazards risk assessment, a new methodology. *International Journal of Health System and Disaster Management*, 3(2), 79-88.

Falconer, R. H., Cobby, D., Smyth, P., Astle, G., Dent, J., & Golding, B. (2009). Pluvial flooding: new approaches in flood warning, mapping and risk management. *Journal of Flood Risk Management*, 2(3), 198-208.

Fang, W.H., et al. (2011). *Integrated Risk Governance: data base, risk map and network platform.* Beijing: Science Press.

FEMA (Federal Emergency Management Agency) (2004). *Using HAZUS-MH for risk assessment.* Retrieved from http://www.fema.gov.

Fernández, D. S., & Lutz, M. A. (2010). Urban flood hazard zoning in Tucumán Province, Argentina, using GIS and multicriteria decision analysis. *Engineering Geology*, 111(1), 90-98.

Fleischhauer, M. (2005). *ARMONIA scientific colloquium: risk assessment and spatial planning in France*. Dortmund, Germany.

Fleischhauer, M., et al. (2005). Multi-risk assessment of spatially relevant hazards in Europe. *International ESMG (European Safety Management Group) symposium 2005.* Hamm (Germany): ESMG.

Fournier d'Albe, E. M. (1979). Objectives of volcanic monitoring and prediction. *Journal of the Geological Society of London*, 136(3), 321-326.

French, J. G., & Holt, K. W. (1989). Floods. In M. B. Gregg (Ed.), *The Public Health Consequences of Disasters* (pp. 69–78). Atlanta, Georgia: US Department of Health and Human Services, Public Health Service.

Friedman, N. (1998). The Bayesian structural EM algorithm. *Proceedings of the Fourteenth conference on Uncertainty in artificial intelligence* (pp. 129-138). Burlington, Massachusetts: Morgan Kaufmann Publishers Inc.

Frigerio S., Kappes M.S., Glade T., & Malet J-P. (2012). *MultiRISK: a platform for Multi-Hazard Risk Modelling and Visualisation.* Retrieved from http://www.mae-srl.it/allegati/3_22_692.pdf.

Frolova, N. I., Larionov, V. I., Sushchev, S. P., & Bonnin, J. (2012). Seismic and integrated risk assessment and management with information technology application. *15th world conference on earthquake engineering*. Lisbon.

Gao, Q. H., et al. (2007). *Natural disaster assessment.* Beijing: Meteorological Press.

Garcia-Aristizabal, A., & Marzocchi, W. (2013). *Scenarios of cascade events*. (ENV.2010.6.1.3.4 New methodologies for multi-hazard and multi-risk assessment).

Ge, Q. S., et al. (2008). *Integrated assessment of natural disaster risk to China*. Beijing: Science Press.

Gill, J. C., & Malamud, B. D. (2014). Reviewing and visualizing the interactions of natural hazards. *Reviews of Geophysics*, 52(4), 680-722.

Gong, P., & Howarth, P. J. (1992). Land-use classification of SPOT HRV data using a cover-frequency method. *International Journal of Remote Sensing*, 13(8), 1459-1471.

Granger, K., & Trevor, J. (2000). A multi-hazard risk assessment. In M. Middelmann, & K. Granger (Eds.), *Community risk in MacKay, A multi-hazard risk assessment*. Australian geological survey organization.

Gray, W. M. (1979). Hurricanes: Their formation, structure and likely role in the tropical circulation. *Meteorology over the tropical oceans*, 77, 155-218.

Grossman, D., & Domingos, P. (2004). Learning Bayesian network classifiers by maximizing conditional likelihood. *Proceedings of the twenty-first international conference on Machine learning*. New York: ACM.

Gruber, F. E., & Mergili, M. (2013). Regional-scale analysis of high-mountain multi-hazard and risk indicators in the Pamir (Tajikistan) with GRASS GIS. *Natural Hazards and Earth System Science*, 13(11), 2779-2796.

Grünthal. G., et al. (2006). Comparative risk assessment for the city of Cologne-storms, floods, earthquake. *Natural Hazards*, 38, 21-44.

Gumbel, E. J. (1958). *Statistics of Extremes.* New York: Columbia University Press.

Guzzetti, F., Carrara, A., Cardinali, M., & Reichenbach, P. (1999). Landslide hazard evaluation: a review of current techniques and their application in a multi-scale study, Central Italy. *Geomorphology*, 31(1), 181-216.

Hahn, H., Villagrán De León, J. C., & Hidajat, R. (2003). *Indicators and other disaster risk management instruments for communities and local Governments.* German Agency for International Cooperation (GTZ), Inter-American Development Bank (IDB).

Hall, J. W., Dawson, R. J., Sayers, P. B., Rosu, C., Chatterton, J. B., & Deakin, R. (2003). A methodology for national-scale flood risk assessment. *Proceedings of the ICE-Water and Maritime Engineering*, 156(3), 235-247.

Haque, C. E. (2000). Risk assessment, emergency preparedness and response to hazards: the case of the 1997 Red River Valley flood, Canada. In *Natural Hazards* (pp. 225-245). Netherlands: Springer.

Henderson-Sellers, A., et al. (1998). Tropical cyclones and global climate change: A post-IPCC assessment. *Bulletin of the American*

Meteorological Society, 79(1), 19-38.

Heckerman, D., Geiger, D., & Chickering, D. M. (1995). Learning Bayesian networks: The combination of knowledge and statistical data. *Machine learning*, 20(3), 197-243.

Hester, R. E., & Harrison, R. M. (Eds.). (1998). *Risk assessment and risk managemen*t (Vol. 9). Royal Society of Chemistry.

Hewitt, K. (Ed.). (1983). *Interpretation of Calamity: From the Viewpoint of Human Ecology*. Boston: Allen.

Hewitt, K. (1997). *Regions of Risk: A Geographical Introduction to Disasters.* Essex: Longman.

Hilhorst, D., & Bankoff, G. (2004). Introduction: mapping vulnerability. In G. Bankoff, G. Frerks, & D. Hilhorst (Eds), *Mapping vulnerability: disasters, development and people* (pp. 1-9). London: Earthscan.

Hisdal, H., & Tallaksen, L. M. (Eds.). (2000). *Drought event definition. Assessment of the Regional Impact of Droughts in Europe.* (Technical Report No. 6). Oslo: Department of Geophysics, University of Oslo.

Ho, C. H., Baik, J. J., Kim, J. H., Gong, D. Y., & Sui, C. H. (2004). Interdecadal changes in summertime typhoon tracks. *Journal of Climate*, 17(9), 1767-1776.

Hohl, R., Schiesses, H., & Aller, D. (2002). Hailfall: The relationship between radar-derived hail kinetic energy and hail damage to buildings. *Atmospheric Research*, 63(1-2), 177-207.

Hsu W. K., Chiang, W. L., & Chen, C. W. (2013). Earthquake risk assessment and optimal risk management strategies for hi-tech fabs in Taiwan. *Natural Hazards*, 65(3), 2063–2076.

Huang, C. F. (1997). Principle of information diffusion. *Fuzzy Sets and Systems*, 91(1), 69-90.

Huang, C. F. (2000). Demonstration of benefit of information distribution for probability estimation. *Signal Process*, 80 (6), 1037-1048.

Huang, C. F., Guo, J., Ai, F. L., & Wu, T. (2013). Basic paradigm of risk analysis in flood disaster and its application. *Journal of natural disaster*, 22(4), 11–23.

Hurst, N. W. (1998). *Risk assessment: the human dimension.* Cambridge: Cambridge University Press.

IFRC(International Federation of Red Cross and Red Crescent Societies). (2013). *Meteorological hazards: Tropical storms, hurricanes, cyclones and typhoons.* Retrieved from https: //www.ifrc.org/en/what-we-do/disaster-management/about-disasters/definition-of-hazard/tropical-storms-hurricanes-typhoons-and-cyclones.

ISDR (Intentional Strategy for Disaster Reduction). (2004). *Living with risk. A global review of disaster reduction initiatives*. Geneva: United Nations publication.

IUGS (International Union of Geological Sciences). (1997). Quantitative risk assessment for slopes and landslides—the state of the art. In D.M. Cruden & R. Fell (Eds.), *Landslide risk assessment*. Rotterdam: Balkema.

Jensen, F. V., & Nielsen, T. D. (2007). *Bayesian Networks and Decision Graphs* (2nd ed.). New York: Springer.

Jolliffe, I. (2002). *Principal component analysis*. John Wiley & Sons, Ltd.

Jonkman, S. N. (2005). Global perspectives on loss of human life caused by floods. *Natural Hazards*, 34(2), 151-175.

JRC (Joint Research Centre). (2004). *European commission: annual report 2003*. Brussels: European Communities.

Kappes, M., Keiler, M., & Glade, T. (2010). From single-to multi-hazard risk analyses: a concept addressing emerging challenges. In J. P. Malet, T. Glade, & N. Casagli (Eds.), *Mountain Risks: Bringing Science to Society* (pp. 351–356). Strasbourg: CERG Editions.

Kappes, M. S., Keiler, M., von Elverfeldt, K., & Glade, T. (2012). Challenges of analyzing multi-hazard risk: a review. *Natural Hazards*, 64(2), 1925-1958.

Kates, R. W. (1978). *Risk assessment of environmental hazard*. Chichester: Wiley [for] the Scientific Committee on Problems of the Environment (SCOPE) of the International Council of Scientific Unions (ICSU).

Keller, A. Z., Wilson, H., & Kara-Zaitri, C. (1990). The Bradford disaster scale. *Disaster Management*, 2(4), 207-213.

Khatsu, P., & van Westen, C. J. (2005). Urban multi-hazard risk analysis using GIS and remote sensing: a case study from Kohima Town, Nagaland, India. *Proceedings of the 26th Asian Conference on remote sensing*. Hanoi, Vietnam.

Komendantova, N., Mrzyglocki, R., Mignan, A., Khazai, B., Wenzel, F., Patt, A., & Fleming, K. (2014). Multi-hazard and multi-risk decision-support tools as a part of participatory risk governance: Feedback from civil protection stakeholders. *International Journal of Disaster Risk Reduction*, 8, 50-67.

Kron, W. (2005). Flood risk= hazard• values• vulnerability. *Water International*, 30(1), 58-68.

Kunz, M., & Hurni, L. (2008). Hazard maps in switzerland. *Proceedings of the 6th ICA Mountain Cartography Workshop* (pp.125–130). Lenk, Switerland.

Kuriakose, S. L., Sankar, G., & Muraleedharan, C. (2009). History of landslide susceptibility and a chorology of landslide-prone areas in the Western Ghats of Kerala, India. *Environmental geology*, 57(7), 1553-1568.

Lane, S. N., et al. (2003). Land management, flooding and environmental risk: new approaches to a very old question. *Proceedings of the Chartered Institution of Water Environmental Management National Conference: the environment–visions, values and innovation* (pp. 10-12). Harrogate, UK.

Lauritzen, S. L. (1995). The EM algorithm for graphical association models with missing data. *Computational Statistics & Data Analysis*, 19(2), 191-201.

Lavalle, C., Barredo, J. I., Roo, A. D., Niemeyer, S., Miguel-Ayanz, J. S., Hiederer, R., Genovese, E., & Camia, A. (2005). *Towards an European integrated map of risk from weather driven events. A contribution to the evaluation of territorial cohesion in Europe*. Brussels: Joint Research Centre, European Commission.

Li, L. F., et al. (2010). Assessment of catastrophic risk using Bayesian network constructed from domain knowledge and spatial data. *Risk Analysis*, 30(7), 1157-1175.

Li, J. L., Zhang, J., Zhang, C., & Chen, Q. G. (2006). Analyze and compare the Spatial Interpolation Methods for climate factor. *Pratacultural Science*, 23(8), 6-11.

Linares-Rivas, A. (2012). C*APRA initiative: integrating disaster risk into development policies in Latin America and the Caribbean. R*etrieved from http://www.ecapra.org/capra-initiative-integrating-disaster-risk-development-policies-latam.

Liao, W., & Ji, Q. (2009). Learning Bayesian network parameters under incomplete data with domain knowledge. *Pattern Recognition*, 42(11), 3046-3056.

Liu, B., Siu, Y. L., Mitchell, G., & Xu, W. (2013). Exceedance probability of multiple natural hazards: risk assessment in China's Yangtze River Delta. *Natural hazards*, 69(3), 2039-2055.

Liu, B., Siu, Y. L., Mitchell, G., & Xu, W. (2014). The danger of mapping risk from multiple natural hazards. *Sustainability Research Institute Working Paper Series*, No. 61.

Lung, T., Lavalle, C., Hiederer, R., Dosio, A., & Bouwer, L. M. (2013). A multi-hazard regional level impact assessment for Europe combining indicators of climatic and non-climatic change. *Global Environmental Change*, 23(2), 522-536.

Macchi, M., Oviedo, G., & Gotheil, S. (2008). *Indigenous and Traditional People and Climate Change*. IUCN (International Union for Conservation of Nature).

Matthies, H. G. (2007). Quantifying uncertainty: modern computational representation of probability and applications. In *Extreme man-made and natural hazards in dynamics of structures* (pp. 105-135). Netherlands: Springer.

Maksimović, Č., Prodanović, D., Boonya-Aroonnet, S., Leitao, J. P., Djordjević, S., & Allitt, R. (2009). Overland flow and pathway analysis for modelling of urban pluvial flooding. *Journal of Hydraulic Research*, 47(4), 512-523.

Marulanda, M. C., Carreño, M. L., Cardona, O. D., Ordaz, M. G., & Barbat, A. H. (2013). Probabilistic earthquake risk assessment using CAPRA: application to the city of Barcelona, Spain. *Natural hazards*, 69(1), 59-84.

Marzocchi, W., et al. (2009). *Principles of multi-risk assessment. Interaction amongst natural and man-induced risks*. Brussels: European Communities.

Marzocchi, W., Garcia-Aristizabal, A., Gasparini, P., Mastellone, M., & Di Ruocco, A. (2012). Basic principles of multi-risk assessment: a case study in Italy. *Natural Hazards*, 62(2), 551–573.

Mccall, G. J. H., Laming, D. J. C., & Scott, S. C. (1992). *Geoharzards-Natural and Man-made*. New York: Chapman Hall.

McGraw, T. F., Mitulla, J. A., & Woll, R. S. (1997). *Disaster warning communications system* (U.S. Patent No. 5,628,050). Washington, DC: U.S. Patent and Trademark Office.

McGuire, B., Mason, I., & Kilburn, C. (2002). *Natural hazards and environmental change*. London: Arnold.

McKee, T. B., Doesken, N. J., & Kleist, J. (1993). The relationship of drought frequency and duration to time scales. *Proceedings of the 8th Conference on Applied Climatology* (Vol. 17, No. 22, pp. 179-183). Boston, MA: American Meteorological Society.

Merz, B., Thieken, A. H., & Gocht, M. (2007). Flood risk mapping at the local scale: concepts and challenges. In *Flood risk management in Europe* (pp. 231-251). Netherlands: Springer.

Mignan, A., Wiemer, S., & Giardini, D. (2014). The quantification of low-probability–high-consequences events: part I. A generic multi-risk approach. *Natural Hazards*, 73(3), 1999-2022.

Moore, I. D., Grayson, R. B., & Ladson, A. R. (1991). Digital terrain modelling: a review of hydrological, geomorphological, and biological applications. *Hydrological processes*, 5(1), 3-30.

Mosquera-Machado, S., & Dilley, M. (2009). A comparison of selected global disaster risk assessment results. *Nauralt Hazards*, 48(3), 439-456.

Moss, R. H., Brenkert, E. L., & Malone, A. L. (2001). *Vulnerability to climate change: A quantitative approach* (Technical Report PNNL-SA-33642). Washington, D.C: Pacific Northwest National Laboratories.

Morrow, B. H. (1999). Identifying and Mapping Community Vulnerability. *Disasters*, 23(1), 11–18.

Munich Re (Munich Reinsurance Company). (2003). *Topics—annual review: natural catastrophes 2002*. Munich: Munich Re Group.

National Aeronautics and Space Administration (NASA). (2011). *Global*

Digital Elevation Map. Retrieved from http://asterweb.jpl.nasa.gov/gdem.asp.

National Atlas Compilation Committee. (1999). *National Economic Atlas of People's Republic of China*. Beijing: China Map Publishing House.

Ngo, E. B. (2001). When disasters and age collide: Reviewing vulnerability of the elderly. *Natural Hazards Review*, 2(2), 80-89.

Nishenko, S. P., & Buland, R. (1987). A generic recurrence interval distribution for earthquake forecasting. *Bulletin of the Seismological Society of America*, 77(4), 1382-1399.

Norio, O., Ye, T., Kajitani, Y., Shi, P., & Tatano, H. (2011). The 2011 eastern Japan great earthquake disaster: overview and comments. *International Journal of Disaster Risk Science*, 2(1), 34-42.

OEP-EOP (Office of Emergency Preparedness, Executive Office of the President of the United States). (1972). *Disaster preparedness* (Report to the Congress). Washington, DC: US Government Printing Office.

Okuyama, Y. (2008). Critical review of methodologies on disaster impact estimation. *Background paper for Joint World Bank—UN assessment on the economics of disaster risk reduction report.* Retrieved from https://gfdrr.org/sites/gfdrr.org/files/New%20Folder/Okuyama_Critical_Review.pdf.

Oreskes, N., Shrader-Frechette, K., & Belitz, K. (1994). Verification, validation, and confirmation of numerical models in the earth sciences. *Science*, 263(5147), 641-646.

Osborne, J. W. (2008). *Best practices in quantitative methods*. London: Sage.

Ou,Y. L., & Wu, H. Y. (2001). *The Taihu lake basin flood in 1999*. Beijing: China Water Power Press.

Pacheco, J. F., Sykes, L. R., & Scholz, C. H. (1993). Nature of seismic coupling along simple plate boundaries of the subduction type. *Journal of Geophysical Research: Solid Earth (1978–2012)*, 98(B8), 14133-14159.

Park, C. (1994). Environment Issues. *Progress in Physical Geography*, 18 (3), 411-424.

Parker, D. (1992). The mismanagement of hazards. In D. J. Parker & J. W.

Handmer (Eds.), *Hazard management and emergency planning: perspectives on Britain*. London: James & James Science Publishers Ltd.

Parsons, M. L. (1995). *Global Warming-the Truth Behind the Myth.* New York: Plenum Press.

Parzen, E. (1962). On estimation of a probability density function and mode. *The Annals of Mathematical Statistics*, 33(3),1065-1076.

Pelling, M. (2003). *The vulnerability of cities. Natural disasters and social resilience*. London: Earthscan Publications.

Penning-Rowsell, E. C., & Chatterton, J. B. (1977). *The benefits of flood alleviation: A manual of assessment techniques.* Hampshire: Gower, Aldershot.

Perry, C. A. (2000). *Significant floods in the United States during the 20th Century – USGS measures a century of floods* (U.S. Geological Survey, Fact Sheet 024–00). Retrieved from http://pubs.er.usgs.gov/publication/fs02400.

Petak, W. J. & Atkisson, A. A. (1982). *Natural Hazard Risk Assessment and Public Policy: Anticipating the unexpected*. New York: Springer-Verlag.

Philander, S. G. (1990). *EL Nino, La Nina, and the Southern Oscillation, California*. San Diego: Academic press, Inc.

Platt, R. H. (1991). Lifelines: An emergency management priority for the United States in the 1990s. *Disasters*, 15(2), 172-176.

Polit, D. F., & Beck, C. T. (2008). *Nursing research: Generating and assessing evidence for nursing practice* (8th ed.). Lippincott Williams & Wilkins.

Pourret, O., Naïm, P., & Marcot, B. (Eds.). (2008). *Bayesian networks: a practical guide to applications* (Vol. 73). Chichester: John Wiley & Sons.

Puente, S. (1999). Social Vulnerability to Disaster in Mexico City. In J. K. Mitchell (Ed.), *Crucibles of Hazard: Mega-Cities and Disasters in Transition* (pp. 295–334). Tokyo: United Nations University Press.

Qi, Y., Wen, F., Wang, K., Li, L., & Singh, S. (2010). A fuzzy comprehensive evaluation and entropy weight decision-making based method for power network structure assessment. *International Journal of Engineering,* *Science and Technology*, 2(5), 92-99.

Qiu, W. H. (2002). *Management decision and applied entropy*. Beijing: China Machine Press.

Rohmer, J. (2012). *Uncertainty quantification: Report on uncertainty quantification and – comparison for single-type risk analyses*. (ENV.2010.6.1.3.4 New methodologies for multi-hazard and multi-risk assessment).

Redner, R. A., & Walker, H. F. (1984). Mixture densities, maximum likelihood and the EM algorithm. *SIAM review*, 26(2), 195-239.

Rosenblatt, M. (1956). Remarks on some nonparametric estimates of a density function. *The Annals of Mathematical Statistics*, 27(3), 832-837.

Rossi, G., Harmancioglu, N., & Yevjevich, V. (1994). *Coping With Floods*. Netherlands: Kluwer Academic Publishers.

Royal Society (1983). *Risk Assessment: Report of a Royal Society Study Group*. London: Royal Society.

Russell, D. W. (2002). In search of underlying dimensions: The use (and abuse) of factor analysis in Personality and Social Psychology Bulletin. *Personality and social psychology bulletin*, 28(12), 1629-1646.

Rutherford, W. H., & De Boer, J. (1983). The definition and classification of disasters. *Injury*, 15(1), 10-12.

Sales, J., Wood, M., & Jelínek, R. (2007). *Risk mapping of industrial hazards in new member states*. Ispra: Joint Research Centre, European Commission.

Sargent, R. G. (2004). Validation and verification of simulation models. *Simulation Conference, 2004. Proceedings of the 2004 Winter* (Vol. 1). IEEE.

SCEMDOAG (South Carolina Emergency Management Division Office of the Adjutant General). (2006). *State of South Carolina hazards assessment 2005*. South Carolina: University of South Carolina, South Carolina Emergency Management Division Office of the Adjutant General, Hazards Research Lab, Department of Geography.

SCEMDOAG (South Carolina Emergency Management Division Office of the Adjutant General). (2009). *State of South Carolina hazards assessment*

2008. South Carolina: University of South Carolina, South Carolina Emergency Management Division Office of the Adjutant General, Hazards Research Lab, Department of Geography.

Schmidt, J., et al. (2011). Quantitative multi-risk analysis for natural hazards: a framework for multi-risk modelling. *Natural Hazards*, 58(3), 1169-1192.

Schmidt-Thomé, P. (2006a). *The spatial effects and management of natural and technological hazards in Europe. European Spatial Planning and Observation Network (ESPON) project 1.3.1*. Geological Survey of Finland, Luxembourg.

Schmidt-Thomé, P. (Ed.), (2006b). *Natural and technological hazards and risks affecting the spatial development of European regions*. Espoo: Geological Survey of Finland.

Schmidt-Thomé, P., et al. (2003). Development of natural hazard maps for European regions. *EU-MEDIN forum on disaster research "The Road to Harmonisation"*. Thessaloniki, Greece.

Schneiderbauer, S., & Ehrlich, D. (2004). *Risk, Hazard and People's Vulnerability to Natural Hazards: A Review of Definitions, Concepts and Data*. Brussels: Joint Research Centre, European Commission.

Scolobig, A., Garcia-Aristizabal, A., Komendatova, N., Patt, A., & Di Ruocco, A., et al. (2014) From multi-risk assessment to multi-risk governance: recommendations for future directions. *Understanding risk: The Evolution of Disaster Risk Assessment*. Washington DC: International Bank for Reconstruction and Development.

Selva, J. (2013). Long-term multi-risk assessment: statistical treatment of interaction among risks. *Natural hazards*, 67(2), 701-722.

Shannon, C E. (1948). A mathematical theory of communications. *Bell Systems Technical Journal*, 27(3), 379-423.

Shi, P. J. (1996). Theory and practice of disaster study. *Journal of natural disaster*, 5(4), 6–17.

Shi, P. J. (2011). *Atlas of natural disaster risk of China.* Beijing: Science Press.

Shi P. J., et al. (2014). *Integrated Risk Governance: integrated natural hazards risk assessment and mapping in the Yangtze River Delta region*. Beijing: Science Press.

Slovic, P. E. (2000). *The perception of risk*. London: Earthscan Publications.

Smith, D.I. (1994). Flood damage estimation-A review of urban stage damage curves and loss functions. *Water SA Manuscript*, 20(3), 231-238.

Smith, K. (1996). *Environmental hazards: Assessing risk and reducing disaster* (2nd ed.). New York: Routledge.

Smith, K. (2000). *Environmental hazards: Assessing risk and reducing disaster* (3rd ed.). New York: Routledge.

Smith, K. (2013). *Environmental hazards: Assessing risk and reducing disaster* (6th ed.). New York: Routledge.

Smith, K., & Petley, D. N. (2009). *Environmental hazards: Assessing risk and reducing disaster* (5th ed.). New York: Routledge.

Stedinger, J. R., Vogel, R. M., & Foufoula-Georgiou, E. (1992). Frequency analysis of extreme events. In D. R. Maidment (Ed.), *Handbook of Hydrology*. New York: McGraw-Hill Inc.

Straub, D. (2005). Natural Hazards Risk Assessment Using Bayesian Networks. *The 9th International Conference on Structural Safety and Reliability*. Rome, Italy.

Suleman, M. S., N'Jai, A., Green, C. H., & Penning-Rowsell, E. C. (1988). *Potential flood damage data: A major update*. London: Middlesex polytechnic flood hazard research centre.

Tabios, G. Q., & Salas, J. D. (1985). A comparative analysis of techniques for spatial interpolation of precipitation. *Journal of the American Water Resources Association*, 21(3), 365–380.

Tabuchi, H. & Bradsher, K. (2011). Japan Nuclear Disaster Put on Par with Chernobyl. *The New York Times*. Retrieved from http://www.nytimes.com/2011/04/12/world/asia/12japan.html?_r=0.

Thacker, B. H., Doebling, S. W., Hemez, F. M., Anderson, M. C., Pepin, J. E., & Rodriguez, E. A. (2004). *Concepts of model verification and validation* (No. LA-14167). Los Alamos: Los Alamos National Lab.

The Office of State Flood Control and Drought Relief Headquarters. (2000). *China's rivers name code* (SL 249-1999). Beijing: Ministry of Water Resources of the People's Republic of China.

Thierry, P., Stieltjes, L., Kouokam, E., Ngueya, P., & Salley, P. (2008). Multi-hazard risk mapping and assessment on an active volcano: the GRINP project at Mount Cameroon. *Natural Hazards*, 45(3), 429–456.

Thirumalaivasan, D., Karmegam, M., & Venugopal, K. (2003). AHP-DRASTIC: software for specific aquifer vulnerability assessment using DRASTIC model and GIS. *Environmental Modelling & Software*, *18*(7), 645-656.

Tobin, G. A., & Montz, B. E. (1997). *Nature hazards: explanation and integration*. New York: The Guilford Press.

Tucker, B. E., Erdik, M., & Hwang, C. N. (1994). *Issues in Urban Earthquake Risk*. Netherlands: Kluwer Academic Publishers.

Turner, B. L., & Meyer, W. B. (1991). Land-use and land cover in global environmental-change-considerations for study. *International Social Science Journal*, 43(4), 669-679.

UNDP (United Nations Development Programme). (2004). *Reducing disaster risk: a challenge for development*. United Nations Development Programme, Bureau for crisis prevention and recovery, New York.

UNDRO (United Nations Office of the Disaster Relief Co-Ordinator). (1991). *Mitigation Natural Disasters: Phenmena, Effects and Options, A Manual for Policy Makers and Planners.* New York: United Nations Press.

Vangelsten, B. V. (2013). *Uncertainties in Multi-risk Assessment: Sources, Types and Quantification.* (ENV.2010.6.1.3.4 New methodologies for multi-hazard and multi-risk assessment).

Van Westen, C. J. (2008). RiskCity: a training package on the use of GIS for urban multi - hazard risk assessment. In D. Sassa & P. Canuti (Eds.), *Proceedings of the First World Landslide Forum* (pp.665-668). Tokyo: United Nations University Press.

Varnes, D. J. (1958). Landslide types and processes. *Highway Research Board Special Report*, 29, 20-47.

Varnes, D. J. (1984). *Landslide Hazard Zonation: A review of Principles and Practice*. France: UNESCO (The United Nations Educational, Scientific and Cultural Organization).

Villagrán de León, J. C. (2006). *Vulnerability: A Conceptual and Methodological Review*. Bonn: UNU - EHS (The United Nations University, Institute for Environment and Human Security).

Wang, J. A., Shi, P. J., Yi, X. S., Jia, H. C., & Zhu, L. Y. (2008). The regionalization of urban natural disasters in China. *Natural Hazards*, 44(2), 169-179.

WBGU (German Advisory Council on Global Change). (2005). *World in Transition: Fighting Poverty through Environmental Policy*. London: Earthscan.

Whittow, J. (1980). *Disasters: the anatomy of environment hazards*. London: Pelican.

Wilhite, D. A., & Glantz, M. H. (1985). Understanding: the drought phenomenon: the role of definitions. *Water international*, 10(3), 111-120.

Wilson, J. P., & Gallant, J. C. (Eds.). (2000). *Terrain analysis: principles and applications*. John Wiley & Sons.

Wipulanusat, W., Nakrod, S., & Prabnarong, P. (2009). Multi-hazard risk assessment using GIS and RS applications: a case study of Pak Phanang basin. *Walailak Journal of Science and Technology*, 6(1), 109-125.

Wisner, B., Blaikie, P., Cannon,T., & Davis, I. (2004). *At Risk: Natural Hazards, People's Vulnerability and Disasters* (2nd ed.). London: Routledge.

Wolman, M. G., & Miller, J. P. (1960). Magnitude and frequency of forces in geomorphic processes. *The Journal of Geology*, 68(1), 54-74.

Wood, M., Arellano, A. L. V., & Mushtaq, F. (2003). *Management of natural and technological hazards in Central and Eastern European countries (PECO). Fifth Framework Programme of Research and Technological Development*. Ispra: Joint Research Centre, European Commission.

World Bank. (2014). *Population density (people per sq. km)*. Retrieved from http://data.worldbank.org/indicator/EN.POP.DNST/countries?display= map.

Wu, H. Y., & Guan, W. Q. (1999). *The Taihu lake basin flood in 1991*. Beijing: China Water Power Press.

Xu, W et al. (2014). *Integrated Risk Governance: Natural hazards and Risk assessment in the Yangtze River Delta region*. Beijing: Science Press.

Yavinsky, R. W. (2012). *Women More Vulnerable Than Men to Climate Change*. Retrieved from http://www.prb.org/Publications/Articles/2012/women-vulnerable-climate-change.aspx.

Yesilnacar, E., & Topal, T. (2005). Landslide susceptibility mapping: a comparison of logistic regression and neural networks methods in a medium scale study, Hendek region (Turkey). *Engineering Geology*, 79(3), 251-266.

Yuan, J. N., Wan, Q. L., Huang, Y. Y., & Ding, W. Y. (2006). The experiments of ensemble prediction of the track of tropical cyclone in South China Sea. *Journal of Tropical Meteorology*, (2), 3-10.

Zhang, Z., et al. (2009). Crustal structure across the Three Gorges area of the Yangtze platform, central China, from seismic refraction/wide-angle reflection data.*Tectonophysics*, 475(3), 423-437.

Zhou, Q., Mikkelsen, P. S., Halsnæs, K., & Arnbjerg-Nielsen, K. (2012). Framework for economic pluvial flood risk assessment considering climate change effects and adaptation benefits. *Journal of Hydrology*, 414, 539-549.

Zschau, J., & Küppers, A. N. (Eds.). (2003). *Early Warning Systems for Natural Disaster Reduction*. New York: Springer Science & Business Media.

Zou, Z. H., Yi, Y., & Sun, J. N. (2006). Entropy method for determination of weight of evaluating indicators in fuzzy synthetic evaluation for water quality assessment. *Journal of Environmental Sciences*, 18(5), 1020-1023.

Appendix A

Susceptibility of each county to each hazard in the Yangtze River Delta

A.1 Susceptibility of each county to each hazard in the Zone I

Zone	County	Typhoon	Slow kinds riverine flood	Fast kinds riverine flood	Coastal flood	Pluvial flood	Landslide
I	Haishu	H	H			H	
I	Minhang	MH	MH			H	
I	Tongxiang	MH	H			H	
I	Songjiang	MH	MH			H	
I	Xiuzhou	MH	MH			H	
I	Jiashan	MH	MH			H	
I	Xuhui	MH	H			H	
I	Luwan	MH	H			H	
I	Huangpu	MH	H			H	
I	Jing'an	MH	H			H	
I	Changning	MH	H			H	
I	Qingpu	MH	MH			H	
I	Putuo*	MH	M			H	
I	Nanxun	M	MH			H	
I	Wujiang	M	MH			H	
I	Kunshan	M	MH			H	
I	Pingjiang	M	H			H	
I	Canglang	M	H			H	
I	Jinchang	M	H			H	
I	Xiangcheng	M	H			H	
I	Nanchang	ML	H			H	
I	Chong'an	ML	H			H	
I	Beitang	ML	H			H	
I	Qishuyan	ML	H			H	
I	Wujin	ML	H			H	
I	Tianning	ML	MH			H	
I	Zhonglou	ML	H			H	
I	Xinbei	ML	M			H	

I	Gaochun	ML	MH			H	
I	Taixing	ML	MH			H	
I	Danyang	ML	M			H	
I	Yangzhong	L	H			H	
I	Gaogang	L	H			H	
I	Jiangyan	L	M			H	
I	Runzhou	L	H			H	
I	Hailing	L	H			H	
I	Weiyang	L	H			H	
I	Guangling	L	H			H	
I	Jiangdu	L	M			H	
I	Hanjiang	L	H			H	
I	Qinhuai	L	H			H	
I	Baixia	L	H			H	
I	Yuhuatai	L	H			H	
I	Gulou	L	H			H	
I	Yizheng	L	ML			H	
I	Xinghua	L	M			H	
I	Gaoyou	L	MH			H	
I	Baoying	L	ML			H	

(H represents high, MH represents medium high, M represents medium, ML represents medium low, L represents low)

A.2 Susceptibility of each county to each hazard in the Zone II

Zone	County	Typhoon	Slow kinds riverine flood	Fast kinds riverine flood	Coastal flood	Pluvial flood	Landslide
II	Jiangdong	H	H		L	H	
II	Fengxian	MH	L		ML	H	
II	Jinshan	MH	M		L	H	
II	Nanhu	MH	MH		L	H	
II	Pudong	MH	M		M	H	
II	Xiacheng	MH	H		H	H	
II	Hongkou	MH	MH		ML	H	
II	Yangpu	MH	H		H	H	
II	Zhabei	MH	ML		L	H	
II	Baoshan	M	L		MH	H	
II	Jiading	M	MH		L	H	
II	Chongming	M	L		H	H	
II	Taicang	M	H		M	H	
II	Qidong	M	ML		MH	H	

II	Haimen	ML	MH		M	H	
II	Zhangjiagang	ML	H		M	H	
II	Tongzhou	ML	M		L	H	
II	Gangzha	ML	MH		M	H	
II	Jingjiang	ML	H		ML	H	
II	Rudong	ML	MH		ML	H	
II	Rugao	ML	MH		L	H	
II	Hai'an	L	M		L	H	

(H represents high, MH represents medium high, M represents medium, ML represents medium low, L represents low)

A.3 Susceptibility of each county to each hazard in the Zone III

Zone	County	Typhoon	Slow kinds riverine flood	Fast kinds riverine flood	Coastal flood	Pluvial flood	Landslide
III	Tiantai	H	L	MH		L	MH
III	Xianju	H	ML	H		L	H
III	Xinchang	H	ML	MH		L	MH
III	Shengzhou	H	M	M		L	M
III	Zhuji	MH	ML	M		L	M
III	Fuyang	MH	ML	MH		L	MH
III	Jiande	MH	ML	MH		L	MH
III	Tonglu	MH	ML	H		L	H
III	Deqing	M	MH	ML		M	ML
III	Wuxing	M	MH	ML		M	ML
III	Wuzhong	M	H	ML		MH	ML
III	Lin'an	M	ML	H		L	H
III	Chun'an	M	M	H		L	H
III	Anji	M	ML	M		L	M
III	Huqiu	M	H	ML		H	ML
III	Changxing	M	M	ML		M	ML
III	Binhu	M	H	ML		H	ML
III	Xishan	ML	MH	L		H	L
III	Huishan	ML	H	L		H	L
III	Yixing	ML	MH	ML		MH	ML
III	Liyang	ML	ML	L		MH	L
III	Jintan	ML	M	L		H	L
III	Lishui	L	MH	L		H	L
III	Jingkou	L	H	ML		H	ML

III	Jurong	L	ML	L		MH	L
III	Dantu	L	ML	L		H	L
III	Jiangning	L	M	L		MH	L
III	Xuanwu	L	M	ML		MH	ML
III	Jianye	L	H	ML		H	ML
III	Qixia	L	H	ML		H	ML
III	Xiaguan	L	H	ML		MH	ML
III	Pukou	L	M	L		MH	L
III	Liuhe	L	ML	L		H	L

(H represents high, MH represents medium high, M represents medium, ML represents medium low, L represents low)

A.4 Susceptibility of each county to each hazard in the Zone IV

Zone	County	Typhoon	Slow kinds riverine flood	Fast kinds riverine flood	Coastal flood	Pluvial flood	Landslide
IV	Luqiao	H	L	L	M	MH	L
IV	Wenling	H	L	ML	M	M	ML
IV	Jiaojiang	H	MH	L	H	H	L
IV	Yuhuan	H	L	ML	H	M	ML
IV	Sanmen	H	L	M	M	L	M
IV	Xiangshan	H	L	ML	H	ML	ML
IV	Huangyan	H	M	MH	L	L	MH
IV	Linhai	H	ML	MH	L	L	MH
IV	Ninghai	H	L	M	ML	L	M
IV	Putuo**	H	L	ML	H	ML	ML
IV	Beicang	H	L	ML	MH	M	ML
IV	Fenghua	H	M	M	L	L	M
IV	Jinzhou	H	L	ML	L	ML	ML
IV	Dinghai	H	L	ML	H	ML	ML
IV	Zhenhai	H	L	L	H	MH	L
IV	Jiangbei	H	M	L	L	MH	L
IV	Daishan	H	L	L	H	MH	L
IV	Yuyao	H	M	M	L	ML	M
IV	Cixi	H	ML	L	MH	MH	L
IV	Shangyu	H	M	ML	L	M	ML
IV	Shengsi	MH	L	L	H	M	L
IV	Shaoxing	MH	ML	ML	L	ML	ML
IV	Yuecheng	MH	MH	L	L	MH	L

IV	Haiyan	MH	M	L	M	H	L
IV	Xiaoshan	MH	MH	ML	ML	MH	ML
IV	Pinghu	MH	MH	L	M	H	L
IV	Haining	MH	M	L	M	H	L
IV	Binjiang	MH	H	ML	MH	H	ML
IV	Jianggan	MH	M	L	H	H	L
IV	Shangcheng	MH	H	ML	H	MH	ML
IV	Xihu	MH	MH	ML	L	M	ML
IV	Gongshu	MH	H	ML	L	H	ML
IV	Yuhang	MH	M	ML	L	M	ML
IV	Changshu	M	H	ML	L	H	ML
IV	Chongchuan	ML	H	ML	H	H	ML
IV	Jiangyin	ML	H	L	L	H	L

(H represents high, MH represents medium high, M represents medium, ML represents medium low, L represents low)

Appendix B

Exceedance probability distribution of daily rainfall and wind speed sets during typhoon in 24 meteorological sites in the Yangtze River Delta

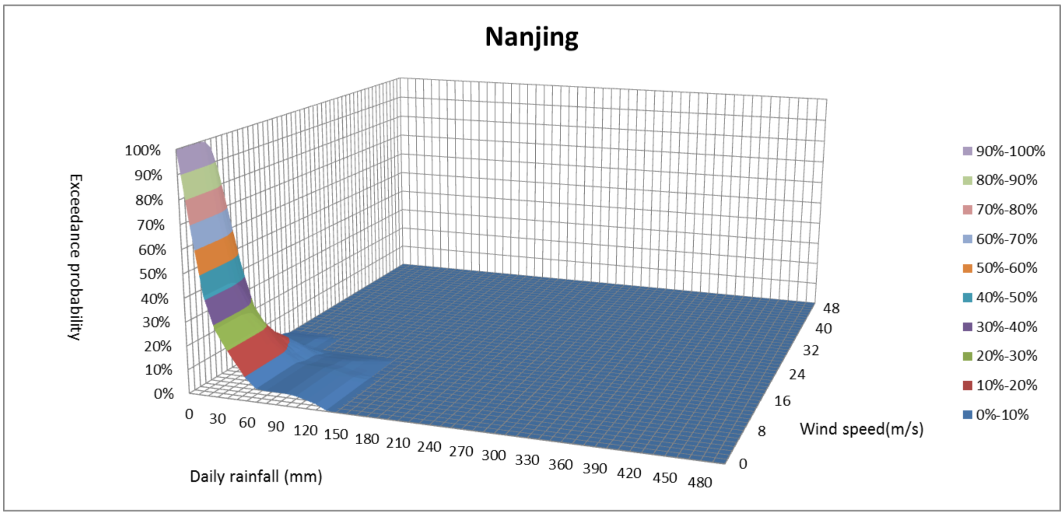

(a) Nanjing

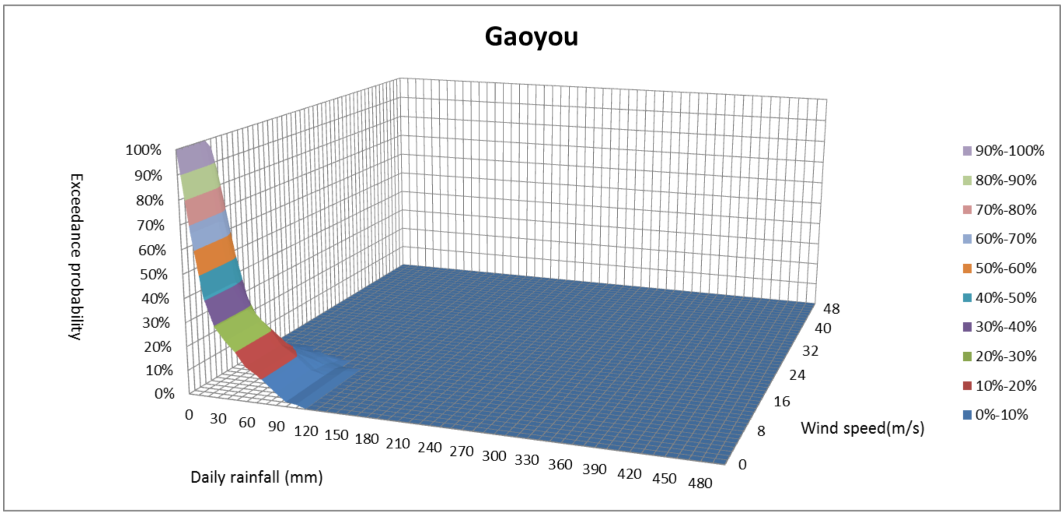

(b) Gaoyou

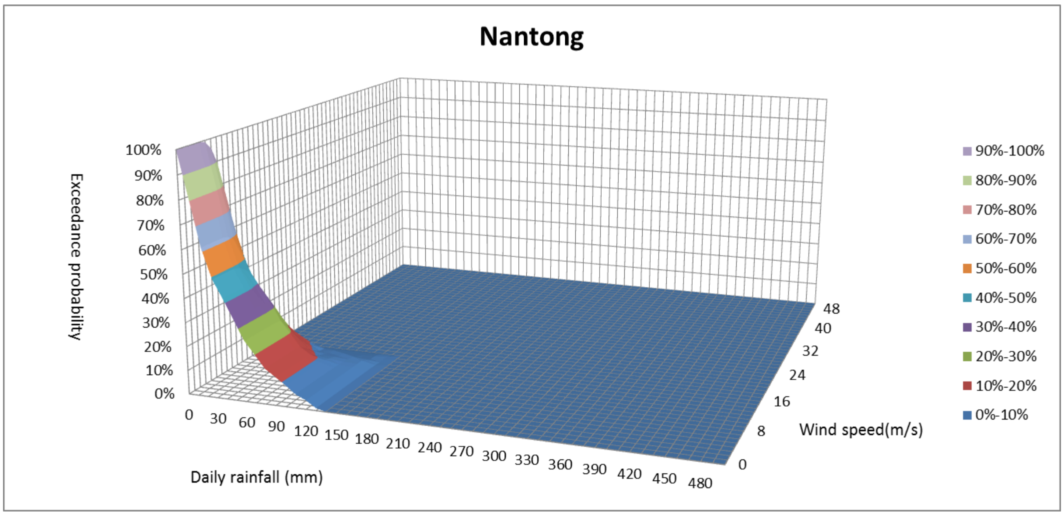

(c) Nantong

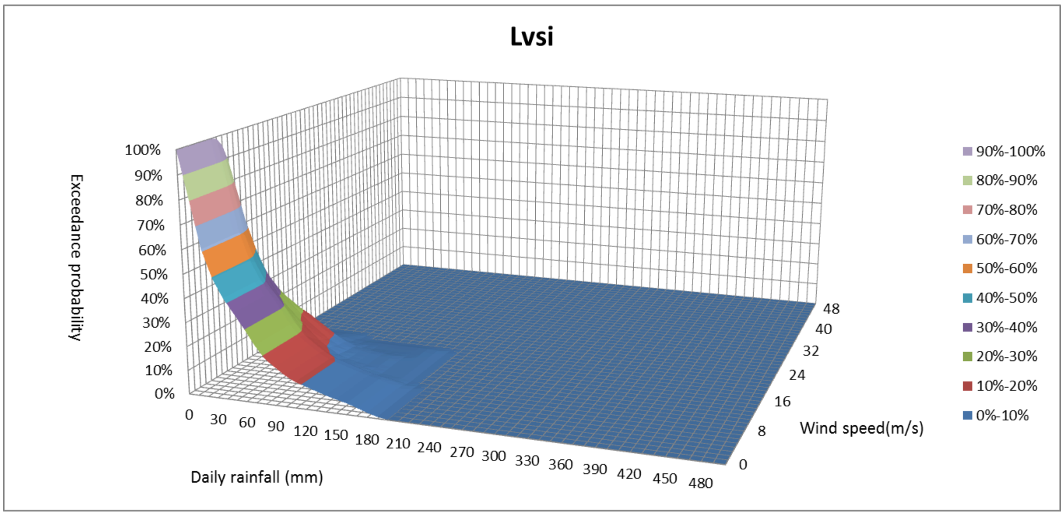

(d) Lvsi

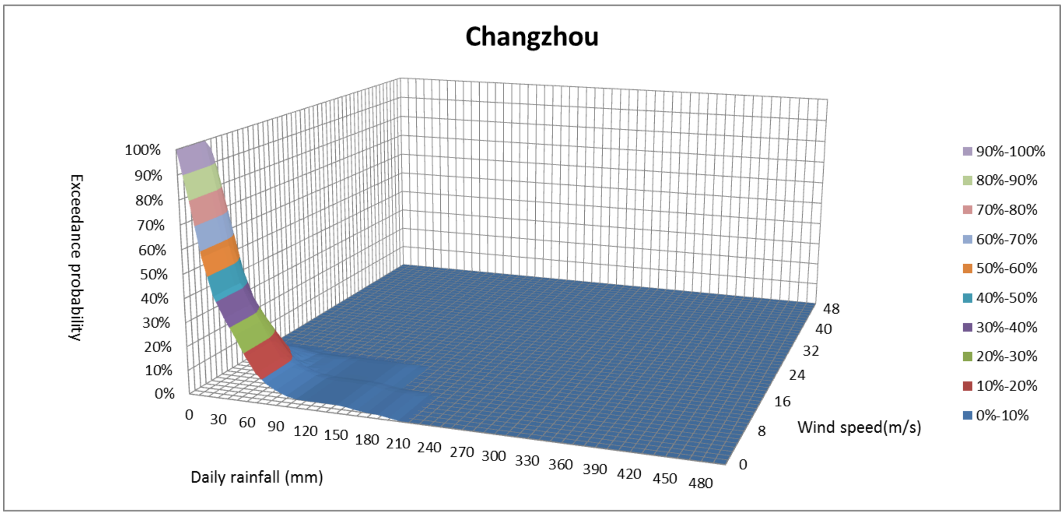

(e) Changzhou

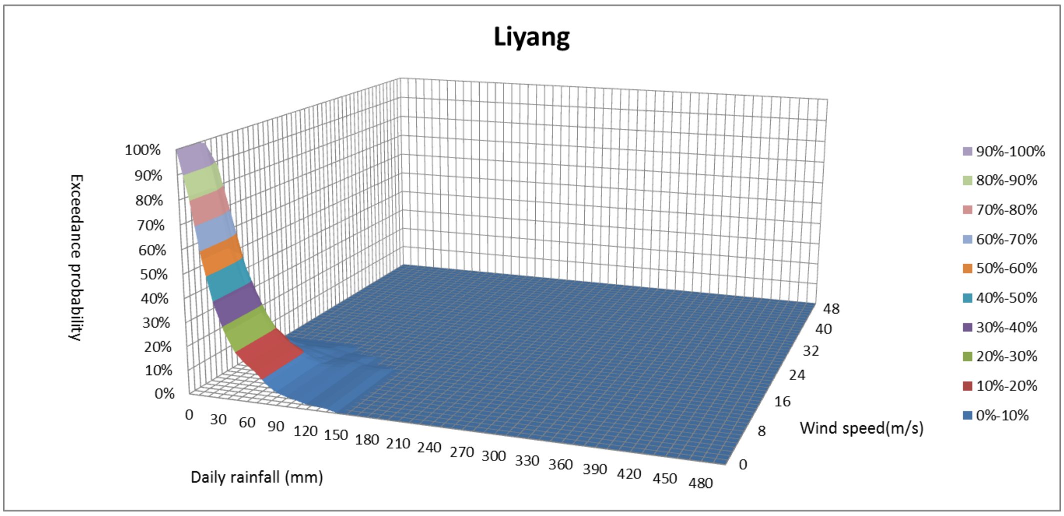

(f) Liyang

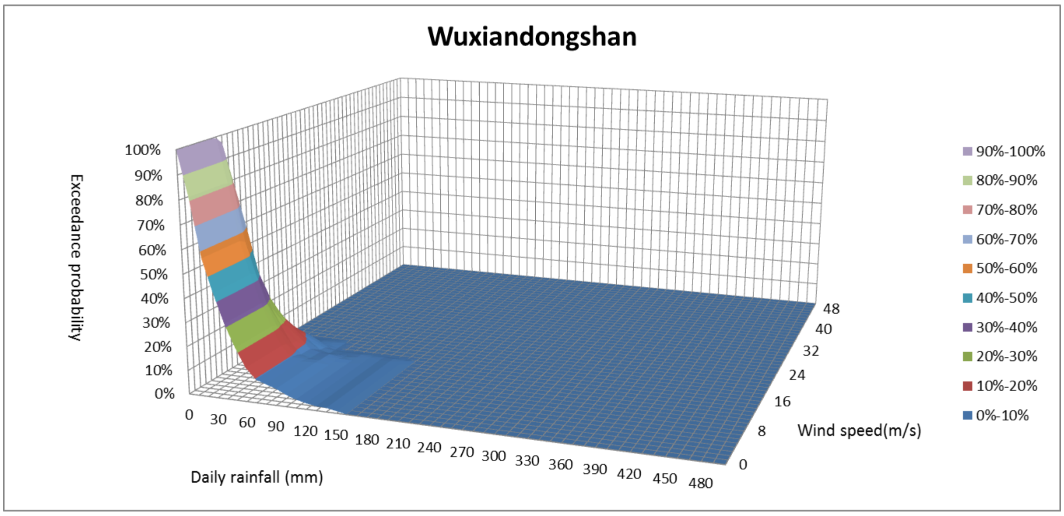

(g) Wuxiandongshan

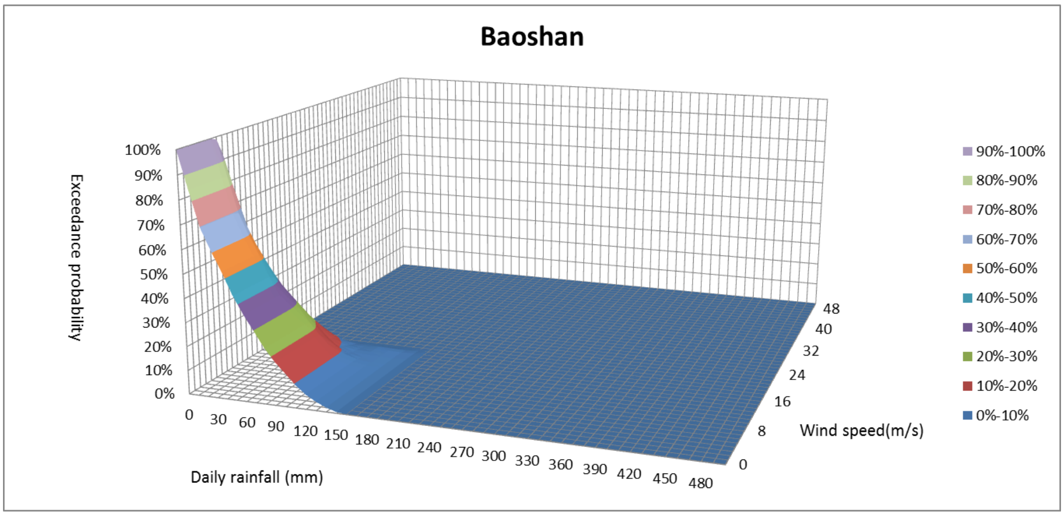

(h) Baoshan

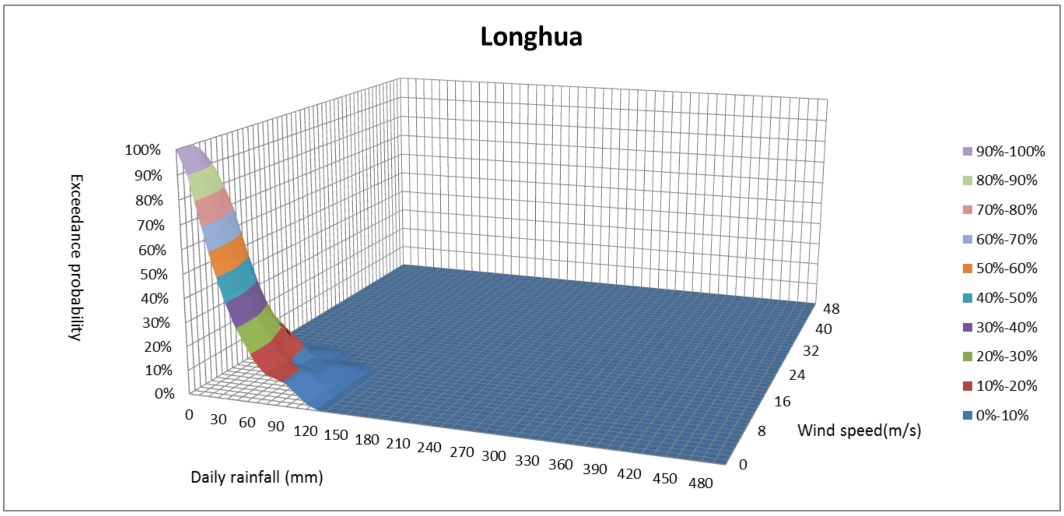

(i) Longhua

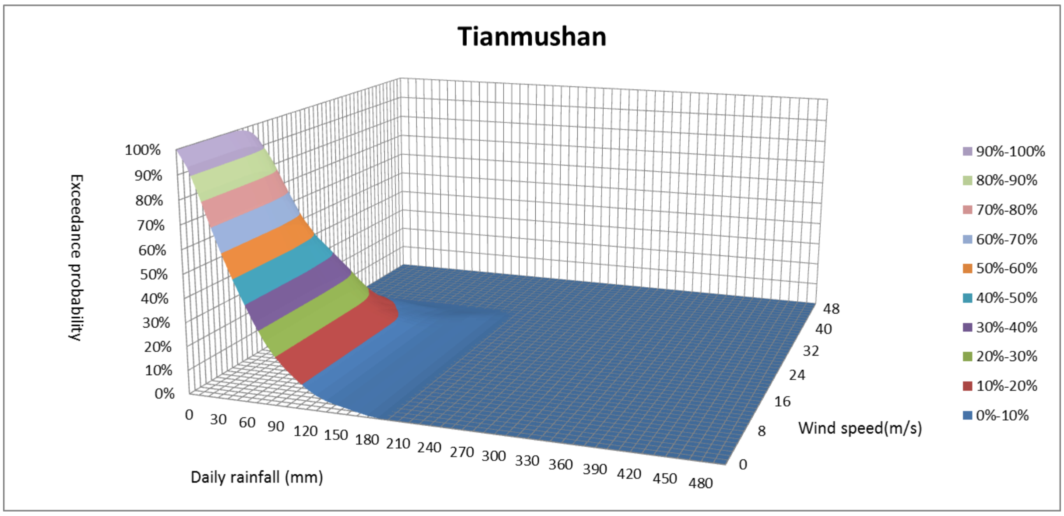

(j) Tianmushan

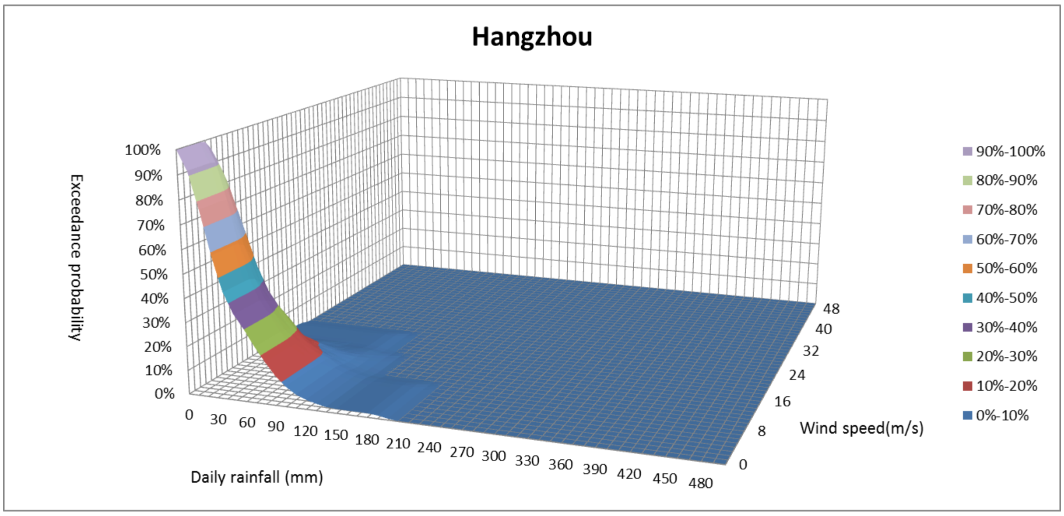

(k) Hangzhou

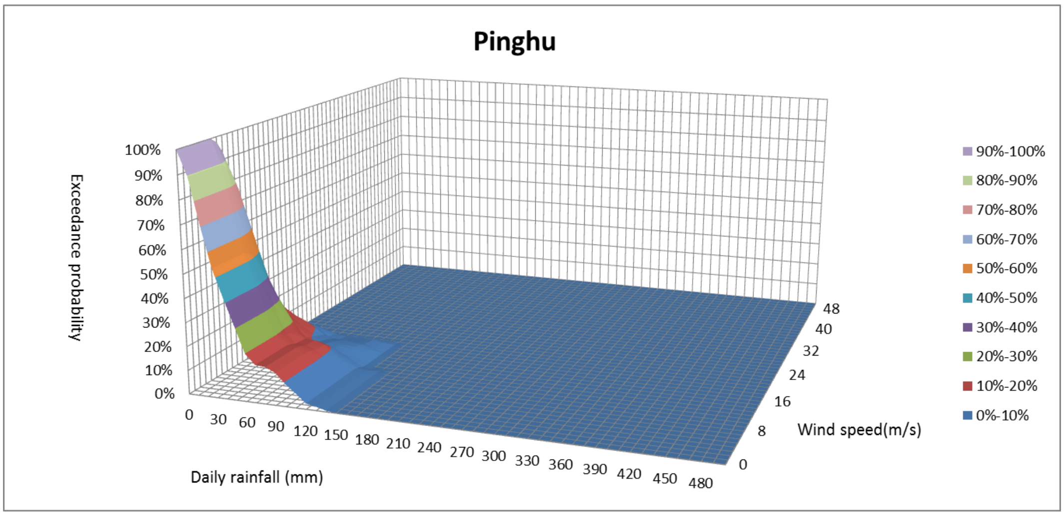

(l) Pinghu

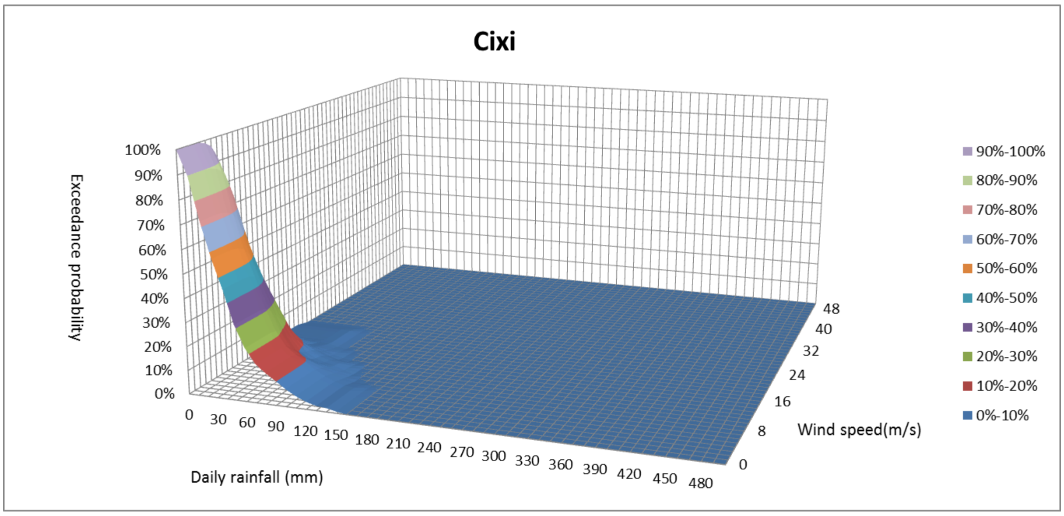

(m) Cixi

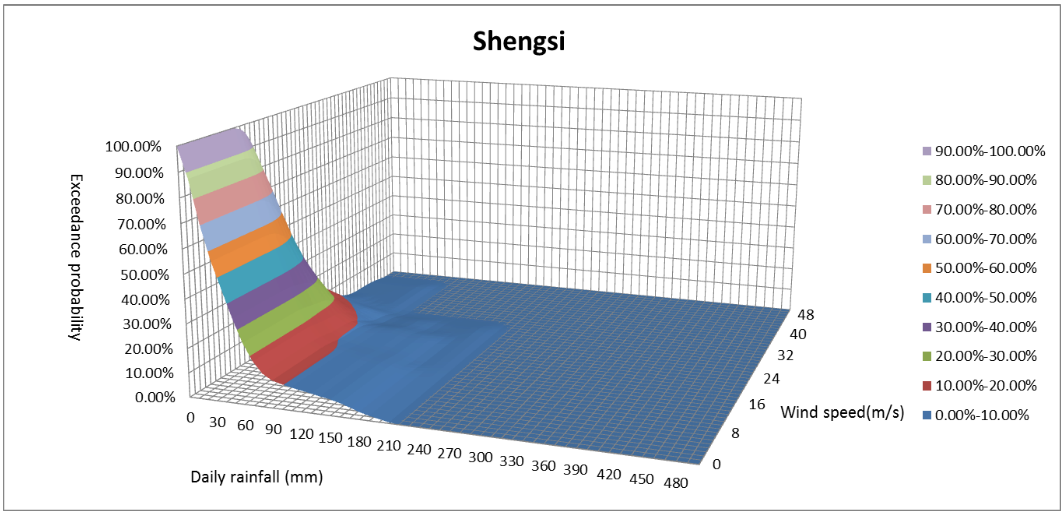

(n) Shengsi

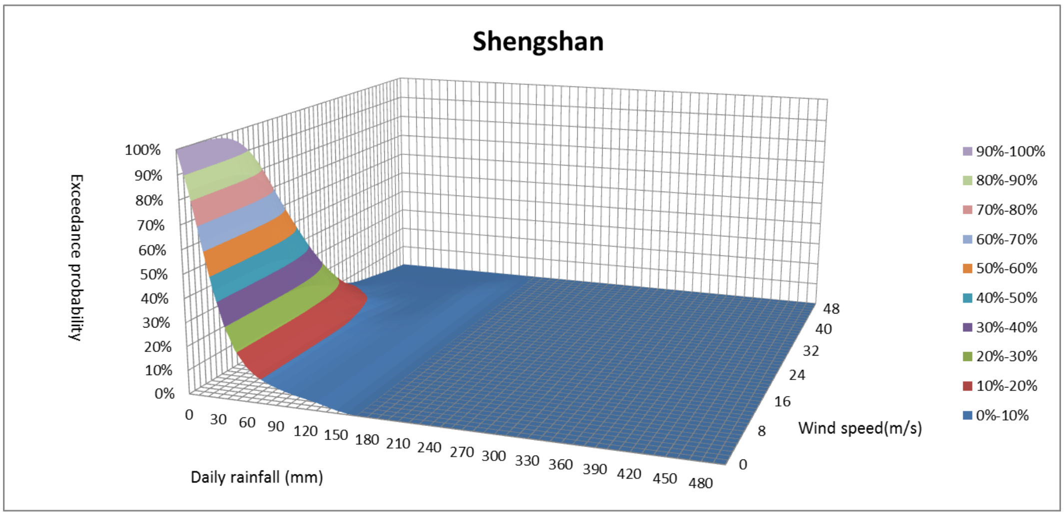

(o) Shengshan

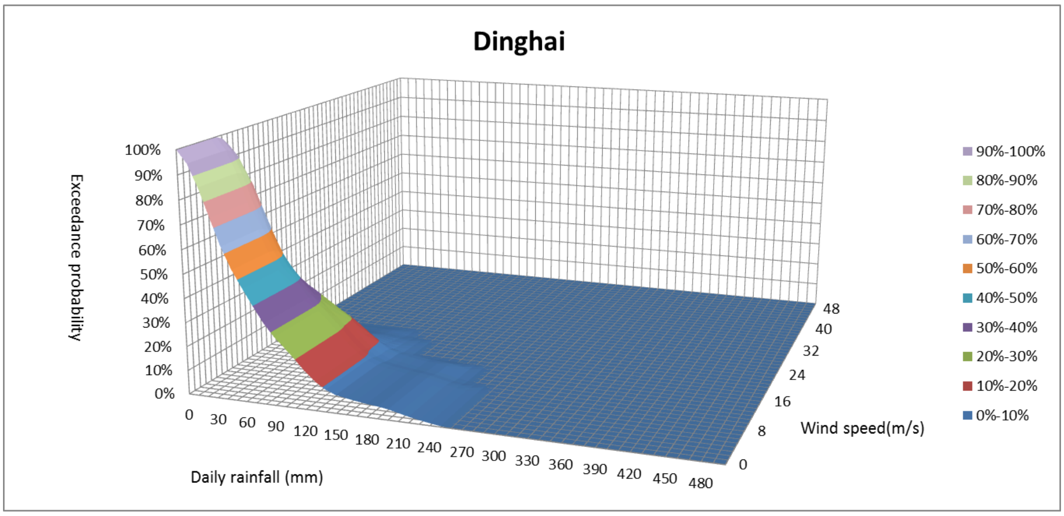

(p) Dinghai

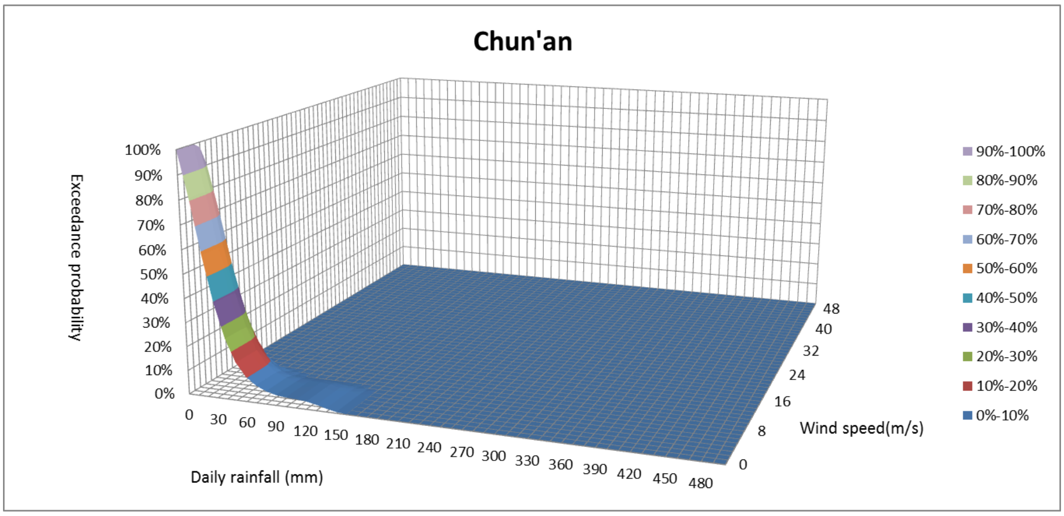

(q) Chun'an

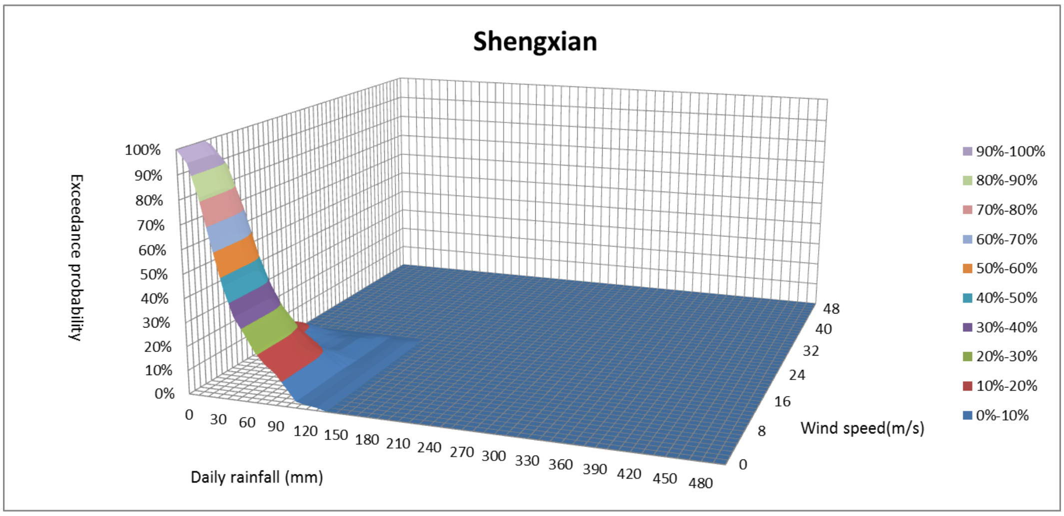

(r) Shengxian

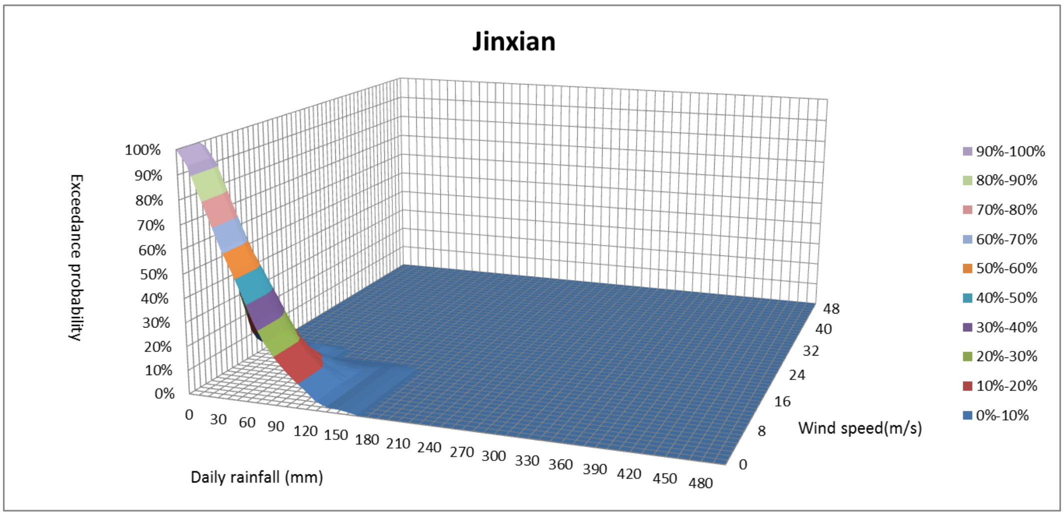

(s) Jinxian

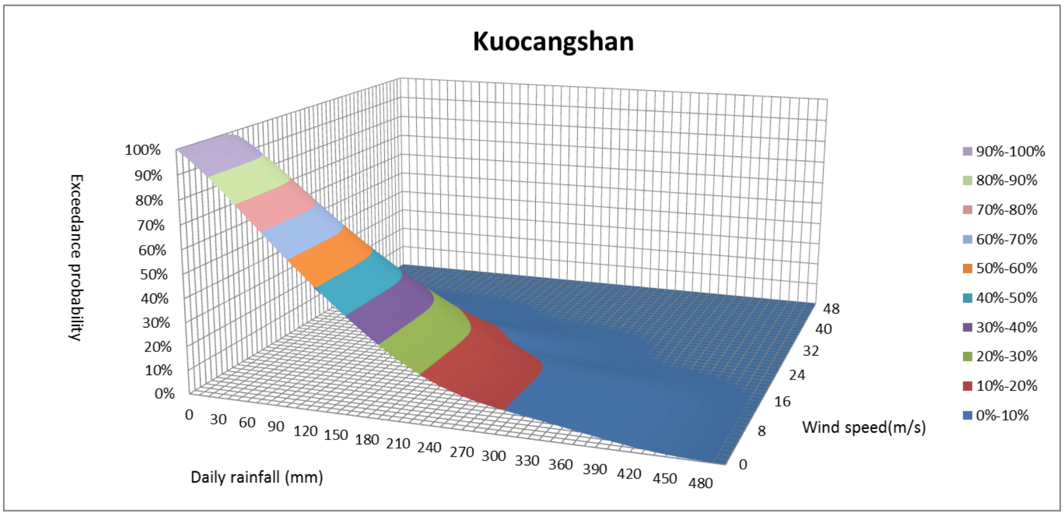

(t) Kuocangshan

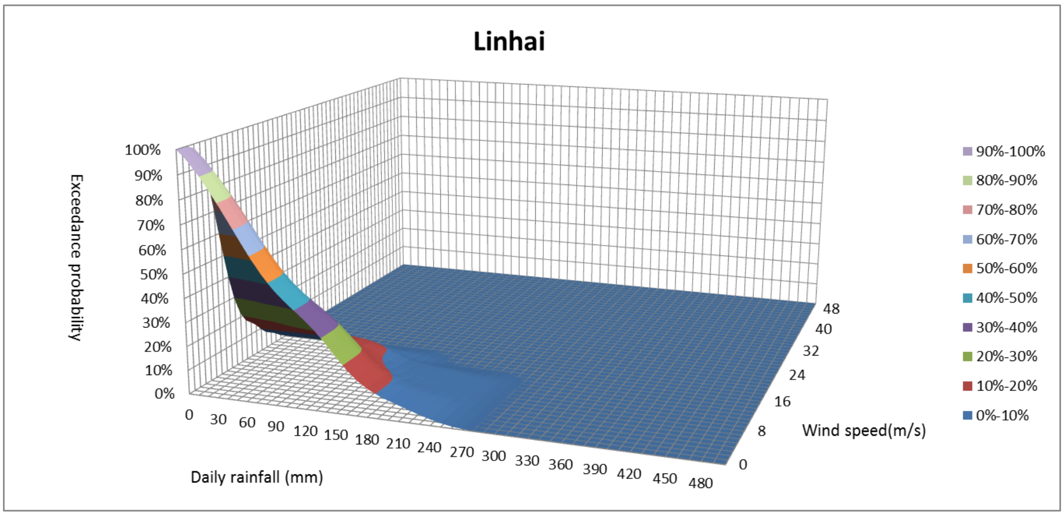

(u) Linhai

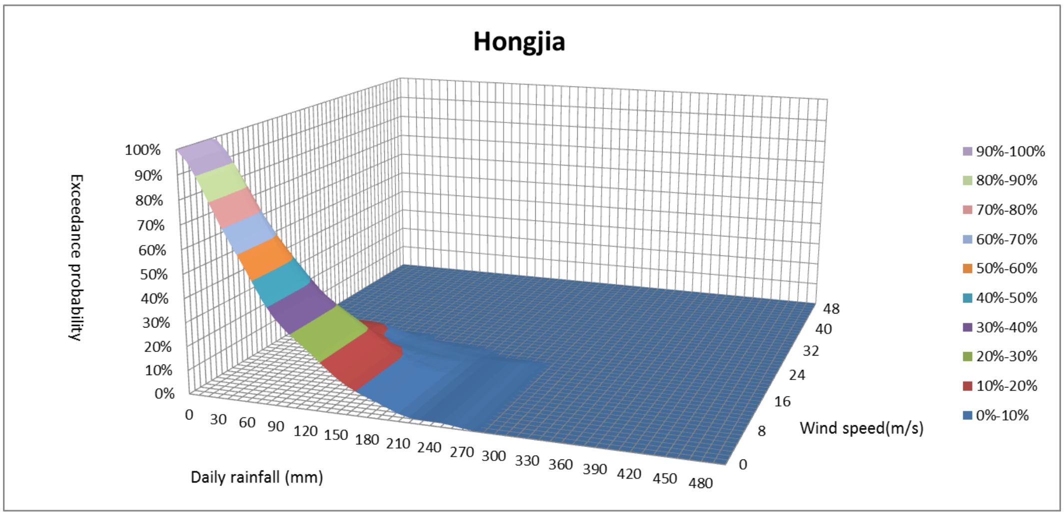

(v) Hongjia

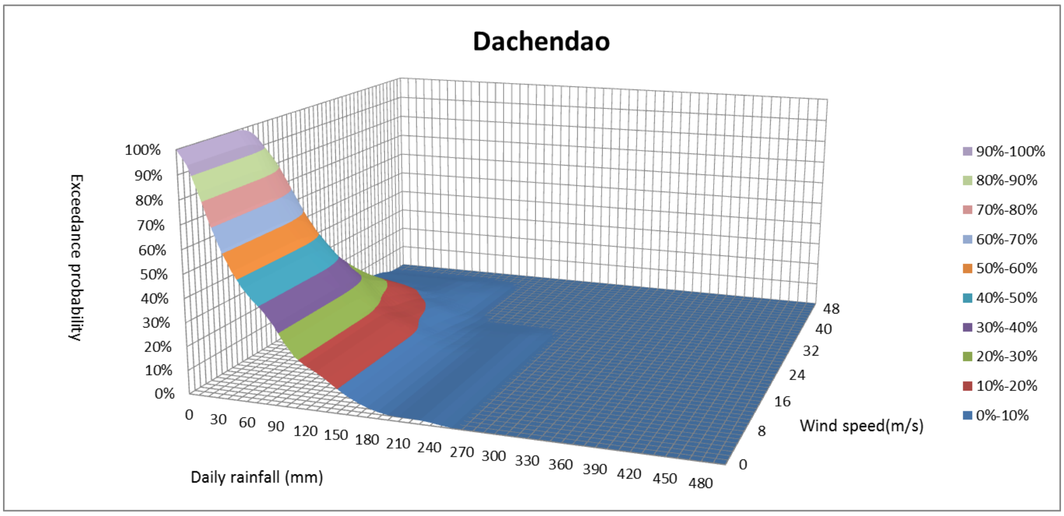

(W) Dachendao

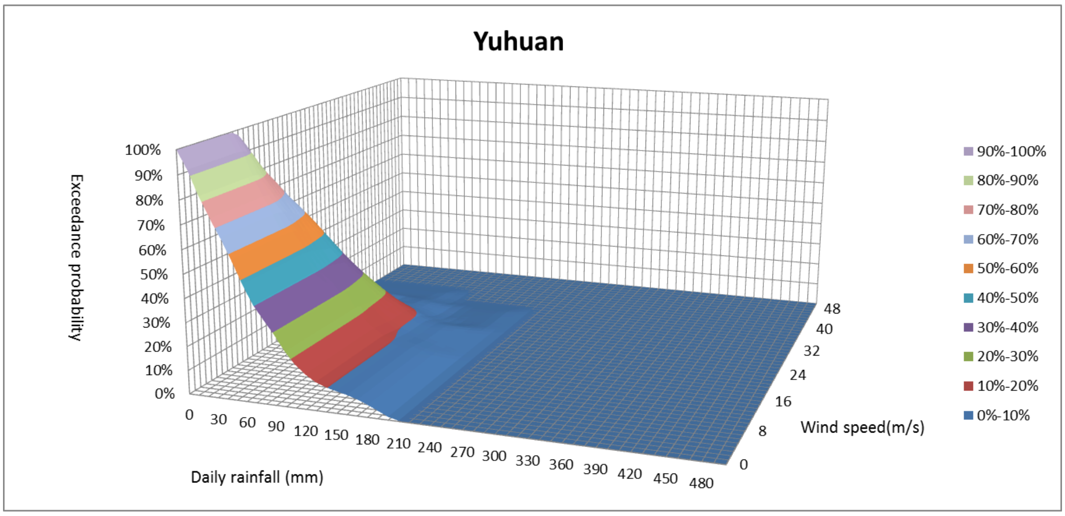
Yuhuan
Exceedance probability
100%
90%
80%
70%
60%
50%
40%
30%
20%
10%
0%
0
30
60
90
120
150
180
210
240
270
300
330
360
390
420
450
480
Daily rainfall (mm)
0
8
16
24
32
40
48
Wind speed(m/s)
90%-100%
80%-90%
70%-80%
60%-70%
50%-60%
40%-50%
30%-40%
20%-30%
10%-20%
0%-10%

(x) Yuhuan

Appendix C

Distribution of maximum daily rainfall and maximum wind speed during typhoon with different exceedance probabilities

C.1 Distribution of maximum daily rainfall and maximum wind speed with exceedance probability of 1%

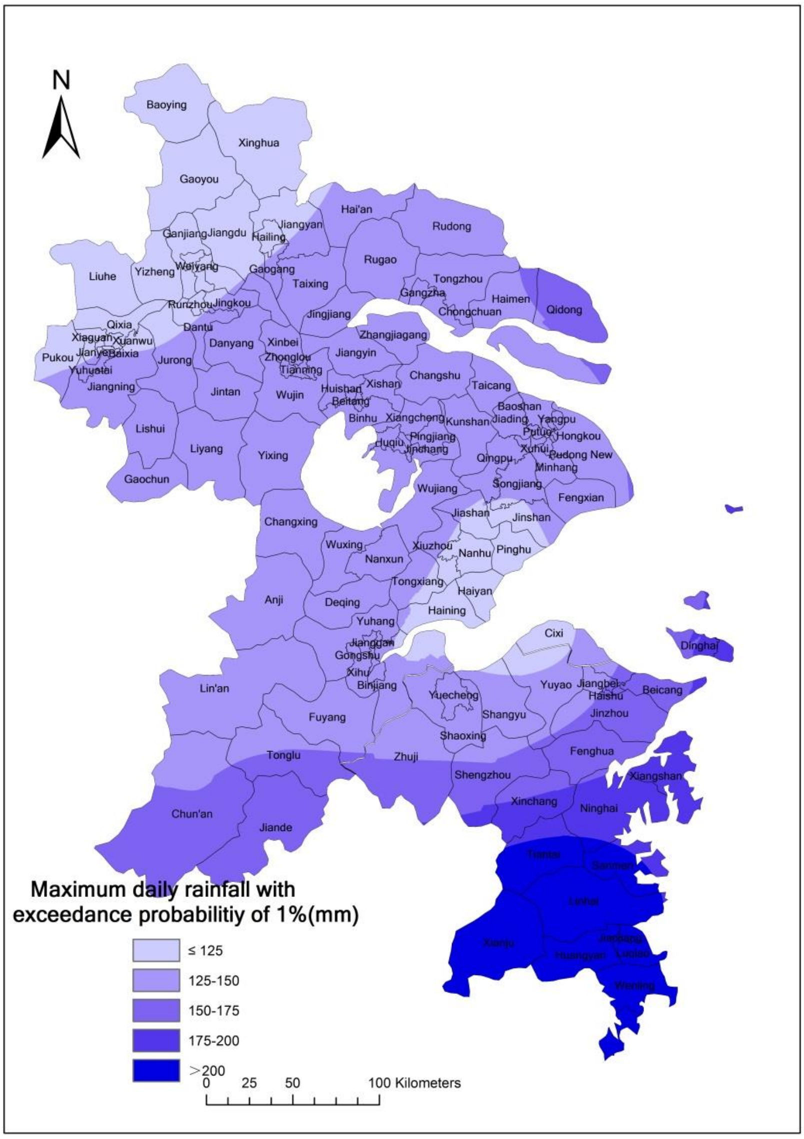

(a) Maximum daily rainfall distribution with exceedance probability of 1%

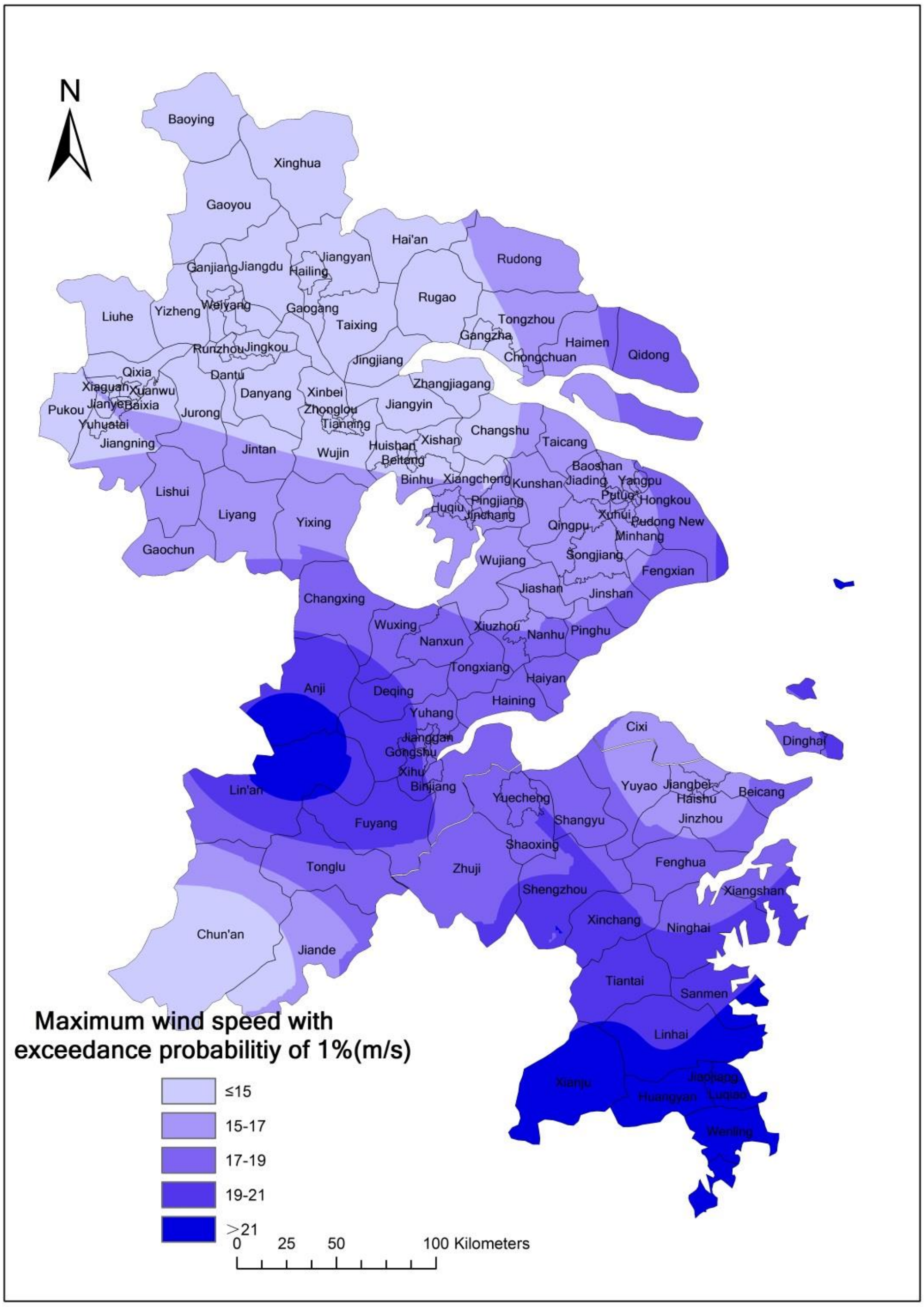

(b) Maximum wind speed distribution with exceedance probability of 1%

C.2 Distribution of maximum daily rainfall and maximum wind speed with exceedance probability of 5%

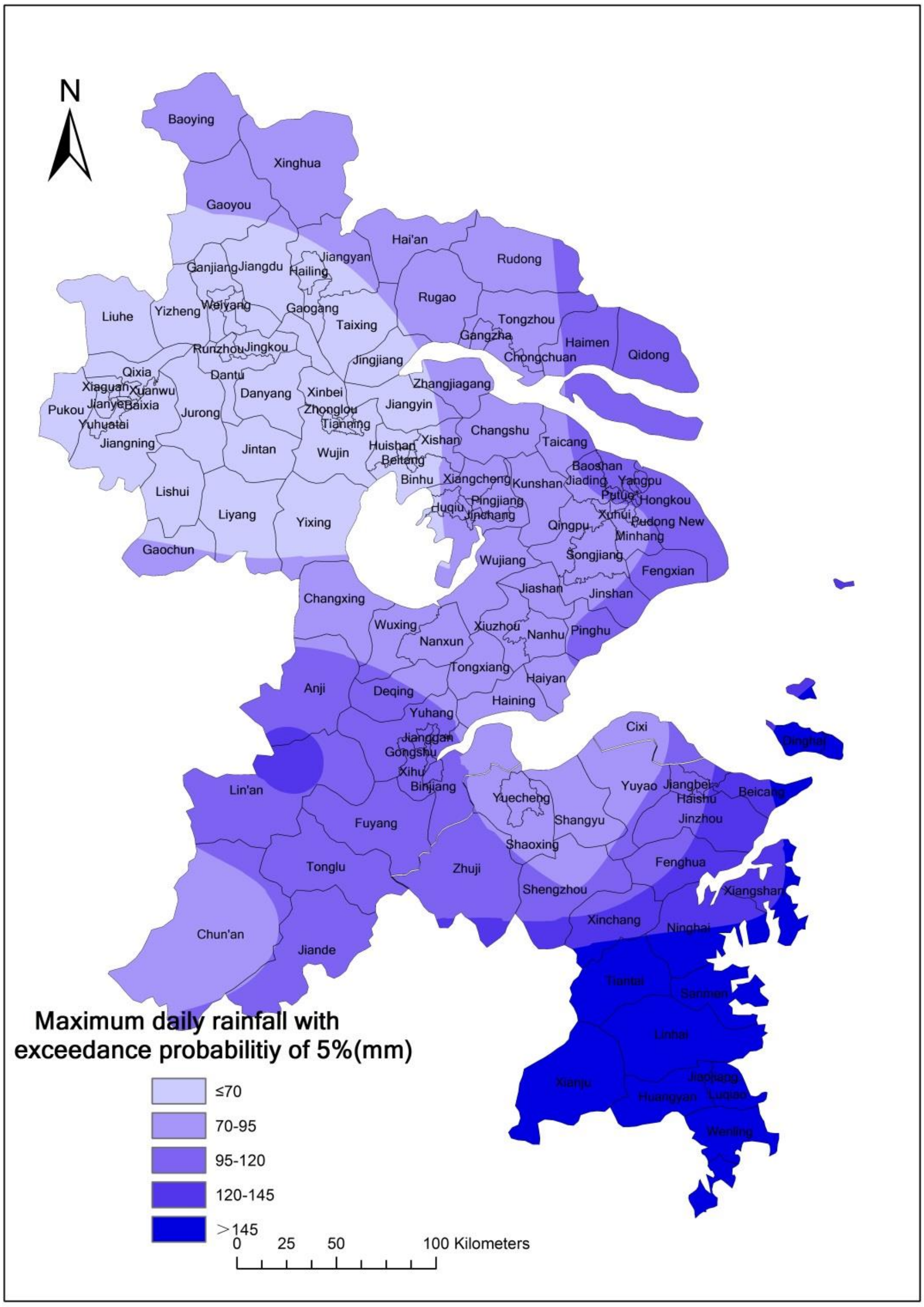

(a) Maximum daily rainfall distribution with exceedance probability of 5%

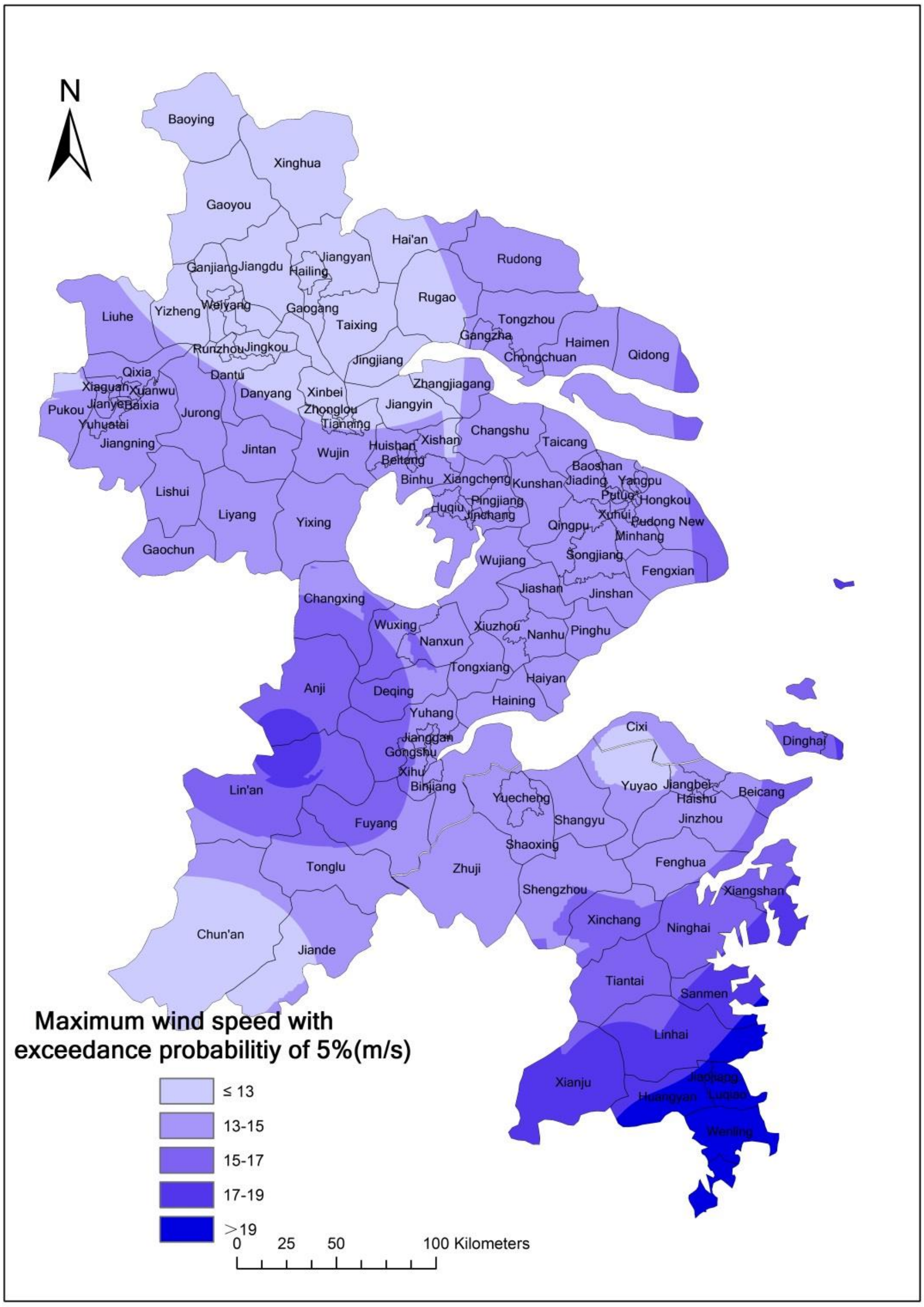

(b) Maximum wind speed distribution with exceedance probability of 5%

C.3 Distribution of maximum daily rainfall and maximum wind speed with exceedance probability of 10%

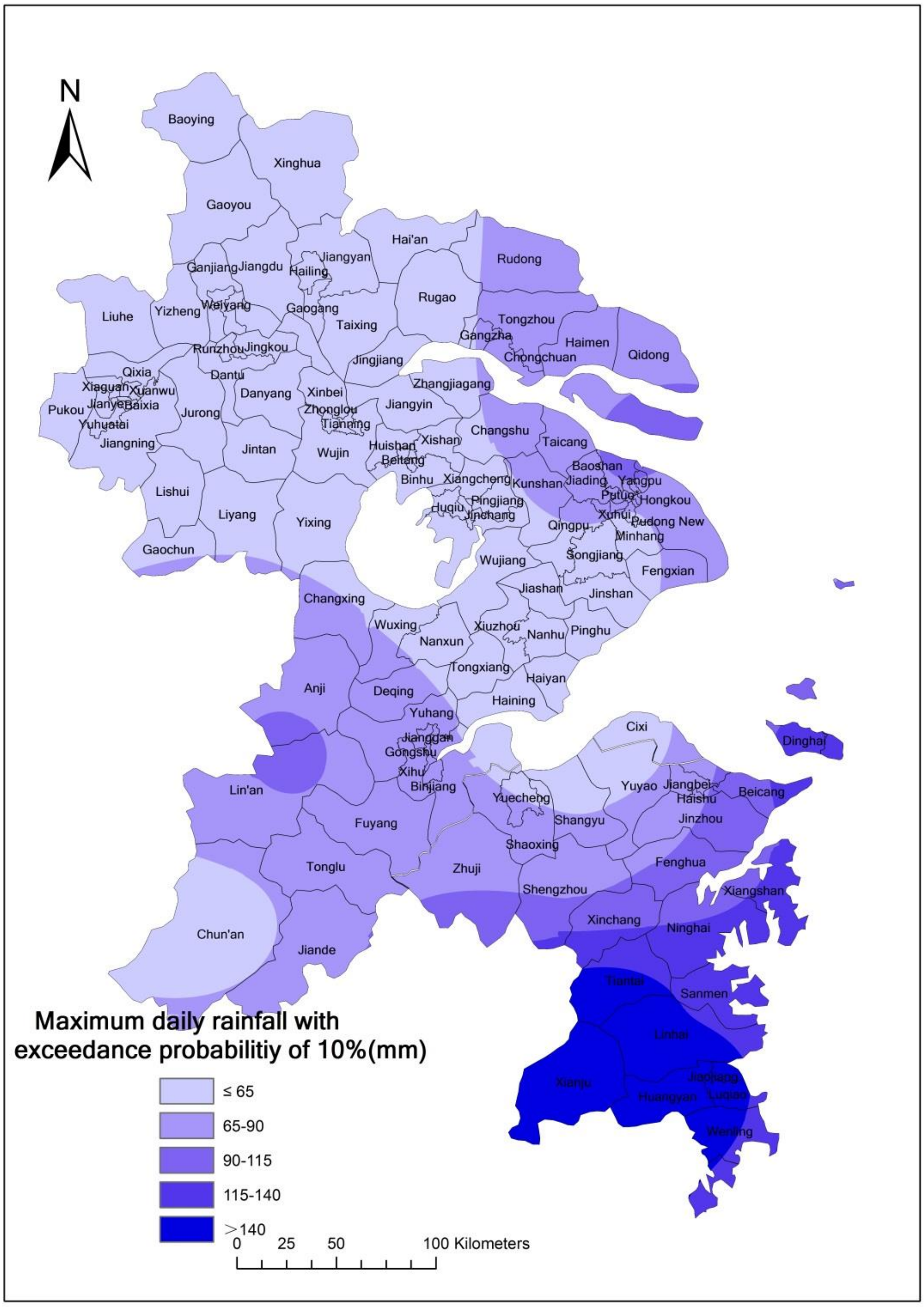

(a) Maximum daily rainfall distribution with exceedance probability of 10%

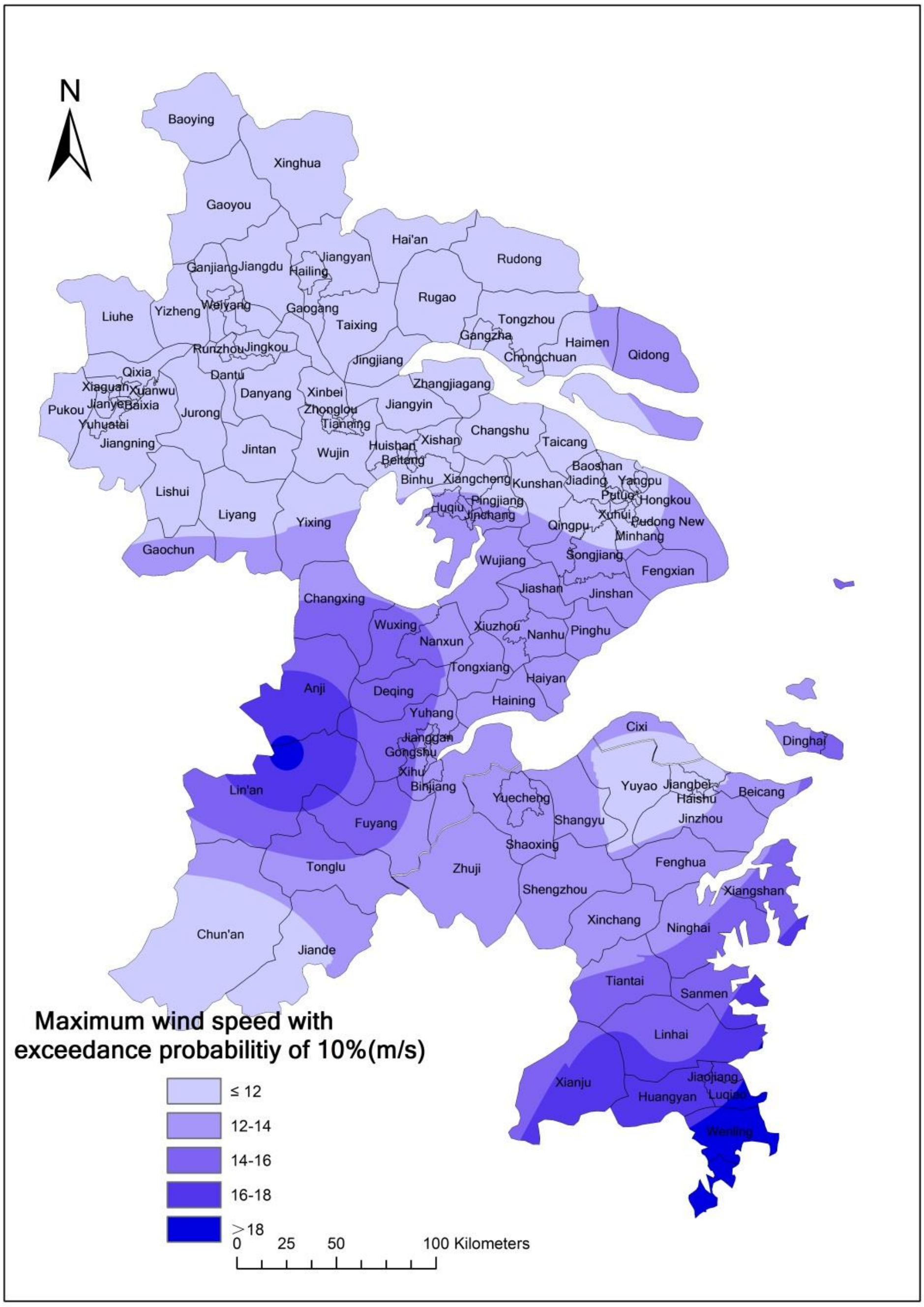

(b) Maximum wind speed distribution with exceedance probability of 10%

C.4 Distribution of maximum daily rainfall and maximum wind speed with exceedance probability of 20%

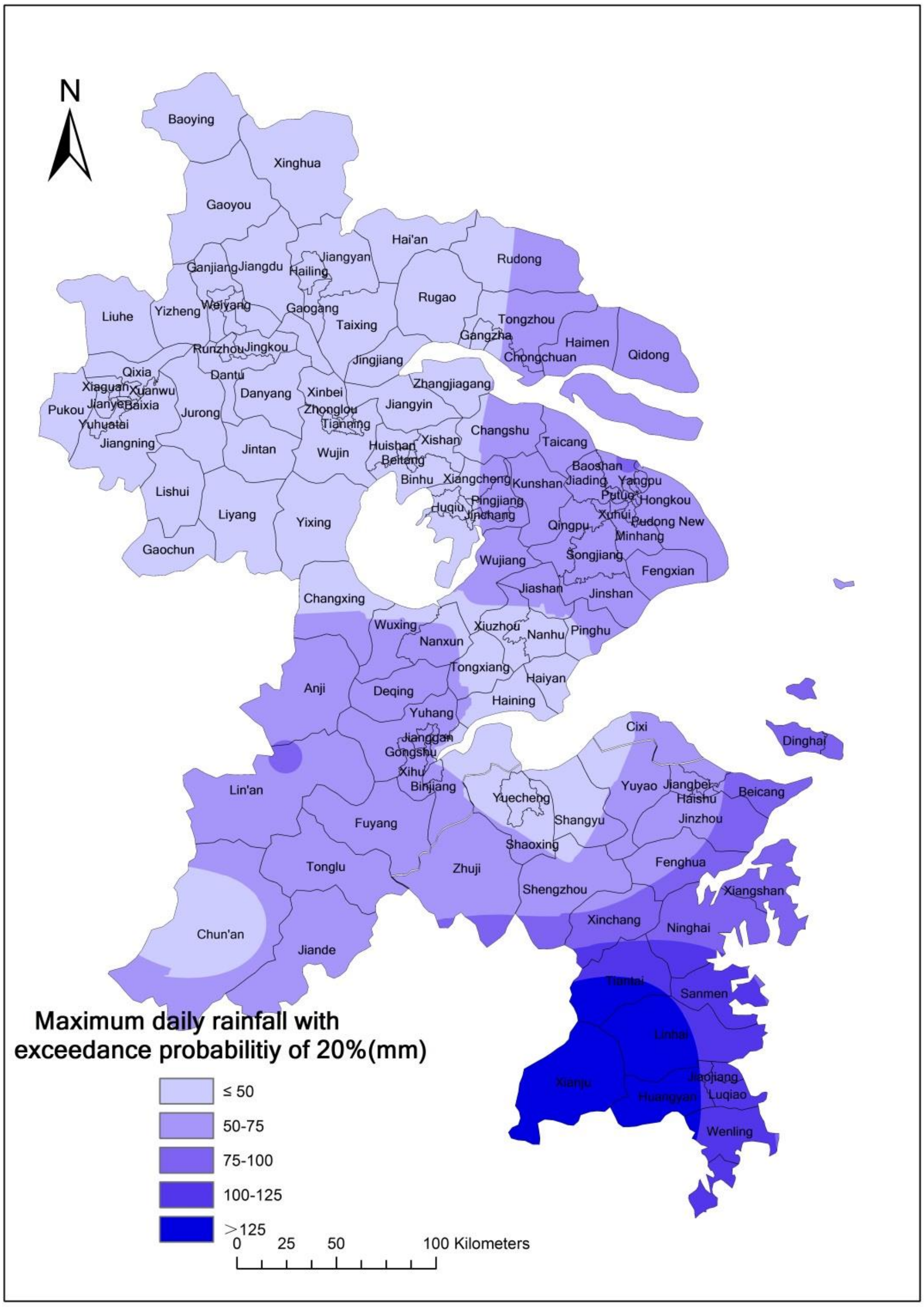

(a) Maximum daily rainfall distribution with exceedance probability of 20%

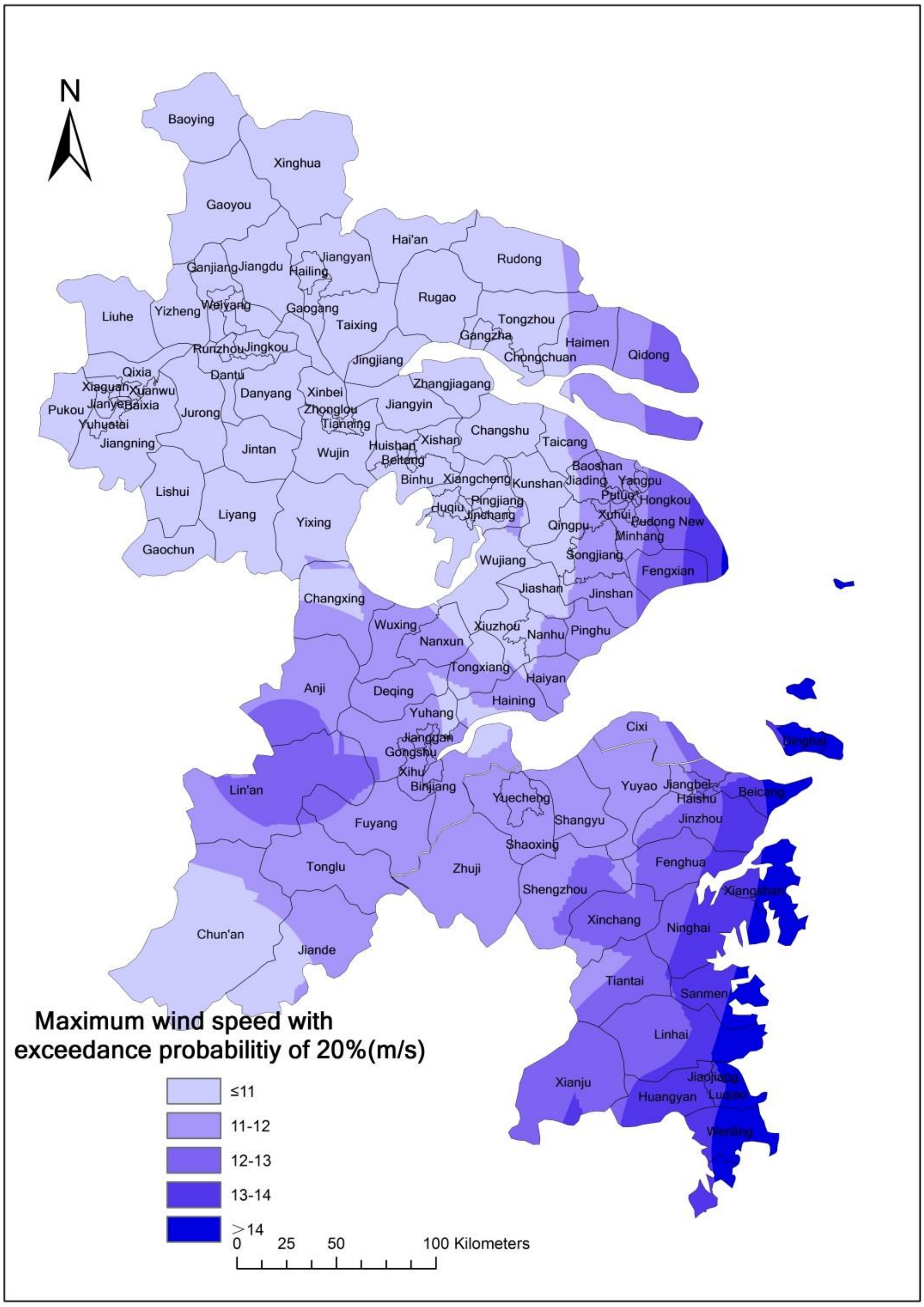

(b) Maximum wind speed distribution with exceedance probability of 20%

Appendix D

Conditional probability tables of vulnerability-related and hazard-related indicators given loss ratio

(a) Conditional probability table of number of mobile phone users per 10,000 persons (M) given loss ratio (L)

p(M/L)	**M_1**	**M_2**	**M_3**	**M_4**	**M_5**
L_1	0.58	0.16	0.1	0.1	0.05
L_2	0.44	0.16	0.19	0.1	0.11
L_3	0.59	0.05	0.25	0.06	0.05
L_4	0.66	0.14	0.14	0.03	0.04
L_5	0.72	0.09	0.15	0.02	0.02
L_6	0.77	0.13	0.07	0.02	0

(b) Conditional probability table of number of doctors per 10,000 persons (D) given loss ratio (L)

p(D/L)	**D_1**	**D_2**	**D_3**	**D_4**	**D_5**
L_1	0.11	0.34	0.36	0.09	0.1
L_2	0.07	0.25	0.37	0.17	0.15
L_3	0.13	0.25	0.5	0.08	0.05
L_4	0.11	0.38	0.33	0.15	0.03
L_5	0.15	0.43	0.3	0.11	0.02
L_6	0.13	0.46	0.33	0.06	0.02

(c) Conditional probability table of reciprocal of the population density (Pd) given loss ratio (L)

p(Pd/L)	**Pd_1**	**Pd_2**	**Pd_3**	**Pd_4**	**Pd_5**
L_1	0.09	0.22	0.22	0.27	0.21
L_2	0.1	0.32	0.28	0.24	0.07
L_3	0.08	0.23	0.36	0.23	0.09
L_4	0.08	0.24	0.19	0.39	0.09
L_5	0.15	0.19	0.17	0.35	0.15
L_6	0.08	0.12	0.13	0.51	0.16

(d) Conditional probability table of reciprocal of the GDP per km^2 (G) given loss ratio (L)

p(G/L)	**G_1**	**G_2**	**G_3**	**G_4**	**G_5**
L_1	0.12	0.07	0.17	0.19	0.45
L_2	0.19	0.13	0.18	0.15	0.34
L_3	0.11	0.05	0.17	0.11	0.56
L_4	0.09	0.04	0.12	0.16	0.58
L_5	0.09	0.02	0.07	0.17	0.65
L_6	0.02	0.02	0.07	0.14	0.73

(e) Conditional probability table of number of medical institutions per km^2 (Mi) given loss ratio (L)

p(Mi /L)	**Mi_1**	**Mi_2**	**Mi_3**	**Mi_4**	**Mi_5**
L_1	0.31	0.29	0.2	0.1	0.1
L_2	0.21	0.24	0.31	0.17	0.08
L_3	0.3	0.2	0.31	0.08	0.11
L_4	0.43	0.22	0.18	0.06	0.1
L_5	0.39	0.2	0.24	0.09	0.07
L_6	0.43	0.31	0.18	0.01	0.06

(f) Conditional probability table of percentage of population with age above 15 and under 65 (Pa) given loss ratio (L)

p(Pa /L)	**Pa_1**	**Pa_2**	**Pa_3**	**Pa_4**	**Pa_5**
L_1	0.14	0.21	0.21	0.32	0.12
L_2	0.19	0.28	0.15	0.25	0.14
L_3	0.06	0.25	0.19	0.3	0.2
L_4	0.07	0.15	0.18	0.46	0.14
L_5	0.07	0.22	0.19	0.48	0.04
L_6	0.1	0.11	0.2	0.55	0.04

(g) Conditional probability table of percentage of male residents (Ma) given loss ratio (L)

p(Ma /L)	**Ma_1**	**Ma_2**	**Ma_3**	**Ma_4**	**Ma_5**
L_1	0.19	0.21	0.18	0.12	0.31
L_2	0.27	0.17	0.2	0.09	0.27
L_3	0.17	0.22	0.16	0.09	0.36
L_4	0.15	0.11	0.11	0.15	0.48
L_5	0.13	0.04	0.07	0.13	0.63
L_6	0.07	0.04	0.1	0.08	0.71

(h) Conditional probability table of Percentage of employed (E) given loss ratio (L)

p(E /L)	E_1	E_2	E_3	E_4	E_5
L_1	0.06	0.27	0.47	0.11	0.08
L_2	0.03	0.24	0.48	0.16	0.1
L_3	0.13	0.28	0.42	0.13	0.05
L_4	0.13	0.37	0.4	0.08	0.02
L_5	0.06	0.57	0.33	0.02	0.02
L_6	0.08	0.49	0.36	0.06	0

(i) Conditional probability table of Maximum daily rainfall and maximum daily wind speed sets (WRf) in the first typhoon given loss ratio (L)

p(WRf/L)	WRf_1	WRf_2	WRf_3	WRf_4	WRf_5	WRf_6	WRf_7	WRf_8
L_1	0.41	0.07	0.37	0.12	0	0.01	0.01	0
L_2	0.27	0.15	0.38	0.17	0	0.01	0.03	0
L_3	0.2	0.13	0.41	0.22	0	0.02	0.03	0
L_4	0.13	0.11	0.24	0.33	0.02	0.02	0.12	0.03
L_5	0.06	0.06	0.2	0.3	0	0.06	0.26	0.07
L_6	0.08	0.05	0.08	0.34	0.07	0.02	0.16	0.19

(j) Conditional probability table of Maximum daily rainfall and maximum daily wind speed sets (WRs) in the second typhoon given loss ratio (L)

p(WRs/L)	WRs_1	WRs_2	WRs_3	WRs_4	WRs_5	WRs_6	WRs_7	WRs_8
L_1	0.5	0.05	0.29	0.13	0	0.01	0.02	0
L_2	0.25	0.19	0.26	0.26	0	0.02	0.02	0
L_3	0.17	0.09	0.28	0.39	0	0	0.05	0.02
L_4	0.11	0.1	0.18	0.42	0.06	0.02	0.1	0.02
L_5	0.04	0.04	0.2	0.31	0.11	0.02	0.17	0.11
L_6	0.13	0.07	0.1	0.27	0.12	0.01	0.16	0.14

(*Note that M_1 to M_5, D_1 to D_5, Pd_1 to Pd_5, G_1 to G_5, Mi_1 to Mi_5, Pa_1 to Pa_5, Ma_1 to Ma_5, E_1 to E_5, WRf_1 to WRf_8, WRs_1 to WRs_8, and L_1 to L_6 are defined in Table 5.7)*

Appendix E

Loss distribution influenced by two consecutive typhoons with different exceedance probabilities

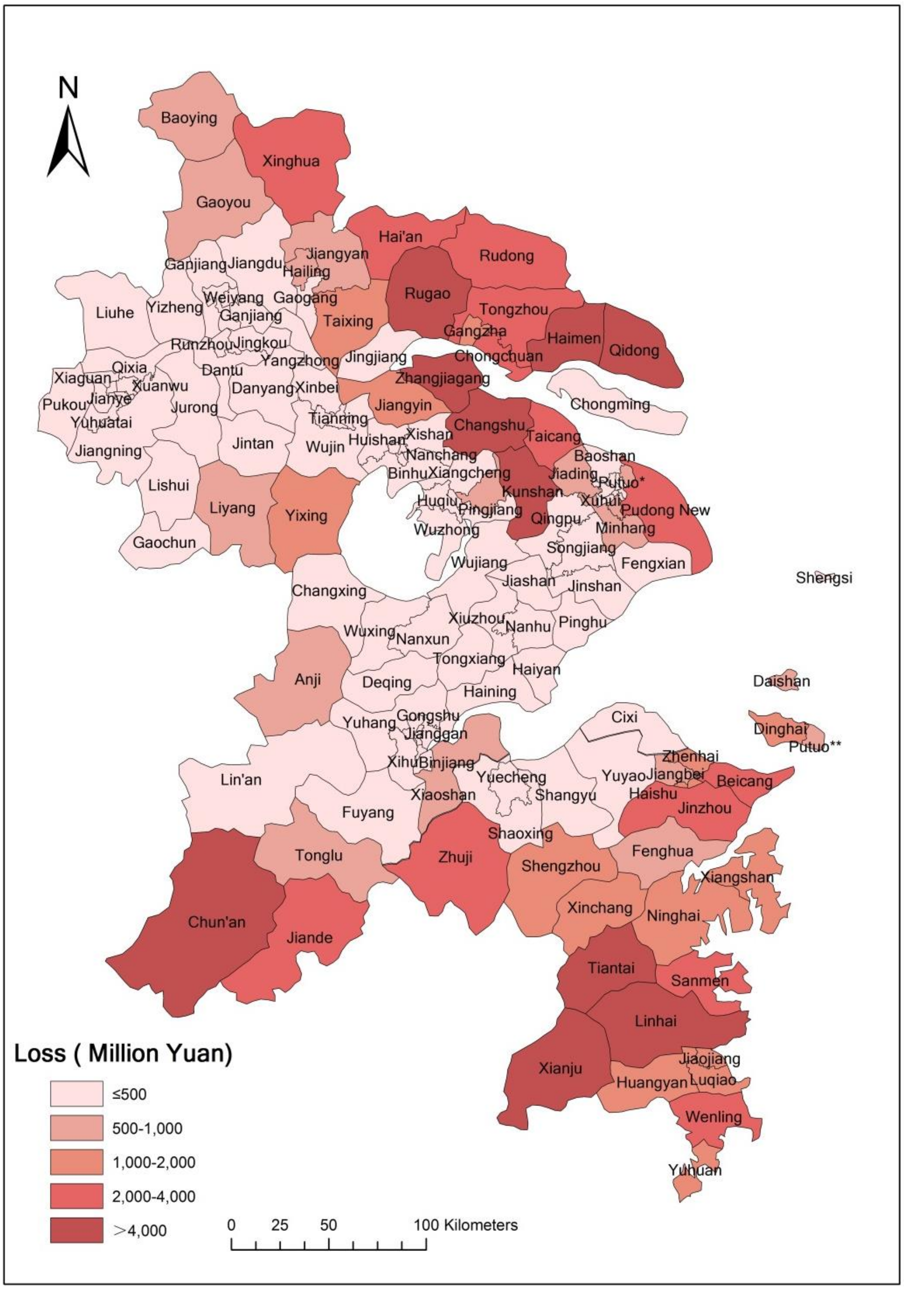

(a) Loss distribution influenced by two typhoons with exceedance probability of 1% and exceedance probability of 10%

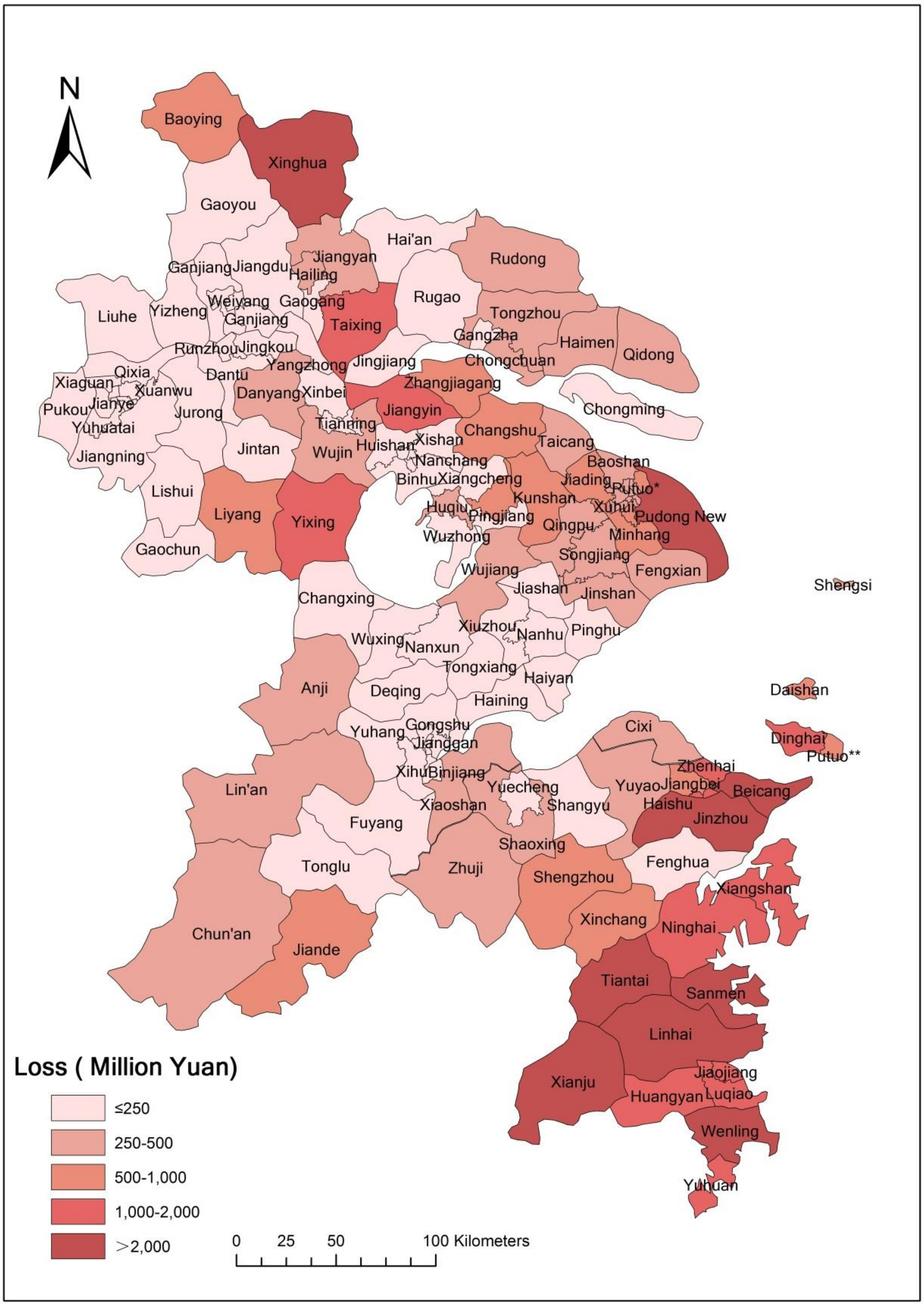

(b) Loss distribution influenced by two typhoons with exceedance probability of 5% and exceedance probability of 10%

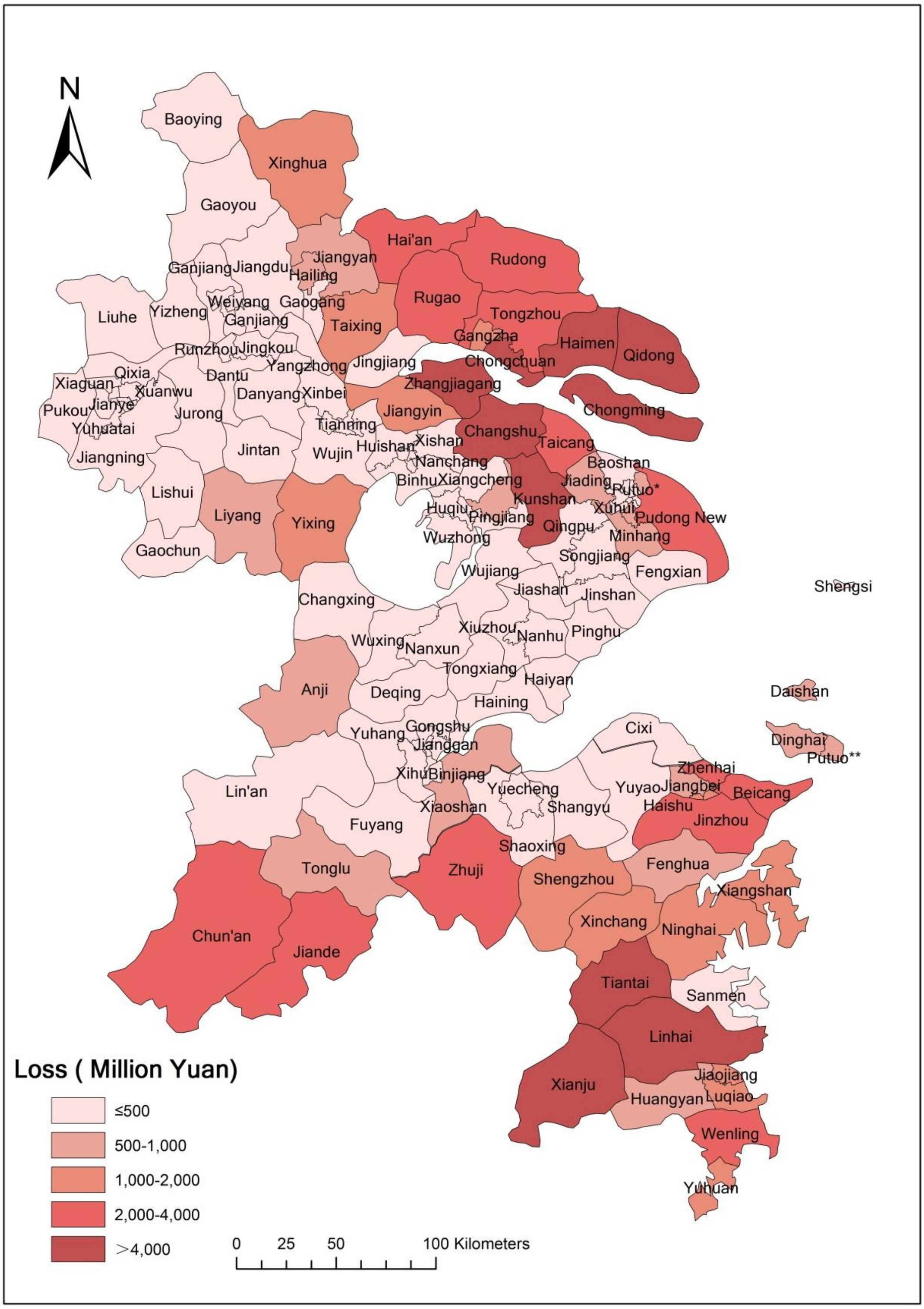

(c) Loss distribution influenced by two typhoons with exceedance probability of 10% and exceedance probability of 1%

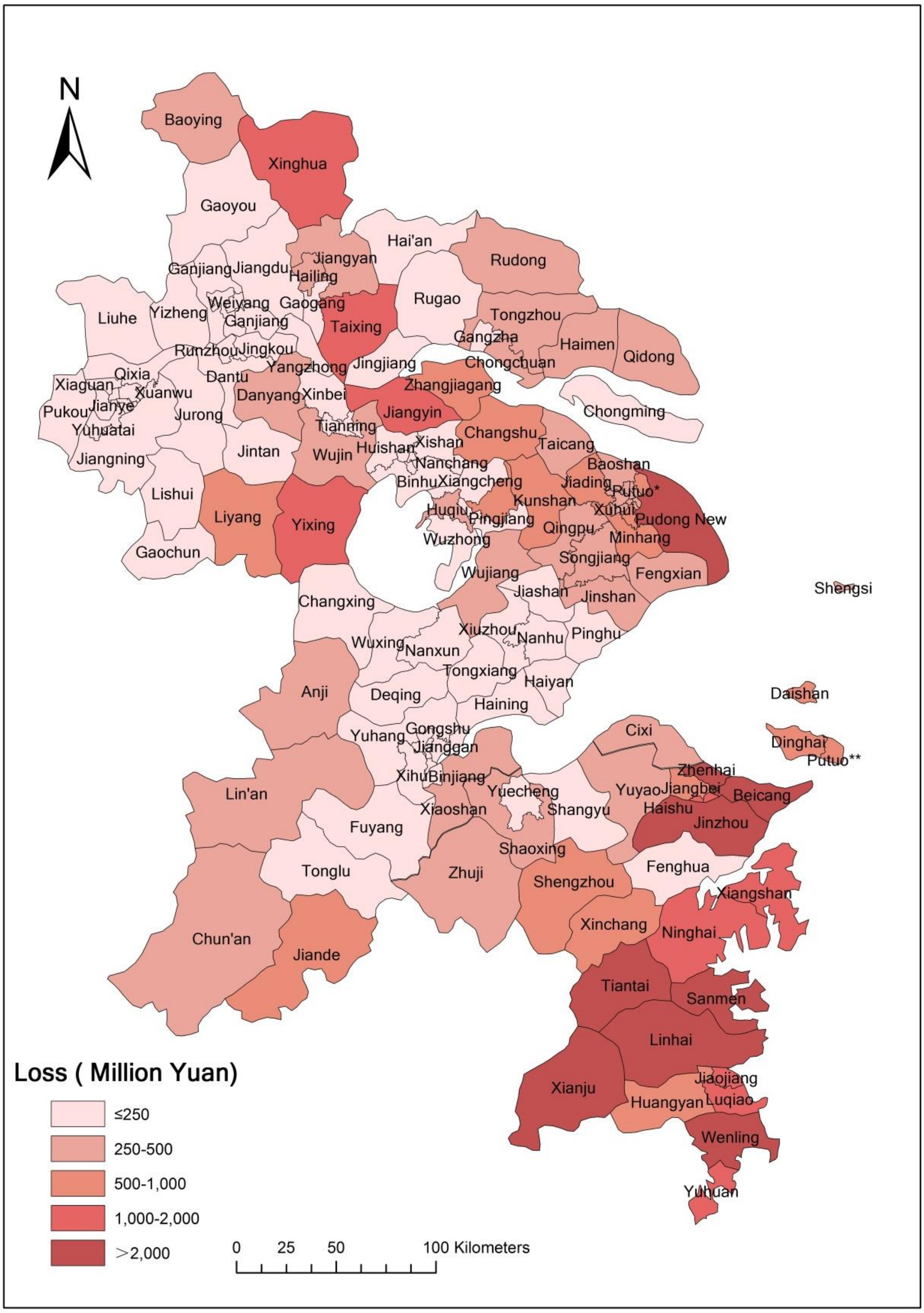

(d) Loss distribution influenced by two typhoons with exceedance probability of 10% and exceedance probability of 5%